Unclassified

SECURITY CLASSIFICATION OF THIS PAGE

REPORT DOCUMENTATION PAGE

1a. REPORT SECURITY CLASSIFICATION: Unclassified	1b. RESTRICTIVE MARKINGS
2a. SECURITY CLASSIFICATION AUTHORITY	3. DISTRIBUTION/AVAILABILITY OF REPORT: Approved for public release; distribution unlimited
2b. DECLASSIFICATION/DOWNGRADING SCHEDULE	
4. PERFORMING ORGANIZATION REPORT NUMBER(S): AFWAL-TR-84-3098	5. MONITORING ORGANIZATION REPORT NUMBER(S)
6a. NAME OF PERFORMING ORGANIZATION: Structural Concepts Branch Structures & Dyn Div (cont'd) / 6b. OFFICE SYMBOL (If applicable): AFWAL/FIBC	7a. NAME OF MONITORING ORGANIZATION
6c. ADDRESS (City, State and ZIP Code): Wright-Patterson Air Force Base, Ohio 45433	7b. ADDRESS (City, State and ZIP Code)
8a. NAME OF FUNDING/SPONSORING ORGANIZATION / 8b. OFFICE SYMBOL (If applicable)	9. PROCUREMENT INSTRUMENT IDENTIFICATION NUMBER
8c. ADDRESS (City, State and ZIP Code)	10. SOURCE OF FUNDING NOS.

PROGRAM ELEMENT NO.	PROJECT NO.	TASK NO.	WORK UNIT NO.
62201F	2401	03	38

11. TITLE (Include Security Classification): On Design of Off-Axis Specimens (unclassified)

12. PERSONAL AUTHOR(S): Sandhu, Raghbir Singh; Sendeckyj, George Peter

13a. TYPE OF REPORT	13b. TIME COVERED	14. DATE OF REPORT (Yr., Mo., Day)	15. PAGE COUNT
Final	FROM 1979 TO 1982	1985 March	162

16. SUPPLEMENTARY NOTATION

17. COSATI CODES			18. SUBJECT TERMS (Continue on reverse if necessary and identify by block number)		
FIELD	GROUP	SUB. GR.			
01	03		Laminate Strength	Nonlinear Analysis	Experimental Data
11	04		Laminated Composites	Stress Analysis	Off-Axis
			Failure Criterion	Mechanical Properties	Specimens

19. ABSTRACT (Continue on reverse if necessary and identify by block number)

The effort reported herein relates to (a) investigation of techniques to achieve uniformity of axial stress distribution in the test area between tabs of an off-axis specimen and (b) assessment of a fixed-angle off-axis specimen to perform as a shear specimen.

On the basis of studies conducted, it is determined that off-axis specimens, subject to uniaxial loading, develop practically uniform axial stress provided (a) rotating end grips are used and (b) the fiber angle of cross-ply tab material and the inclination of tab ends are simultaneously optimized. This tab design retains its superior characteristics even in the nonlinear material range.

The performance of off-axis specimens to function as shear specimens was assessed using both linear and nonlinear material behavior. Three failure criteria, namely,

(continued)

20. DISTRIBUTION/AVAILABILITY OF ABSTRACT: UNCLASSIFIED/UNLIMITED ☒ SAME AS RPT. ☐ DTIC USERS ☐	21. ABSTRACT SECURITY CLASSIFICATION: Unclassified

22a. NAME OF RESPONSIBLE INDIVIDUAL	22b. TELEPHONE NUMBER (Include Area Code)	22c. OFFICE SYMBOL
R S Sandhu	(513) 255-5864	AFWAL/FIBCA

DD FORM 1473, 83 APR EDITION OF 1 JAN 73 IS OBSOLETE.

Unclassified

SECURITY CLASSIFICATION OF THIS PAGE

6a. Continued
Flight Dynamics Laboratory
Air Force Wright Aeronautical Laboratories
Air Force Systems Command

19. Continued
Norris Criterion, Tsai Criterion and Chamis Criterion were used in the linear analysis. In the case of nonlinear material behavior, a criterion based upon axial, transverse and shear energies of unidirectional laminates under simple load conditions was used. The results of studies, based upon linear and nonlinear material behavior, indicate that the off-axis angle required to generate the maximum shear response is not a fixed entity. It changes with changes of material and material behavior.

AFWAL-TR-84-3098

ON DESIGN OF OFF-AXIS SPECIMENS

R. S. Sandhu
Structural Concepts Branch
G. P. Sendeckyj
Structural Integrity Branch
Structures and Dynamics Division

March 1985

FINAL TECHNICAL REPORT

FLIGHT DYNAMICS LABORATORY
AIR FORCE WRIGHT AERONAUTICAL LABORATORIES
AIR FORCE SYSTEMS COMMAND
WRIGHT-PATTERSON AIR FORCE BASE, OHIO 45433

NOTICE

When Government drawings, specifications, or other data are used for any purpose other than in connection with a definitely related Government procurement operation, the United States Government thereby incurs no responsibility nor any obligation whatsoever; and the fact that the government may have formulated, furnished, or in any way supplied the said drawings, specifications, or other data, is not to be regarded by implication or otherwise as in any manner licensing the holder or any other person or corporation, or conveying any rights or permission to manufacture use, or sell any patented invention that may in any way be related thereto.

This report has been reviewed by the Office of Public Affairs (ASD/PA) and is releasable to the National Technical Information Service (NTIS). At NTIS, it will be available to the general public, including foreign nations.

This technical report has been reviewed and is approved for publication.

Raghbir S. Sandhu

RAGHBIR S. SANDHU
Project Engineer

Larry G. Kelly

LARRY G. KELLY, Chief
Structural Concepts Branch
Structures and Dynamics Division

FOR THE COMMANDER

ROGER J. HEGSTROM, Colonel, USAF
Chief, Structures and Dynamics Division
Flight Dynamics Laboratory

"If your address has changed, if you wish to be removed from our mailing list, or if the addressee is no longer employed by your organization please notify AFWAL/FIBC, W-PAFB, OH 45433 to help us maintain a current mailing list".

Copies of this report should not be returned unless return is required by security considerations, contractual obligations, or notice on a specific document.

FOREWORD

This effort was initiated by the Structural Concepts Branch, Structures and Dynamics Division, Flight Dynamics Laboratory, Air Force Wright Aeronautical Laboratories, under Project No. 2401, Task No.240103, and Work Unit No. 24010321, "Analytical Technique Development for Advanced USAF Aircraft," but a major portion of this study was conducted under Work Unit No. 24010338, "Preliminary Design of Military Aircraft Structures."

The experimental work was performed by the Structures Test Branch, Structures and Dynamics Division, Flight Dynamics Laboratory. Messrs H.D. Stalnaker and J.V. Smith were the Test Engineers. The Instrumentation and Data Acquisition Engineers were Mr R.C. Taylor and Mr J.E. Pappas. The data was processed by Mrs Artie Vahldiek and Mr B.F. Davis.

The specimens were fabricated by the Composites Concepts Group of the Structural Concepts Branch with Mr E.E. Zink as the lead technician.

TABLE OF CONTENTS

TABLE OF CONTINUED (CONTINUED)

LIST OF ILLUSTRATIONS

LIST OF ILLUSTRATIONS (CONTINUED)

LIST OF ILLUSTRATIONS (CONTINUED)

LIST OF ILLUSTRATIONS (CONTINUED)

LIST OF ILLUSTRATIONS (CONTINUED)

LIST OF ILLUSTRATIONS (CONTINUED)

LIST OF ILLUSTRATIONS (CONTINUED)

LIST OF ILLUSTRATIONS (CONTINUED)

LIST OF TABLES

SECTION I

INTRODUCTION

Off-axis specimens normally are fabricated from unidirectional composite materials. In the specimens, the fibers are oriented at an angle to the specimen axis (Figure 1).* When loaded uniaxially ($\sigma_x \neq 0, \sigma_y = \tau_{xy} = 0$), the specimen develops normal and shear stresses (σ_1, σ_2 and τ_{12}) with respect to the material axes 1 and 2. Available experimental data confirms the assumption made in mechanics of composite materials that the unidirectional lamina is orthotropic, i.e. the stresses σ_1 and σ_2 produce ε_1 and ε_2 strains and the stress τ_{12} generates γ_{12} strain, respectively. This uncoupling of normal and shear responses with respect to the material axes presents a possibility of the off-axis specimen being used to study the behavior of composite laminates subjected to biaxial stresses.

The simplistic and attractive concept of the specimen changes when we consider methods of load introduction. The introduction of tensile loads into the specimens requires that the specimens with or without tabs be gripped in the loading machine. The use of standard non-rotating grips causes the axial stress σ_x to become non-uniform in the area between grips or tabs if provided. Various techniques have been suggested and used with some success to remedy this

---

*Figures and Tables are located on pgs 34-147.

undesirable situation. These techniques are discussed in chronological order in the following paragraphs.

Tsai (References 1 thru 3) used off-axis specimens to experimentally verify a strength theory based upon strength parameters obtained in simple (single load) tests. Ideally this secimen should have uniform axial stress σ_x. However, he observed that specimens of uniform cross section tended to fail in the region under the grips of the specimen. To ensure failure in the test section, Tsai reduced the specimen cross-section in 'dog-bone' fashion. Lauraitis (Reference 4), to correlate the experimental data and the analytical results based upon fracture mechanics and Tsai criterion, reduced the test section using a continuous large radius of curvature but for the same reasons as Tsai.

Effects of restraints caused by clamping devices were investigated by Pagano and Halpin (Reference 5). Using a simple analytical model, they showed that end constraints indeed introduced in-plane bending effects (See Figure 1b) in the specimens. The presence of in-plane bending stresses introduces non-uniformity of normal stresses. This analytical observation was supported by qualitative experimental data obtained by testing specimens of nylon-reinforced rubber. Moreover, they concluded that long off-axis specimens could be used to obtain initial elastic moduli but not strength data. For strength data, specimen end-gripping techniques would require modification to generate uniform stress states between grips.

Rizzo (Reference 6) used the finite element method to determine the influence of rigid clamping with and without end rotation on the distribution of stresses. He observed that a marked improvement in the uniformity of stress distribution occurred when rotation of end-grips was permitted. He further observed that for long specimens (length/width ratio exceeding ten) the stress field at the center of the specimens was unaffected by the end-clamping arrangements.

Wu and Thomas (Reference 7) designed a fixture which permitted end rotations about axes normal to the specimen planform. The fixture was used to test strain gaged 15^{o} off-axis specimens with length/width ratios of 5, 4 and 2.5. The width was kept constant at 1.5 inches and the length was progressively adjusted. On the basis of data from these tests, they concluded that at the low stress level and within the aspect ratios (length/width) investigated the use of the rotating end fixture resulted in a relatively uniform stress state. Using a 45^{o} off-axis specimen with an aspect ratio of 12, Richard et al (Reference 8) reconfirmed the findings of Reference 5.

To improve uniformity of stress state, Cole and Pipes (References 9 and 10) selected the fiber orientation of highly tapered end tabs to be the same as the fiber direction in the off-axis specimens. Their selection of the tab fiber orientation was not supported by quantitative assessment. However, their study yielded an important finding. They observed that boron/epoxy laminas retained their

orthotropic characteristics at all load levels (shear and normal stress strain response were uncoupled). As a result of this observation, the use of the off-axis specimen to determine shear stress-strain response was suggested implicitly in Reference 11 and 12. The use of a 10^{o} off-axis specimen for the same purpose was advocated explicitly in References 13 through 15.

The off-axis specimens (presently used by investigators for verification of failure criterion, fracture mechanics and fatigue studies, and to determine the shear stress-strain response of unidirectional laminates) often incorporate the design modifications described in the preceding paragraphs. In spite of these efforts, deficiencies in the design of the specimen and the test fixture exist. The present study is aimed at removing some of the shortcomings. Specifically the objective of this two-fold effort is to investigate the following:

a. Necessary changes in the design to improve uniformity of stress (σ_x) so that the specimen could indeed be used to study the effects of biaxial stress states upon composite laminates.

b. Validity of the off-axis specimen for determining the shear stress-strain (τ_{12}, γ_{12}) response of undirectional composite laminates. This requires that other stress components must vanish, which is not possible in the off-axis specimen. Therefore, the next best possible thing to do is to maximize the shear effects relative to the

normal effects caused by the presence of normal stresses σ_1 and σ_2.

The improved specimen design is described in Section II. Experimental and analytical data verifying the improvements are included in Section III. Finally, the evaluation of the results and the conclusions drawn therefrom are presented in Section IV.

SECTION II

SPECIMEN DESIGN

An axially loaded ($\sigma_x \neq 0, \sigma_y = \tau_{xy} = 0$) off-axis specimen develops a biaxial stress state (σ_1, σ_2, τ_{12}) relative to the material axes such that normal stresses (σ_1, σ_2)are functions only of normal strains (ε_1, ε_2) and shear stress (τ_{12}) is a function only of shear strain (γ_{12}) (References 9 and 10). This behavior of the specimen suggests that the specimen can be used for the following purposes:

a. Determination of the shear stress-strain responses of unidirectional composite laminates.

b. Limited verification of failure criteria (Figure 2).

c. Fatigue and fracture mechanics studies under biaxial stress states.

The stress state in the test area of the specimen must be uniform for any of these three purposes. This condition is the basic requirement for achieving meaningful results. The means for improving stress uniformity and the shear stress-strain response determination are described in the following paragraphs.

The study of the off-axis specimen reported herein includes the following:

a. Point-stress state

b. Shear stress-strain response based upon

(i). Linear material behavior

(ii). Nonlinear material behavior

c. Effects of end constraints upon the stress distribution and the means to achieve uniformity of the stress state.

1. Specimen Point Stress State

A biaxial stress state exists along the material axes 1, 2 of a uniaxially loaded ($\sigma_x \neq 0, \sigma_y = \tau_{xy} = 0$) flat unidirectional composite laminate specimen when the load axes X, Y do not coincide with the material axes. If the angle between the only load (σ_x) and material axis 1 is α, the resulting stresses and strains referred to the material axes 1 and 2 are given by

$$\sigma_1 = m^2 \sigma_x \tag{1}$$

$$\sigma_2 = n^2 \sigma_x \tag{2}$$

$$\tau_{12} = mn\sigma_x \tag{3}$$

$$\varepsilon_1 = \sigma_1/E_{11} - \mu_{12}\sigma_2/E_{11} \tag{4}$$

$$\varepsilon_2 = -\mu_{12}\sigma_1/E_{11} + \sigma_2/E_{22} \tag{5}$$

$$\gamma_{12} = \tau_{12}/G_{12} \tag{6}$$

$$\mu_{21} = \mu_{12}E_{22}/E_{11} \tag{7}$$

where

σ_x = normal stress in x-direction

σ_1, ε_1 = normal stress and strain in the fiber direction (1-axis)

σ_2, ε_2 = normal stress and strain in the direction transverse to the fibers (2-axis)

τ_{12}, γ_{12} = in-plane shear stress and strain

E_{11}, E_{22} = Young's moduli in 1 and 2 directions

G_{12} = shear modulus

μ_{12} = major Poisson's ratio

m = $\cos \alpha$

n = $\sin \alpha$

α = angle between the 1 and x directions (positive when counterclockwise going from 1 to x)

2. Specimen Optimization for Shear

In the off-axis specimen, though uncoupled, both normal and shear stresses and strains exist relative to the material axes. For the off-axis specimen to perform as a shear specimen, the shear response as compared to the normal responses should be a maximum. In the following paragraphs, we determine the off-axis angle which (a) maximizes the shear response to failure and (b) minimizes the transverse strain. Since the shear stress-strain response of unidirectional composite laminates is in general nonlinear, the off-axis angles maximizing the shear response for linear and nonlinear material behaviors are likely to be different. We show that this is so and the off-axis angle maximizing the shear response is not a fixed entity.

2.1 Maximizing Shear Response-Linear Material

The failure of the off-axis specimen subjected to the biaxial stress state (Equations 1 to 3) is governed by the following expression that incorporates three criteria, Norris, Tsai and Chamis (Reference 16):

$$(\sigma_1 /F_{11})^2 +(\sigma_2 /F_{22})^2 - \bar{K}(\sigma_1\sigma_2 /F_{11}F_{22})+(\tau_{12}/F_{66})^2 \geq 1 \quad (8)$$

where

F_{11} = strength in the fiber direction

F_{22} = strength in the direction transverse to the fibers

F_{66} = shear strength

$\bar{K}$ = 1 for Norris criterion

= F_{22} /F_{11} for Tsai criterion

= K_{12} for Chamis criterion, is a combined strength coefficient to be chosen such that the predicted and experimental results are in good agreement

F_{11} and F_{22} can assume positive or negative values depending upon whether σ_1 and σ_2 are tensile or compressive. Upon using σ_1, σ_2 and τ_{12} from Equations 1 to 3, Equation 8 can be written as

$$\sigma_x^2 \geq 1/(m^4/F_{11}^2+ n^4/F_{22}^2- \bar{K}m^2n^2/F_{11}F_{22}+ m^2n^2/F_{66}^2) \quad (9)$$

In Equation 8, the expression $(\tau_{12} /F_{66})^2$ represents the contribution, X_s, made by the shear stress towards failure.

It can be written as

$$X_s = (\tau_{12}/F_{66})^2 \tag{10}$$

or

$$X_s = \sigma_x^2 (m^2 n^2 / F_{66}^2) \tag{11}$$

Substituting Equation 9 for the case of equality into Equation 11, we get

$$X_s = 1/(F_{66}^2/F_{11}^2 \cot^2\alpha + F_{66}^2/F_{22}^2 \tan^2\alpha - \bar{K}F_{66}^2 / F_{11}F_{22} + 1) \tag{12}$$

X_s attains a maximum value, when

$$dX_s/d\alpha = 0 \tag{13}$$

On simplification, Equation 13 reduces to

$$\tan \alpha' = \sqrt{F_{22}/F_{11}} \tag{14}$$

where α' is the off-axis angle for which X_s becomes maximum. Equation 14 indicates that the off-axis angle, α', maximizing the shear contribution to failure is a function of the normal strength parameters only. The coupling and shear strength terms of the interacting type failure criterion do not affect the off-axis angle α'.

2.2 Minimizing Transverse Strain-Linear Material

Using Equations 1 and 2, the transverse strain ε_2 in Equation 5 can be written as

$$\varepsilon_2 = [-\mu_{12}\cos^2\alpha/E_{11} + \sin^2\alpha/E_{22}]\ \sigma_x \tag{15}$$

The transverse strain ε_2 vanishes for

$$\tan^2 \alpha = \mu_{12} E_{22}/E_{11} \tag{16}$$

and α assumes a specific optimum value $\alpha"$. Thus

$$\tan^2 \alpha" = \mu_{21} \tag{17}$$

$$\tan \alpha" = \sqrt{\mu_{21}} \tag{18}$$

Off-axis angles α' and $\alpha"$ computed for various material systems are shown in Table 1. It is evident from the table that α' and $\alpha"$ for the same material system are not the same. This means that when fibers are oriented to maximize shear contribution to failure, the specimen is not simultaneously free of transverse strain. When fibers are oriented at $\alpha"$ to eliminate transverse strain, shear contribution to failure is not maximum. Hence, for linear material there is no fiber orientation for which both conditions (maximum shear contribution to failure and zero ε_2) are satisfied at the same time.

2.3 Maximizing Shear Response-Nonlinear Material

In this paragraph the effect of nonlinearity of material behavior upon the off-axis angle maximizing the shear response is studied. The concepts developed in References 11 and 12 and incorporated in the computer program "NOLAST" (Reference 17) are used. These concepts are described in paragraphs 2.3.1 thru 2.3.5.

2.3.1 Constitutive Releationship for Nonlinear Elastic Material

$$d\varepsilon_i = S_{ij}(\varepsilon_i)\, d\sigma_j \quad (i, j = 1,2,6) \tag{19}$$

where $d\varepsilon_i$, $d\sigma_j$ and $S_{ij}(\varepsilon_i)$ are the increments of strain, and stress components and elements of the compliance matrix, respectively. The compliances $S_{ij}(\varepsilon_i)$ depend upon current strain level and are obtained from the basic stress-strain data of the unidirectional lamina represented analytically by piecewise cubic spline interpolation functions.

2.3.2 Laminate Strain Increments

$$\{d\varepsilon^0\} = [A]^{-1} \{d\bar{N}\} \tag{20}$$

where

$\{d\varepsilon^0\}$ = laminate strain increments

$[A]^{-1}$ = laminate compliance matrix

$\{d\bar{N}\}$ = increments of stress resultants

In the application of Equation 20, a predictor-corrector and iterative procedure is used to improve the accuracy of the laminate stress-strain increments. In this technique, the matrix $[A]^{-1}$ is computed using elastic constants which correspond to the end of the previous load increment and, hence, the strain increment. Then a new increment of load $\{d\bar{N}\}$ is applied and the resulting strain increment $\{d\varepsilon^0\}$ is calcuated using the matrix $[A]^{-1}$. This strain increment is used to determine a new set of average elastic constants and a new matrix $[A]^{-1}$ is computed. The above cycle is repeated by applying the current load increment and a new set of

strain increments $\{d\varepsilon^0\}$ through the use of the updated matrix $[A]^{-1}$ is calculated. This procedure is continued until the ratio of change of the strain increment to the strain increment in two consecutive cycles is less than 0.001.

2.3.3 Equivalent Strain Increments

In the procedure described in paragraph 2.3.2 the lamina biaxial strains (ε_1 and ε_2) are modified before being used to determine the elastic constants from the experimental stress-strain curves. This modification is required to allow for the simultaneous existence of longitudinal and transverse stresses in the lamina whereas in the experimental data only one component of stress is present. The effects of the existence of transverse or longitudinal stresses are taken into account by assuming that simple equivalent strain increments can be computed from

$$d\varepsilon_1\Big|_{\text{Equivalent}} = d\varepsilon_1 /(1-\mu_{12}B) \qquad (21)$$

$$d\varepsilon_2\Big|_{\text{Equivalent}} = d\varepsilon_2 /(1-\mu_{21}/B) \qquad (22)$$

where μ_{12} = major Poisson's ratio and

$$B = d\,\sigma_2 / d\,\sigma_1$$

2.3.4 Failure Criterion

The incremental loading technique described in paragraph 2.3.2 is a finite process. It culminates in failure of the lamina. To determine the failure state, various failure criteria (Reference 16) have been proposed.

These criteria assume linear material behavior and are not applicable to materials exhibiting nonlinear behavior. For this reason, the failure criterion developed in References 11 and 12 for nonlinear material behavior was used. This criterion is a function of both stress and strain states. For plane stress conditions, the criterion is written as:

$$\sum_{i = 1,2,6} (W_i / \bar{W}_i)^{mi} = 1 \qquad (23)$$

where W_i = area under the simple stress-strain curve up to the strain due to the applied load

$\bar{W}_i$ = area under the simple stress-strain curve to failure due to uniaxial lamina loading

m_i = parameter to be determined by biaxial experimental data

Since biaxial data are not available for fixing the values of m_i, it is assumed that $m_1 = m_2 = m_6 = 1$, and it reduces the criterion to a simple strain energy relationship. For this condition the criterion corresponds to the following equation:

$$\bar{X}_n + \bar{X}_s = 1 \qquad (24)$$

where

$$\bar{X}_n = W_1 / \bar{W}_1 + W_2 / \bar{W}_2 \qquad (25)$$

$$\bar{X}_s = W_6 / \bar{W}_6$$

where $\bar{X}_n$ = normal stress contribution to failure

$\bar{X}_s$ = shear stress contribution to failure

2.3.5 Contribution of Shear to Degradation Process of Off-Axis Specimen

The shear contribution to failure of the unidirectional laminates from Equations (25) is

$$\bar{X}_s = W_6 / \bar{W}_6 \qquad (26)$$

Using the "NOLAST" Program (Reference 17), values of $\bar{X}_s$ were computed for different off-axis angles for AS/3501-5 graphite-epoxy. A plot of the analytical data is shown in Figure 3. The nonlinear material peak value of $\bar{X}_s$ = 88.0% occurs when the off-axis angle is 13.0° which is greater than the α' = 11° 23' computed using linear analysis (Table I) for the same AS/3501-5 graphite- epoxy material system. The data based upon the nonlinear analysis for the boron-epoxy material system indicate that the off-axis angle for the boron-epoxy material systems is 15.0° (Reference 11 and 12) with the maximum $\bar{X}_s$ = 94.14%. The corresponding off-axis angle using linear analysis is 11° 40' (Table I).

Thus, for AS/3501-5 graphite epoxy and the boron-epoxy material systems, the more realistic nonlinear material behavior analysis yields higher off-axis angles than the simpler, but less realistic linear material behavior analysis. Moreover, the value of the angle that maximizes shear contribution to failure is not the same for different material systems in either linear or nonlinear analyses.

3.0 Specimen Optimization for Uniform Stress

In the discussion of paragraph 2 of this Section, it was tacitly assumed that the specimens examined were subjected to a uniform σ_x applied at the specimen ends, ie., the means of introduction of loads in the specimen did not generate any stresses other than σ_x uniformly across the width as shown in Figure 1a. However, for realistic load introduction, the specimens usually are tabbed and tabs are gripped in the gripping device of the test machine. This constrains the specimen ends from natural rotation and causes the specimen to deform to the shape shown exaggerated in Figure 1b, thereby creating a non-uniform stress state in the test section. Analyses of off-axis specimens are conducted on the basis that uniform stress states exist. In order to verify the theoretical results, it is imperative to design the experiments to reproduce the analytical conditions as closely as possible. For this reason the uniformity of state becomes important. Various techniques devised to alleviate the undesired effects end constraints are described below.

3.1 Improved Grips

The use of standard grips prevents rotation of the ends of the off-axis specimen. Such constraint causes non-uniform stresses in the test section. If the ends are permitted to rotate, considerable improvement in the uniformity of the stress state can be achieved (Reference 6 and 7). A grip design with a provision for rotation of

specimen ends is essential to reduce the effects of the end constraints.

3.2 Aspect Ratio (Length/Width Ratio)

The aspect ratio (length/width) is an important factor in designing the specimen if determination of the longitudinal shear modulus of the specimens' fibrous composite material is the primary objective. The effect of the non-rotating grips on the longitudinal shear modulus of specimen material is minimal if the aspect ratio of the specimen exceeds 12.0 (Reference 6). Compliance with the aspect ratio requirements assures the uniformity of the stress state only in the central region of the specimen. Everywhere else the stress is far from uniform. For this reason the aspect ratio is not important when it is desired to determine the strength of the off-axis specimen.

3.3 Improved Tabs

Tabs, if required to introduce loads into the specimen through shear irrespective of the grip rotation, are fabricated from crossplied glass-epoxy. The suitability of the tab design to transfer loads from the grips of the machine to the specimen with minimal contraints will depend upon the following factors (Figure 4):

(i) Orientation β of the fibers of the tabs with respect to the specimen axis.

(ii) Inclination $\tan \lambda = \delta/B$ ($\tan \lambda = \delta$ when $B = 1$) of the tab ends where B is width of the specimen.

A parametric study was conducted to investigate the effects of β and δ on the state of stress in the specimens. It consisted of finite element analyses with hinged boundary conditions and linear material behavior. The finite element models are shown in Figures 5 and 6. For each off-axis angle α, combinations of β and δ were determined that minimized the variation σ_x in the test section between tabs. The detailed results of the study are tabulated in Table II for $\alpha = 4^{\circ}, 6^{\circ}, 8^{\circ}$ and 10° and in Table III for $80^{\circ} \geq \alpha \geq 12^{\circ}$ while the maximum stress variations for α between 4° and 80° are summarized in Table IV. Examination of the tables and Figure 7, indicates that if $\beta = \delta = 0$, very large stress differences exist and their magnitude depends upon the off-axis angle α. The maximum difference occurs for 45°. If recommendations of References 9 and 10 are followed, the fiber orientation in both the composite and the tabs are matched (i.e., $\beta = \alpha$, and $\delta = 0$) some relief in the severity of the stress differences is obtained. However by optimizing β with $\delta = 0$, the stress differences are further reduced except for $\alpha = 35^{\circ}$ through 65°, for which further improvements over $\beta = \alpha$ and $\delta = 0$ case are almost negligible. The maximum reduction in the stress differences is achieved by varying β and δ. As a result the stress field becomes practically uniform.

To verify the analytical results presented here, tests for two groups α, β, δ combinations were conducted:

(a) $\beta = \alpha$, and $\delta = 0$; (b) optimized β and δ. Results of these experiments are discussed in Section III.

SECTION III

EXPERIMENTAL AND ANALYTICAL DATA

The investigation reported herein consisted of two parts experimental and analytical (nonlinear material behavior). These two parts are described in the following paragraphs.

1. Experimental Part

1.1 Material System

The material system used in the study was AS/3501-5, graphite/epoxy, supplied by Hercules Incorporated in the form of a 12.0 inch wide prepreg tape.

1.2 Cure Cycle

The prepreg material was used to fabricate three 16-ply panels: two 3.5 feet by 5.0 feet and one plate 9.0 inches by 7.0 inches. Fibers in the large panels were aligned parallel the short direction, while a $(\pm 45_4)_s$ layup was used in the small panel. All three panels were cured at the same time in accordance with the following cure cycle:

a. Apply full vacuum pressure (8-10 psi).

b. Heat to 225°F at 5°F to 8°F per minute.

c. Upon reaching 225°F, apply sufficient pressure to reach a total of 85 psi and continue heating to 350°F.

d. Hold for 60 minutes at 350°F and 85 psi pressure (autoclave plus full vacuum).

e. Cool to 150°F or less under pressure.

1.3 Specimens (basic properties and off-axis)

The large panels were used to cut various subpanels for the intended off-axis angles as shown in Figures 8 and 9. All the subpanels were subjected to ultrasonic through-transmission C-scan and X-ray inspection for flaws before being cut into test specimens. The inspection did not reveal significant defects. In addition, the resin content and densities of the panels were determined using ASTM Standards D792 and D2734 and they are tabulated in Table V. The specimens fabricated from the subpanels and the $(\pm 45_4)_s$ panel were of two types: those for determining basic panel properties and those for validating the analytical results of off-axis specimen studies.

1.3.1 Specimens for Basic Properties

The specimens for basic properties determination were cut from (0_{16}), (90_{16}) and $(\pm 45_4)_s$ panels and had the dimensions shown in Figures 10 and 11 except that (0_{16}) tensile specimens were 0.75 inches wide. This reduction in width was mandated by the load capacity of the test machine used in the testing part of the program. In addition, specimens of (0/90) glass epoxy tabbing material with dimensions shown in Figure 10 were fabricated. In the three types of these specimens fibers were aligned at 0, 90 and ±45 respectively to the loading axes.

1.3.2 Off-axis Specimens

Off-axis specimens were cut from the sub-panels marked 4°, 6°, 8°, 10°, 12°, 14°, 16°, 20°, 30°, 40°, 45°, 50°, 60°, 70°, and 80° . Dimensions of these specimens are shown in Figure 10. For each of the off-axis angles, specimens with either square or inclined tabs were machined. They were designated as XXOAA or XXOAB. Where XX represented the off-axis angle, OAA - specimens with square tabs and OAB - inclined tabs.

1.4 Instrumentation

All specimens were instrumented with two 3-element strain gage rosettes, one on each face at the center of the test section of the specimen.

1.5 Testing

An Instron Test Machine, Floor Model TT-1115, was used to test all specimens at ambient environments (RTA). The crosshead speed for compression specimens was 0.05 inches per minute while it was 0.2 inches per minute for tensile specimens.

Tension tests for determination of basic properties of laminates (graphite/epoxy and glass/epoxy) with 0°, 90° and $\pm 45^{\circ}$ layups were conducted using standard grips. For basic compression properties tests of 0° and 90° laminates, a test fixture (Figure 12) designed by Northrop Corporation and modified locally (R.L. Rolfes, AFWAL/FIBCC) was used.

All the off-axis specimens were loaded in tension. Some of the square tab specimens were tested in standard fixed grips. For the rest of the square tab and all inclined tab specimen, the test fixture had hinged grips as shown in Figure 13. The designation for the former group was XX0AA while for the latter - XX0AAH and XX0ABH.

1.6 Data

For each of the basic mechanical properties, two sets of stress-strain data from the two strain gages located on opposite faces of the specimen were obtained. To determine the average data, piecewise cubic spline interpolation functions were employed to represent each set of data. The stresses at prescribed strain values were determined. The results were then averaged to determine stress-strain curves for both the graphite/epoxy and glass/epoxy material systems. The averaged data are tabulated in Table VI and VII, and engineering elastic constants are presented in Table VIII.

Ultimate stresses and strains for all off-axis specimens (test series XXOAA, XXOAAH and XXOABH) are presented in Table IX. Experimental and analytical stress-strain plots for off-axis specimens obtained in this study are shown in Figures 14 thru 100. In each of the figures, experimental data for the test specimem are plotted individually using different symbols. Test sequence numbers are given for each of the symbols in the plots.

2.0 Analytical Part

The basic property data for graphite-epoxy and glass-epoxy material systems and the nonlinear analysis were used to determine the cumulative stress strain response of the off-axis specimens modelled as shown in Figures 5 and 6. In determining the cumulative responses, appropriate boundary conditions were incorporated in the finite element analyses. The analytical stress-strain curves corresponding to the locations of strain gages were obtained. These curves are plotted in Figures 14 through 100 using solid and dashed lines. The data shown in these figures are compared and evaluated in Section IV.

SECTION IV

EVALUATION OF DATA AND CONCLUSIONS

On the basis of data generated in this study, some observations can be made. They are arranged in the following order:

a. Use of off-axis specimen as a shear specimen.

b. Design of off-axis specimen to improve uniformity of stress σ_x.

c. Analytical-Experimental correlation

1. Use of Off-axis Specimen as a Shear Specimen

For linear materials, the optimum angle α' that maximizes shear contribution to failure was found to be given by Equation 14. In addition to the maximum shear contribution hypothesis, the optimum angle α'' corresponding to the minimum transverse strain condition was determined. This yielded Equation 18. The resulting data in Table I indicate that maximum shear and minimum transverse strain cannot be obtained simultaneously, and that the optimum off-axis angle α' is a material-dependent quantity that is different for different material systems.

In the case of nonlinear materials, an equation similar to Equation 14 could not be derived. However, using the nonlinear material properties (Table VI) a nonlinear point stress analysis computer program "NOLAST" (References 17) was employed to compute shear contributions to failure $\bar{X}s$ (Equation 26) for off-axis angles 0^{O} to 90^{C} in AS/3501-5

material system. The results of this analyis are shown in Figure 3. $\bar{X}_s$ reaches the peak value of 88.0%, at the off-axis angle of 13^o. The values of $\bar{X}_s$ drop sharply for off-axis angles less than 11^o and for those exceeding 14^o. In the range of 11^o thru 14^o, the values of $\bar{X}_s$ are 87.5%, 87.78%, 88.0% and 87.6% (averaging to 87.72%) for 11^o, 12^o, 13^o and 14^o respectively.

These results indicate that the optimum off-axis angle is not a fixed entity. It changes with material and material behavior. In addition, the off-axis shear response does not cover the entire range of shear behavior of unidirectional laminates. For the AS/3501-5 material system used in this study, the off-axis shear response, $\bar{X}_s$, was 88.0% of the area under the pure shear stress strain plot obtained by testing $(\pm 45)_{4s}$ coupons while the normal stress contributions $\bar{X}_n$ (Equation 25) accounted for the remaining 12% towards failure. On the basis of findings in this study, it is difficult to justify a recommendation of a fixed value of fiber orientation (α) in an off-axis specimen for determining the shear response of unidirectional laminates for different material systems.

2. Design of Off-Axis Specimen to Improve Uniformity of Stress σ_x

Tabbing the specimens and the use of standard grips constrains end rotations of the specimens. These constraints cause in-plane bending stresses (Reference 5). Resulting deformations are illustrated in Figure 1(b). To

reduce the effects of end constraints, various techniques including the one evolved in this study are discussed below.

2.1 Rotation Grips

Finite element analyses based upon linear material properties of off-axis specimens were conducted in Reference 6 to assess the effects of different specimen end boundary conditions on uniformity of stress distribution. Those analyses indicated that considerable improvement in stress distribution uniformity in the test section of the specimen could be achieved by using a hinged fixture to transfer loads from the loading machine to the specimen even with non-optimum tab fiber direction and square tabs. This assessment was later substantiated experimentally (Reference 7). On the basis of those results and the analyses conducted in this study, the use of hinged grips to load the specimen appears imperative.

2.2 Tab Design with Hinged Grips and Linear Material

A parametric study of the tab design was conducted for AS/3501-5 off-axis specimens with glass epoxy tabs. Finite element models of Figures 5 and 6, material properties tabulated in Tables VI thru VIII and hinged boundary conditions were used. The parameters were α and β, the fiber orientation in the specimens, tab material, and $\delta = \tan \lambda$ where λ is the inclination of tabs on the specimens as shown in Figure 4. The variation of α was limited to the values specified in paragraph 1.3.2 of Section III. The procedure used in the parametric study

consisted of using a linear elastic finite element analysis and varying β and δ to minimize maximum axial stress σ_x difference between any two elements inside the test section.

This procedure was used for the following combinations of α, β and δ under a constant thickness of one tabbing material system and a constant applied load.

2.2.1 $\alpha \neq 0$, $\beta = \delta = 0$

This condition corresponds to the use of square ended tabs with fibers of tabs aligned along the longitudinal axis of the specimen. The stress σ_x difference percentages obtained for this combination are tabulated in Table IV and stress differences are plotted in Figure 7.

2.2.2 $\alpha \neq 0$, $\beta = \alpha$, $\delta = 0$

To improve distribution of stresses in off-axis specimens, Pipes (References 9 and 10) suggested the use of square ended tabs with fibers of tabs aligned along the specimen fiber direction. This design has been used ever since. The stress difference percentages for this condition are also given in Table IV and stress differences are plotted in Figure 7.

2.2.3 $\alpha \neq 0$, optimized β, $\delta = 0$

This condition corresponds to the use of specimens with square ended tabs in which tab fiber directions are determined to produce minimum variations of the axial stress σ_x. For this condition and for each off-axis angle, α , (listed in paragraphs 1.3.2 of Section III), the tab angle β was varied until the maximum stress

differences attained the minimum values. The resulting stress difference percentages corresponding to optimum values of β for square tabs are given in Table IV, and stress differences are plotted in Figure 7 .

2.2.4 $\alpha \neq 0$, $\beta \neq 0$, $\beta \neq \alpha$, $\delta \neq 0$

This condition corresponds to the use of optimized orientation of tab fibers and tab ends. In this case, for each of the values of α ,both β and δ were varied to obtain the minimum stress σ_x differences. The optimum α , β , δ and the corresponding stress difference percentages are tabulated in Table IV. The axial stresses in various elements are given in Tables II and III. This condition produced practically uniform axial stress states in all of the off-axis specimens.

Plots of stress differences for the square tab specimens for tab fiber orientations $\beta = 0$, $\beta = \alpha$ and optimized β for different off axis angle α are shown in Figure 7. It is obvious from the plots that by making the tab fiber orientation the same as the off-axis angle ($\alpha = \beta$) a dramatic improvement over the $\beta = 0$ case in stress distribution was achieved. However, the optimization of the tab fiber angle β although improving results for condition 2.2.2, ($\beta = \alpha$) did not improve the results to the same extent as did condition 2.2.2 ($\beta = \alpha$) over condition 2.2.1 ($\beta = 0$). Results for the optimized β and δ condition 2.2.4 are not shown in Figure 7 since the ordinate values were too small for the resulting plot to be distinguished from the

abscissa at most of the points, with the maximum value of stress difference being 4.7 psi.

2.3 Effect of Material Nonlinearity on Tab Design

It was observed in paragraph 2.2 of this Section that the stress field was practically uniform in an off-axis specimen with tabs designed for optimum combinations of tab fiber orientation (β) and tab inclination (δ). In this condition linear material behavior was assumed for both the specimens and the tabs. However, off-axis specimens loaded to failure are known to exhibit nonlinear stress-strain response. This raises a question about the validity of the tab design based upon linear material behavior. To assess the effect of material nonlinearity on the tab design, two studies were conducted. These studies consisted of nonlinear finite element analyses (finite element models as per Figure 5 and 6) of hinged ended off-axis specimens with tabs designed as per conditions 2.2.2 ($\beta = \alpha$) and 2.2.4 (optimized β and δ). From each of the analyses, stress differences $\Delta\sigma_x$ and load levels were determined. Stress differences, stress difference percentages, and axial stress levels corresponding to the first and the next to the last increment are tabulated in Table X. From the data of Table X, it is concluded that the effect of material nonlinearity on the tab design results in degrading the uniformity of stress σ_x, but the stress distribution corresponding to design condition 2.2.4 (optimized β and δ) is far more uniform than that for condition 2.2.2 ($\beta = \alpha$).

3. Analytical - Experimental Correlation

The experimental part of the effort was intended to evaluate tab designs for conditions 2.2.2 and 2.2.4 with rotating grips (hinged grips). Unfortunately half of the specimens for condition 2.2.2 were tested with standard Instron grips instead of rotating grips. The remaining specimens were split into two groups with square end and inclined tabs as originally intended and tested with rotating grips. The test data (Figures 14 thru 100) show a good deal of scatter. To find the reason for the data scatter, actual off-axis angles were measured for the available failed specimens. These angles are tabulated in Table XI. As can be seen from the table, the actual angles deviated considerably from the planned angles. Accounting for these differences decreases the scatter somewhat. The remaining scatter is probably due to material variability, but the possibility of technique related variability cannot be dismissed.

Due to the scatter in the current data, no definite conclusions about the improvements resulting from orienting the tab ends can be drawn. But since the analytical results very strongly favor tab end orientation, it is only logical that the analytical indications should be verified with a new set of experiments. Considering the data shown in Table X off-axis angles α for these experiments need not assume values greater than thirty degrees, because square end tabs cause the greatest non-uniformity of stress for $0^\circ < \alpha \leq 30^\circ$.

REFERENCES

1. S.W. Tsai, "Strength Characteristics of Composite Materials," NASA-CR 224, April 1965.

2. V.D. Azzi and S.W. Tsai, "Anistropic Strength of Composites," presented at the Spring Meeting, Society for Stress Analysis, May 1965.

3. S.W. Tsai, " Strength Theories of Filamentary Structures" Proceedings of a Conference on Fundamental Aspects of Fiber Reinforced Plastic Composites, Wiley Interscience, New York, 1968.

4. K. Lauraitis, "Tensile Strength of Off-Axis Unidirectional Composites," T. & A.M. Report No 344, Department of Theoretical and Applied Mechanics, University of Illinois, Urbana, Illinois, August 1971.

5. N.J. Pagano and J.C. Halpin, "Influence of End Constraint in the Testing of Anisotropic Bodies," Journal of Composite Materials, Vol 2, No 1, January 1968, pp 18-31.6.

6. R. R. Rizzo, "More on the Influence of End Constraints on Off-Axis Tensile Tests," Journal of Composite Materials, Vol 3, April 1969, 202-219.

7. E. M. Wu and R.L. Thomas, "Off-Axis Test of a Composite," Journal of Composite Materials, Vol 2, No 4, October 1969, pp 523-526.

8. G.L. Richards, T.P. Airhart, and J.E. Ashton, "Off-Axis Tensile Coupon Testing," Journal of Composite Materials, Vol 3, July 1969, pp 586-589.

9. B .W. Cole and R.B. Pipes,"Filamentry Composite Laminates Subjected to Biaxial Stress Fields," AFFDL-TR-73-115, AD785362, 1973, Air Force Flight Dynamics Laboratory, Wright-Patterson Air Force Base, Ohio.

10. R.B. Pipes and B.W. Cole, "On the Off-Axis Strength Test for Anisotropic Materials," Journal of Composite Materials, Vol 7, April 1973, pp 246-256.

11. R.S. Sandhu,"Ultimate Strength Analysis of Symmetric Laminates," AFFDL-TR-73-137, AD 779927, 1974, Air Force Flight Dynamics Laboratory, Wright-Patterson Air Force Base, Ohio.

12. R.S. Sandhu, "Nonlinear Behavior Of Unidirectional and Angle Ply Laminates," Journal of Aircraft, Vol 13, No 2, February 1976, pp 104-111.

13. I.M. Daniel and T. Liber, "Lamination Residual Stresses in Fiber Composites," NASA CR-134826, 1975.

14. C.C. Chamis and J.H. Sinclair, "10^{o} Off-Axis Tensile Test for Interlaminar Shear Chacterization of Fiber Composites," NASA TN D-8215, April 1976.

15. I.M. Daniel, "Biaxial Testing of Graphite/Epoxy Composites Containing Stress Concentrations," AFML-TR-76-244, Part 1, December 1976, Air Force Materials Laboratory, Wright-Patterson Air Force Base, Ohio.

16. R.S. Sandhu, "A Survey of Failure Theories of Isotropic and Anisotropic Materials," AFFDL-TR-72-71, AD 756889, January 1972, Air Force Flight Dynamics Laboratory, Wright-Patterson Air Force Base, Ohio.

17. R.S. Sandhu, "Computer Program (NOLAST) for Nonlinear Analysis of Composite Laminates," AFFDL-TR-76-1, ADB 010592, February 1976, Air Force Flight Dynamics Laboratory, Wright-Patterson Air Force Base, Ohio.

TABLE I

OFF-AXIS ANGLE FOR MAXIMIZING SHEAR RESPONSE AND MINIMIZING TRANSVERSE RESPONSE-LINEAR ANALYSIS

MATERIAL	E_{11} $x10^6$psi	E_{22} $x10^6$psi	υ_{12}	F_{11} ksi	F_{22} ksi	α'	α''
**MOD-I/EPOXY	34.9	1.12	0.218	81.7	4.0	12° 28.5'	4° 47'
BORON/EPOXY	30.8	2.59	0.24	197.8	8.4	11° 40'	8° 5'
GLASS/EPOXY	6.45	1.84	0.245	248.	10.0	11° 21'	14° 49'
**T-300/5208	21.4	1.35	0.25	204.0	7.0	10° 30'	7° 10'
*AS/3501-5	17.87	1.52	0.25	225.2	9.12	11° 23'	8° 18'

*The material system used in this study

**Reference 14

TABLE II

LONGITUDINAL STRESSES σ_x IN OFF-AXIS SPECIMEN WITH ORIENTATION ANGLE $\alpha \leq 10^{\circ}$ *

ALPHA=	4.0000	6.0000	8.0000	10.0000
BETA =	62.0000	56.0000	5.5000	6.0000
DELTA=	0.0000	0.0000	.1500	.1520
ELEMENT NO.	σ_x STRESS PSI			
25	7392.8	7392.0	7392.2	7391.6
26	7389.5	7390.6	7390.7	7390.9
27	7390.6	7390.7	7391.0	7390.2
28	7392.3	7392.0	7391.4	7392.4
29	7390.2	7391.4	7391.4	7392.0
30	7392.1	7391.1	7391.2	7390.6
31	7393.0	7391.4	7391.5	7390.4
32	7389.8	7391.3	7391.1	7392.2
33	7390.0	7391.2	7391.2	7391.9
34	7392.6	7391.4	7391.4	7390.6
35	7392.7	7391.5	7391.5	7390.9
36	7389.9	7391.1	7391.1	7391.9
37	7390.9	7391.2	7391.2	7391.4
38	7391.9	7391.4	7391.4	7391.0
39	7391.7	7391.4	7391.4	7391.3
40	7390.8	7391.2	7391.2	7391.5
41	7391.3	7391.3	7391.3	7391.3
42	7391.3	7391.3	7391.3	7391.3
43	7391.3	7391.3	7391.3	7391.3
44	7391.3	7391.3	7391.3	7391.3
45	7391.3	7391.3	7391.3	7391.3
46	7391.3	7391.3	7391.3	7391.3
47	7391.3	7391.3	7391.3	7391.3
48	7391.3	7391.3	7391.3	7391.3

*Linear Material and Finite Element Analyses

TABLE III

LONGITUDINAL STRESSES σ_x IN OFF-AXIS SPECIMEN WITH ORIENTATION ANGLE $\alpha \geq 12^{\circ}$ *

ALPHA=	12.0000	14.0000	16.0000	20.0000	30.0000	40.0000	45.0000	50.0000	60.0000	70.0000	80.0000
BETA =	6.5000	7.5000	8.0000	9.0000	12.0000	16.0000	17.5000	19.0000	25.0000	30.0000	36.0000
DELTA=	.1600	.1600	.1720	.1940	.2552	.3030	.3235	.3379	.3176	.2510	.1120
ELEMENT NO.					σ_x STRESS PSI						
25	7390.9	7389.9	7389.2	7388.7	7391.2	7390.0	7391.2	7392.1	7390.4	7390.2	7391.3
26	7391.1	7392.1	7392.3	7392.4	7391.3	7391.9	7391.3	7390.0	7392.5	7393.1	7391.3
27	7389.1	7390.7	7390.0	7390.2	7391.3	7391.5	7391.3	7391.0	7391.6	7391.8	7391.3
28	7393.7	7392.2	7393.2	7393.3	7391.4	7391.3	7391.3	7391.8	7390.7	7390.2	7391.4
29	7392.6	7391.6	7391.9	7391.6	7391.3	7391.0	7391.3	7391.5	7390.7	7390.8	7391.3
30	7389.8	7390.9	7390.4	7390.4	7391.3	7391.4	7391.3	7391.0	7391.7	7391.9	7391.3
31	7389.2	7390.2	7389.4	7389.6	7391.3	7391.1	7391.3	7391.4	7391.2	7391.4	7391.3
32	7393.5	7392.5	7393.4	7393.4	7391.3	7391.6	7391.3	7391.4	7391.2	7391.1	7391.3
33	7392.7	7392.0	7392.4	7392.3	7391.3	7391.4	7391.3	7391.3	7391.3	7391.2	7391.3
34	7389.7	7390.5	7389.9	7390.0	7391.3	7391.2	7391.3	7391.4	7391.3	7391.3	7391.3
35	7390.2	7390.6	7390.3	7390.5	7391.3	7391.2	7391.3	7391.4	7391.3	7391.4	7391.3
36	7392.7	7392.1	7392.7	7392.6	7391.3	7391.5	7391.3	7391.2	7391.4	7391.3	7391.3
37	7391.6	7391.4	7391.4	7391.3	7391.3	7391.3	7391.3	7391.3	7391.3	7391.3	7391.3
38	7390.7	7391.0	7390.8	7390.9	7391.3	7391.3	7391.3	7391.3	7391.3	7391.3	7391.3
39	7391.3	7391.3	7391.4	7391.4	7391.3	7391.3	7391.3	7391.3	7391.3	7391.3	7391.3
40	7391.7	7391.5	7391.7	7391.6	7391.3	7391.3	7391.3	7391.3	7391.3	7391.3	7391.3
41	7391.2	7391.3	7391.2	7391.2	7391.3	7391.3	7391.3	7391.3	7391.3	7391.3	7391.3
42	7391.4	7391.4	7391.4	7391.4	7391.3	7391.3	7391.3	7391.3	7391.3	7391.3	7391.3
43	7391.4	7391.4	7391.4	7391.4	7391.3	7391.3	7391.3	7391.3	7391.3	7391.3	7391.3
44	7391.2	7391.3	7391.2	7391.2	7391.3	7391.3	7391.3	7391.3	7391.3	7391.3	7391.3

*Linear Material and Finite Element Analyses

TABLE IV

MAXIMUM STRESS DIFFERENCES (Δ) FOR LINEAR MATERIAL

SPECIMEN FIBER ORIENTATION α	PERCENTAGE OF MAXIMUM STRESS DIFFERENCE (Δ)						
	SQUARE TABS δ=0				INCLINED TABS δ≠0		
	β=0	β=α	β≠α		β≠α		
	Δ %	Δ %	β	Δ %	β	δ	Δ %
4	0.5777	0.5006	62.0°	0.0474	62.0°	0.	0.0474
6	0.7346	0.5547	56.0°	0.0189	56.0°	0.	0.0189
8	0.9065	0.6224	50.0°	0.0866	5.5°	0.1500	0.0203
10	1.1419	0.6954	45.5°	0.2043	6.0°	0.1520	0.0271
12	1.4071	0.8023	41.0°	0.3301	6.5°	0.1600	0.0622
14	1.7196	0.9444	36.5°	0.4979	7.5°	0.1600	0.0352
16	2.0538	1.0959	34.0°	0.6765	8.0°	0.1720	0.0568
20	2.7911	1.4206	33.5°	1.0783	9.0°	0.1940	0.0636
30	4.7421	1.9604	36.5°	1.7669	12.0°	0.2552	0.0027
40	6.6281	2.5395	32.0°	2.5016	16.0°	0.3030	0.0257
45	6.7877	2.5422	35.0°	2.5422	17.5°	0.3235	0.0014
50	5.9570	2.7505	48.5°	2.7451	19.0°	0.3379	0.0230
60	3.9046	1.9780	55.0°	1.9009	25.0°	0.3176	0.0284
70	1.8143	1.0350	58.5°	0.8402	30.0°	0.2510	0.0392
80	0.6156	0.3572	43.0°	0.0988	36.0°	0.1120	.0014

TABLE V

RESIN CONTENT AND DENSITY *

Panel	Subpanel	Density	Resin	Percent Volume		
			w/o	Resin	Fiber	Voids
A (Figure 8)	4	1.590	32.9	41.1	59.9	-1.0
	6	1.593	31.6	39.5	61.2	-0.7
	8	1.589	32.8	40.9	60.0	-0.9
	10	1.594	31.8	39.8	61.1	-0.9
	12	1.585	33.0	41.1	59.6	-0.7
B (Figure 9)	14	1.600	30.7	38.6	62.3	-0.9
	16	1.598	31.4	39.3	61.6	-0.9
	20	1.599	30.7	38.6	62.3	-0.9
	30	1.598	31.2	39.1	61.8	-0.9
	40	1.598	30.7	38.5	62.3	-0.8
	45	1.601	30.3	38.1	62.7	-0.8
	50	1.594	31.4	39.3	61.4	-0.7
	60	1.601	30.6	38.4	62.4	-0.8
	70	1.599	30.6	38.4	62.4	-0.8
A (Figure 8)	80	1.591	31.8	39.7	60.9	-0.7

* Assumed Resin Density = 1.2733 gm/cc and Fiber Density = 1.7798 gm/cc

TABLE VI

UNIDIRECTIONAL MATERIAL PROPERTIES (STRESS-STRAIN DATA)
AS/3501-5 GRAPHITE EPOXY

0° TENSION 2 SAMPLES/SECOND			0° COMPRESSION 2 SAMPLES/SECOND			90° TENSION 4 SAMPLES/SECOND		90° COMPRESSION 2 SAMPLES/SECOND		SHEAR 2 SAMPLES/SECOND	
STRAIN IN/IN	STRESS KSI	POISSONS' RATIO	STRAIN IN/IN	STRESS KSI	POISSONS' RATIO	STRAIN IN/IN	STRESS KSI	STRAIN IN/IN	STRESS KSI	STRAIN IN/IN	STRESS KSI
0.	0.	.200	0.	0.	.300	0.	0.	0.	0.	0.	0.
.0005	8.93	.281	.0005	10.02	.302	.0005	0.76	.001	1.65	.004	3.13
.001	18.49	.306	.001	19.87	.308	.001	1.51	.002	3.24	.008	5.70
.0015	28.11	.317	.0015	29.39	.313	.0015	2.26	.003	4.80	.012	7.67
.002	37.91	.322	.002	38.62	.317	.002	3.01	.004	6.33	.016	9.13
.0025	47.80	.324	.0025	47.73	.321	.0025	3.74	.005	7.87	.02	10.25
.003	57.75	.325	.003	56.80	.325	.003	4.48	.006	9.41	.024	11.15
.0035	67.87	.326	.0035	65.77	.329	.0035	5.20	.007	10.92	.028	11.86
.004	78.00	.326	.004	74.66	.335	.004	5.90	.008	12.41	.032	12.45
.0045	88.23	.326	.0045	83.56	.338	.0045	6.59	.009	13.88	.036	12.96
.005	98.60	.326	.005	92.62	.342	.005	7.28	.01	15.32	.04	13.40
.0055	108.95	.326	.0055	101.85	.346	.0055	7.96	.011	16.74	.042	13.58
.006	119.40	.325	.0059	110.19	.349	* .0064	9.12	.012	18.13	.044	13.73
.0065	129.90	.324	* .00813	141.73	.368			.013	19.48	.046	13.90
.007	140.40	.323						.014	20.82	.048	14.07
.0075	150.89	.322						.015	22.17	.05	14.23
.008	161.51	.320						.016	23.49	.052	14.36
.0085	172.05	.319						.017	24.70	* .09247	15.27
.009	182.69	.318						.018	25.88		
.0095	193.18	.316						.0185	26.49		
* .011	225.20	.312						* .03125	37.15		

*Ultimate Stress-Strain Values

TABLE VII

$(0^{\circ}/90^{\circ})$ MATERIAL PROPERTIES (STRESS-STRAIN DATA)
Glass/Epoxy

$0^{\circ}/90^{\circ}$ TENSION			SHEAR	
STRAIN IN/IN	STRESS KSI	POISSONS' RATIO	STRAIN IN/IN	STRESS KSI
0.	0.	0.130	0.	0.
0.001	4.14	0.130	.005	2.86
.002	8.12	0.129	.01	4.47
.003	11.93	0.128	.015	5.44
.004	15.50	0.122	.02	5.97
.005	18.74	0.113	.025	6.41
.006	21.99	0.105	.03	6.69
.007	25.05	0.098	.035	6.90
.008	28.18	0.093	.04	7.05
.009	31.30	0.088	.045	7.18
.01	34.29	0.084	.05	7.29
.011	37.33	0.081	.055	7.40
.012	40.38	0.078	.06	7.46
.013	43.41	0.075	.065	7.59
.014	46.42	0.071	.07	7.69
.015	49.39	0.068	.075	7.75
.016	52.32	0.064	.08	7.90
0.17	55.18	0.059	.085	8.04
0.18	58.00	0.054	.09	8.19
.019	60.86	0.050	.15174	9.43
.020	63.72	0.046		
.021	66.51	0.041		
.022	69.30	0.038		
.023	72.09	0.034		
.02757	83.22	0.026		

TABLE VIII

ENGINEERING ELASTIC CONSTANTS
AS/3501-5 GRAPHITE EPOXY

SYMBOL	DESCRIPTION	ELASTIC CONSTANT	COEFFICIENT OF VARIATION
E_{11t}	Tensile Longitudinal Tangent Modulus of Elasticity	17.87×10^6 psi	8.4
E_{11c}	Compressive Longitudinal Tangent Modulus of Elasticity	20.05×10^6 psi	27.9
E_{22t}	Tensile Transverse Tangent Modulus of Elasticity	1.52×10^6 psi	12.0
E_{22c}	Compressive Transverse Tangent Modulus of Elasticity	1.65×10^6 psi	34.7
G_{12}	Shear Tangent Modulus of Elasticity	0.78×10^6 psi	2.4
μ_{12t}	Major Tensile Poisson's Ratio	0.2	
μ_{12c}	Major Compressive Poisson's Ratio	0.3	
S_{11t}	Tensile Longitudinal Strength	225.20 ksi	8.8
S_{11c}	Compressive Longitudinal Strength	141.73 ksi	3.7
S_{22t}	Tensile Transverse Strength	9.12 ksi	6.5
S_{22c}	Compressive Transverse Strength	37.15 ksi	5.0

TABLE VIII (CON'T)

ENGINEERING ELASTIC CONSTANTS
(Graphite/Epoxy)

SYMBOL	DESCRIPTION	ELASTIC CONSTANT	COEFFICIENT OF VARIATION
S_{12}	In-plane Shear Strength	15.27 ksi	2.3
ε^{u}_{11t}	Tensile Ultimate Longitudinal Strain	.010995	7.5
ε^{u}_{11c}	Compressive Ultimate Longitudinal Strain	.008131	19.3
ε^{u}_{22t}	Tensile Ultimate Transverse Strain	.006399	7.2
ε^{u}_{22c}	Compressive Ultimate Transverse Strain	.031248	17.2
γ^{u}_{12}	Ultimate Shear Strain	.09247	33.8

TABLE IX

TEST NUMBERS:AREAS:ULTIMATE STRESSES AND STRAINS

	TEST	154	153	152	151	150	MEAN	COV	239	257	256	MEAN	COV	329	330	331	332	333	MEAN	COV
	AREA	.08330	.08310	.08140	.08220	.08210	.08242	.9	.08220	.08090	.08200	.08170	.9	.08220	.08350	.08400	.08390	.08350	.08342	.9
4	SIGX	146.51	128.21	112.12	64.16	94.68	109.18	28.9	115.77	140.10	131.16	129.01	9.5	145.45	142.31	136.34	132.21	115.73	134.41	8.7
	EPSX	.00949	.00797	.00674	.00392	.00605	.00683	30.6	.00831	.00844	.00810	.00828	2.0	.00932	.00857	.00875	.00830	.00680	.00835	11.3
	EPSY	.00327	.00263	.00206	.00176	.00187	.00222	34.5	.00267	.00268	.00220	.00251	10.9	.00331	.00271	.00307	.00297	.00219	.00285	14.9
	EPSXY	.02351	.01642	.01681	.00678	.01251	.01561	40.4	.02064	.01409	.01028	.01500	34.9	.02387	.02246	.02123	.02066	.01378	.02040	19.1
	SIG2	.71	.62	.55	.31	.46	.53	28.9	.56	.68	.64	.63	9.5	.71	.69	.66	.64	.56	.65	8.7
	TAU12	10.20	8.92	7.80	4.46	6.60	7.60	28.9	8.06	9.75	9.13	8.98	9.5	10.12	9.90	9.49	9.20	8.05	9.35	8.7
	EPS12	.02506	.01977	.01787	.00744	.01349	.01671	39.7	.02197	.01550	.01161	.01636	32.0	.02540	.02381	.02267	.02202	.01490	.02176	18.6

	TEST	155	156	157	158	159	MEAN	COV	245	259	255	MEAN	COV	324	325	326	327	328	MEAN	COV
	AREA	.09300	.09200	.09400	.09240	.09210	.09270	.9	.09310	.09100	.09210	.09207	1.1	.09130	.09020	.09130	.09050	.09070	.09080	.5
6	SIGX	107.98	103.91	104.75	102.25	98.21	103.40	3.4	104.03	124.35	119.74	116.04	9.2	113.76	104.72	105.35	107.01	107.17	107.60	3.3
	EPSX	.00867	.00809	.00872	.00916	.00731	.00839	8.5	.00781	.00896	.00874	.00850	7.2	.00939	.00804	.00789	.00831	.00861	.00845	7.0
	EPSY	.00318	.00311	.00313	.00361	.00222	.00305	16.6	.00211	.00265	.00305	.00260	18.2	.00336	.00310	.00316	.00342	.00326	.00326	4.1
	EPSXY	.02623	.02236	.02437	.02290	.02326	.02382	6.4	.02833	.02642	.02658	.02777	3.7	.03330	.02434	.02310	.02780	.02617	.02694	14.8
	SIG2	1.18	1.14	1.14	1.12	1.07	1.13	3.4	1.14	1.36	1.31	1.27	9.2	1.24	1.14	1.15	1.17	1.17	1.18	3.3
	TAU12	11.21	10.80	10.89	10.63	10.21	10.75	3.4	10.81	12.93	12.45	12.06	9.2	11.83	10.89	10.95	11.12	11.14	11.19	3.3
	EPS12	.02612	.02420	.02630	.02505	.02474	.02568	6.1	.02977	.03021	.02845	.02948	3.1	.03522	.02612	.02489	.02963	.02807	.02879	14.0

	TEST	160	161	162	163	164	MEAN	COV	242	254	258	MEAN	COV	320	321	322	323		MEAN	COV
	AREA	.09250	.09220	.09220	.09190	.09110	.09198	.6	.09210	.09180	.09300	.09230	.7	.09170	.09090	.09100	.09160		.09130	.4
8	SIGX	87.70	87.45	88.35	80.45	82.76	85.34	4.1	87.90	90.36	54.99	77.75	25.4	88.23	82.13	89.50	77.74		84.40	6.5
	EPSX	.00888	.00806	.00940	.00832	.01058	.00905	11.0	.00868	.00848	.00434	.00717	34.2	.00864	.00790	.00952	.00683		.00822	13.9
	EPSY	.00299	.00258	.00394	.00329	.00430	.00342	20.5	.00335	.00294	.00152	.00260	36.9	.00410	.00346	.00414	.00287		.00364	16.6
	EPSXY	.02861	.03027	.03462	.02561	.02936	.02969	11.0	.02642	.02822	.00977	.02147	47.4	.03009	.02378	.02901	.01996		.02571	18.4
	SIG2	1.70	1.69	1.71	1.56	1.60	1.65	4.1	1.70	1.75	1.07	1.51	25.4	1.71	1.59	1.73	1.51		1.63	6.5
	TAU12	12.09	12.05	12.19	11.09	11.41	11.76	4.1	12.11	12.45	7.58	10.72	25.4	12.16	11.32	12.33	10.71		11.63	6.5
	EPS12	.03077	.03203	.03696	.02782	.03232	.03198	10.3	.02872	.03027	.01100	.02333	45.9	.03243	.02599	.03165	.02186		.02798	17.8

	TEST	165	166	167	168	169	MEAN	COV	230	253	252	MEAN	COV	316	317	318	319		MEAN	COV
	AREA	.09400	.09320	.09390	.09440	.09410	.09392	.5	.09300	.09260	.09400	.09320	.8	.09290	.09290	.09290	.09230		.09275	.3
10	SIGX	73.65	67.95	70.48	71.15	66.67	69.98	3.9	63.62	83.64	88.12	78.46	16.6	49.03	66.87	64.83	69.53		62.57	14.7
	EPSX	.01107	.01016	.01229	.01072	.00969	.01079	9.2	.01026	.01131	.01216	.01124	8.5	.00542	.00962	.00943	.01080		.00882	26.6
	EPSY	.00504	.00431	.00589	.00531	.00495	.00510	11.2	.00506	.00397	.00533	.00479	15.0	.00272	.00486	.00444	.00581		.00446	29.0
	EPSXY	.03804	.03048	.03556	.03699	.03420	.03545	9.5	.03105	.03179	.03590	.03291	7.9	.01325	.02757	.02712	.03199		.02498	32.3
	SIG2	2.22	2.05	2.13	2.15	2.01	2.11	3.9	1.92	2.52	2.66	2.37	16.6	1.48	2.02	1.95	2.10		1.89	14.7
	TAU12	12.59	11.62	12.05	12.17	11.40	11.97	3.9	10.88	14.30	15.07	13.42	16.6	8.38	11.44	11.09	11.89		10.70	14.7
	EPS12	.04126	.03359	.03963	.04212	.03714	.03875	8.9	.03442	.03510	.03971	.03641	7.9	.01523	.03086	.03023	.03574		.02802	31.7

	TEST	170	171	172	173	174	MEAN	COV	231	249	250	MEAN	COV	312	313	314	315		MEAN	COV
	AREA	.09310	.09310	.09310	.09410	.09410	.09350	.6	.09420	.09250	.09300	.09323	.9	.09240	.09270	.09290	.09210		.09252	.4
12	SIGX	61.22	57.38	59.70	61.14	47.84	57.46	9.7	56.57	73.68	52.54	60.93	18.4	59.30	61.16	56.70	58.70		58.97	3.1
	EPSX	.01046	.00974	.01120	.01149	.00729	.01004	16.7	.01026	.01224	.00617	.00956	32.4	.00888	.01223	.00860	.00939		.00978	17.1
	EPSY	.00515	.00448	.00514	.00588	.00286	.00470	24.3	.00453	.00522	.00240	.00405	36.3	.00468	.00495	.00399	.00450		.00453	8.9
	EPSXY	.03045	.02717	.02914	.03434	.01912	.02804	20.1	.03524	.03571	.01434	.02843	42.9	.02763	.03533	.02572	.03072		.02985	14.1
	SIG2	2.65	2.48	2.58	2.64	2.07	2.48	9.7	2.45	3.18	2.27	2.63	18.4	2.56	2.64	2.45	2.54		2.55	3.1
	TAU12	12.45	11.67	12.14	12.43	9.73	11.68	9.7	11.50	14.98	10.68	12.39	18.4	12.06	12.44	11.53	11.94		11.99	3.1
	EPS12	.03417	.03061	.03326	.03844	.02160	.03162	19.8	.03821	.03972	.01658	.03151	41.1	.03076	.03927	.02862	.03372		.03309	14.0

TABLE IX (CON'T)

TEST NUMBERS;AREAS;ULTIMATE STRESSES AND STRAINS

	TEST	175	176	177	178	179	MEAN	COV	232	247	248	MEAN	COV	289	290	291	MEAN	COV
	AREA	.09290	.09280	.09190	.09080	.09070	.09182	1.1	.09090	.09170	.09300	.09187	1.2	.09010	.09250	.08990	.09083	1.6
14	SIGX	39.76	37.96	36.99	47.52	41.67	40.78	10.2	44.65	56.97	51.64	51.15	11.9	49.47	50.85	52.74	51.02	3.2
	EPSX	.00611	.00568	.00547	.00837	.00614	.00636	16.3	.00834	.01276	.00961	.01024	22.2	.00817	.00900	.00961	.00893	8.1
	EPSY	.00267	.00264	.00220	.00387	.00276	.00283	22.1	.00394	.00656	.00443	.00497	28.0	.00495	.00496	.00667	.00553	17.9
	EPSXY	.01412	.01337	.01299	.02049	.01500	.01529	19.6	.02171	.03540	.02532	.02748	25.8	.02066	.02531	.02579	.02392	11.8
	SIG2	2.33	2.22	2.16	2.78	2.44	2.39	10.2	2.62	3.33	3.02	2.99	11.9	2.90	2.98	3.09	2.99	3.2
	TAU12	9.33	8.91	8.68	11.15	9.78	9.57	10.2	10.53	13.37	12.12	12.01	11.9	11.61	11.94	12.38	11.98	3.2
	EPS12	.01659	.01614	.01507	.02384	.01744	.01781	19.5	.02493	.04033	.02894	.03140	25.4	.02440	.02890	.03042	.02791	11.2

	TEST	185	186	187	188	189	MEAN	COV	233	269	263	MEAN	COV	292	293	294	295	MEAN	COV
	AREA	.09270	.09170	.09150	.09060	.08960	.09122	1.3	.09060	.09090	.09110	.09087	.3	.08840	.09100	.09040	.09070	.09013	1.3
16	SIGX	34.19	42.13	34.25	41.13	38.72	38.08	9.8	38.45	50.45	51.40	46.77	15.4	45.43	45.52	48.06	43.52	45.63	4.1
	EPSX	.00540	.00788	.00551	.00797	.00717	.00677	18.3	.00705	.01223	.01179	.01036	27.7	.00916	.01053	.01140	.00879	.00997	12.2
	EPSY	.00229	.00330	.00248	.00366	.00332	.00301	19.8	.00346	.00576	.00568	.00497	26.3	.00455	.00568	.00710	.00492	.00556	20.3
	EPSXY	.01219	.01760	.01425	.01631	.01519	.01511	13.6	.01516	.03187	.03120	.02608	36.3	.02371	.02713	.02951	.02219	.02563	12.9
	SIG2	2.60	3.20	2.60	3.12	2.94	2.89	9.8	2.92	3.83	3.91	3.55	15.4	3.45	3.46	3.65	3.31	3.47	4.1
	TAU12	9.06	11.16	9.07	10.90	10.26	10.09	9.8	10.19	13.37	13.62	12.39	15.4	12.04	12.06	12.73	11.53	12.09	4.1
	EPS12	.01441	.02081	.01632	.01999	.01843	.01799	14.6	.01843	.03056	.03572	.03024	33.9	.02738	.03159	.03483	.02608	.02997	13.4

	TEST	190	191	192	193	194	MEAN	COV	234	276	264	MEAN	COV	296	297	298	MEAN	COV
	AREA	.09320	.09200	.09100	.09000	.09010	.09126	1.5	.09200	.09180	.09220	.09200	.2	.08860	.08920	.09020	.08933	.9
20	SIGX	38.05	38.80	37.34	32.79	36.57	36.71	6.4	38.56	38.73	40.70	39.33	3.0	36.02	36.94	34.61	35.86	3.3
	EPSX	.01210	.01249	.01081	.00883	.01134	.01123	13.2	.01204	.01275	.01260	.01246	3.0	.00966	.01312	.01280	.01186	16.1
	EPSY	.00625	.00674	.00512	.00419	.00634	.00573	18.3	.00542	.00704	.00663	.00636	13.3	.00580	.00665	.00479	.00575	16.2
	EPSXY	.02450	.02682	.02071	.01680	.02348	.02246	17.1	.02506	.02656	.02895	.02686	7.3	.02084	.02694	.02282	.02353	13.2
	SIG2	4.45	4.54	4.37	3.84	4.28	4.29	6.4	4.51	4.53	4.76	4.60	3.0	4.21	4.32	4.05	4.19	3.3
	TAU12	12.23	12.47	12.00	10.54	11.75	11.80	6.4	12.39	12.45	13.08	12.64	3.0	11.58	11.87	11.12	11.52	3.3
	EPS12	.03056	.03291	.02611	.02124	.02973	.02811	16.2	.03042	.03307	.03454	.03268	6.4	.02590	.03334	.02879	.02934	12.8

	TEST	195	196	197	198	199	MEAN	COV	235	273	265	MEAN	COV	299	300	301	MEAN	COV
	AREA	.09190	.09040	.09100	.09100	.09120	.09110	.6	.09220	.09100	.09100	.09140	.8	.08900	.08940	.08920	.08920	.2
30	SIGX	25.18	23.97	26.98	26.51	26.30	25.79	4.7	24.28	26.23	28.89	26.47	8.7	8.63	22.12	11.81	14.19	49.7
	EPSX	.01371	.01269	.01657	.01515	.01668	.01496	11.7	.01183	.01286	.01429	.01299	9.5	.00228	.00955	.00352	.00511	76.1
	EPSY	.00705	.00651	.00861	.00810	.00852	.00776	12.0	.00577	.00624	.00933	.00711	27.2	.00108	.00516	.00166	.00263	83.9
	EPSXY	.01757	.01535	.01880	.01883	.01901	.01791	8.6	.01451	.01704	.03113	.02089	42.9	.00282	.01227	.00426	.00645	78.9
	SIG2	6.30	5.99	6.75	6.63	6.58	6.45	4.7	6.07	6.56	7.22	6.62	8.7	2.16	5.53	2.95	3.55	49.7
	TAU12	10.90	10.38	11.68	11.48	11.39	11.17	4.7	10.51	11.36	12.51	11.46	8.7	3.74	9.58	5.11	6.14	49.7
	EPS12	.02676	.02431	.03121	.02955	.03133	.02863	10.6	.02250	.02506	.03603	.02786	25.8	.00431	.01888	.00661	.00993	78.8

	TEST	200	201	202	203	204	MEAN	COV	236	266	267	MEAN	COV	303	304	305	306	302	MEAN	COV
	AREA	.08990	.08880	.09080	.09100	.09060	.09022	1.0	.09090	.09000	.09110	.09067	.6	.09040	.09090	.08990	.08990	.09110	.09044	.6
40	SIGX	16.10	19.59	17.72	18.65	18.08	18.03	7.1	18.51	18.33	17.06	17.97	4.4	15.52	18.53	16.88	16.17	16.40	16.70	6.8
	EPSX	.00948	.01307	.01094	.01092	.01099	.01108	11.6	.01109	.01124	.00915	.01049	11.1	.00780	.01233	.00924	.00859	.00915	.00942	18.3
	EPSY	.00380	.00649	.00390	.00465	.00414	.00460	24.1	.00454	.00472	.00365	.00430	13.3	.00358	.00581	.00417	.00371	.00415	.00428	20.8
	EPSXY	.00762	.00853	.00864	.00904	.00888	.00854	6.5	.00183	.00777	.00684	.00548	58.3	.00552	.00884	.00677	.00668	.01404	.00837	40.5
	SIG2	6.65	8.09	7.32	7.71	7.47	7.45	7.1	7.65	7.57	7.05	7.42	4.4	6.41	7.66	6.97	6.68	6.78	6.90	6.8
	TAU12	7.93	9.65	8.73	9.18	8.90	8.88	7.1	9.11	9.03	8.40	8.85	4.4	7.64	9.12	8.31	7.96	8.08	8.22	6.8
	EPS12	.01440	.02074	.01612	.01691	.01644	.01692	13.8	.01571	.01706	.01379	.01552	10.6	.01217	.01940	.01438	.01328	.01553	.01495	18.6

TABLE IX (CON'T)

TEST NUMBERS:AREAS:ULTIMATE STRESSES AND STRAINS

	TEST	205	206	207	208	209	MEAN	COV	238	268	274	MEAN	COV	277	278	279	MEAN	COV
	AREA	.09030	.08950	.09060	.08970	.08970	.08996	.5	.08880	.09000	.09210	.09030	1.8	.08810	.09090	.09130	.09010	1.9
45	SIGX	18.04	16.27	16.49	16.00	14.99	16.36	6.7	14.59	16.37	14.61	15.19	6.7	16.97	16.60	16.53	16.70	1.4
	EPSX	.01263	.00994	.01038	.00992	.00872	.01032	13.9	.00617	.01019	.00883	.00906	11.3	.01181	.01228	.01167	.01192	2.7
	EPSY	.00461	.00393	.00370	.00345	.00310	.00376	15.1	.00279	.00370	.00303	.00317	14.9	.00520	.00473	.00439	.00477	8.5
	EPSXY	.00811	.00556	.00569	.00730	.00576	.00668	15.9	.00550	.00524	.00497	.00524	5.0	.00631	.00754	.00680	.00688	9.8
	SIG2	9.02	8.14	8.25	8.00	7.50	8.18	6.7	7.30	8.19	7.31	7.60	6.7	8.49	8.30	8.27	8.35	1.4
	TAU12	9.02	8.14	8.25	8.00	7.50	8.18	6.7	7.30	8.19	7.31	7.60	6.7	8.49	8.30	8.27	8.35	1.4
	EPS12	.01723	.01367	.01408	.01337	.01182	.01408	14.0	.01096	.01389	.01186	.01224	12.3	.01701	.01702	.01606	.01670	3.3

	TEST	210	211	212	213	214	MEAN	COV	237	275	270	MEAN	COV	280	281	282	MEAN	COV
	AREA	.09110	.09010	.09130	.09000	.09090	.09068	.7	.08980	.09000	.09210	.09063	1.4	.09000	.09110	.09060	.09057	.6
50	SIGX	16.47	15.76	16.10	14.78	15.89	15.80	4.0	12.14	16.58	16.35	15.02	16.6	12.02	14.65	13.80	13.49	9.9
	EPSX	.01184	.01124	.01133	.00993	.01194	.01126	7.1	.00751	.01237	.01141	.01043	24.7	.00674	.01012	.00834	.00840	20.2
	EPSY	.00383	.00348	.00361	.00283	.00361	.00347	11.0	.00202	.00415	.00364	.00327	33.9	.00203	.00331	.00321	.00285	25.0
	EPSXY	.00396	.00483	.00501	.00367	.00574	.00468	16.7	.00350	.00435	.00534	.00439	21.0	.00275	.00406	.00320	.00334	20.0
	SIG2	9.66	9.25	9.45	8.67	9.32	9.27	4.0	7.12	9.73	9.59	8.82	16.6	7.05	8.60	8.10	7.92	9.9
	TAU12	8.11	7.76	7.93	7.28	7.82	7.78	4.0	5.98	8.16	8.05	7.40	16.6	5.92	7.21	6.80	6.64	9.9
	EPS12	.01475	.01366	.01395	.01189	.01432	.01370	8.0	.00878	.01351	.01389	.01273	27.6	.00815	.01252	.01082	.01050	21.0

	TEST	215	216	217	218	219	MEAN	COV	240	271	272	MEAN	COV	307	308	309	310	311	MEAN	COV
	AREA	.08920	.08950	.08760	.08760	.08840	.08846	1.0	.08870	.09100	.09040	.09020	1.4	.09250	.09140	.09040	.09040	.09080	.09110	1.0
60	SIGX	10.80	12.24	12.83	13.35	12.58	12.36	7.8	12.18	12.35	10.70	11.74	7.7	12.02	10.05	12.06	9.55	9.96	10.73	11.3
	EPSX	.00713	.00898	.00861	.00878	.00853	.00841	8.7	.00876	.00832	.00692	.00800	12.0	.00836	.00627	.00798	.00570	.00654	.00697	16.4
	EPSY	.00153	.00161	.00194	.00201	.00176	.00177	11.6	.00149	.00168	.00131	.00150	12.5	.00194	.00146	.00198	.00133	.00147	.00164	18.4
	EPSXY	.00160	.00253	.00203	.00137	.00231	.00197	24.5	.00234	.00201	.00181	.00205	13.1	.00139	.00095	.00148	.00109	.00136	.00125	18.0
	SIG2	8.10	9.18	9.62	10.01	9.44	9.27	7.8	9.14	9.26	8.03	8.81	7.7	9.02	7.54	9.05	7.16	7.47	8.05	11.3
	TAU12	4.68	5.30	5.56	5.78	5.45	5.35	7.8	5.27	5.35	4.63	5.09	7.7	5.20	4.35	5.22	4.14	4.31	4.65	11.3
	EPS12	.00669	.00791	.00812	.00866	.00776	.00783	9.2	.00771	.00766	.00622	.00720	11.8	.00823	.00622	.00789	.00555	.00625	.00683	17.0

	TEST	220	221	222	223	224	MEAN	COV	241	260	251	MEAN	COV	283	284	285	MEAN	COV
	AREA	.08840	.08730	.08720	.08720	.08810	.08764	.6	.08810	.09200	.09010	.09007	2.2	.08940	.08960	.08930	.08943	.2
70	SIGX	12.48	10.54	11.42	11.63	10.61	11.34	7.1	8.70	10.84	9.65	9.73	11.0	10.20	9.94	9.88	10.01	1.7
	EPSX	.00924	.00735	.00766	.00828	.00730	.00797	10.2	.00581	.00774	.00662	.00672	14.4	.00712	.00675	.00679	.00688	2.9
	EPSY	.00112	.00080	.00097	.00099	.00090	.00095	12.4	.00067	.00083	.00071	.00074	10.8	.00082	.00084	.00081	.00082	2.1
	EPSXY	.00080	.00096	.00061	.00103	.00096	.00087	19.4	.00086	.00135	.00132	.00118	23.1	.00032	.00027	.00054	.00038	37.8
	SIG2	11.02	9.31	10.08	10.27	9.37	10.01	7.1	7.68	9.57	8.52	8.59	11.0	9.01	8.78	8.72	8.84	1.7
	TAU12	4.01	3.39	3.67	3.74	3.41	3.64	7.1	2.80	3.48	3.10	3.13	11.0	3.28	3.19	3.18	3.22	1.7
	EPS12	.00605	.00450	.00508	.00517	.00454	.00507	12.4	.00351	.00447	.00370	.00389	13.1	.00485	.00467	.00447	.00466	4.1

	TEST	225	226	227	228	229	MEAN	COV	243	262	261	MEAN	COV	286	287	228	MEAN	COV
	AREA	.09340	.09240	.09240	.09250	.09250	.09264	.5	.09240	.08990	.08990	.09073	1.6	.09230	.09270	.09130	.09210	.8
80	SIGX	8.43	10.10	10.18	8.74	9.89	9.47	8.7	8.74	8.32	8.56	8.54	2.5	8.78	7.02	8.13	7.98	11.2
	EPSX	.00617	.00733	.00718	.00629	.00722	.00684	8.1	.00657	.00560	.00607	.00608	8.0	.00615	.00480	.00579	.00558	12.5
	EPSY	.00031	.00037	.00035	.00032	.00036	.00034	7.2	.00033	.00029	.00029	.00030	7.5	.00024	.00026	.00027	.00025	7.0
	EPSXY	.00038	.00041	.00043	.00041	.00023	.00037	21.7	.00022	.00030	.00072	.00041	64.5	.00000	.00001	.00018	.00006	157.5
	SIG2	9.18	9.80	9.87	8.48	9.59	9.18	8.7	8.48	8.07	8.30	8.28	2.5	8.52	6.81	7.88	7.74	11.2
	TAU12	1.44	1.73	1.74	1.49	1.69	1.62	8.7	1.49	1.42	1.46	1.46	2.5	1.50	1.20	1.39	1.36	11.2
	EPS12	.00186	.00224	.00217	.00187	.00238	.00210	10.9	.00215	.00173	.00150	.00180	18.4	.00218	.00172	.00191	.00194	11.8

TABLE X

STRESS DIFFERENCES FOR NONLINEAR ANALYSIS

Off-Axis Angle	SQUARF TABS*						INCLINED TABS*						
	1st. Increment			Last But One Increment			1st. Increment				Last But One Increment		
	σ_x**	$\Delta\sigma_x$**	%	σ_x	$\Delta\sigma_x$	%	δ	σ_x	$\Delta\sigma_x$	%	σ_x	$\Delta\sigma_x$	%
4°	18,360.	100.	0.5447	165,200.	600.	0.3632	0.	18,360.	10.	0.0545	165,215.	200.	0.1211
6°	14,090.	80.	0.5678	140,900.	1,000.	0.7097	0.	14,089.	10.	0.0710	140,857.	300.	0.2130
8°	10,870.	60.	0.5520	108,600.	700.	0.6446	0.1500	10,870.	10.	0.092	108,662.	100.	0.0920
10°	9,130.	57.	0.6243	82,090.	930.	1.1329	0.1520	9,130.	13.	0.1424	82,159.	50.	0.0609
12°	7,391.	54.	0.7306	73,800.	1,410.	1.9106	0.1600	7,391.	15.	0.2029	73,850.	140.	0.1896
14°	6,521.	54.	0.8281	58,610.	1,260.	2.1498	0.1600	6,522.	13.	0.1993	58,691.	290.	0.4941
16°	5,652.	54.	0.9554	56,390.	1,470.	2.6068	0.1720	5,652.	12.	0.2123	50,865.	350.	0.6881
20°	4,782.	58.	1.2129	42,960.	1,720.	4.0037	0.1940	4,782.	12.	0.2509	43,035.	590.	1.3710
30°	3,478.	135.	3.8815	28,025.	1,750.	6.2444	0.2552	3,478.	14.	0.4025	24,337.	650.	2.6708
40°	2,174.	46.	2.1159	17,400.	930.	5.3448	0.3030	2,174.	14.	0.6440	17,389.	510.	2.9329
45°	1,826.	41.	2.2453	16,440.	910.	5.5353	0.3235	1,826.	13.	0.7119	16,434.	480.	2.9208
50°	1,565.	34.	2.1725	14,090.	560.	3.9744	0.3379	1,565.	9.	0.5751	14,086.	260.	1.8458
60°	1,304.	31.	2.3773	11,740.	240.	2.0443	0.3176	1,304.	8.	0.6135	11,739.	10.	0.0852
70°	1,043.	8.	1.8234	10,300.	80.	0.7767	0.2510	1,043.	4.	0.3835	9,389.	51.	0.5432
80°	956.5	2.6	0.2718	9,382.	22.	0.2345	0.1120	956.5	2.	0.2091	8,607.	27.	0.3137

* Hinged End Conditions

** All Stresses in psi

TABLE XI

NOMINAL AND ACTUAL OFF-AXIS ANGLES

NOMINAL ANGLE	STANDARD INSTRON GRIPS		ROTATING GRIPS	
	TEST #	ACTUAL ANGLE	TEST #	ACTUAL ANGLE
4°	154	4.60°	244	
	153	4.90°	257	
	152	4.35°	256	3.3°
	151	4.82°		
	150	4.93°		
6°	155	6.40°	245	7.08°
	156	6.47°	259	5.47°
	157	6.67°	255	5.37°
	158	6.35°		
	159	6.42°		
8°	160	8.55°	242	7.78°
	161	8.02°	254	7.68°
	162	7.90°	258	7.60°
	163	8.67°		
	164	9.22°		
10°	165	11.30°	230	11.85°
	166	10.77°	253	8.67°
	167	11.12°	252	9.35°
	168	11.37°		
	169	12.03°		
12°	170	12.75°	231	
	171	12.97°	249	10.65°
	172	13.02°	250	10.98°
	173	12.95°		
	174	13.27°		
14°	175	14.00°	232	
	176	13.98°	247	15.27°
	177	14.07°	248	
	178	13.47°		
	179	13.43°		
16°	185	15.80°	233	
	186		269	15.47°
	187	16.28°	263	15.57°
	188	16.25°		
	189	16.18°		
20°			234	
			276	19.90°
			264	19.92°

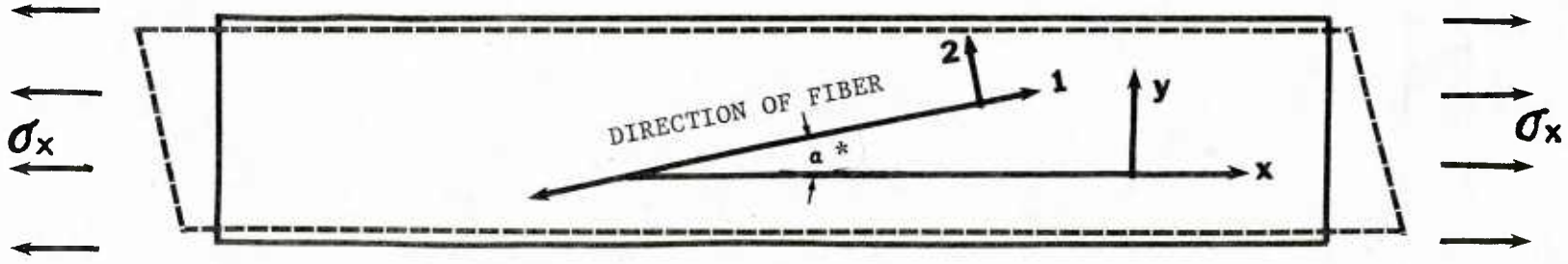

* Negative as shown

(a) Unconstrained Boundary Conditions

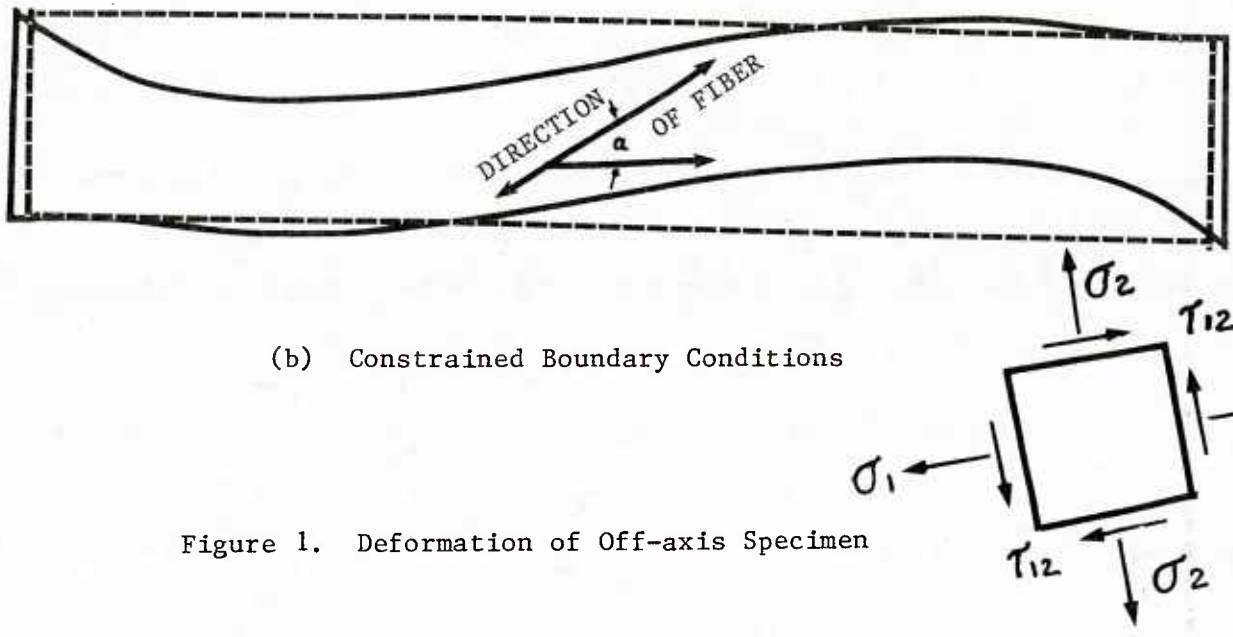

(b) Constrained Boundary Conditions

Figure 1. Deformation of Off-axis Specimen

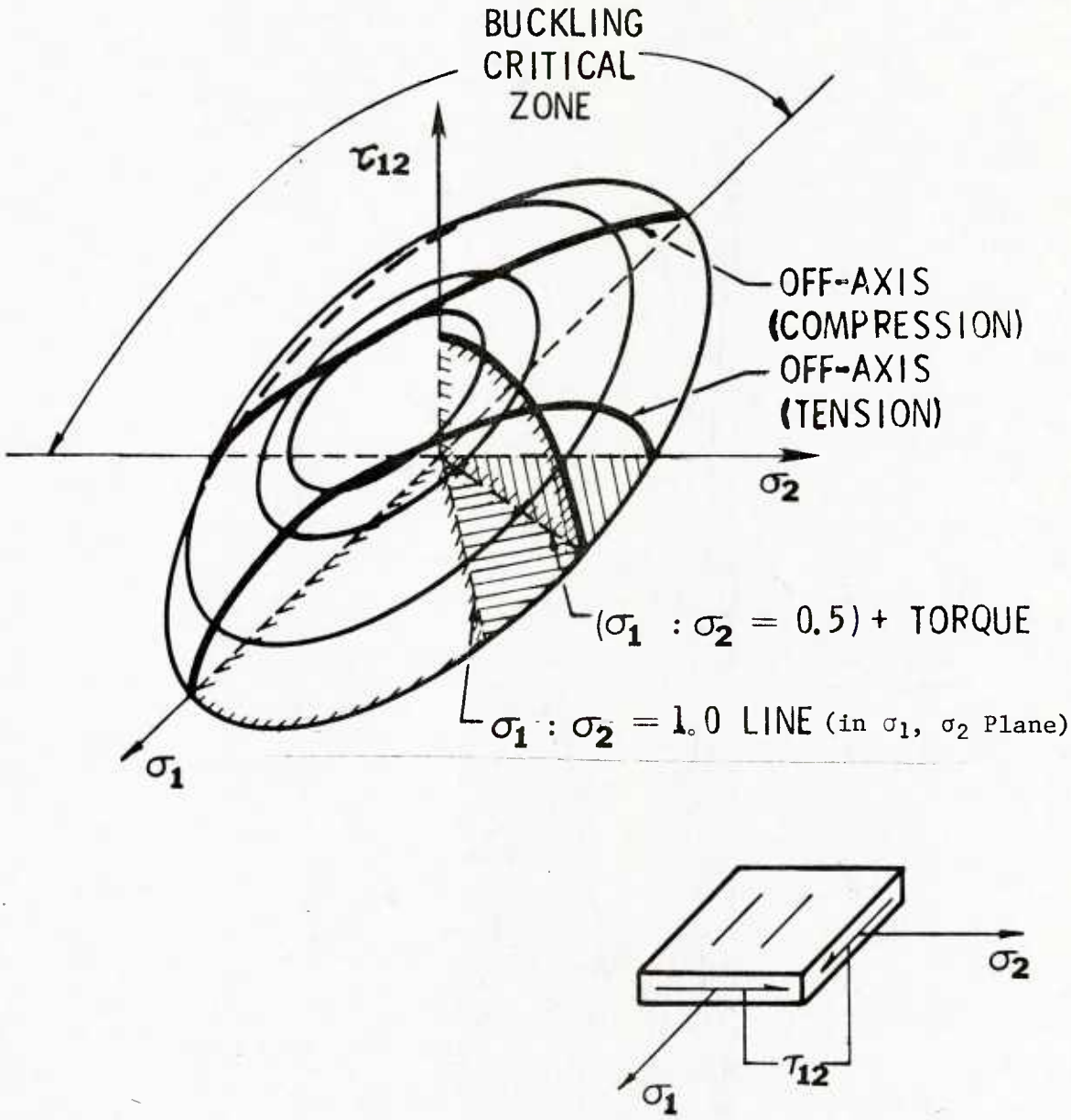

Figure 2. Hypothetical Failure Surface

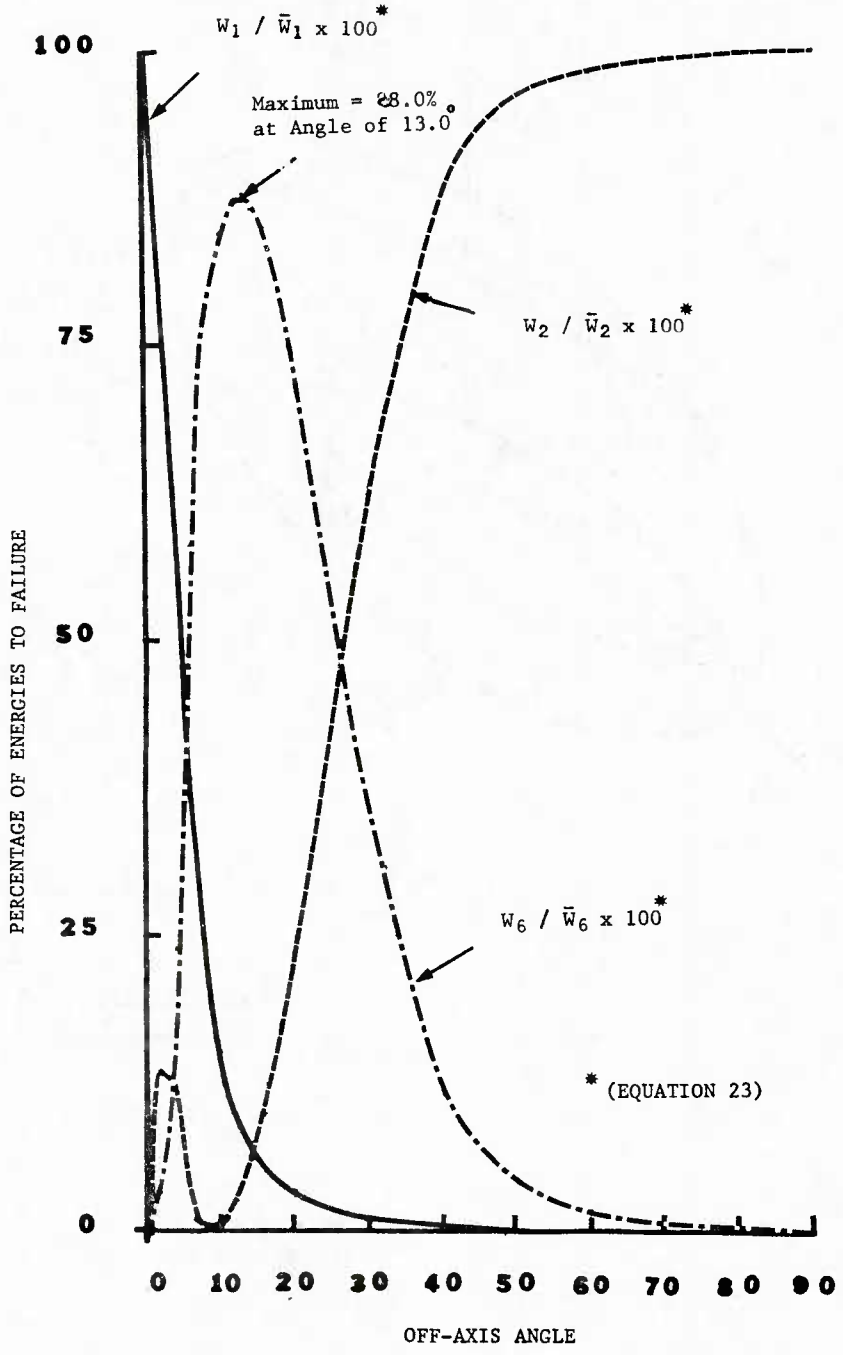

Figure 3. Percentage of Energy Contributions to Failure for Various Off-axis Angles obtained using Nonlinear Point Stress Analysis

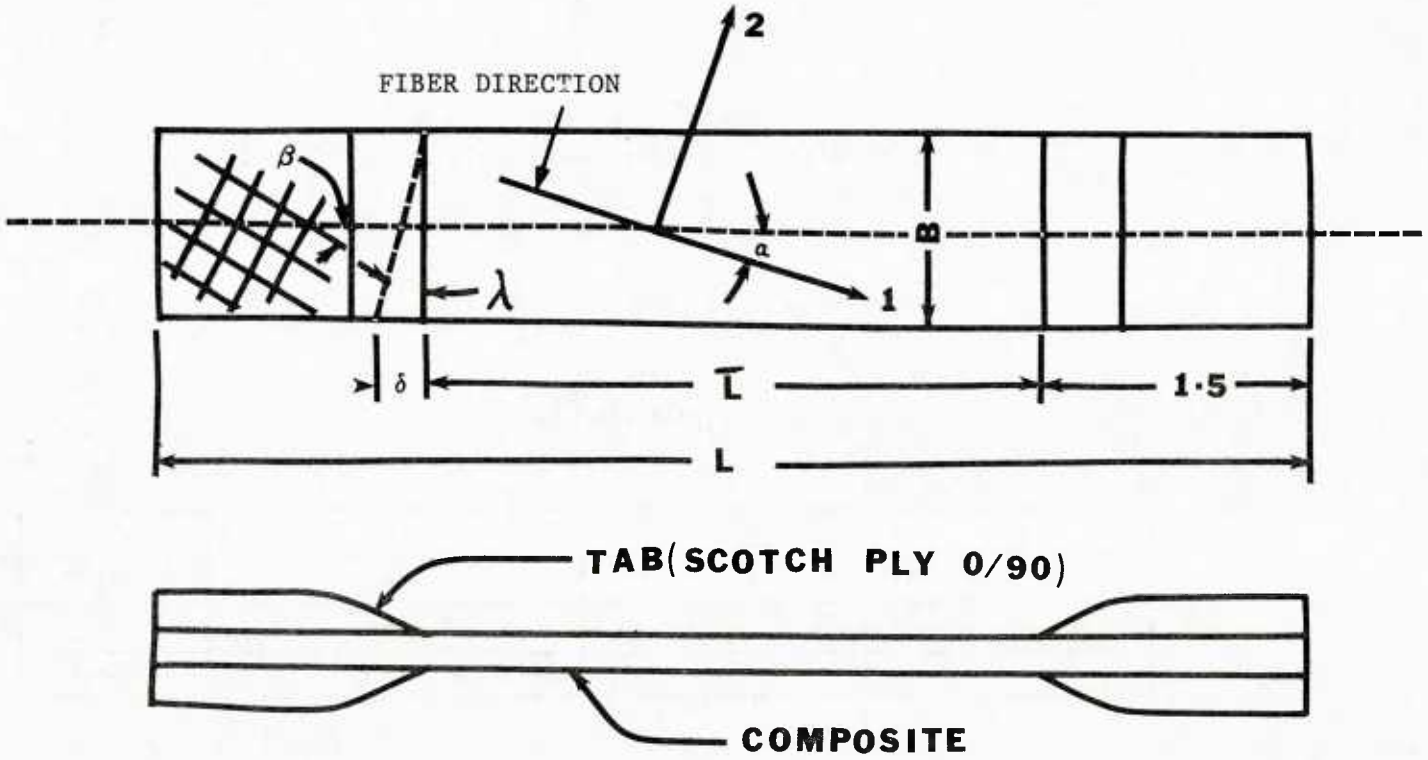

NOTE:
1. B = 1.0 inch except for $\alpha = 4°$ for which it is 0.9 inch.
2. L = 17.0, 15.0, 14.0, 12.0 inch for $\alpha = 4°, 6°, 8°$ and $10°$ respectively.
   L = 10.0 inch for $\alpha = 12°, 14°, 16°, 20°, 30°, 40°, 45°, 50°, 60°, 70°$ and $80°$.
3. No. of coupon = 6 for square end tabs.
4. No. of coupon = 6 for inclined tabs.

Figure 4. Off-axis Specimen

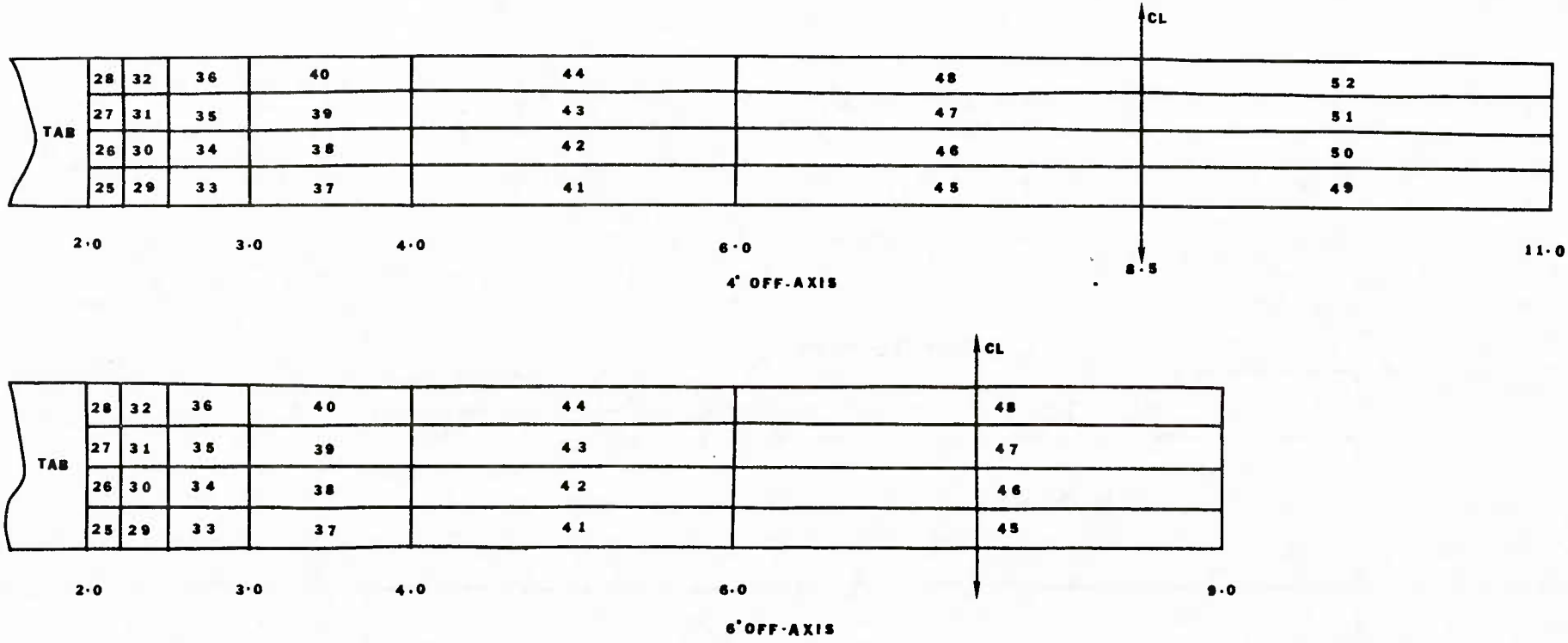

Figure 5. Finite Element Models for 4^{o} and 6^{o} Off-axis Specimens

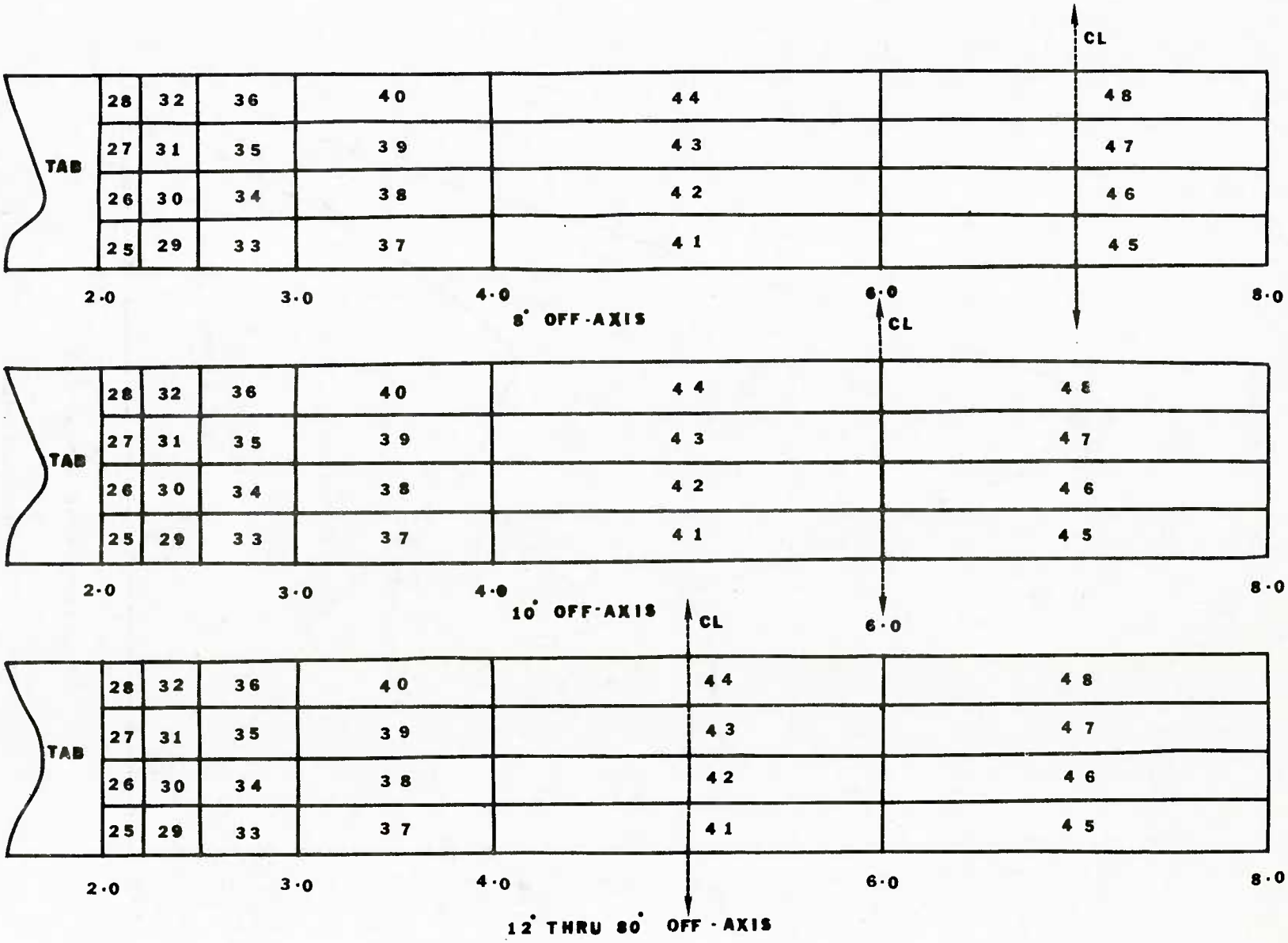

Figure 6. Finite Element Models of 8^{o}, 10^{o}, 12^{o} thru 80^{o} Off-axis Specimens

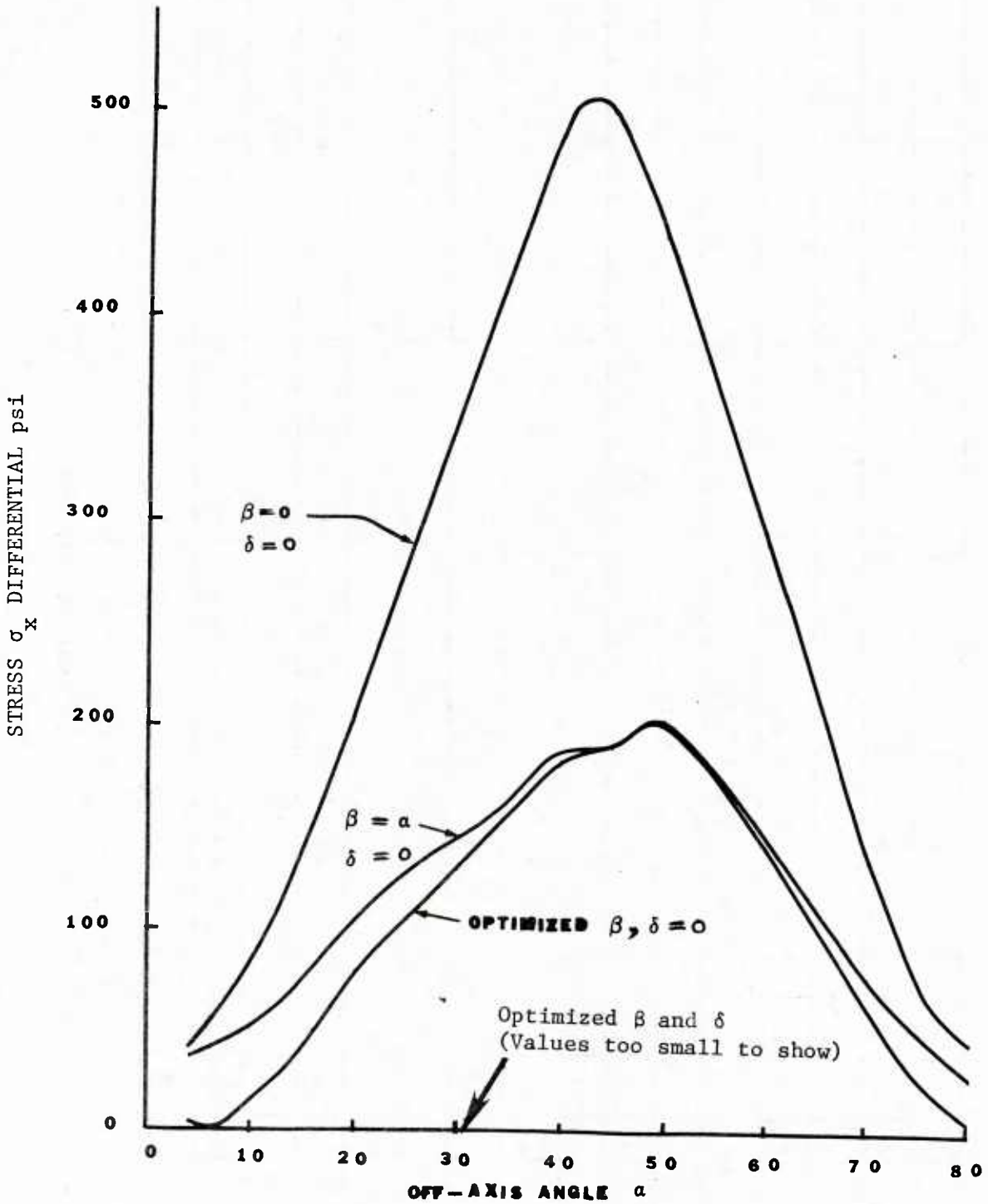

Figure 7. Stress σ_x Differential versus Off-axis Angle α, for $\beta = 0$ ($\delta = 0$), $\beta = a$ ($\delta = 0$), Optimized β ($\delta = 0$) and Optimized β and δ, for Hinged Grips

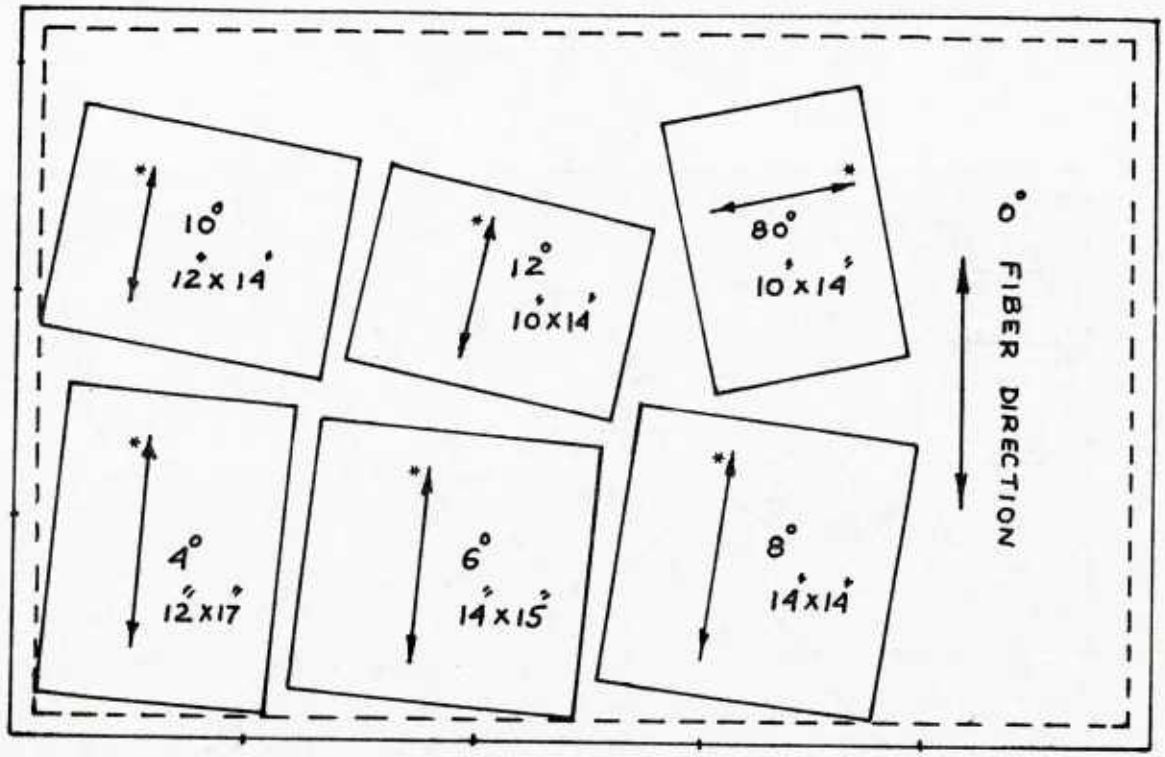

* Load Direction in each Panel

Figure 8. Fabrication Schedule for Sub Panels for 4^{o}, 6^{o}, 8^{o}, 10^{o}, 12^{o}, and 80^{o} Off-axis Specimens

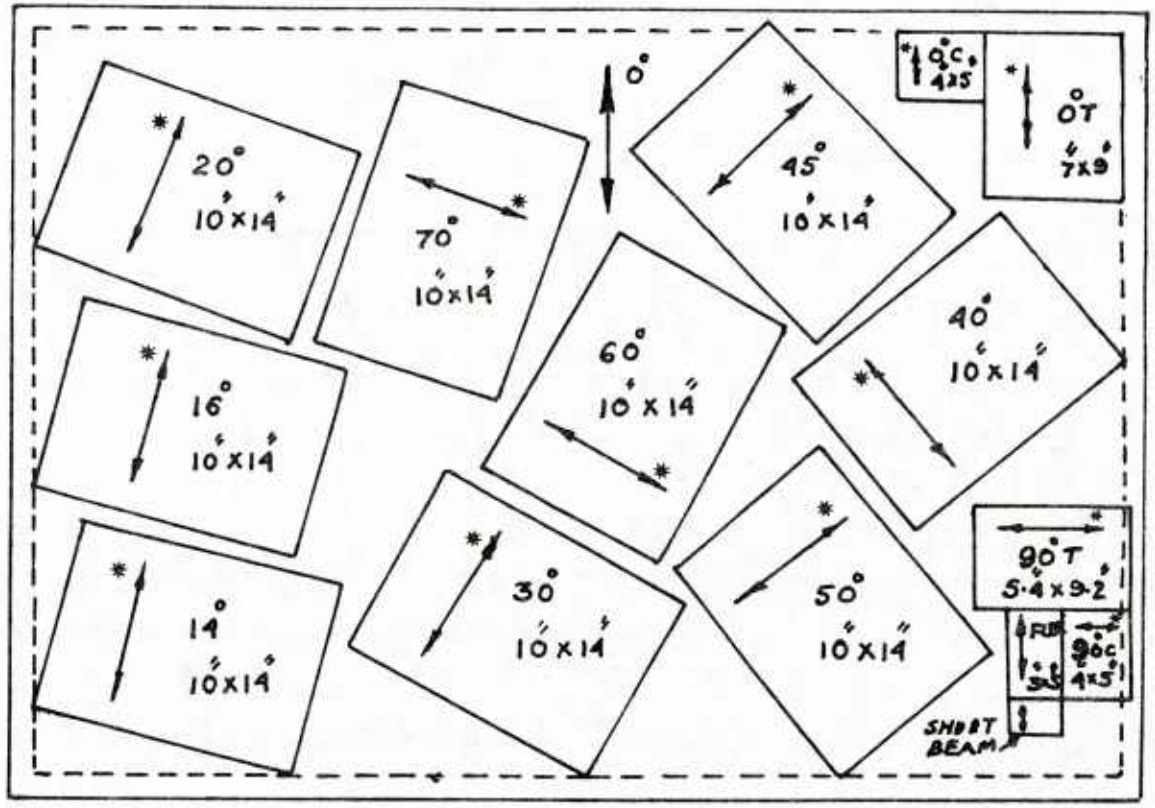

* Load Direction in each Panel

Figure 9. Fabrication Schedule for Sub Panels for 14^{o}, 16^{o}, 20^{o}, 30^{o}, 40^{o}, 45^{o}, 50^{o}, 60^{o}, 70^{o} Off-axis and 0^{o} and 90^{o} Tensile and Compresive Specimens

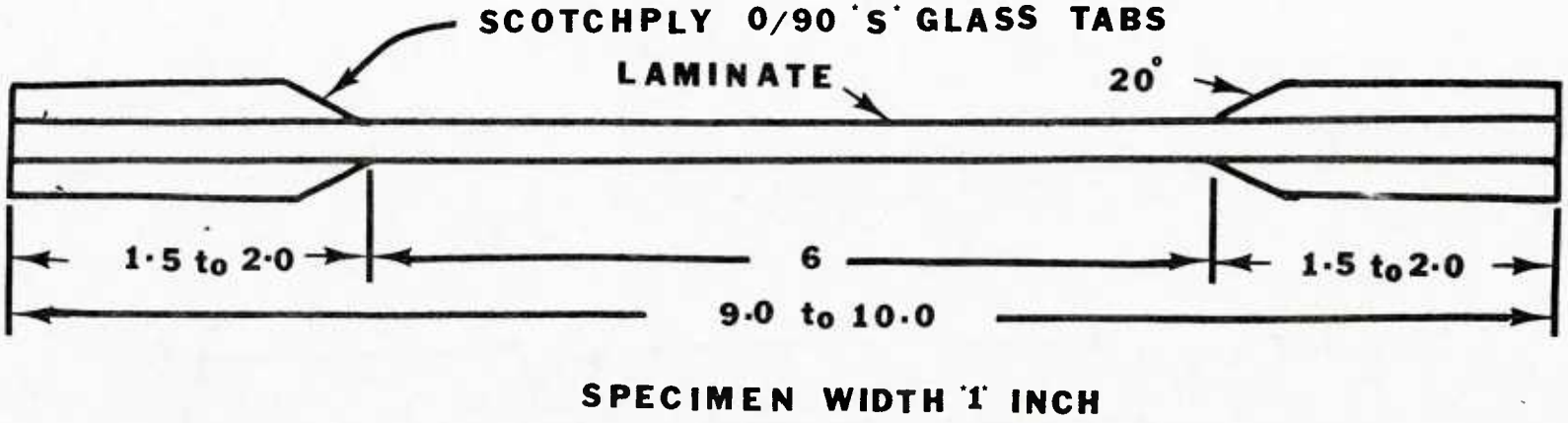

Figure 10. 0°, 90° and $\pm 45^{\circ}$ Tension Test Specimen

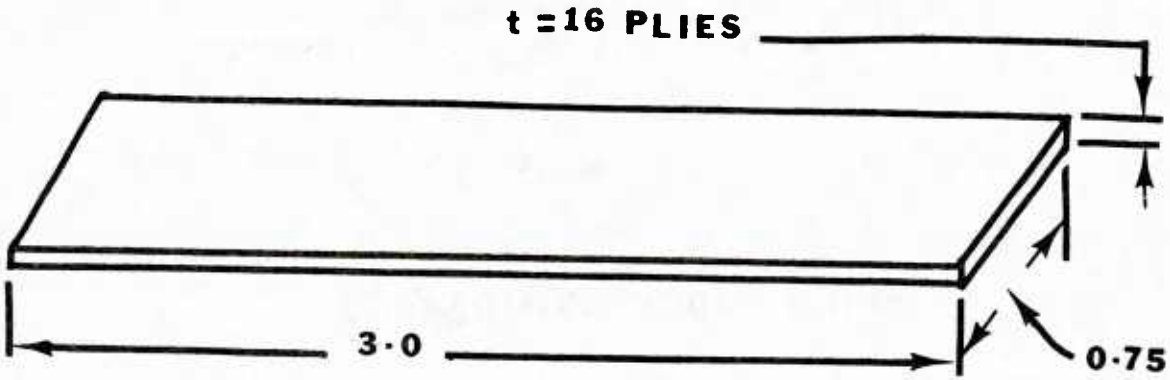

Figure 11. 0^{o} and 90^{o} Compression Test Specimen

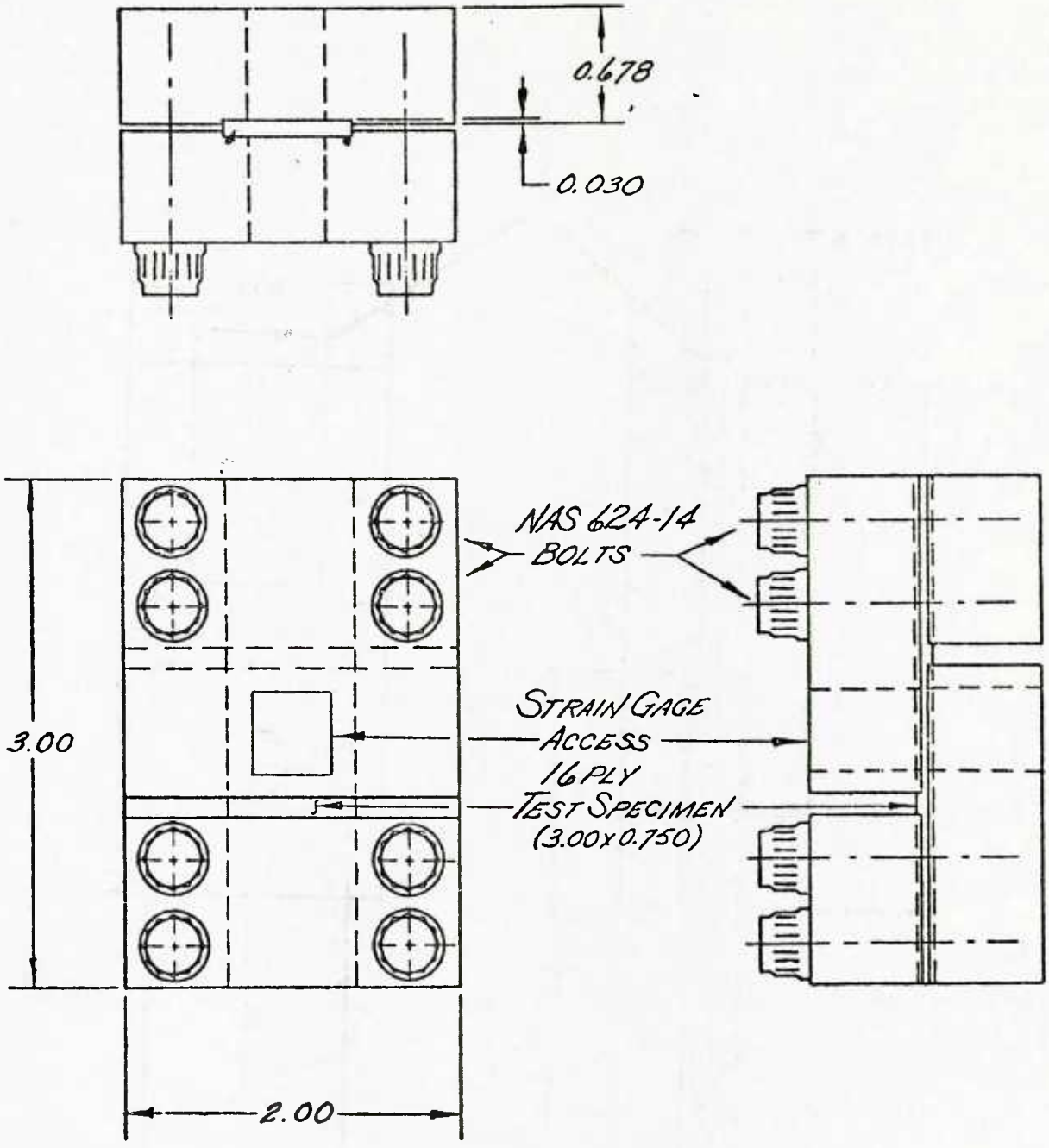

Figure 12. Compression Test Fixture

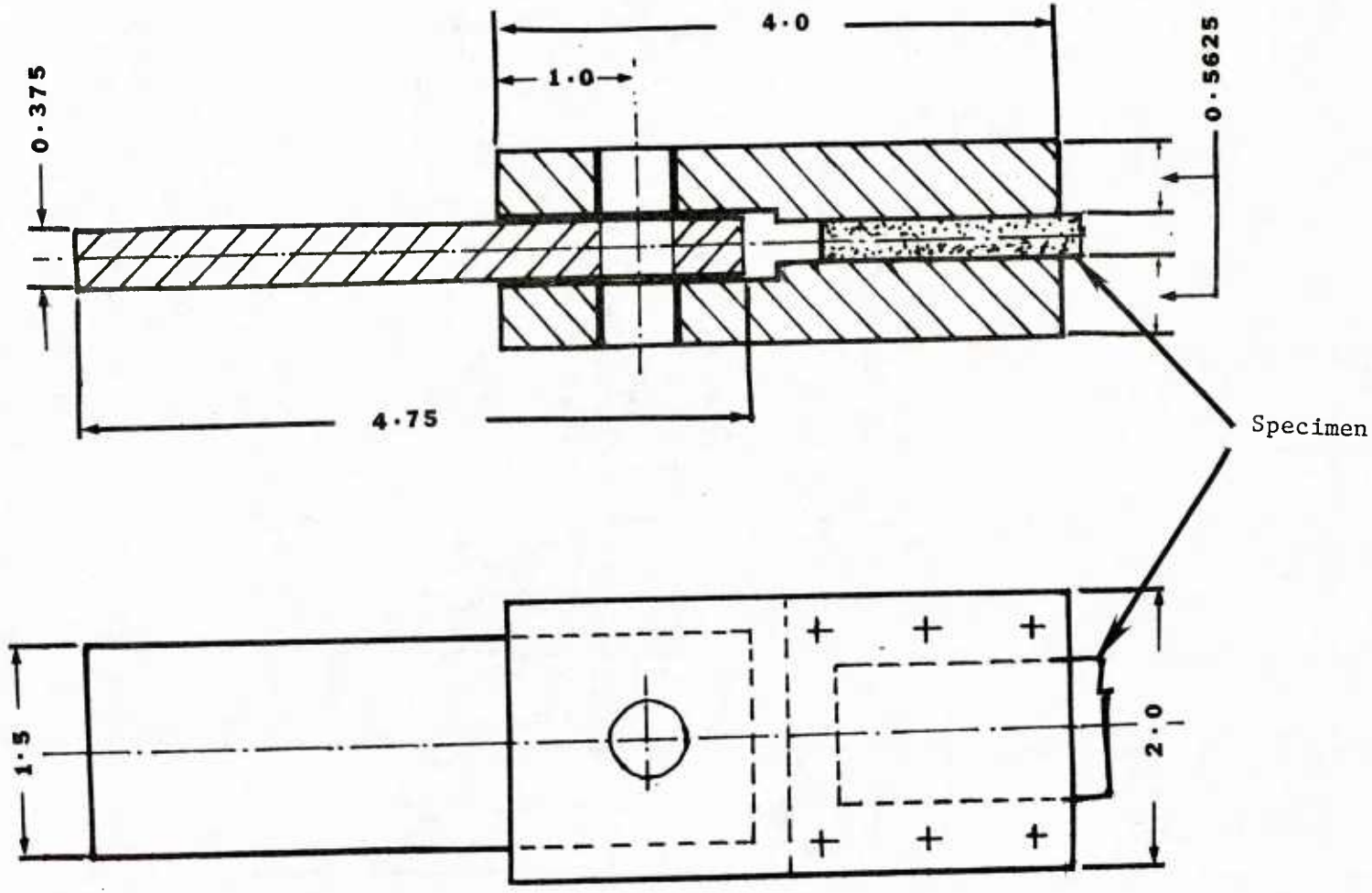

Figure 13. Fixture with Rotation Grips

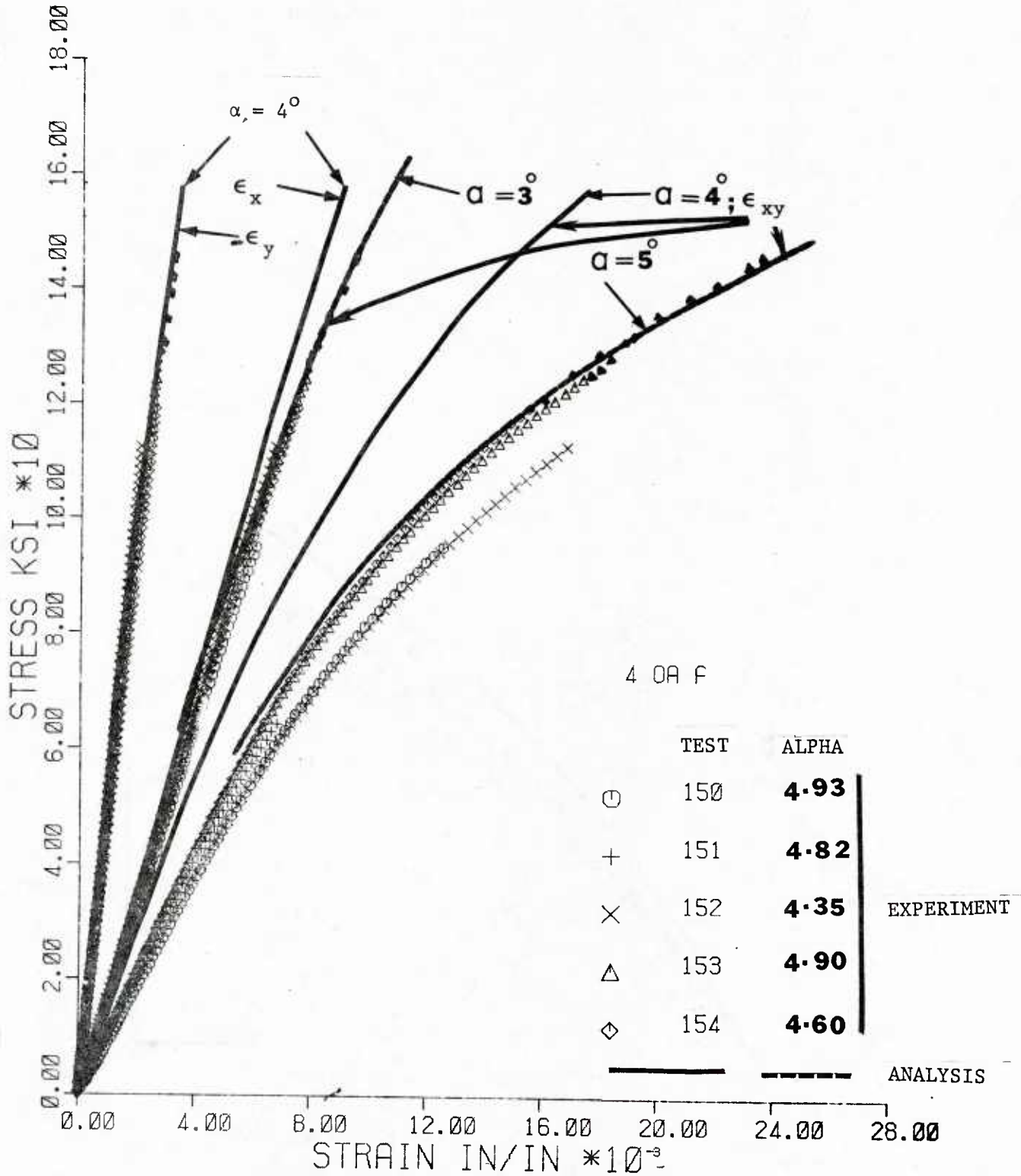

Figure 14. Axial Stress versus Axial, Transverse, and Shear Strain Curves for 4° (nominal) Off-axis Specimens with Square Tabs and Fixed Grips

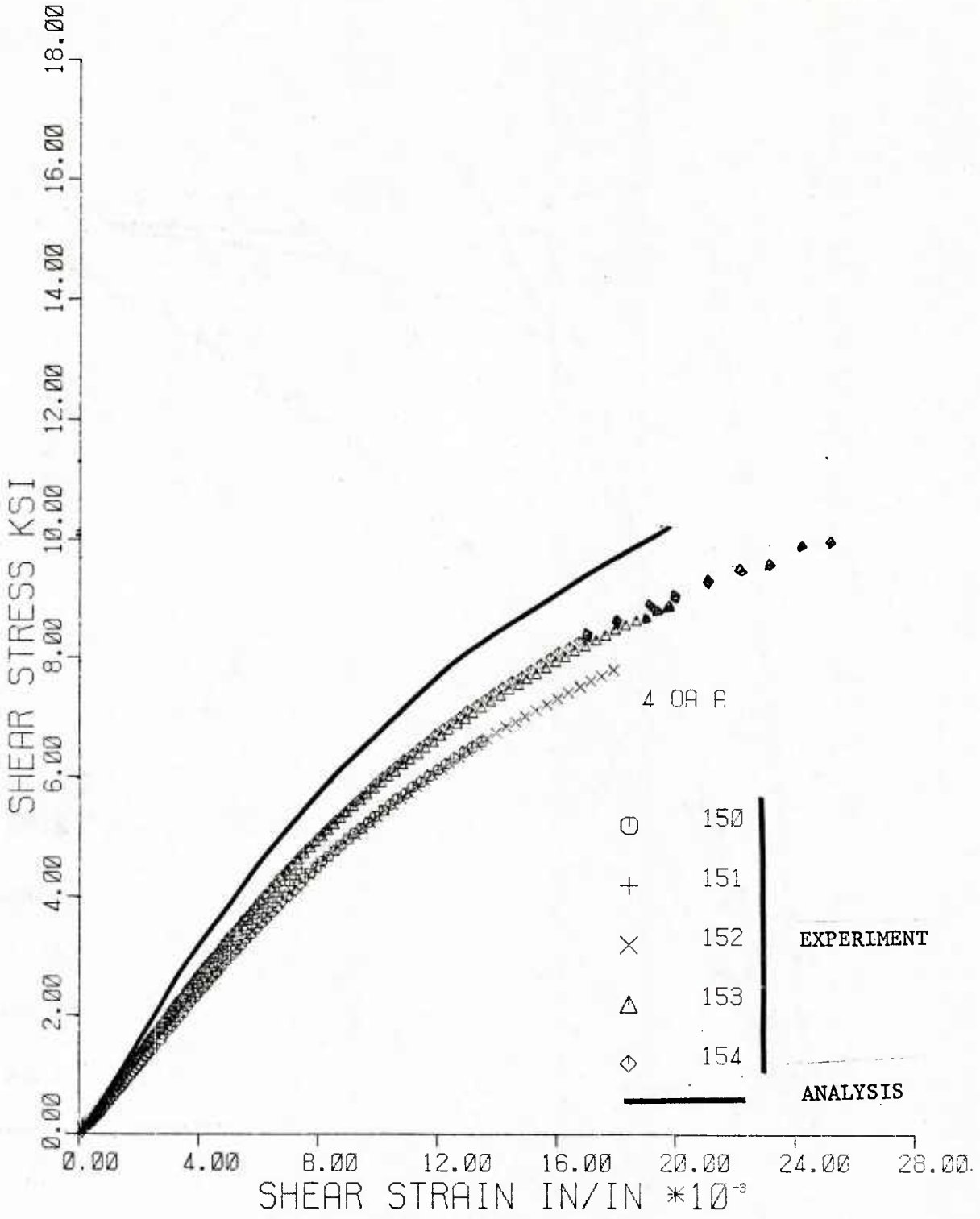

Figure 15. Shear Stress (τ_{12}) versus Shear Strain (γ_{12}) Curves for 4° Off-axis Specimens with Square Tabs and Fixed Grips

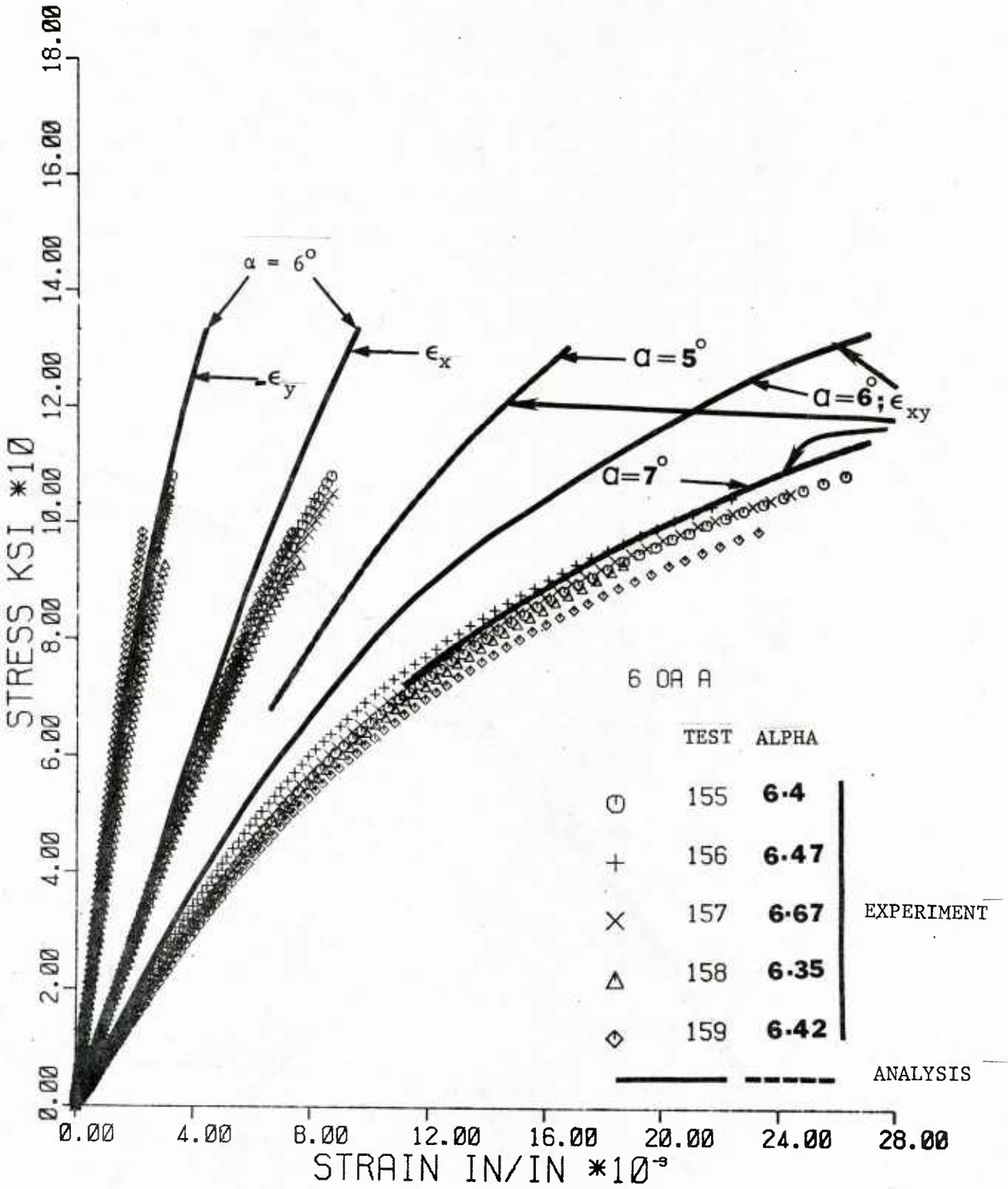

Figure 16. Axial Stress versus Axial, Transverse, and Shear Strain Curves for 6° (nominal) Off-axis Specimens with Square Tabs and Fixed Grips

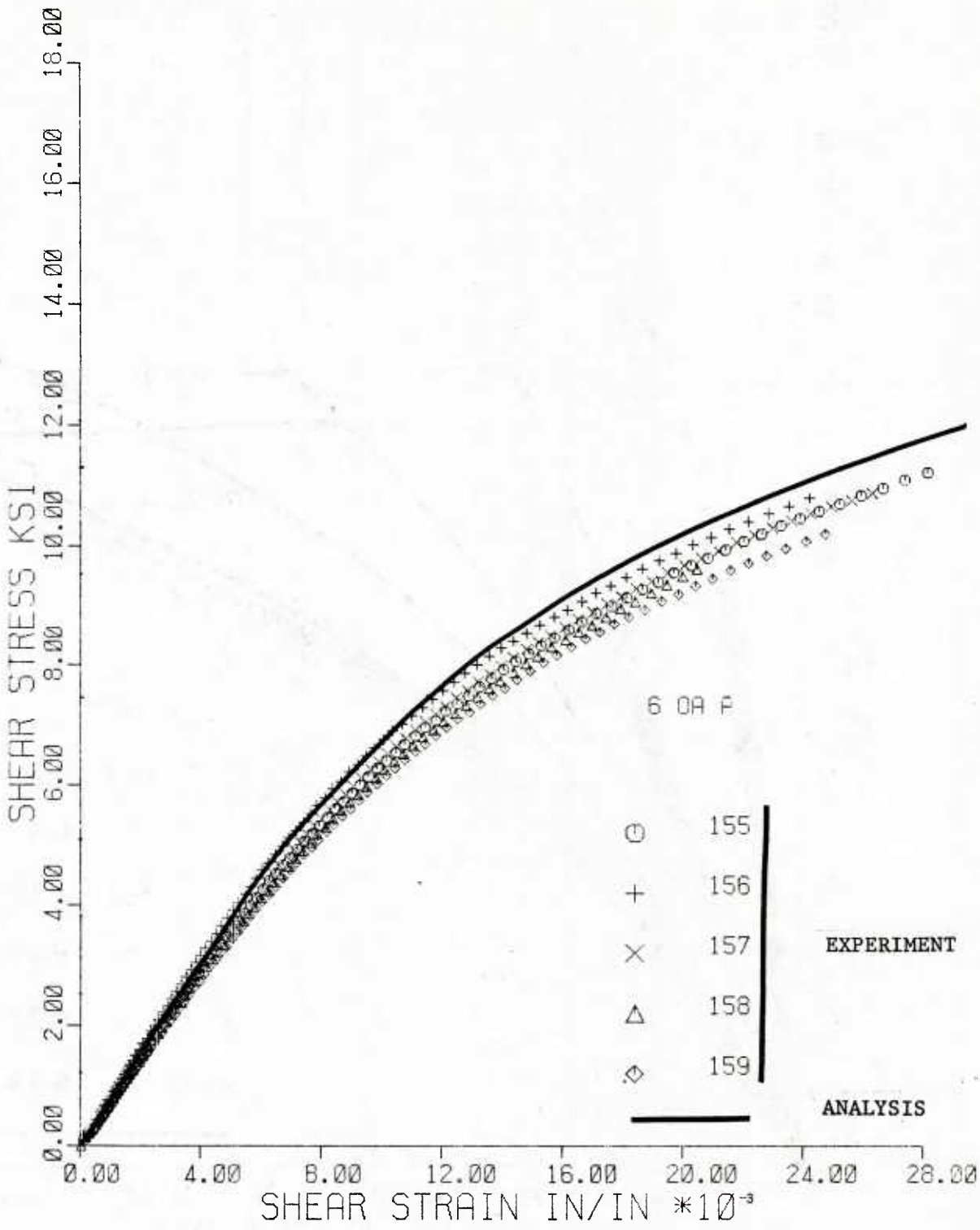

Figure 17. Shear Stress (τ_{12}) versus Shear Strain (γ_{12}) Curves for 6^{o} Off-axis Specimens with Square Tabs and Fixed Grips

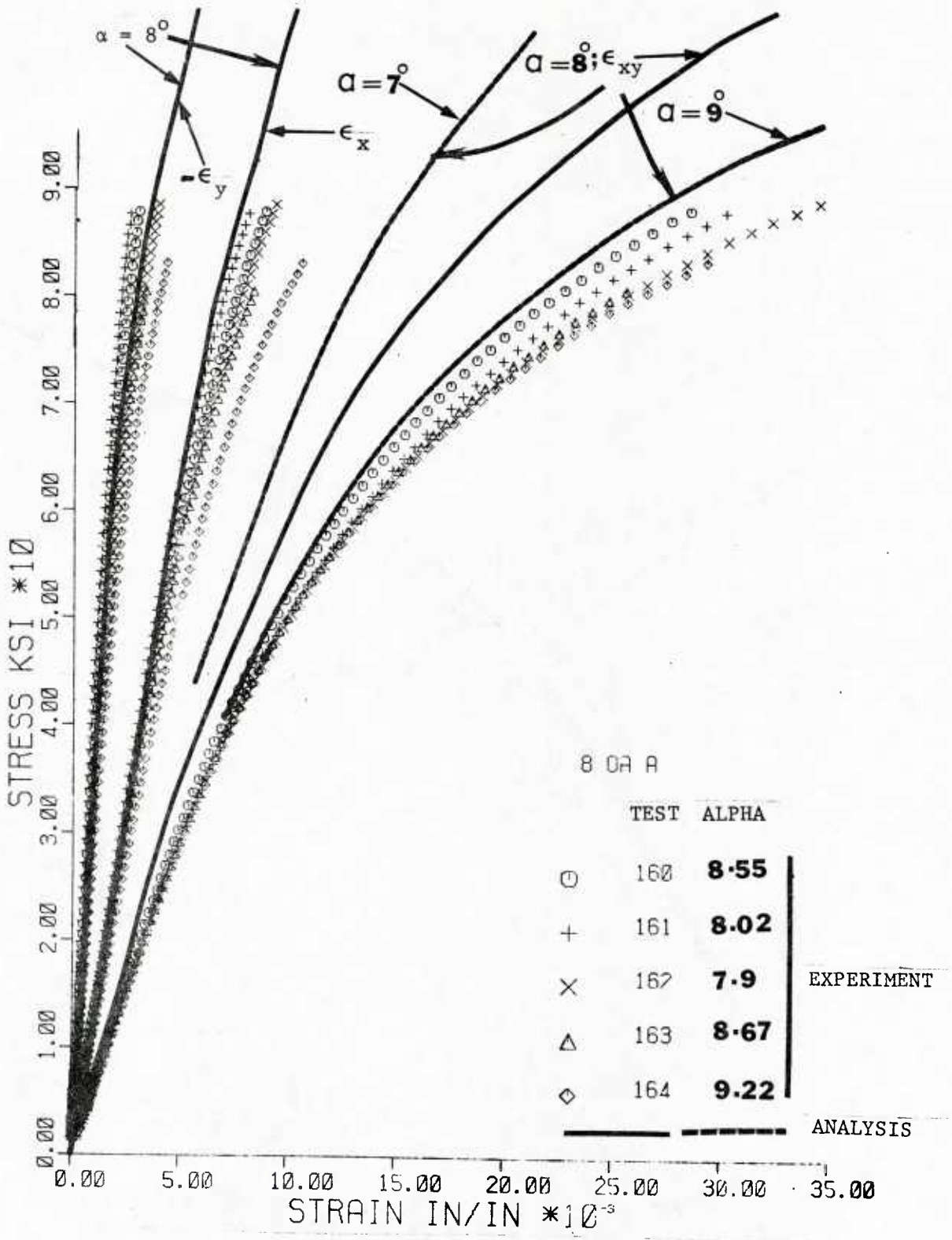

Figure 18. Axial Stress versus Axial, Transverse, and Shear Strain Curves for 8° (nominal) Off-axis Specimens with Square Tabs and Fixed Grips.

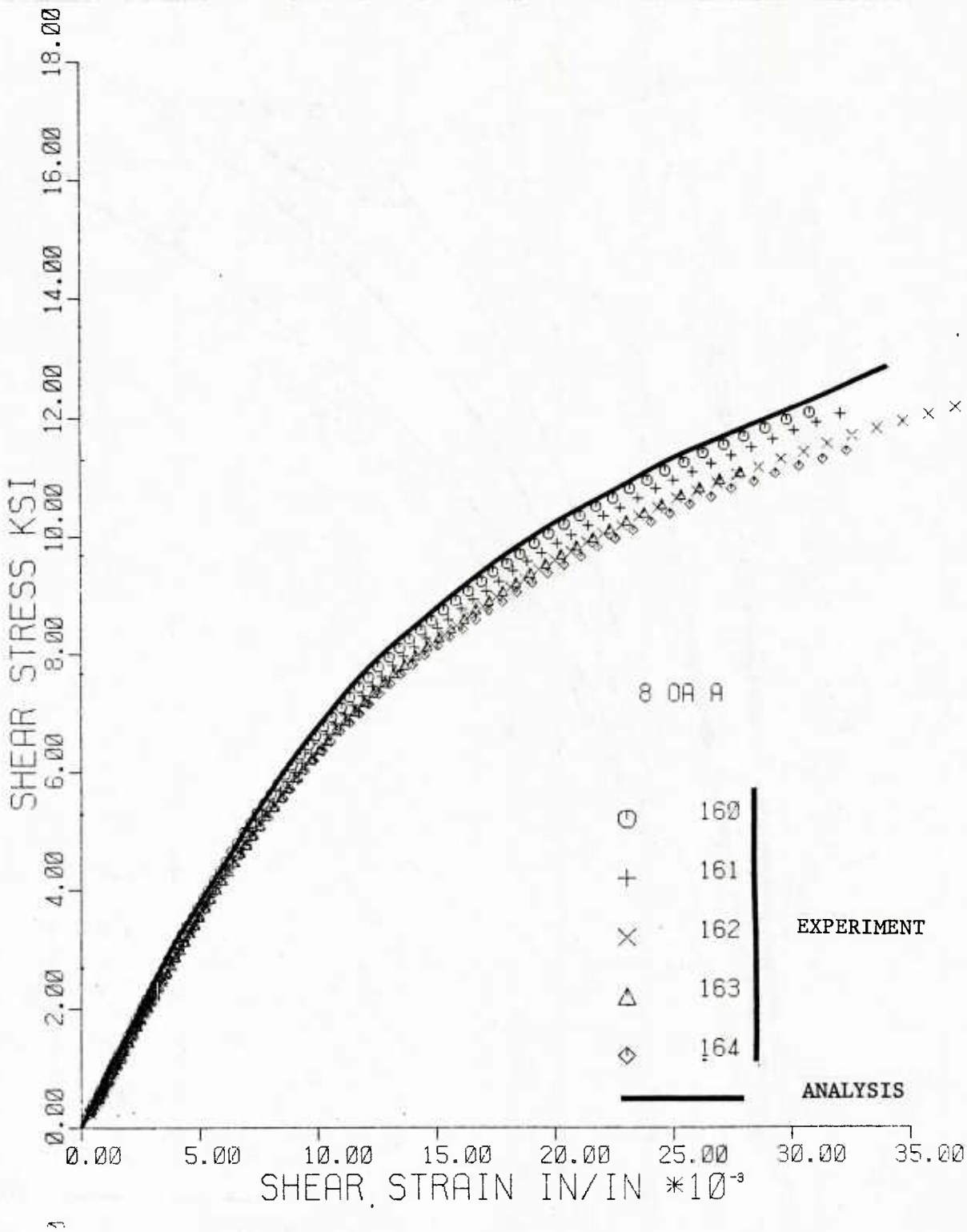

Figure 19. Shear Stress (τ_{12}) versus Shear Strain (γ_{12}) Curves for 8° Off-axis Specimens with Square Tabs and Fixed Grips

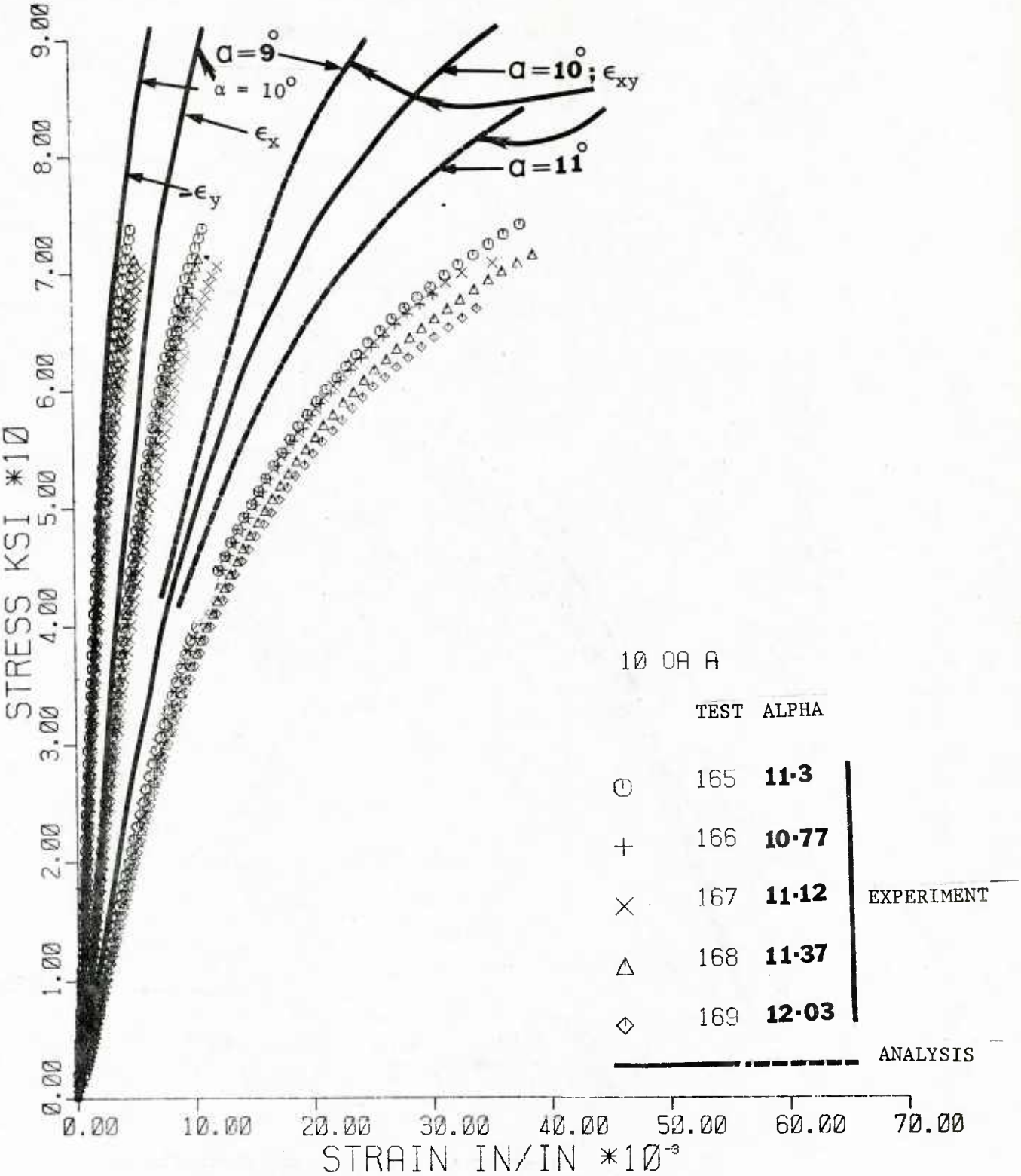

Figure 20. Axial Stress versus Axial, Transverse, and Shear Strain Curves for 10° (nominal) Off-axis Specimens with Square Tabs and Fixed Grips

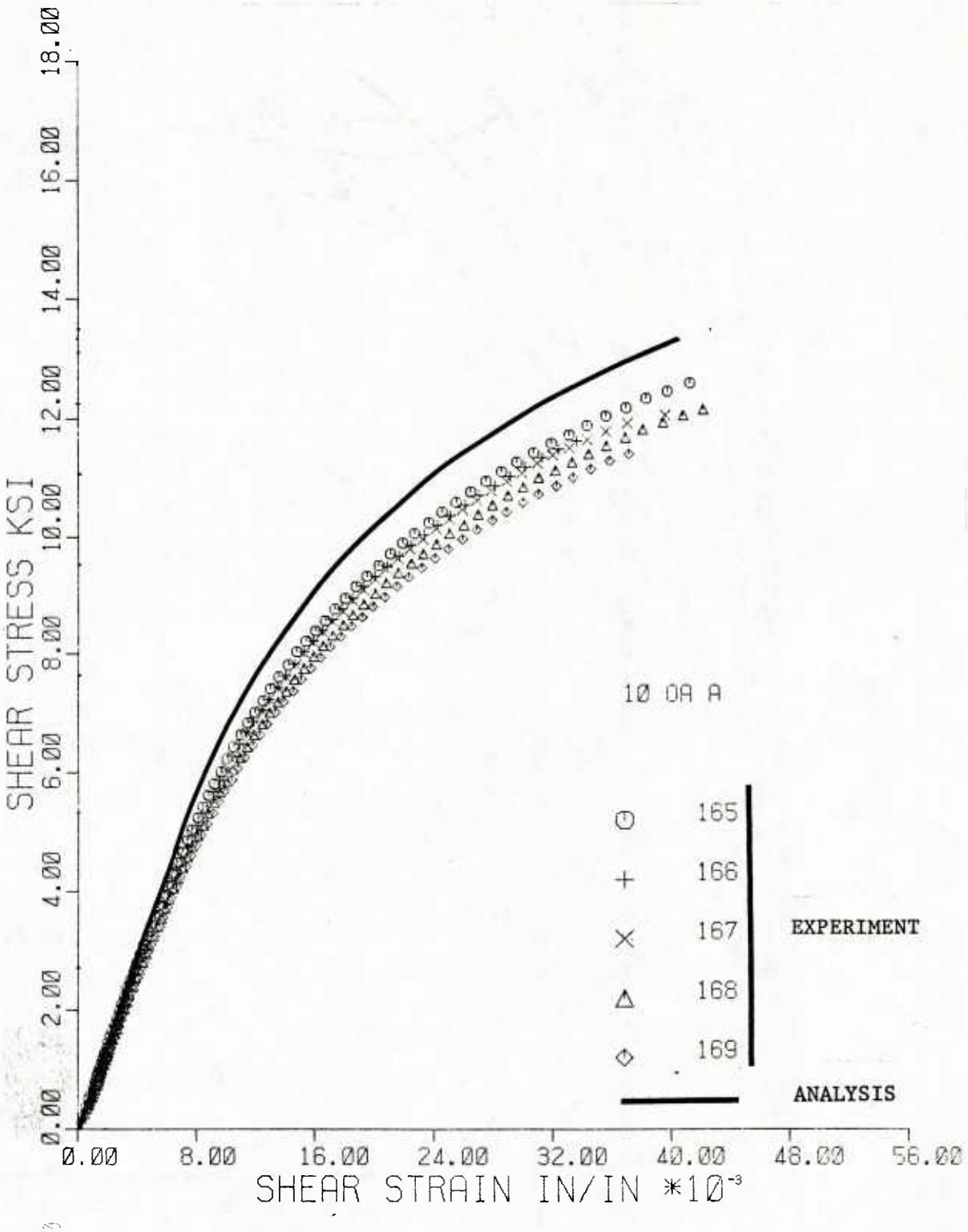

Figure 21. Shear Stress (τ_{12}) versus Shear Strain (γ_{12}) Curves for 10^{o} Off-axis Specimens with Square Tabs and Fixed Grips

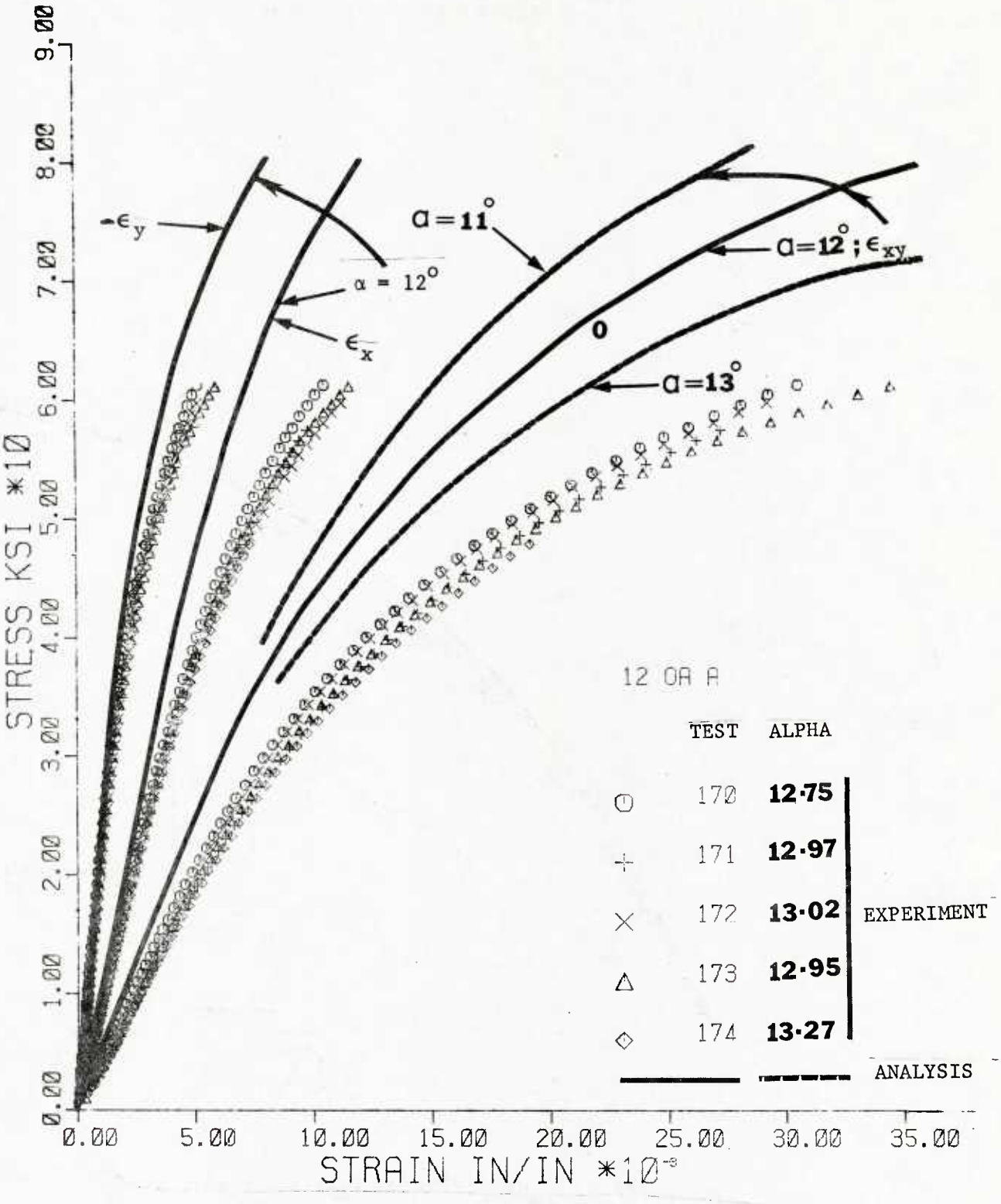

Figure 22. Axial Stress versus Axial, Transverse, and Shear Strain Curves for 12° (nominal) Off-axis Specimens with Square Tabs and Fixed Grips

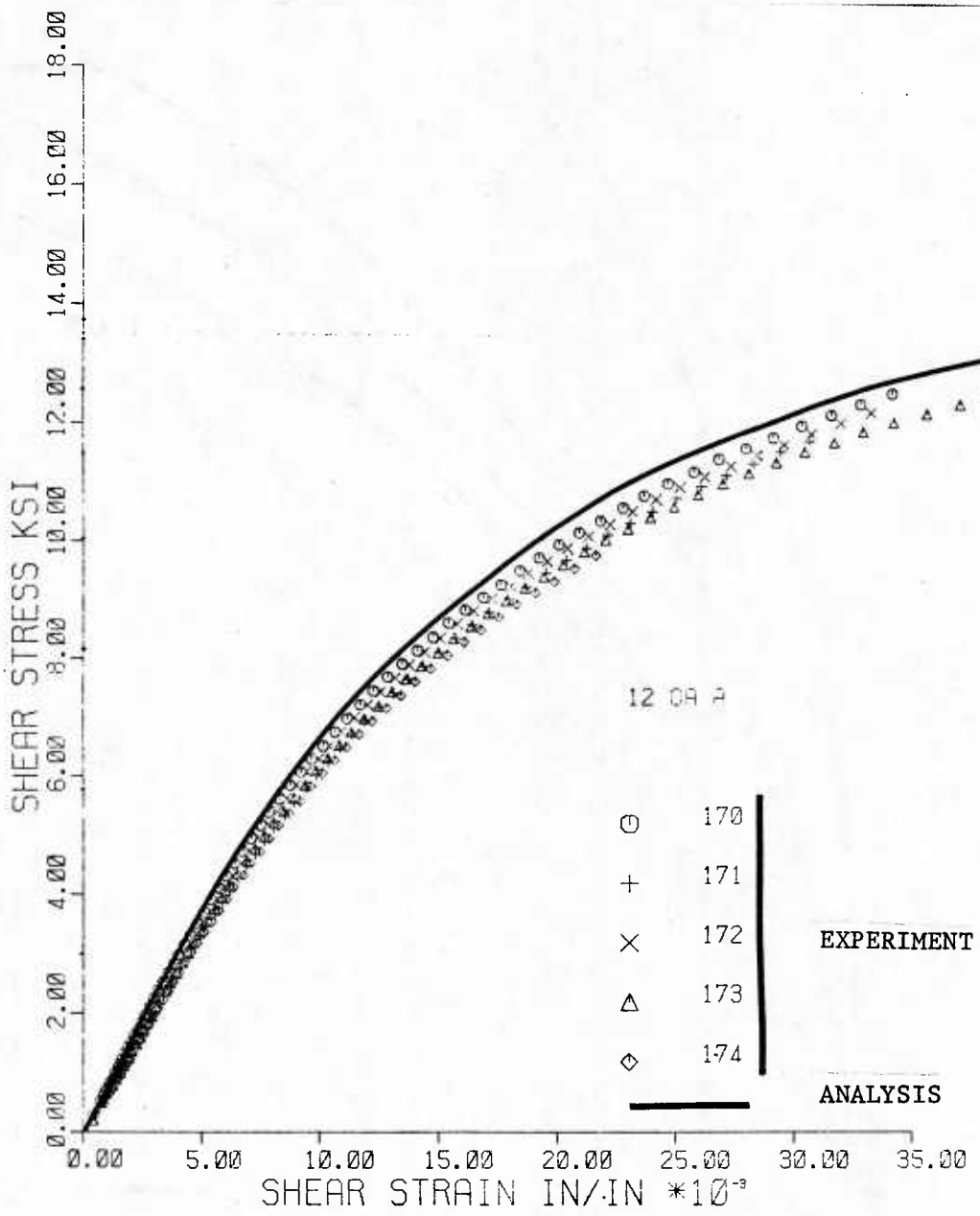

Figure 23. Shear Stress (τ_{12}) and Shear Strain (γ_{12}) Curves for 12° Off-axis Specimens with Square Tabs and Fixed Grips

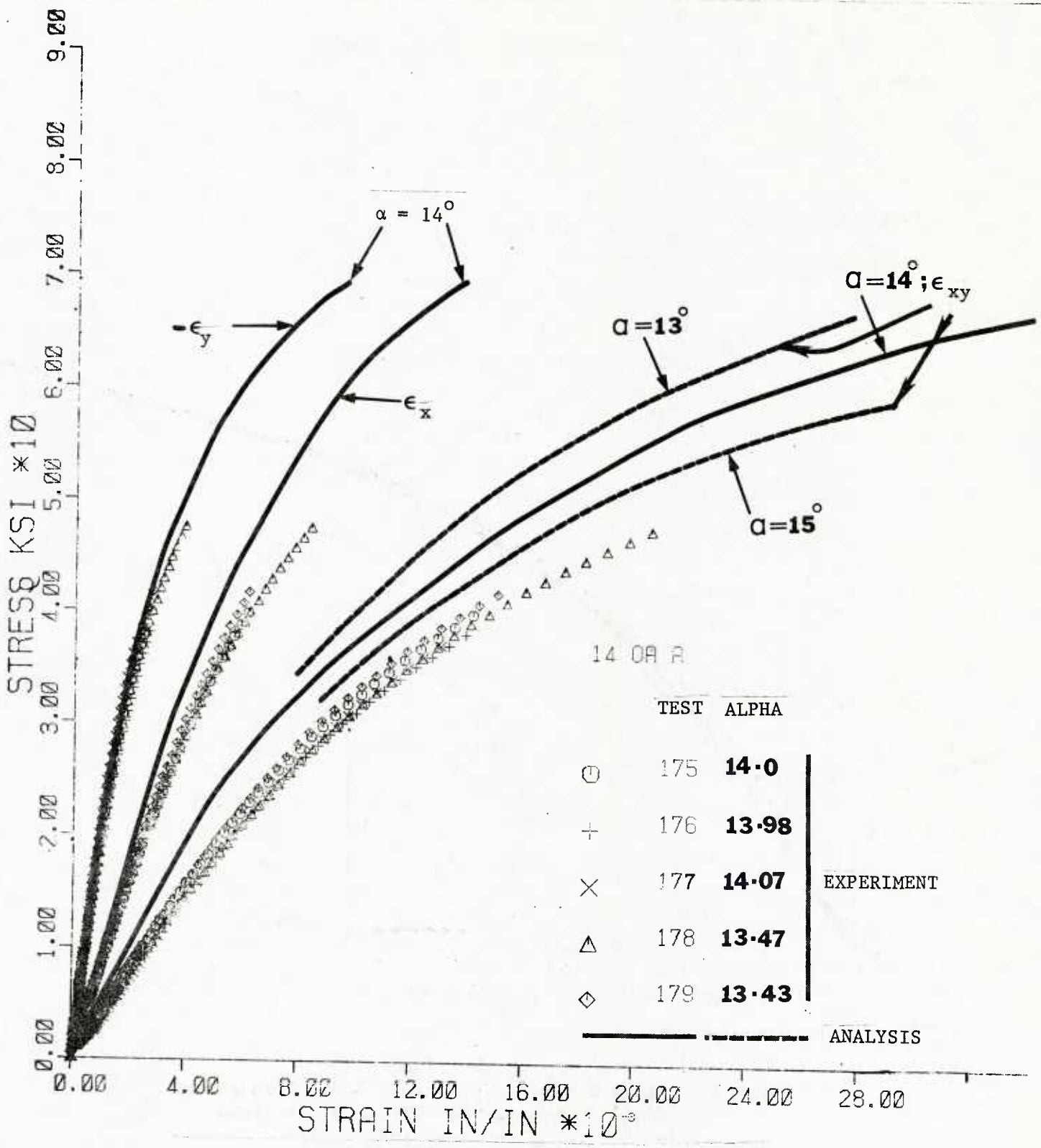

Figure 24. Axial Stress versus Axial, Transverse, and Shear Strain Curves for 14° (nominal) Off-axis Specimens with Square Tabs and Fixed Grips

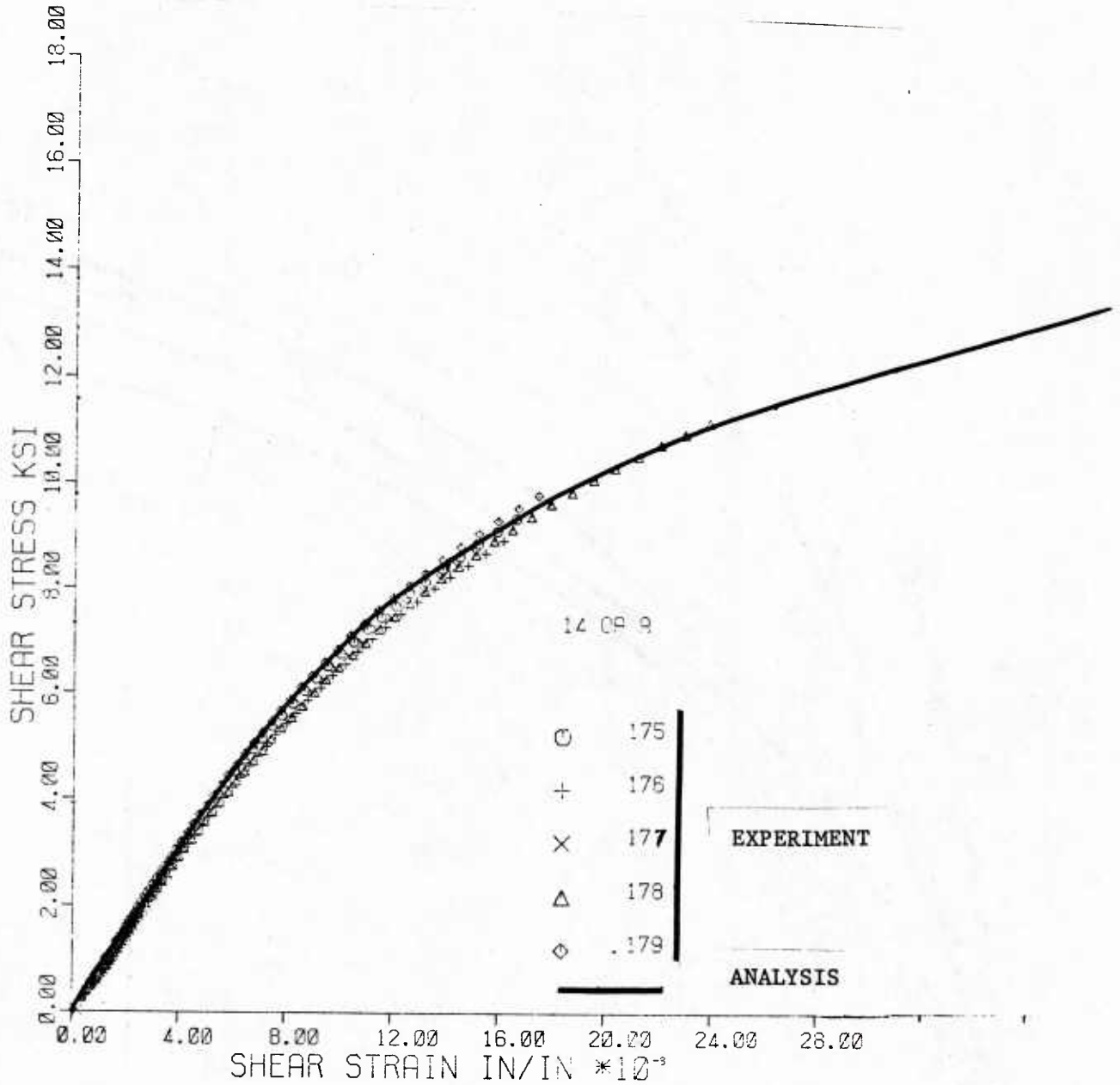

Figure 25. Shear Stress (τ_{12}) versus Shear Strain (γ_{12}) Curves for 14° Off-axis Specimens with Square Tabs and Fixed Grips

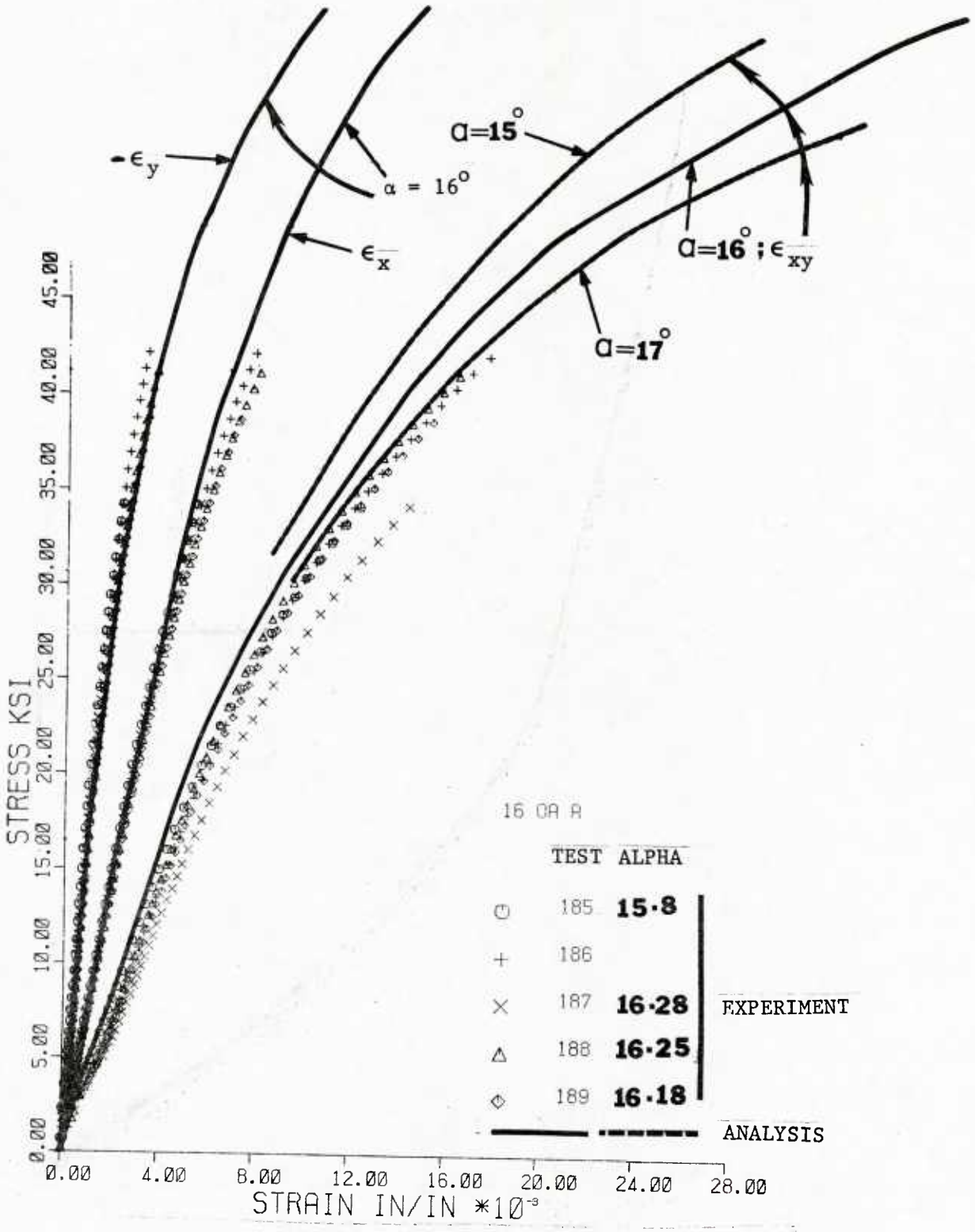

Figure 26. Axial Stress versus Axial, Transverse, and Shear Strain Curves for 16° (nominal) Off-axis Specimens with Square Tabs and Fixed Grips

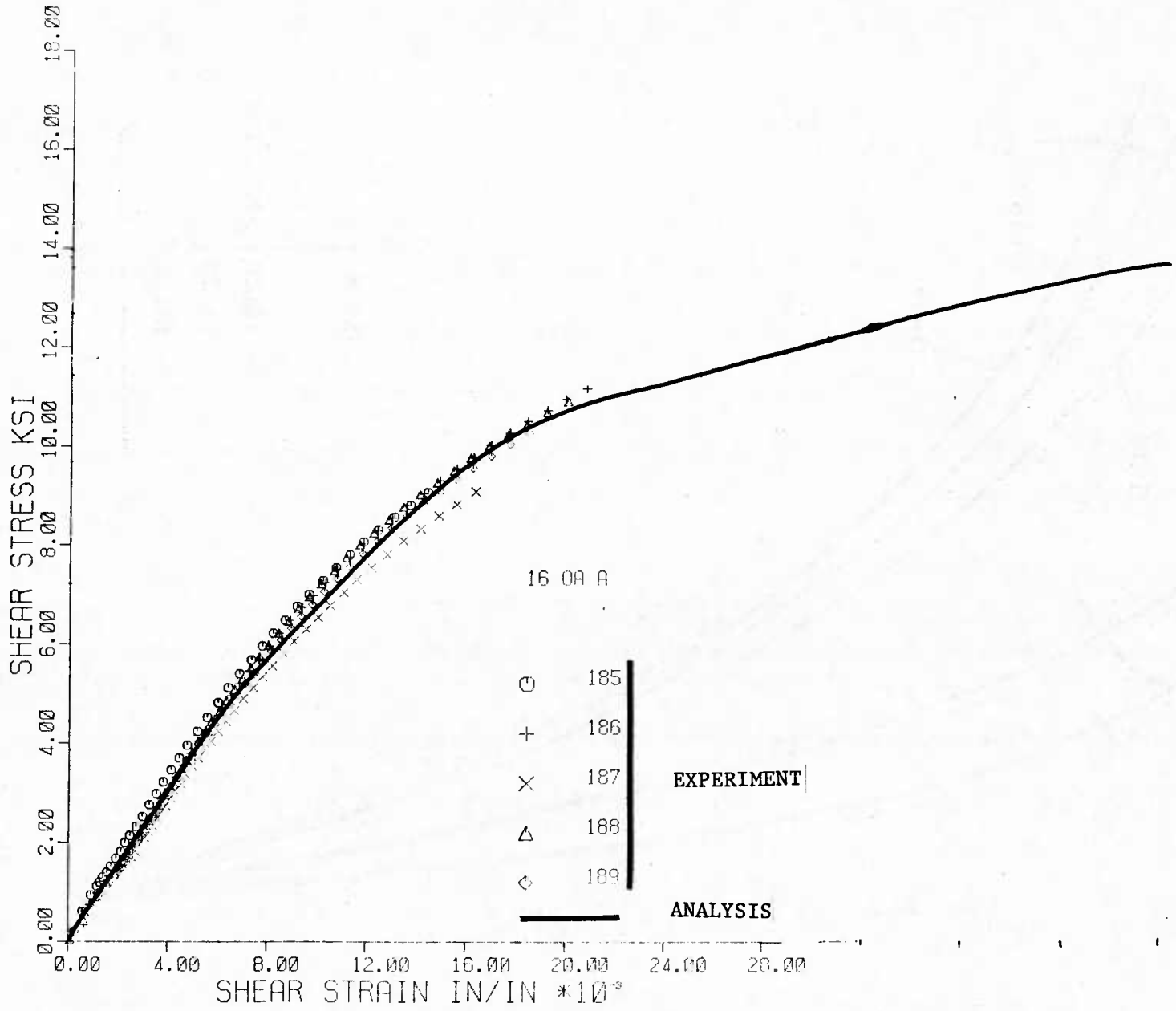

Figure 27. Shear Stress (τ_{12}) versus Shear Strain (γ_{12}) Curves for 16° Off-axis Specimens with Square Tabs and Fixed Grips

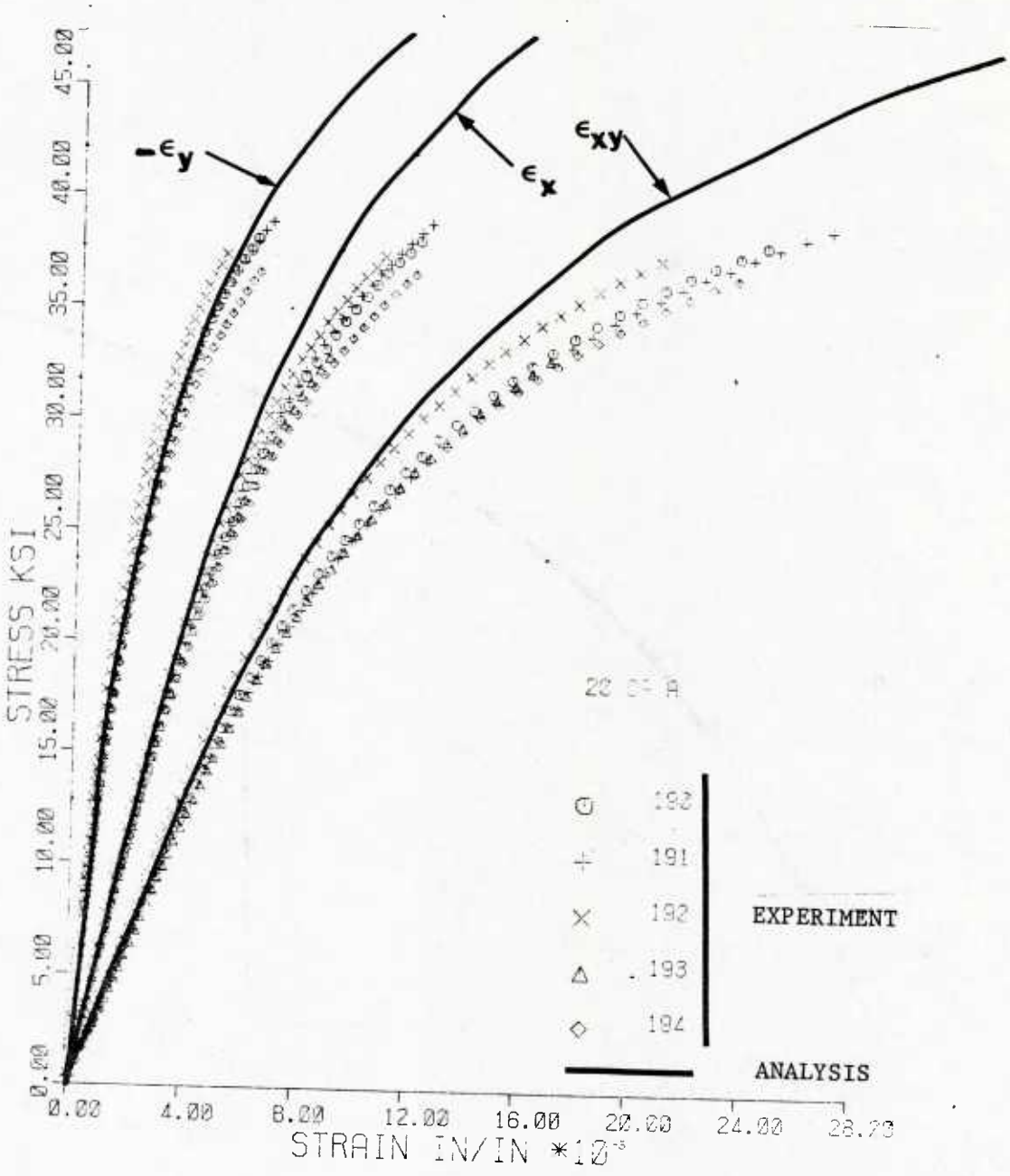

Figure 28. Axial Stress versus Axial, Transverse, and Shear Strain Curves for 20° Off-axis Specimens with Square Tabs and Fixed Grips

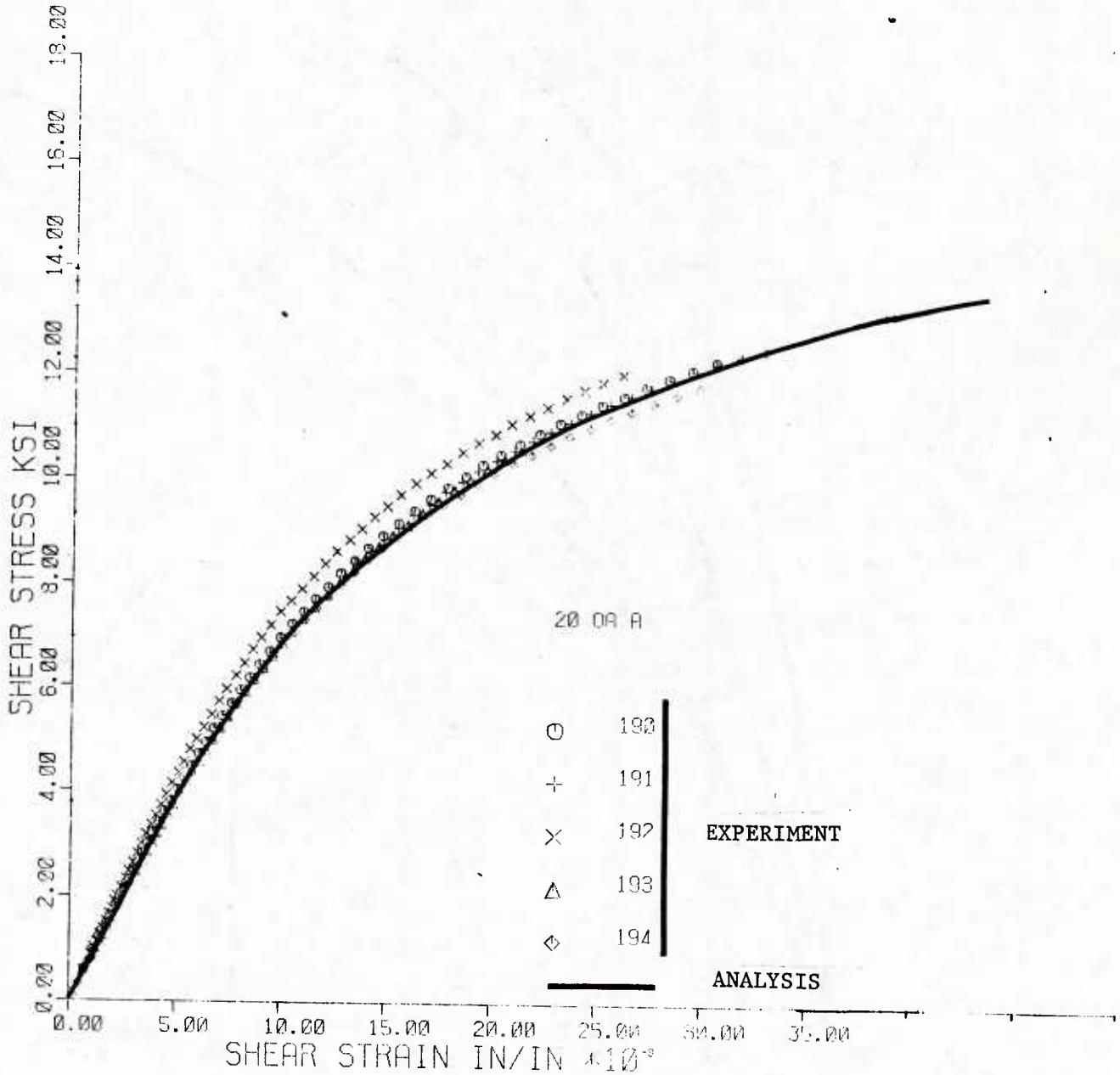

Figure 29. Shear Stress (τ_{12}) versus Shear Strain (γ_{12}) Curves for 20^{o} Off-axis Specimens with Square Tabs and Fixed Grips

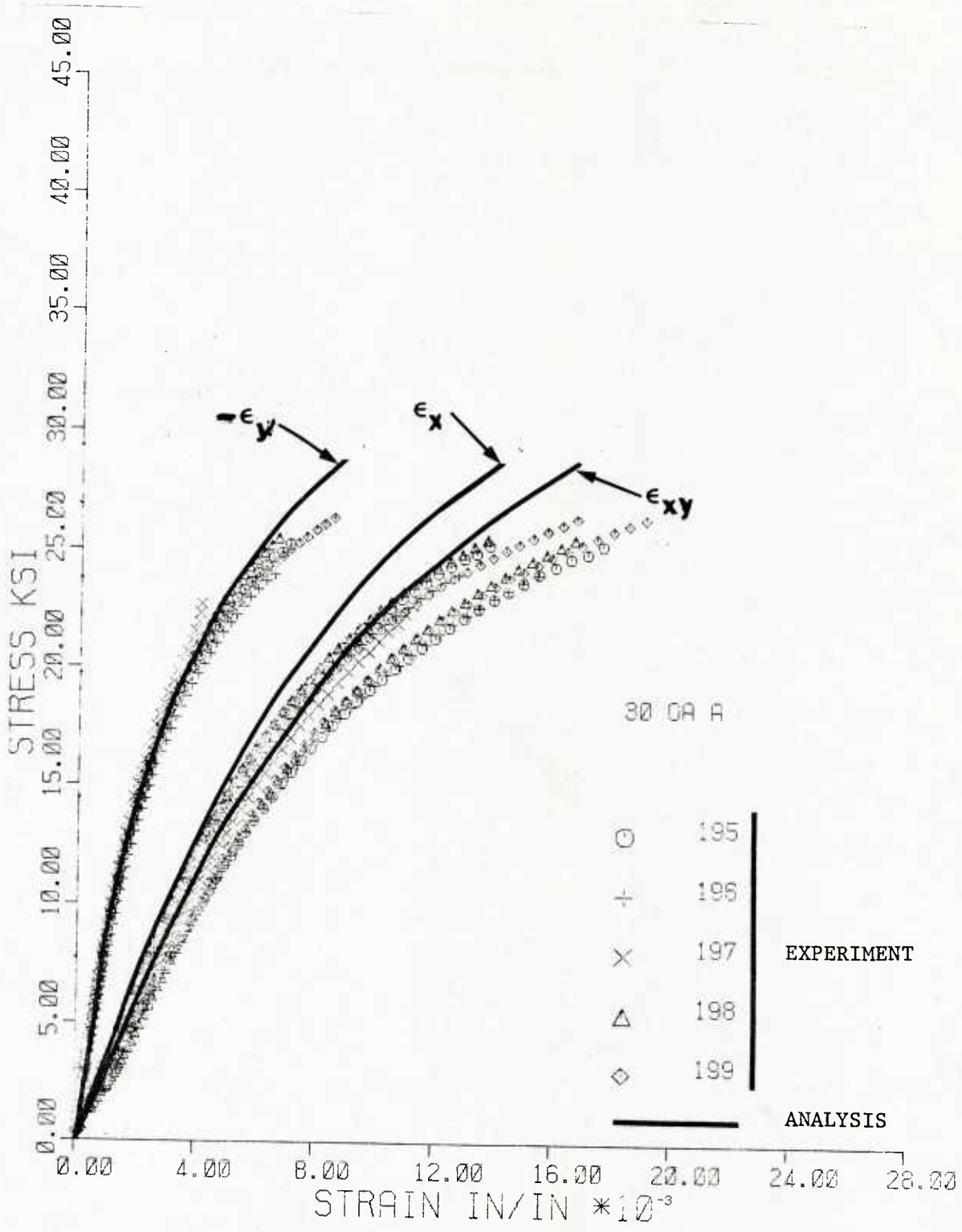

Figure 30. Axial Stress versus Axial, Transverse, and Shear Strain Curves for 30° Off-axis Specimens with Square Tabs and Fixed Grips

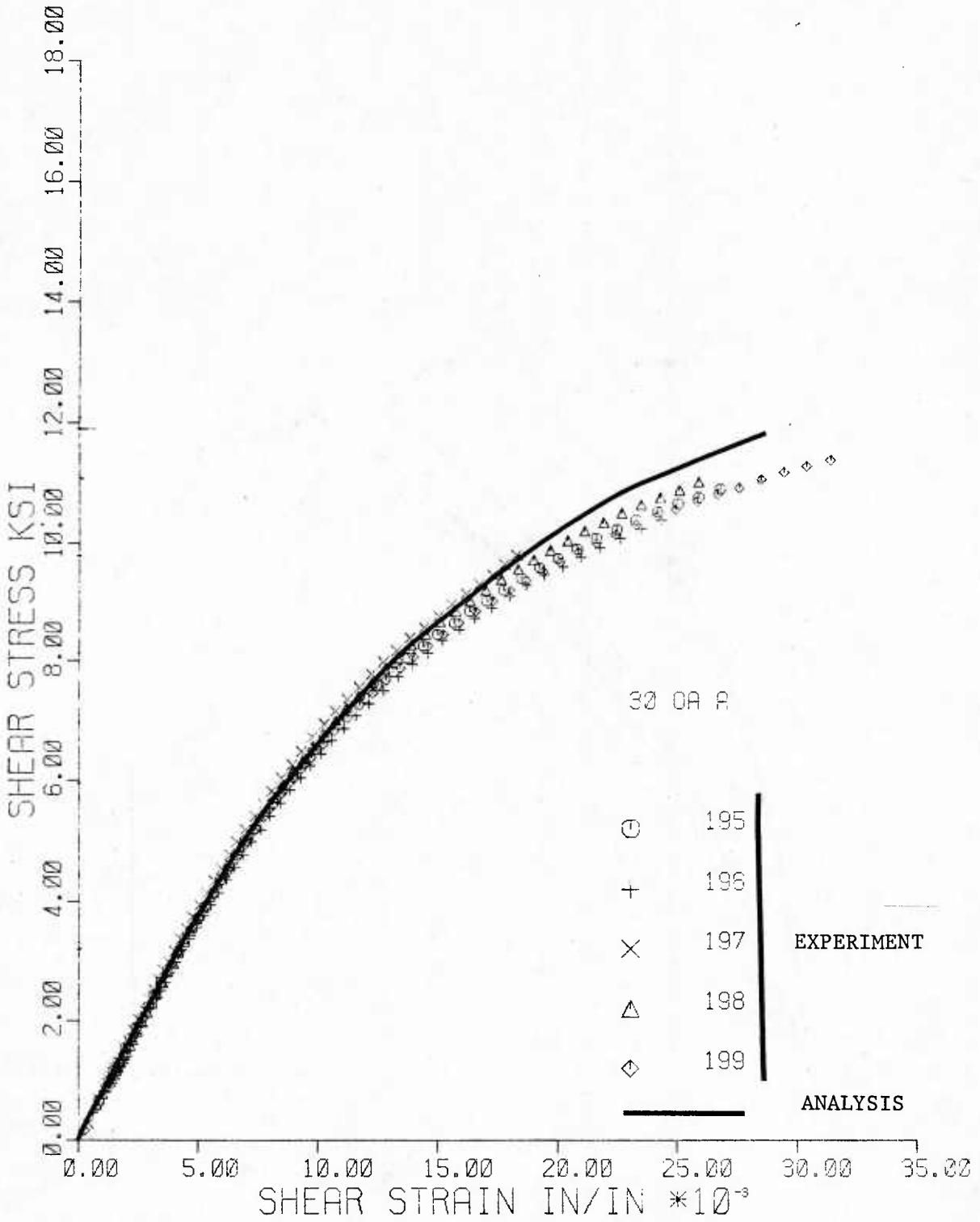

Figure 31. Shear Stress (τ_{12}) versus Shear Strain (γ_{12}) Curves for 30° Off-axis Specimens with Square Tabs and Fixed Grips

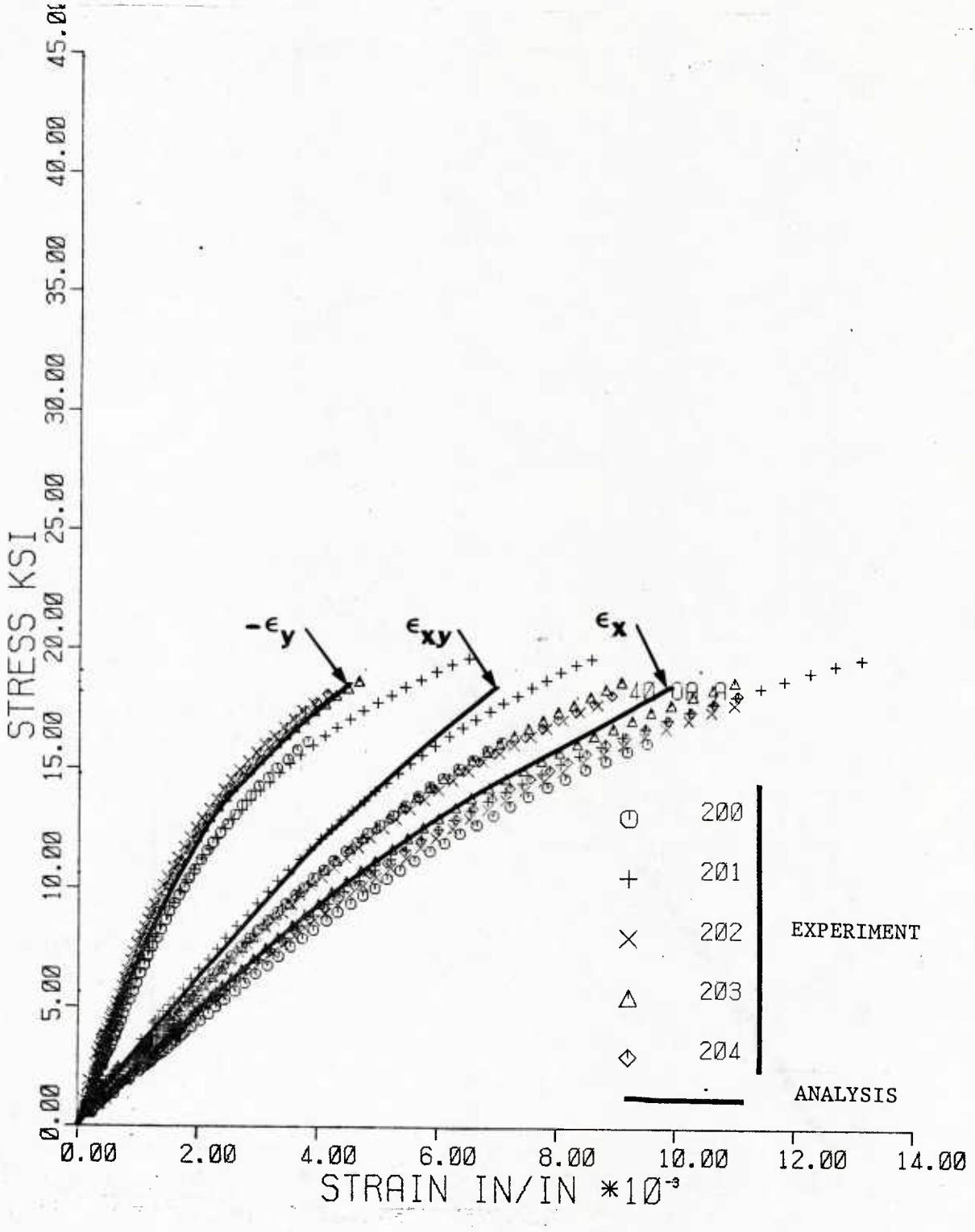

Figure 32. Axial Stress versus Axial, Transverse, and Shear Strain Curves for 40^{o} Off-axis Specimens with Square Tabs and Fixed Grips

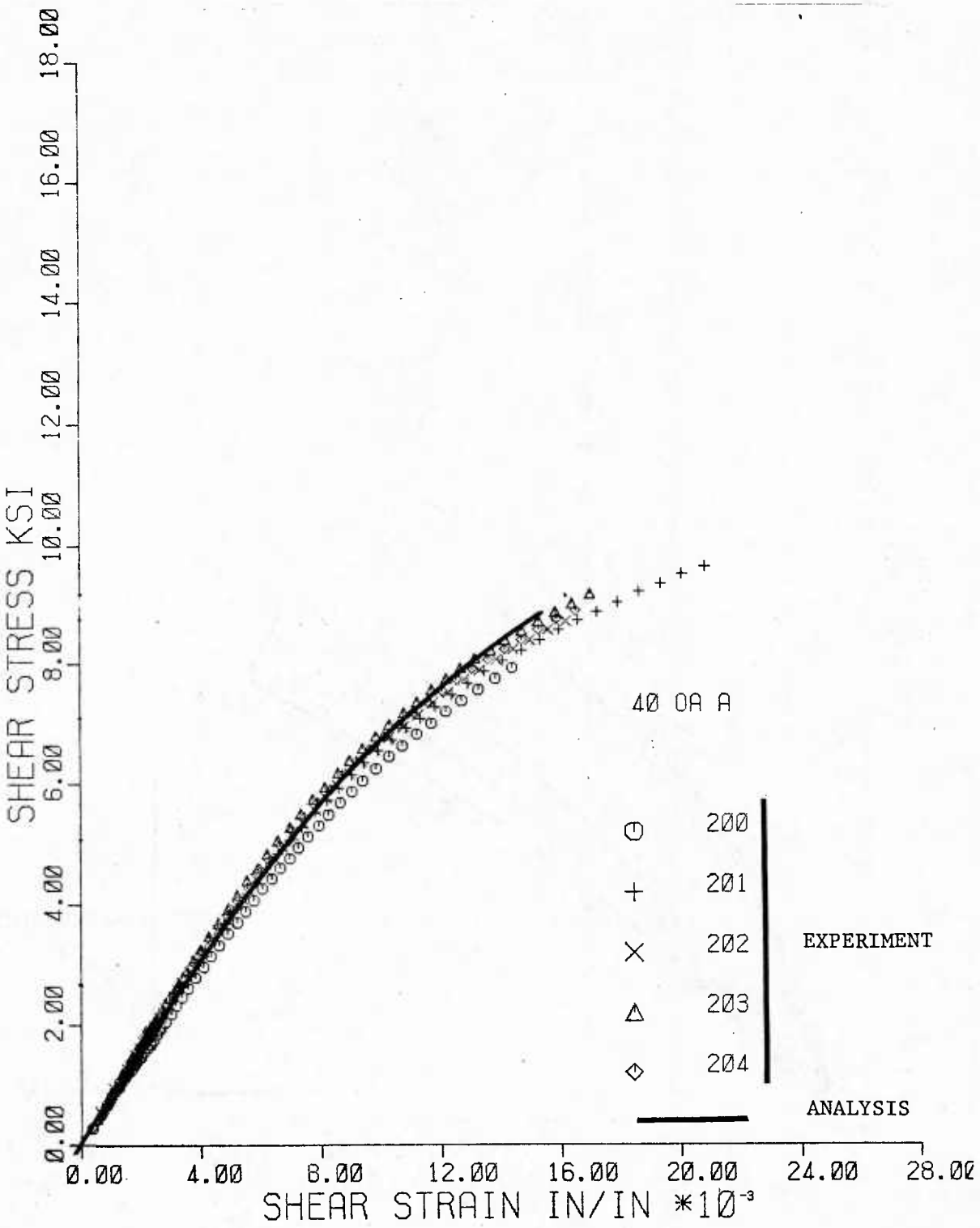

Figure 33. Shear Stress (τ_{12}) versus Shear Strain (γ_{12}) Curves for 40^{o} Off-axis Specimens with Square Tabs and Fixed Grips

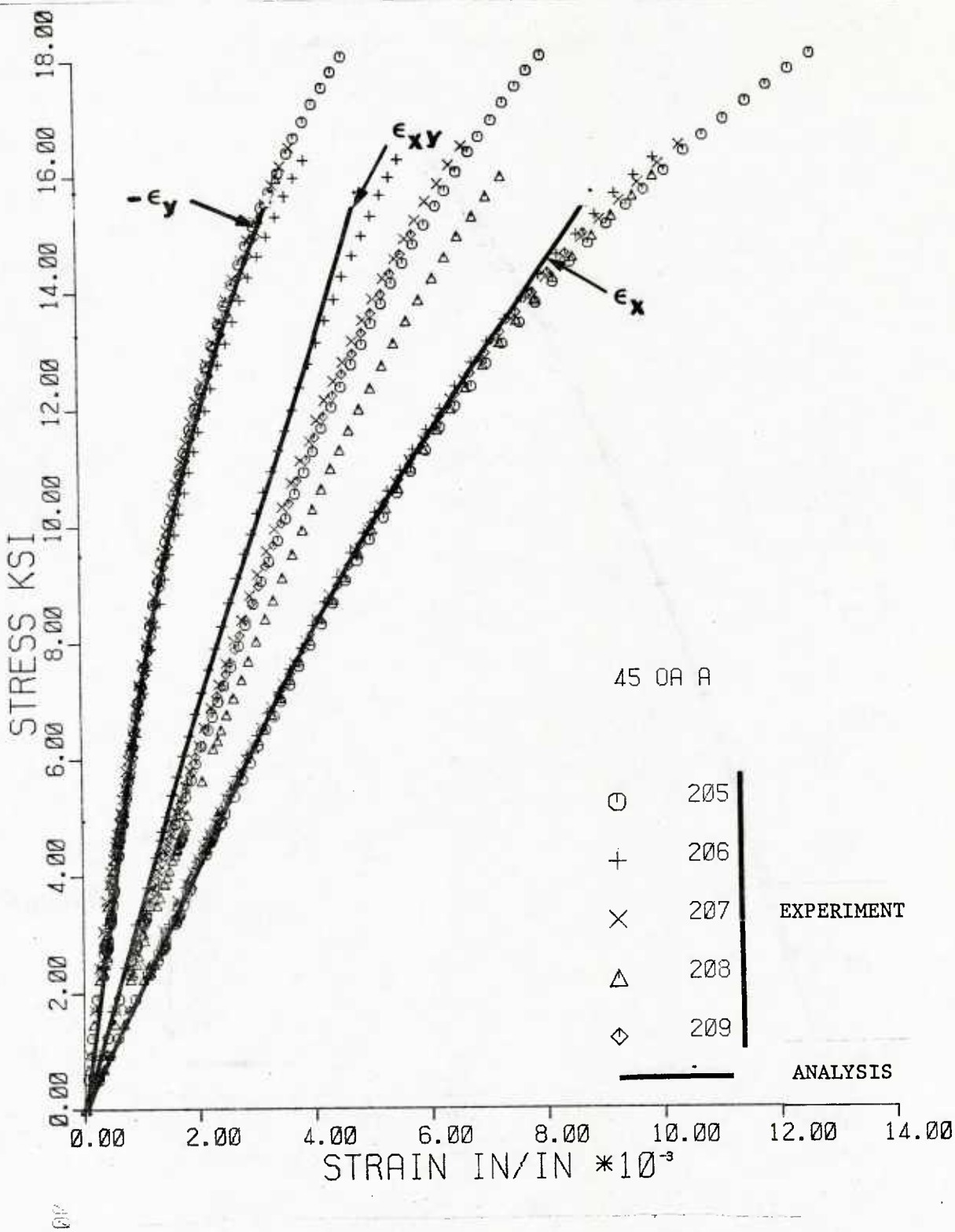

Figure 34. Axial Stress versus Axial, Transverse, and Shear Strain Curves for 45° Off-axis Specimens with Square Tabs and Fixed Grips

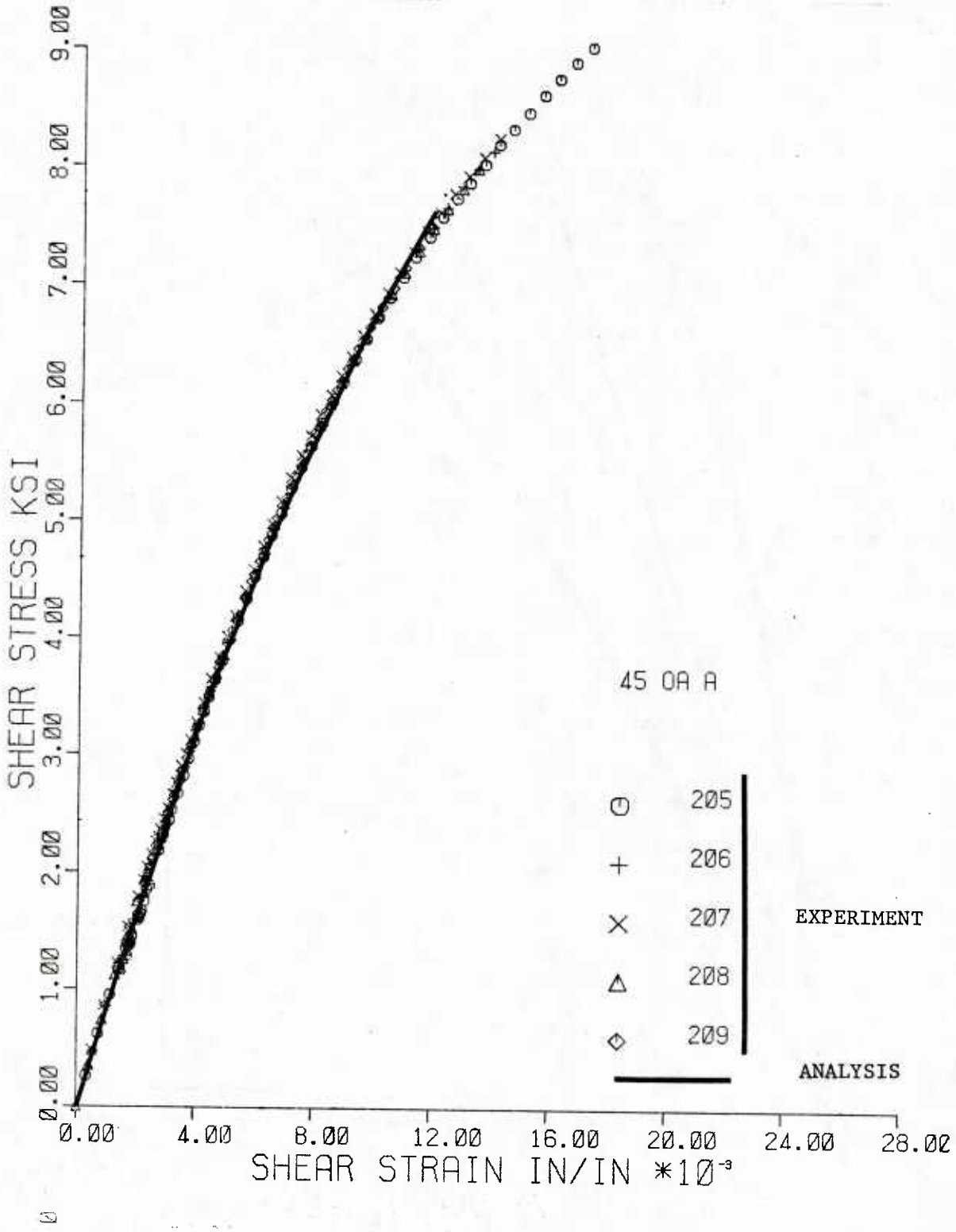

Figure 35. Shear Stress (τ_{12}) versus Shear Strain (γ_{12}) Curves for 45° Off-axis Specimens with Square Tabs and Fixed Grips

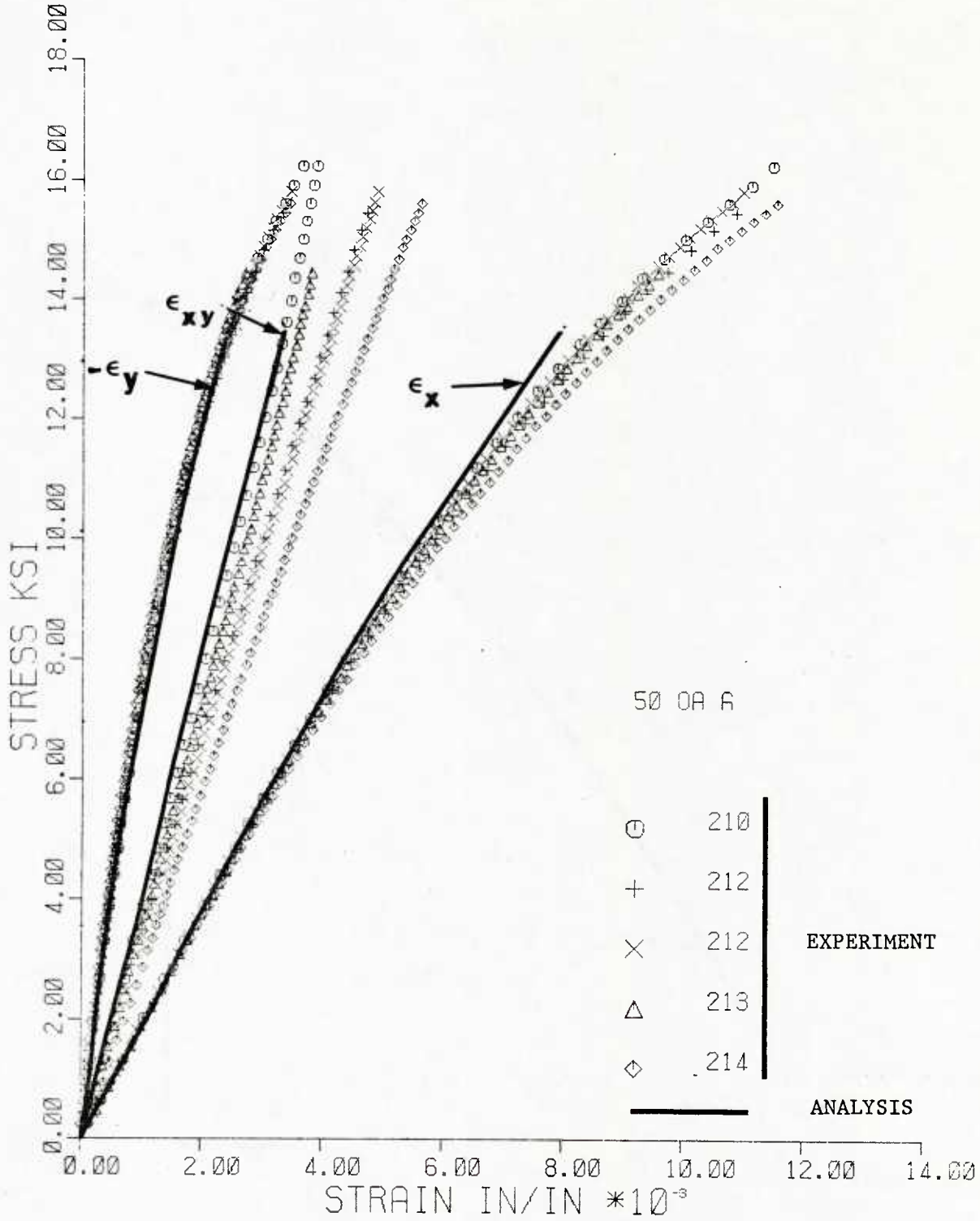

Figure 36. Axial Stress versus Axial, Transverse, and Shear Strain Curves for 50° Off-axis Specimens with Square Tabs and Fixed Grips

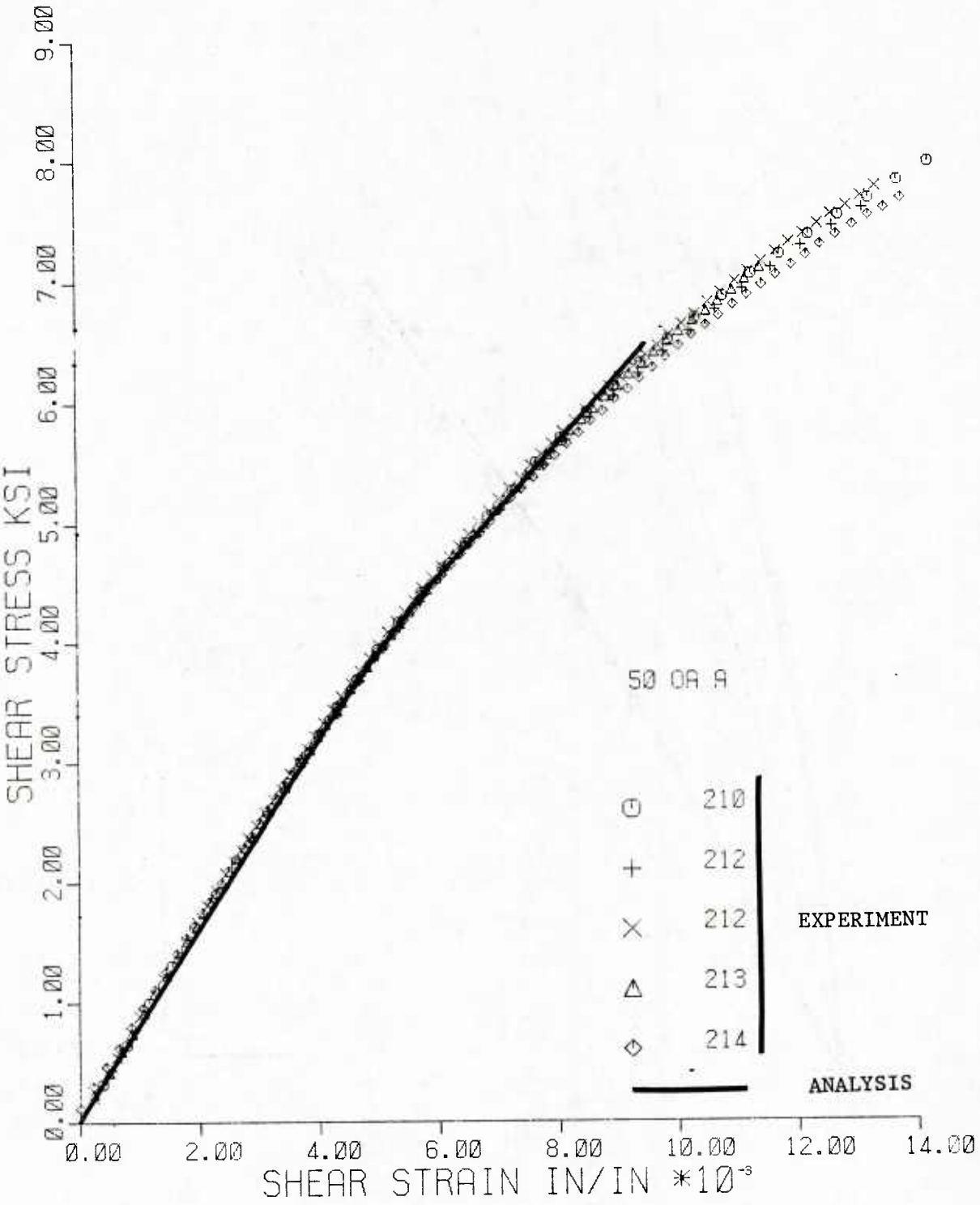

Figure 37. Shear Stress (τ_{12}) versus Shear Strain (γ_{12}) Curves for 50^{o} Off-axis Specimens with Square Tabs and Fixed Grips

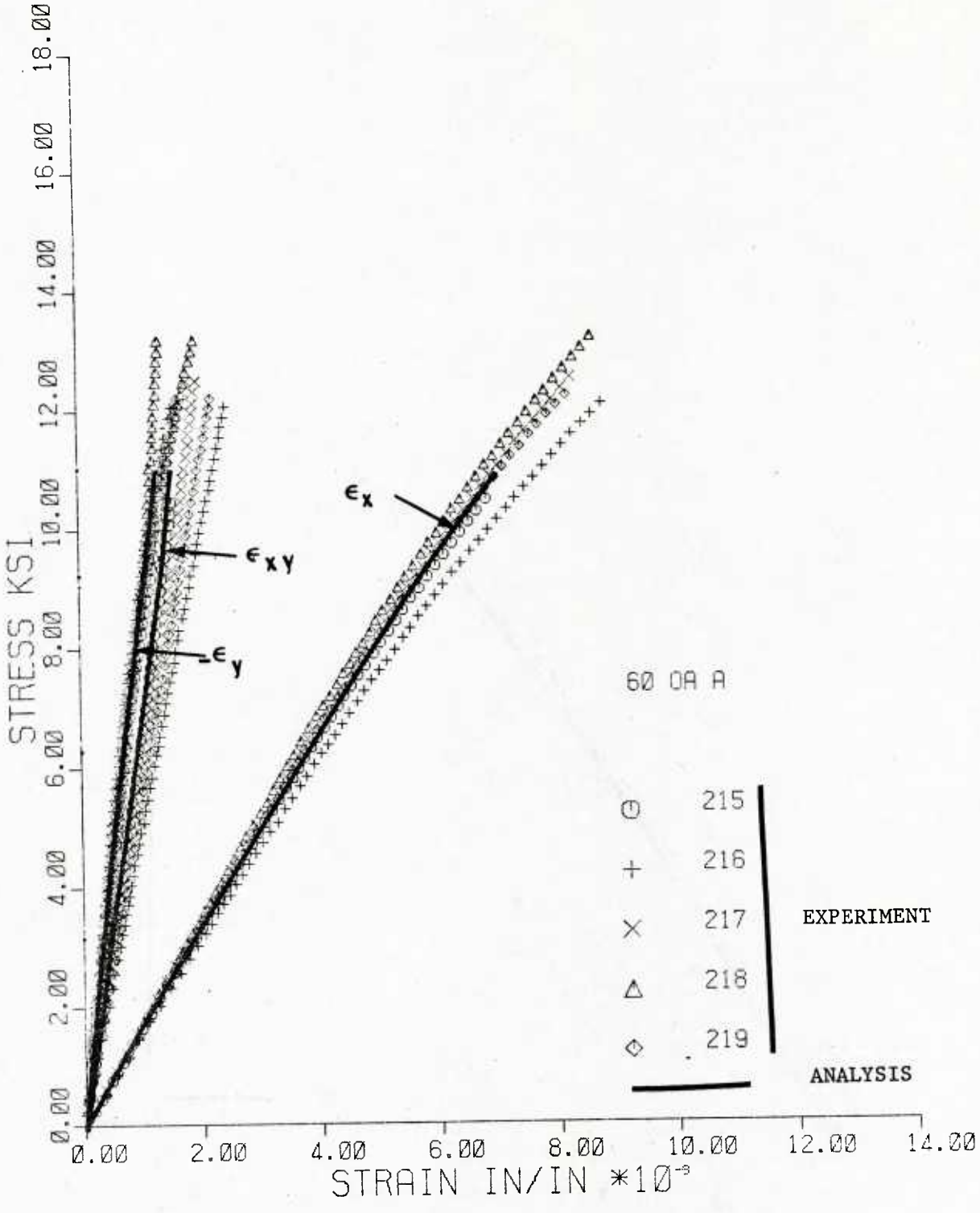

Figure 38. Axial Stress versus Axial, Transverse, and Shear Strain Curves for 60° Off-axis Specimens with Square Tabs and Fixed Grips

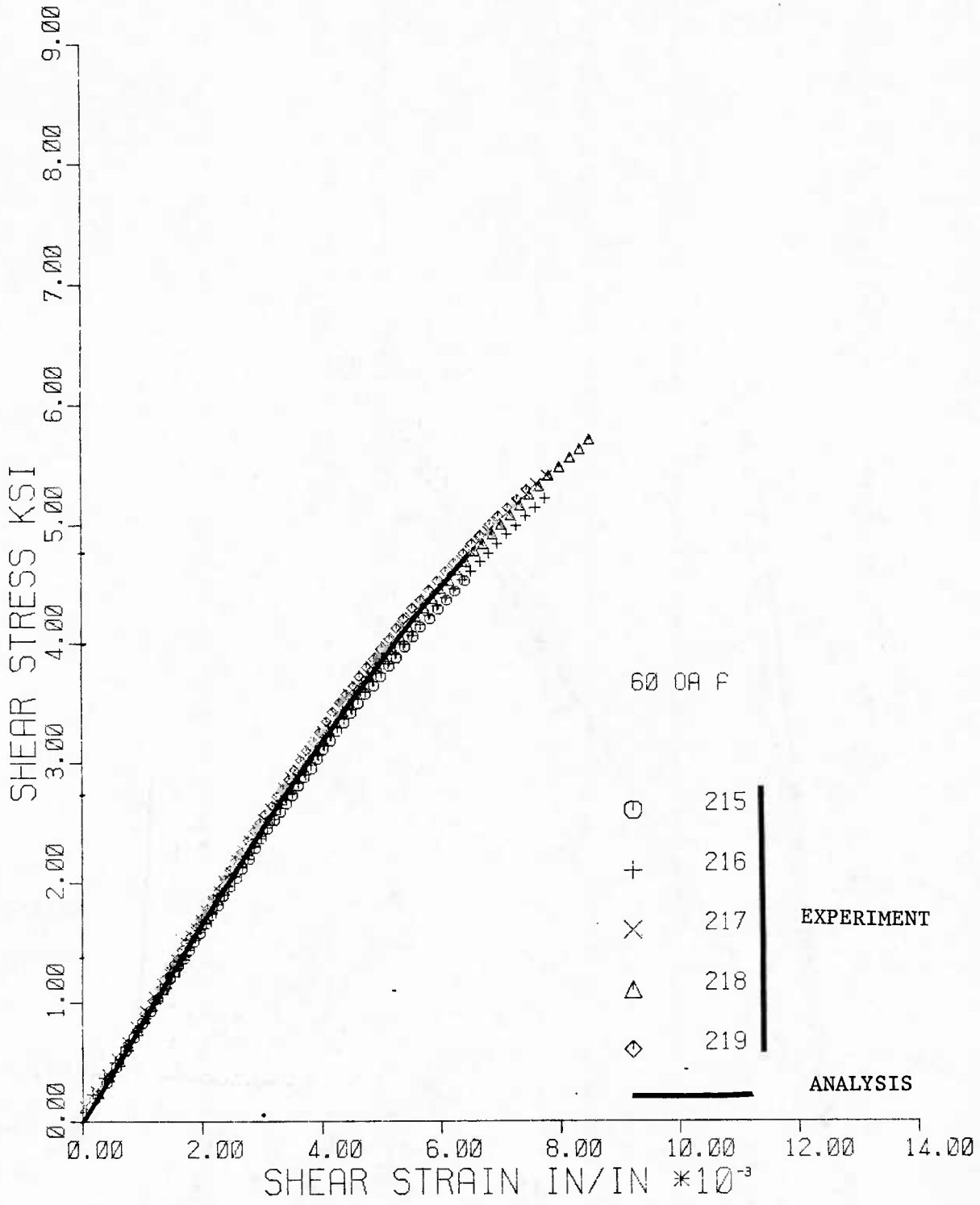

Figure 39. Shear Stress (τ_{12}) versus Shear Strain (γ_{12}) Curves for 60° Off-axis Specimens with Square Tabs and Fixed Grips

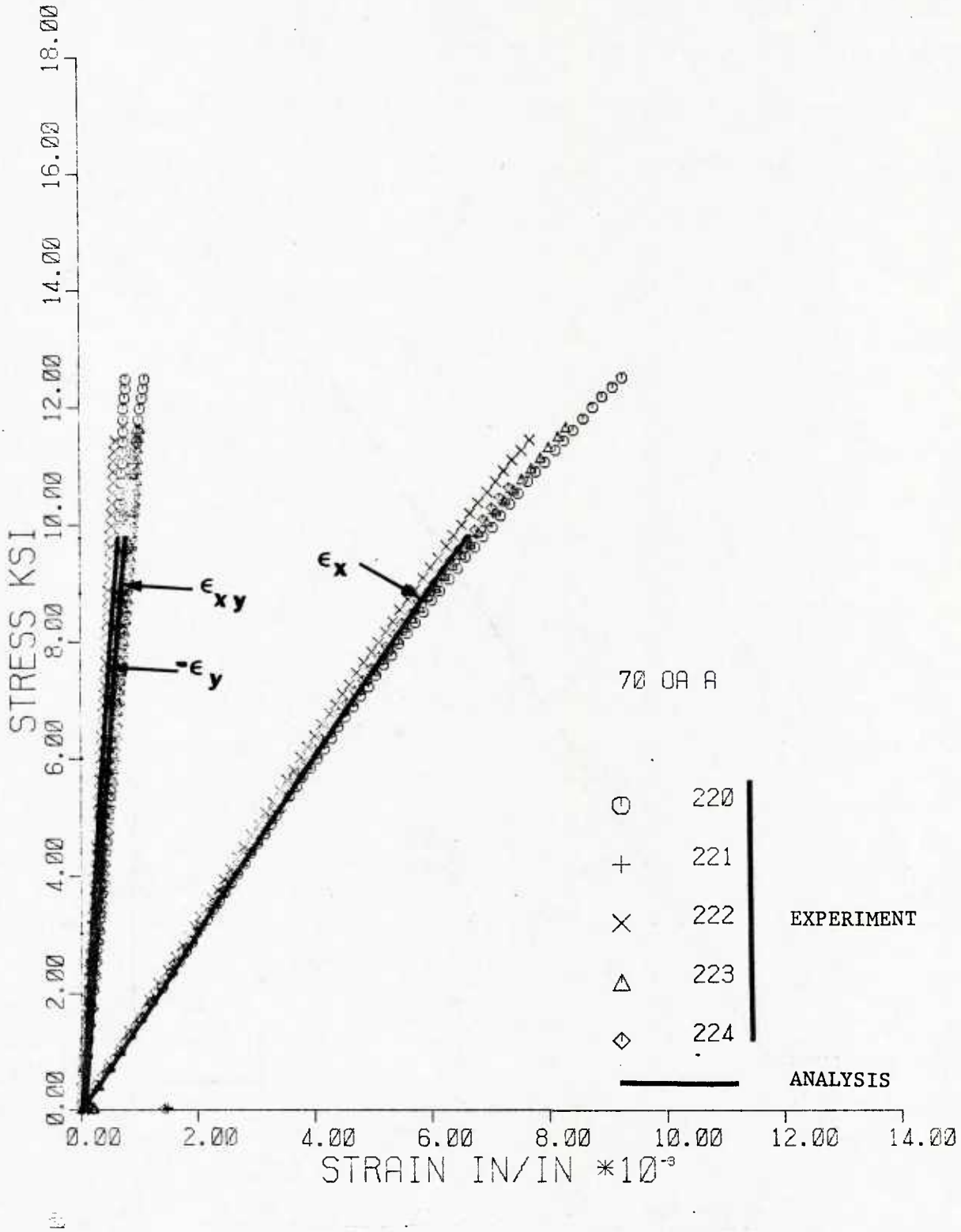

Figure 40. Axial Stress versus Axial, Transverse, and Shear Strain Curves for 70° Off-axis Specimens with Square Tabs and Fixed Grips

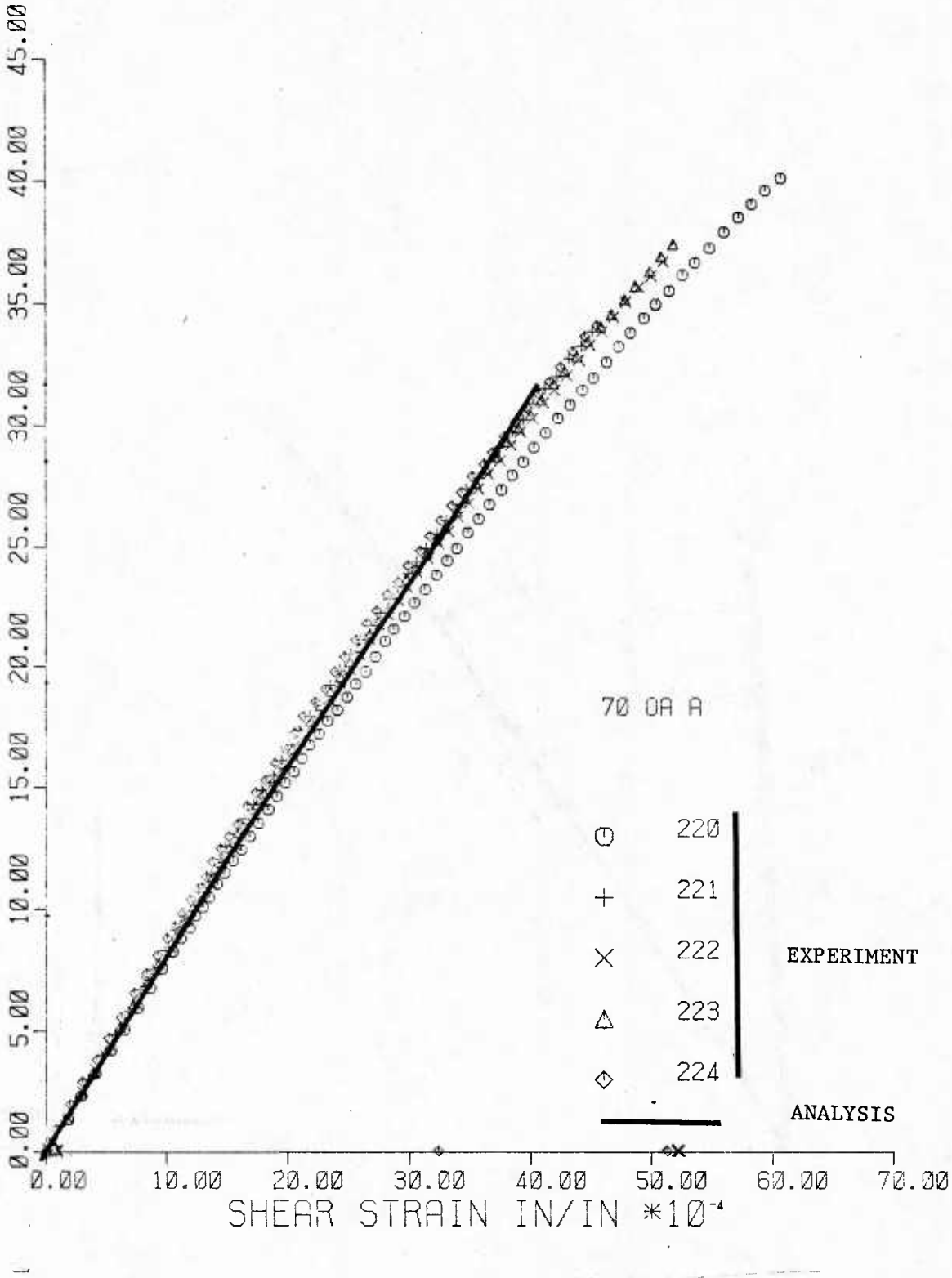

Figure 41. Shear Stress (τ_{12}) versus Shear Strain (γ_{12}) Curves for 70^{o} Off-axis Specimens with Square Tabs and Fixed Grips

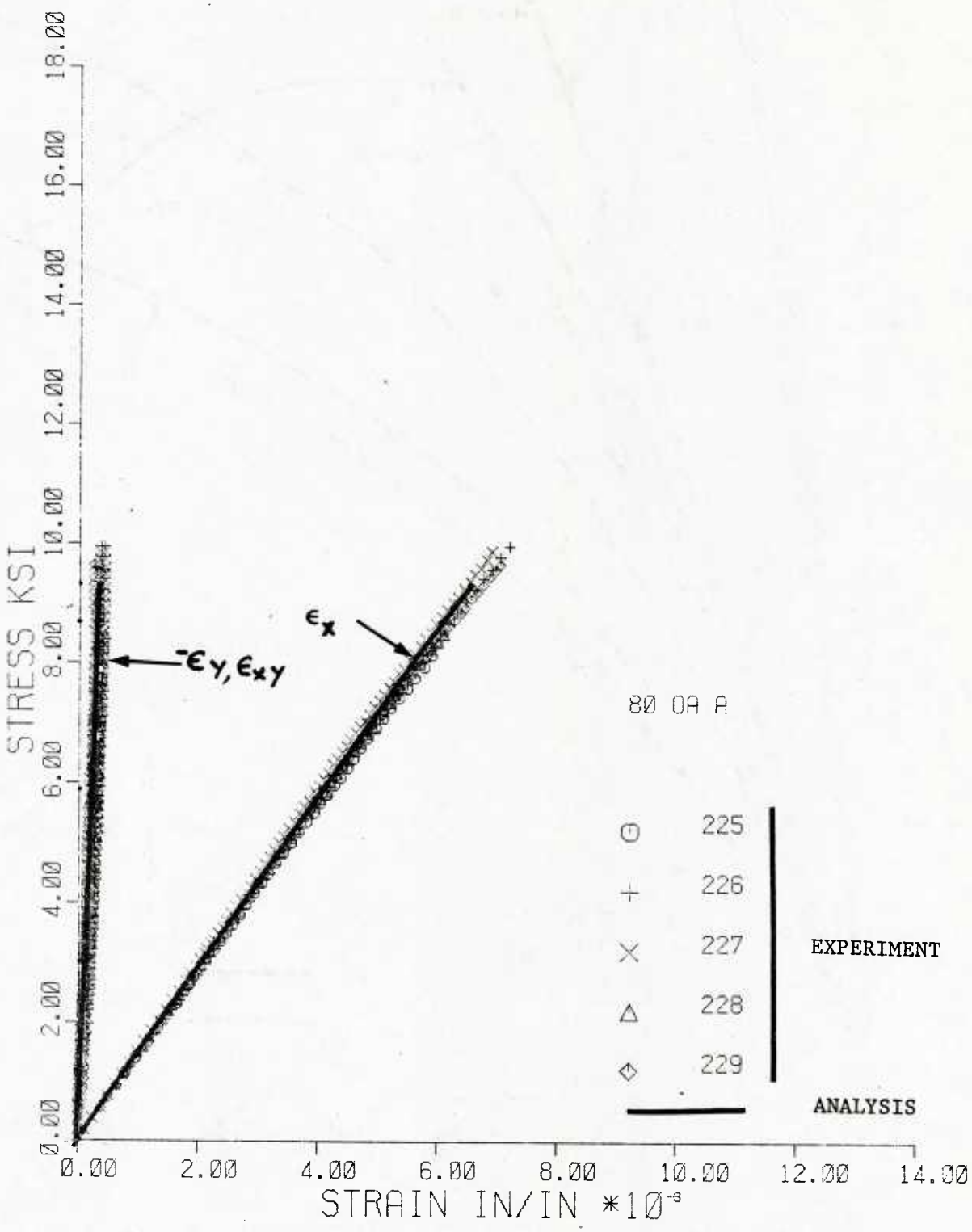

Figure 42. Axial Stress versus Axial, Transverse, and Shear Strain Curves for 80° Off-axis Specimens with Square Tabs and Fixed Grips

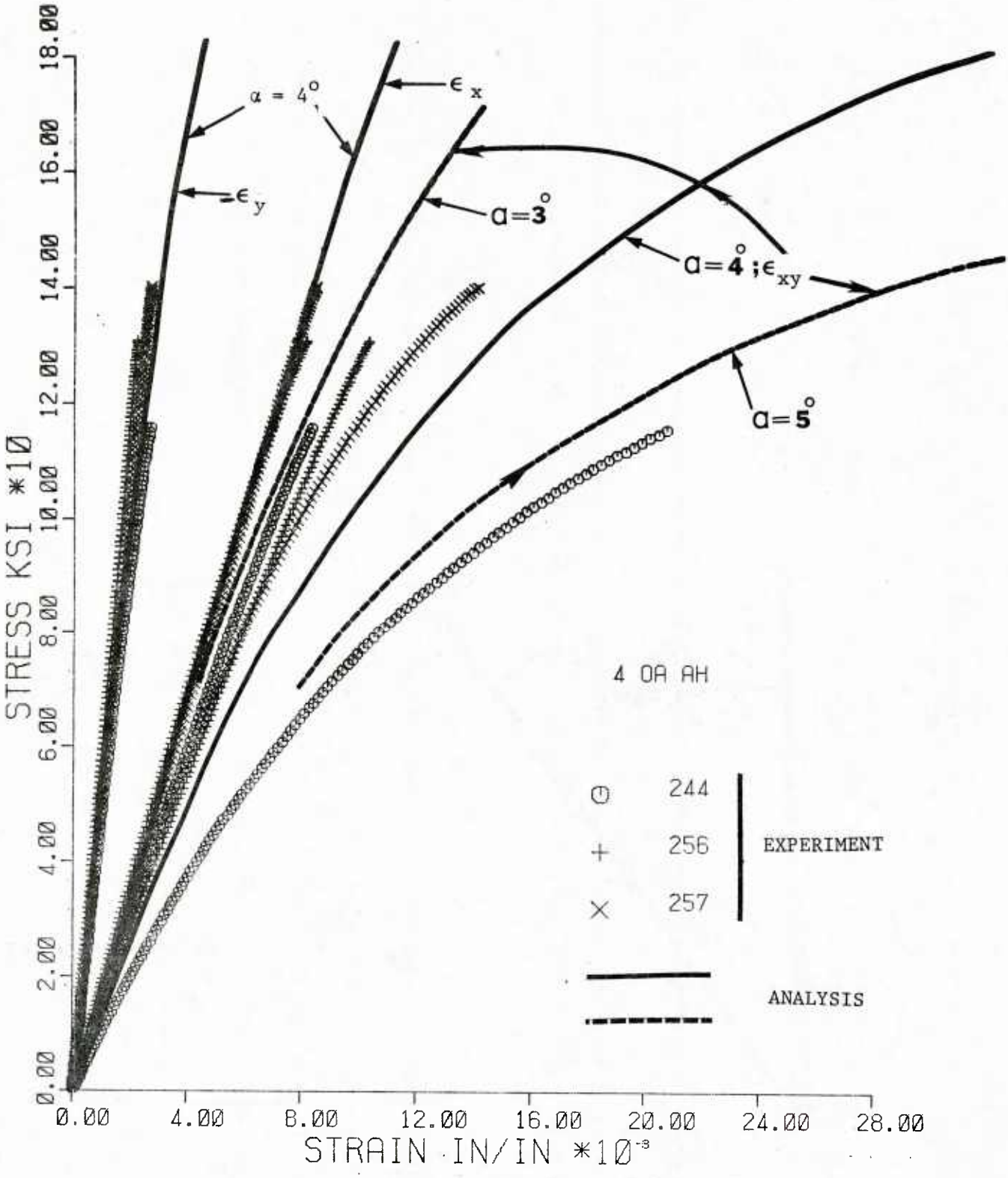

Figure 43. Axial Stress versus Axial, Transverse, and Shear Stain Curves for 4° (nominal) Off-axis Specimens with Square Tabs and Hinged Grips

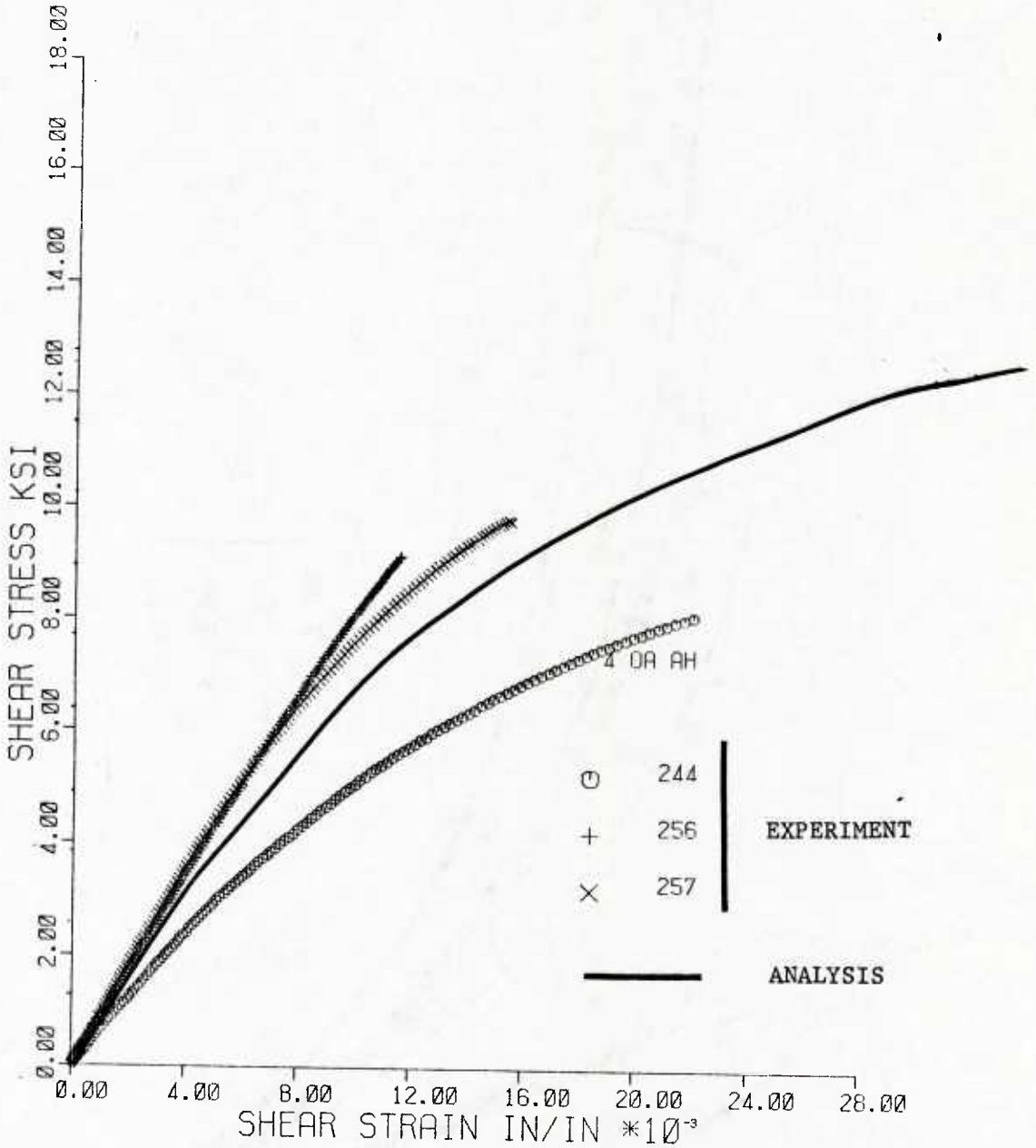

Figure 44. Shear Stress (τ_{12}) versus Shear Strain (γ_{12}) Curves for 4° Off-axis Specimens with Square Tabs and Hinged Grips

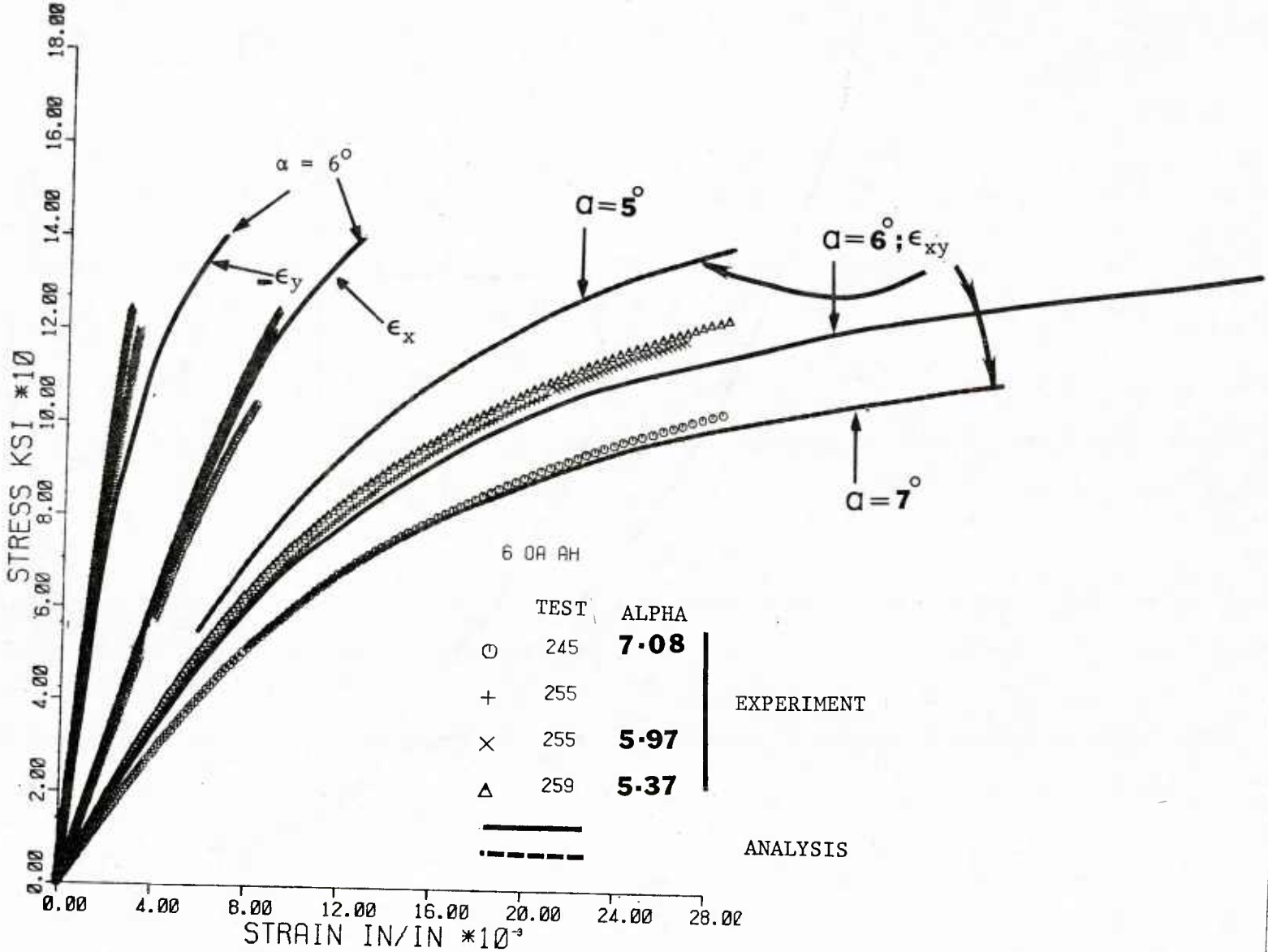

Figure 45. Axial Stress versus Axial, Transverse, and Shear Strain Curves for 6° (nominal) Off-axis Specimens with Square Tabs and Hinged Grips

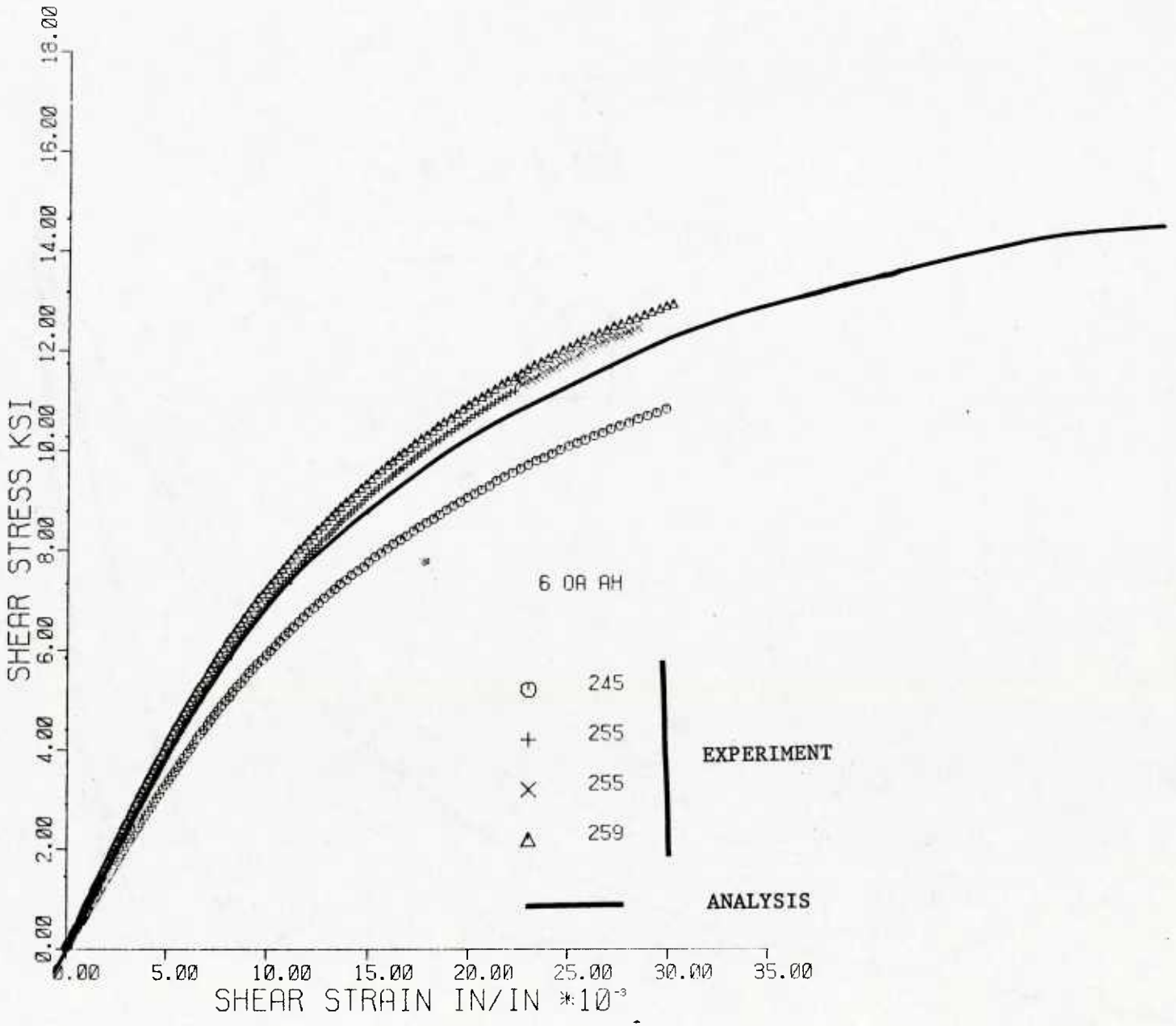

Figure 46. Shear Stress (τ_{12}) versus Shear Strain (γ_{12}) Curves for 6^{o} Off-axis Specimens with Square Tabs and Hinged Grips

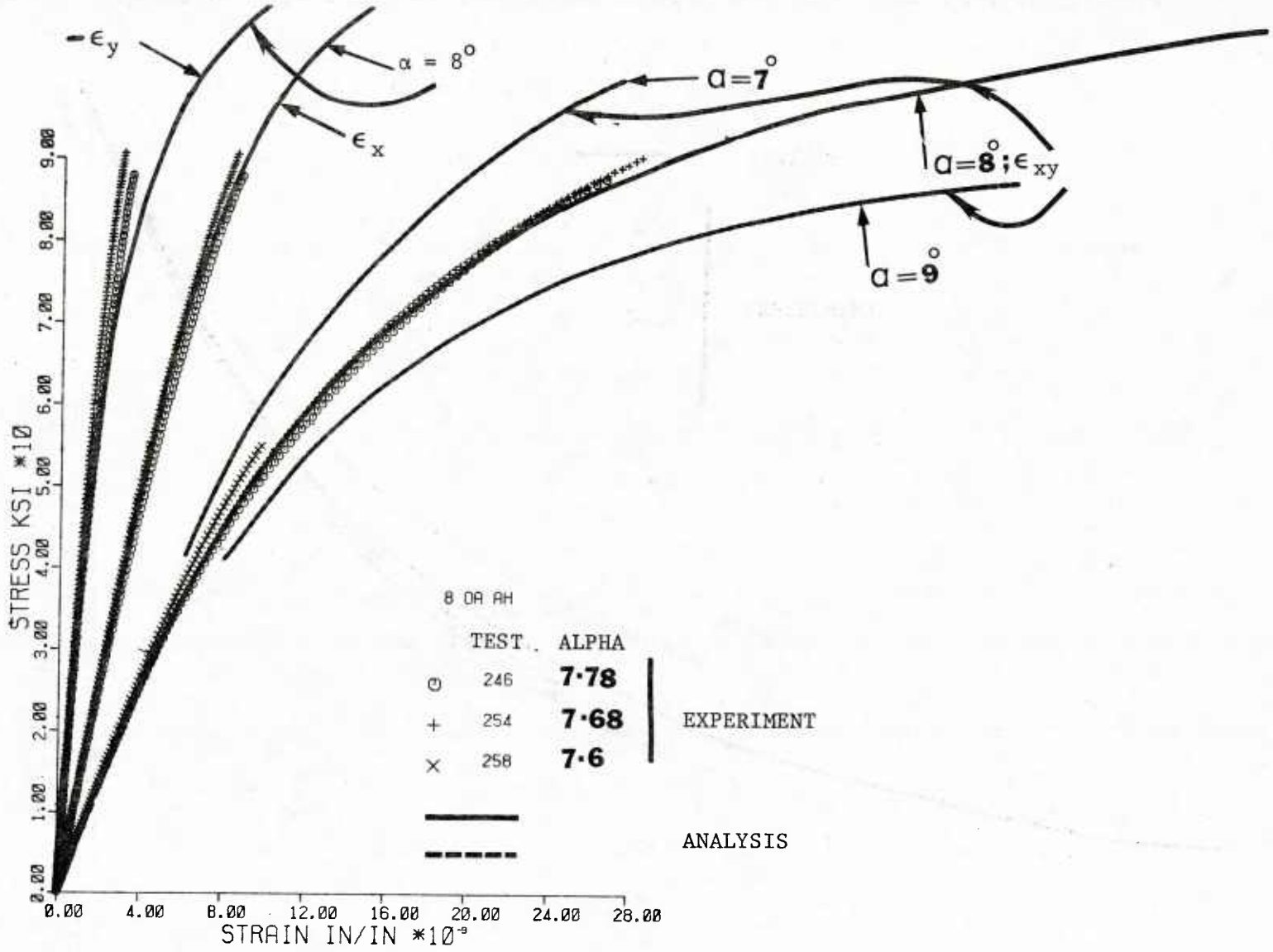

Figure 47. Axial Stress versus Axial, Transverse and Shear Strain Curves for 8° (nominal) Off-axis Specimens with Square Tabs and Hinged Grips

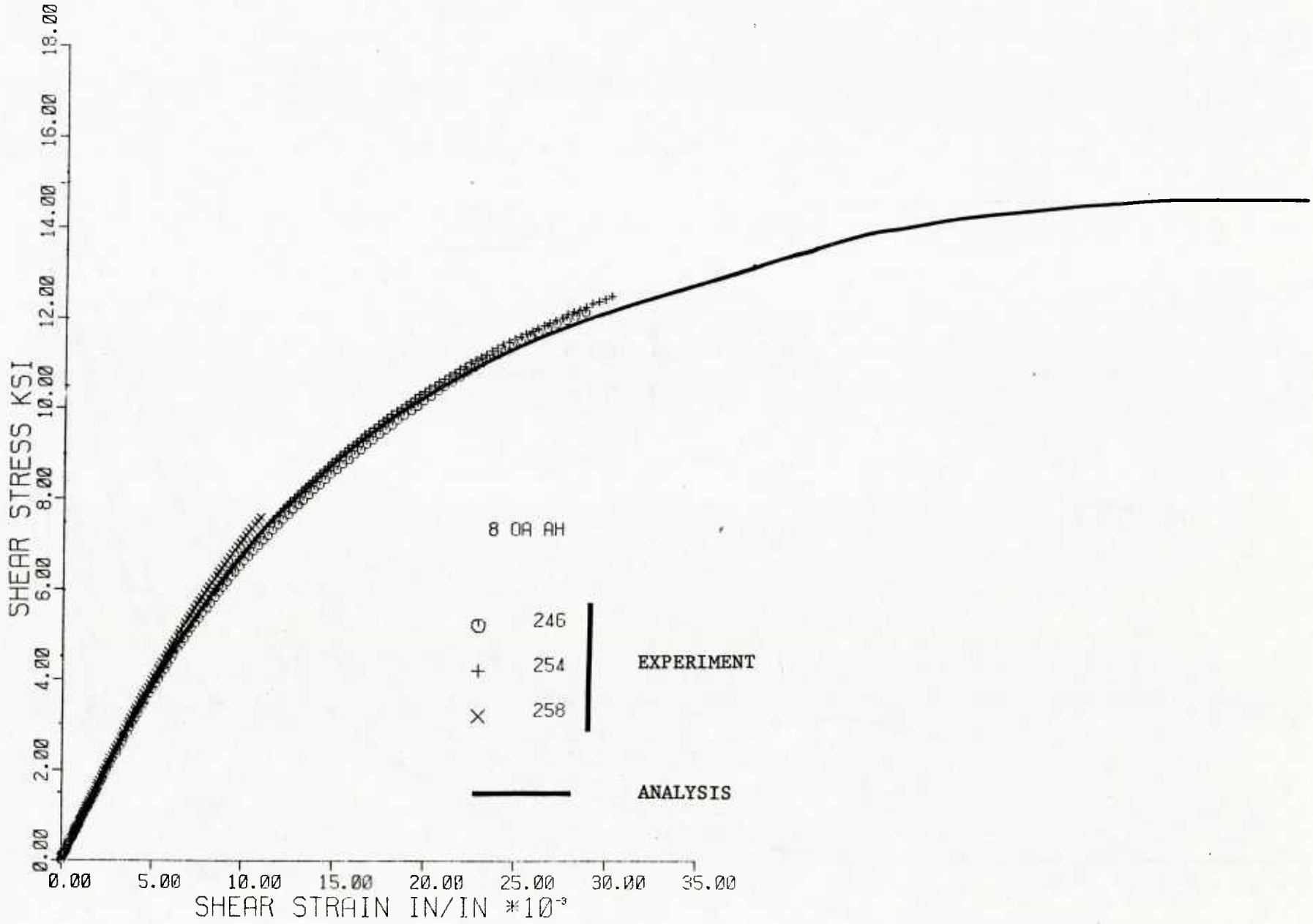

Figure 48. Shear Stress (τ_{12}) versus Shear Strain (γ_{12}) Curves for 8° Off-axis Specimens with Square Tabs and Hinged Grips

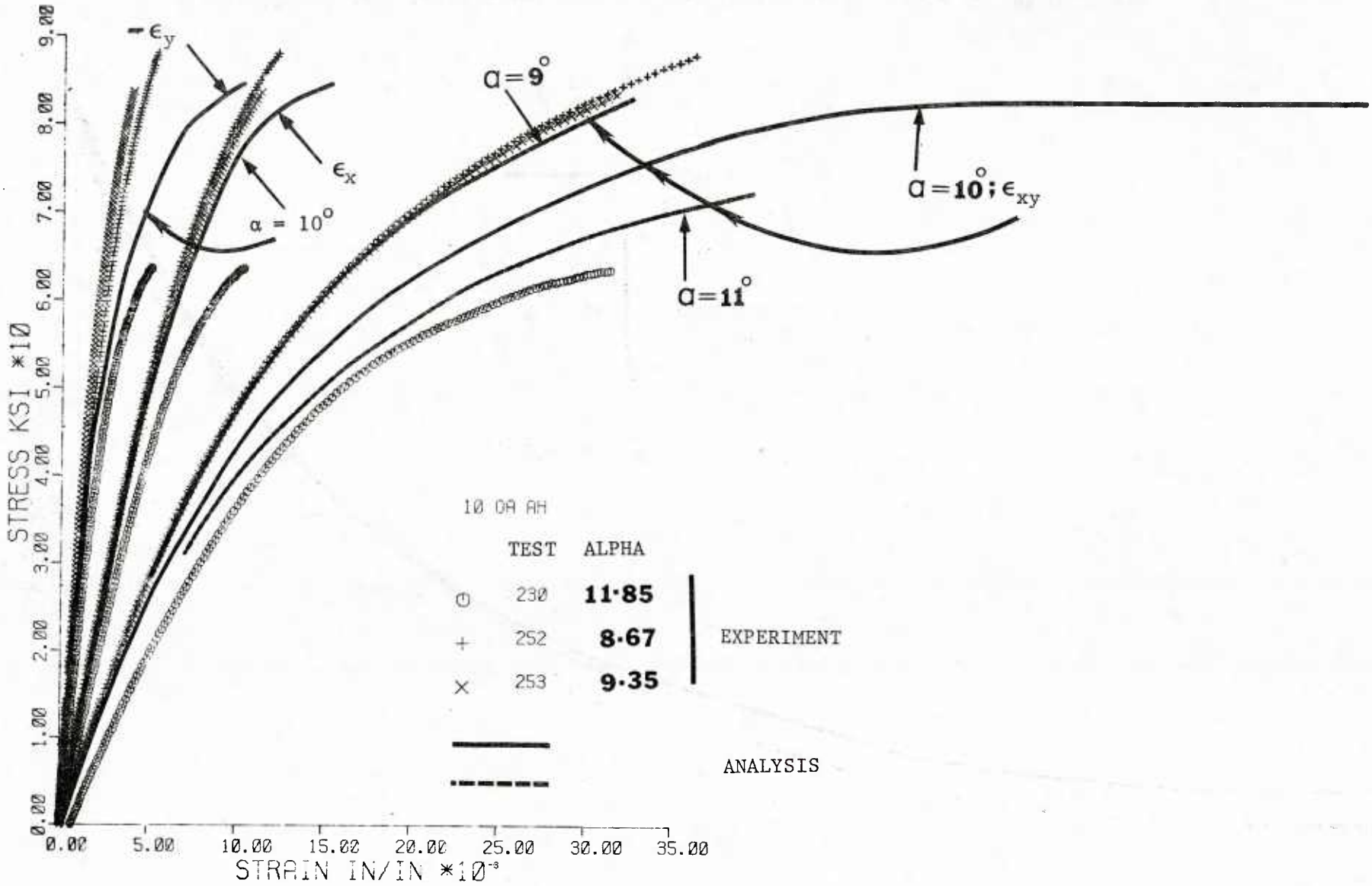

Figure 49. Axial Stress versus Axial, Transverse and Shear Strain Curves for 10° (nominal) Off-axis Specimens with Square Tabs and Hinged Grips

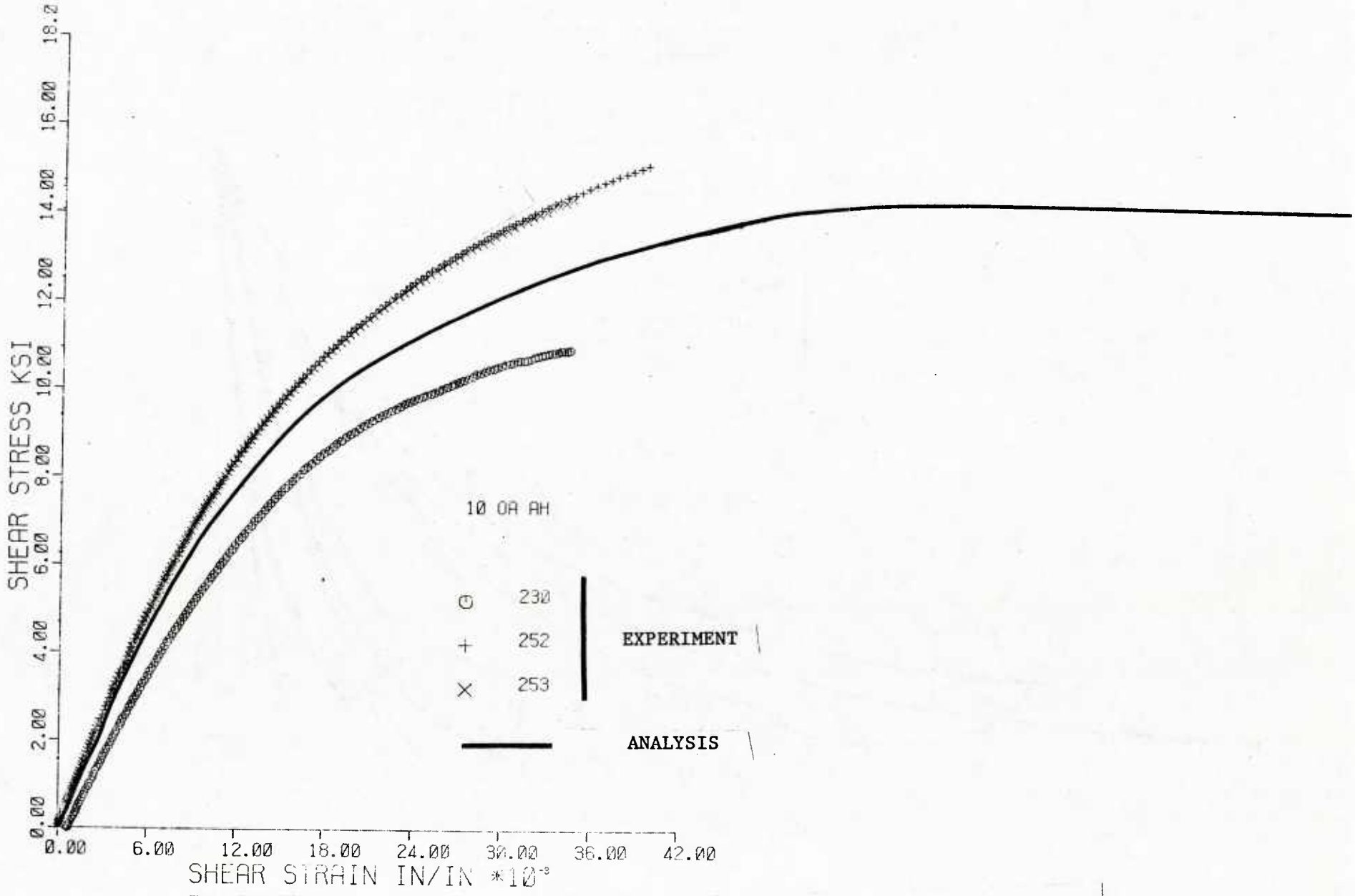

Figure 50. Shear Stress (τ_{12}) versus Shear Strain (γ_{12}) Curves for 10^{o} Off-axis Specimens with Square Tabs and Hinged Grips

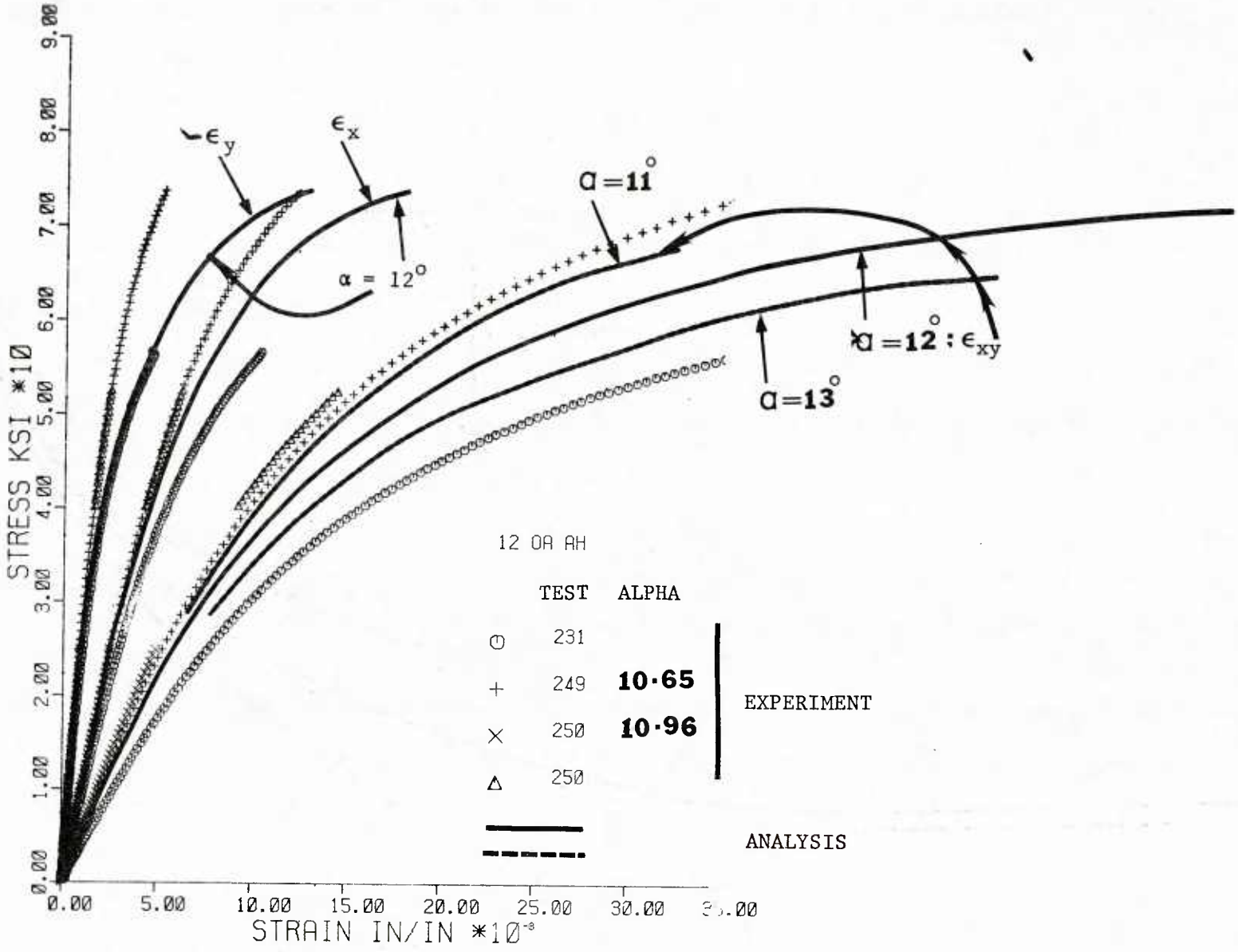

Figure 51. Axial Stress versus Axial, Transverse and Shear Strain Curves for 12° (nominal) Off-axis Specimens with Square Tabs and Hinged Grips

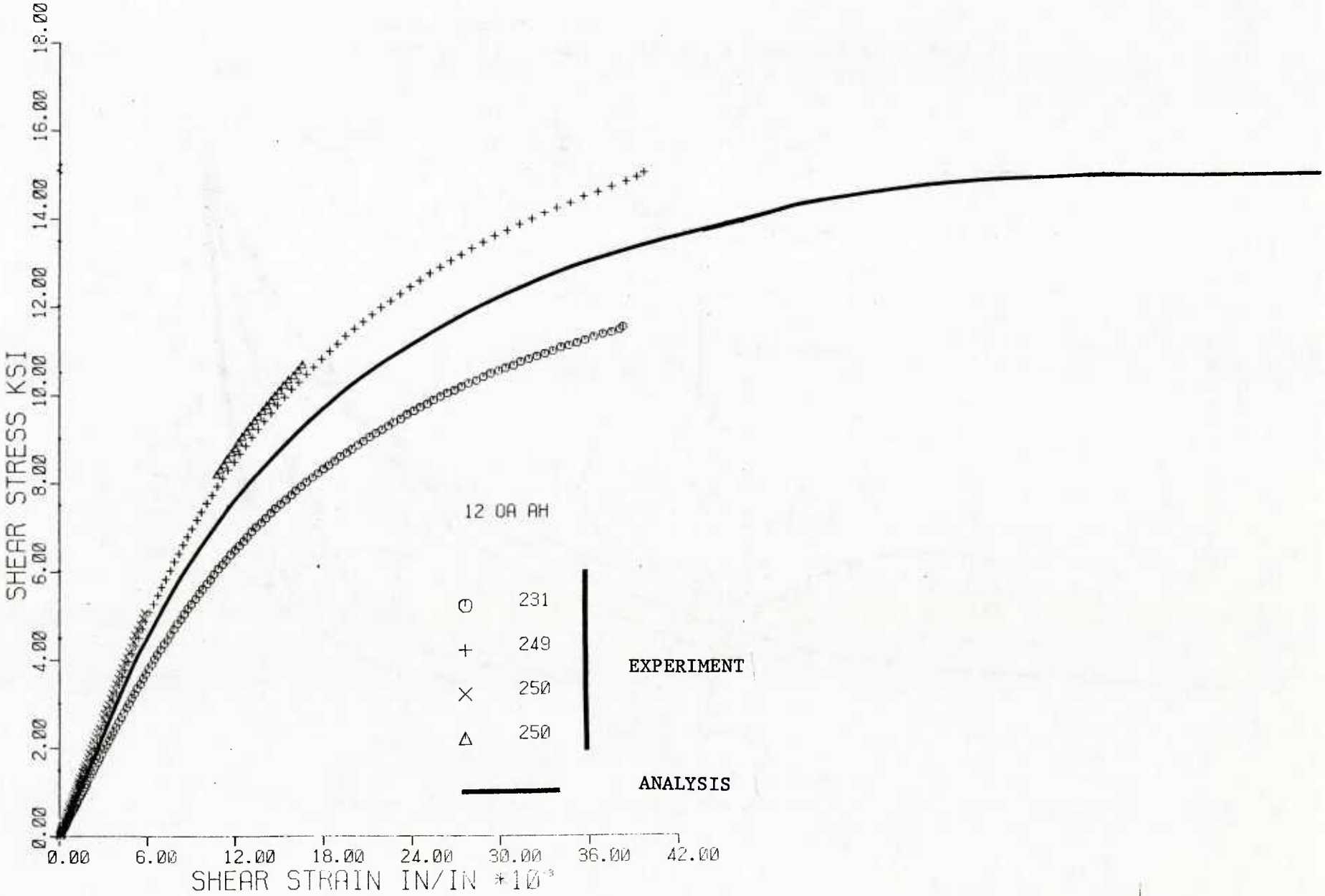

Figure 52. Shear Stress (τ_{12}) versus Shear Strain (γ_{12}) Curves for 12^{o} Off-axis Specimens with Square Tabs and Hinged Grips

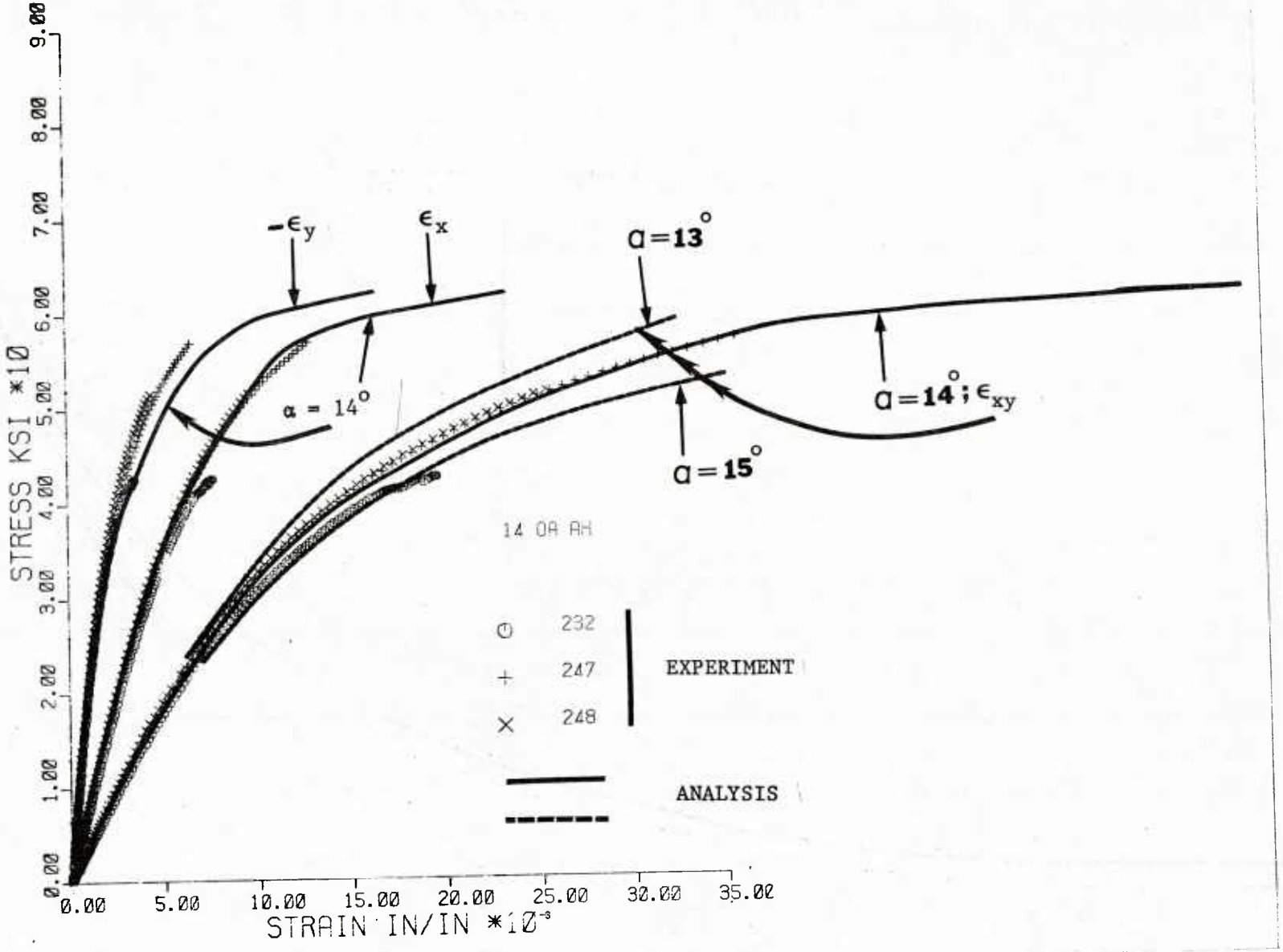

Figure 53. Axial Stress versus Axial, Transverse and Shear Strain Curves for 14° (nominal) Off-axis Specimens with Square Tabs and Hinged Grips

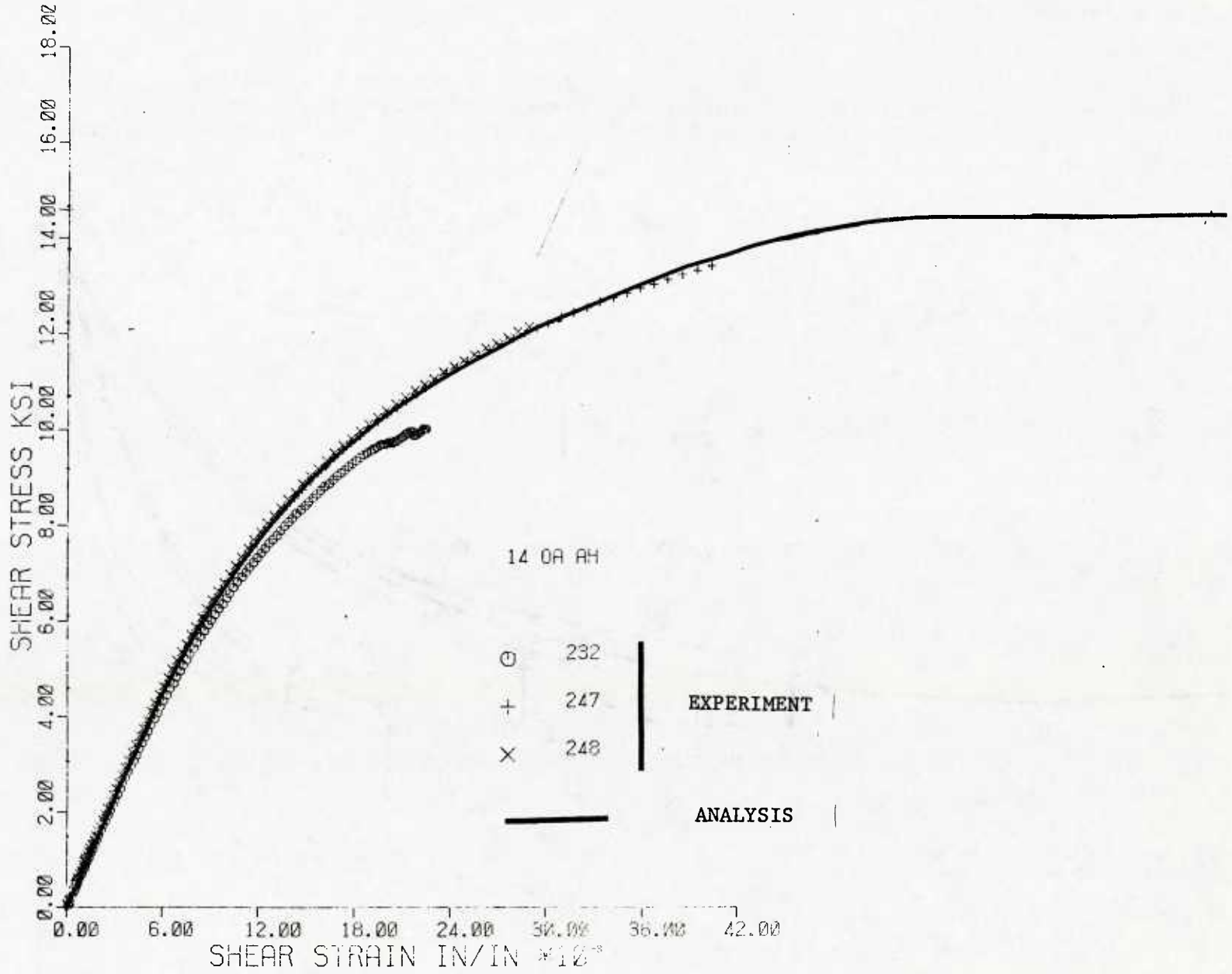

Figure 54. Shear Stress (τ_{12}) versus Shear Strain (γ_{12}) Curves for 14° Off-axis Specimens with Square Tabs and Hinged Grips

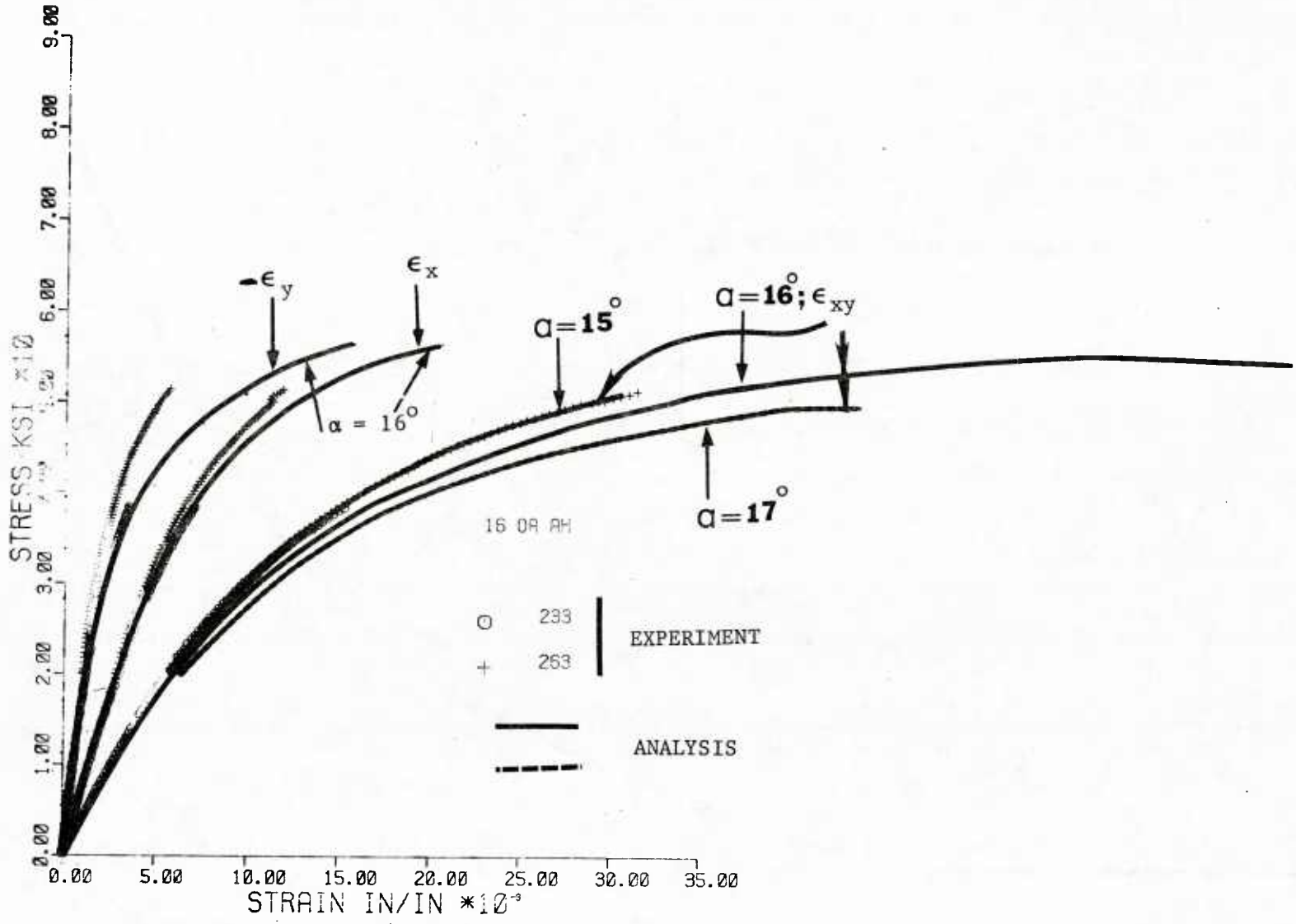

Figure 55. Axial Stress versus Axial, Transverse and Shear Strain Curves for 16° (nominal) Off-axis Specimens with Square Tabs and Hinged Grips

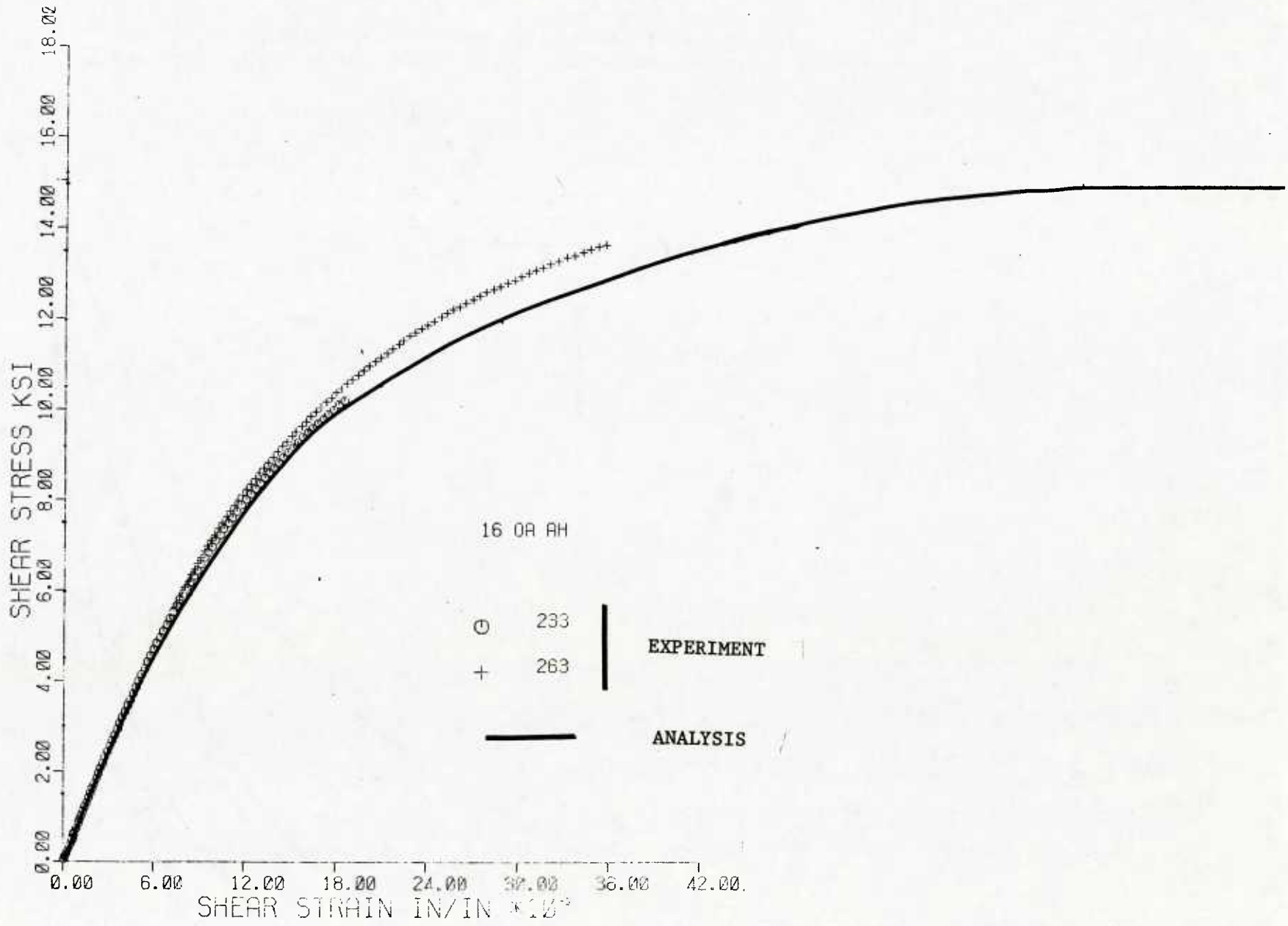

Figure 56. Shear Stress (τ_{12}) versus Shear Strain (γ_{12}) Curves for 16° Off-axis Specimens with Square Tabs and Hinged Grips

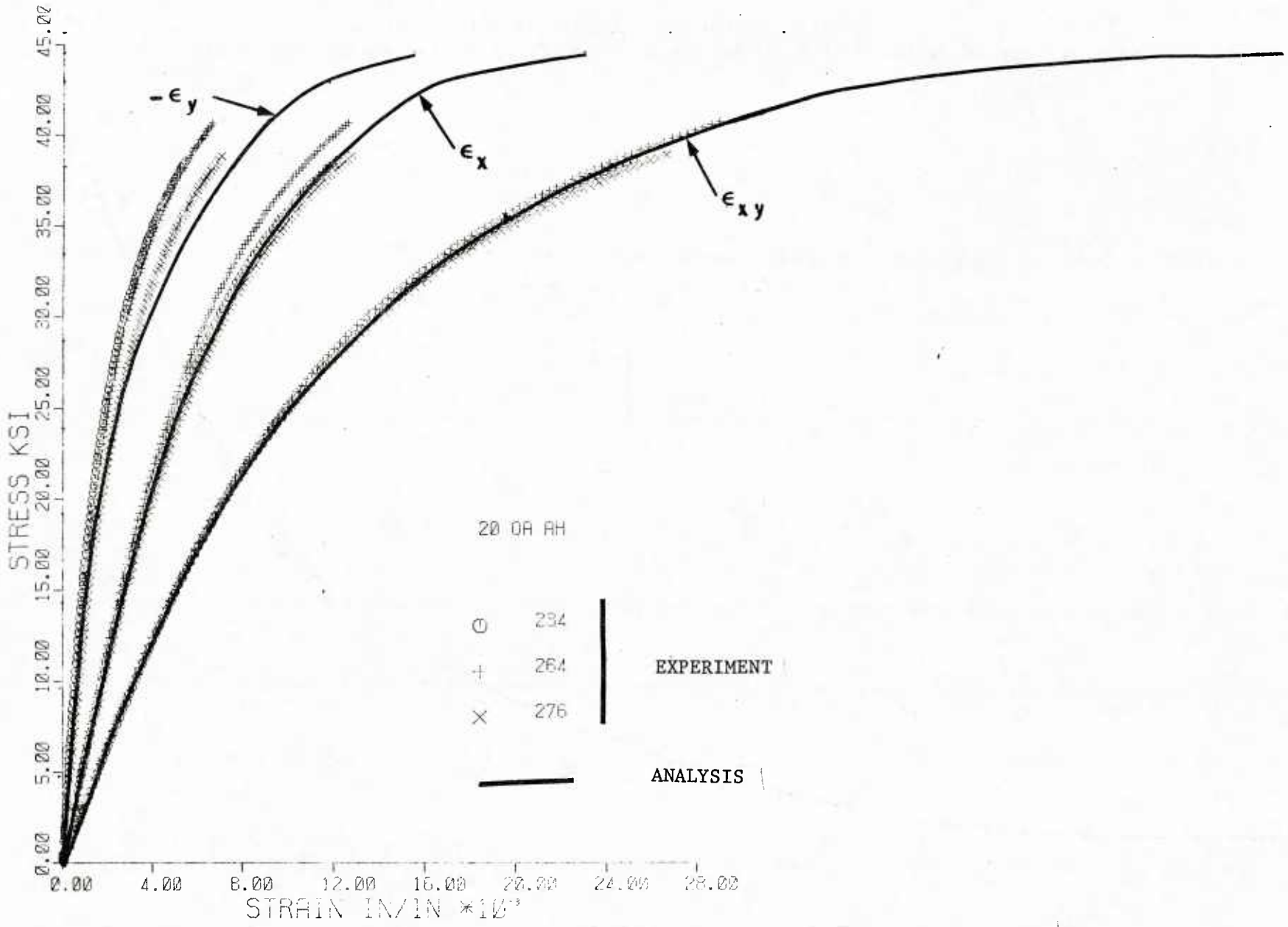

Figure 57. Axial Stress versus Axial, Transverse and Shear Strain Curves for 20^{o} Off-axis Specimens with Square Tabs and Hinged Grips

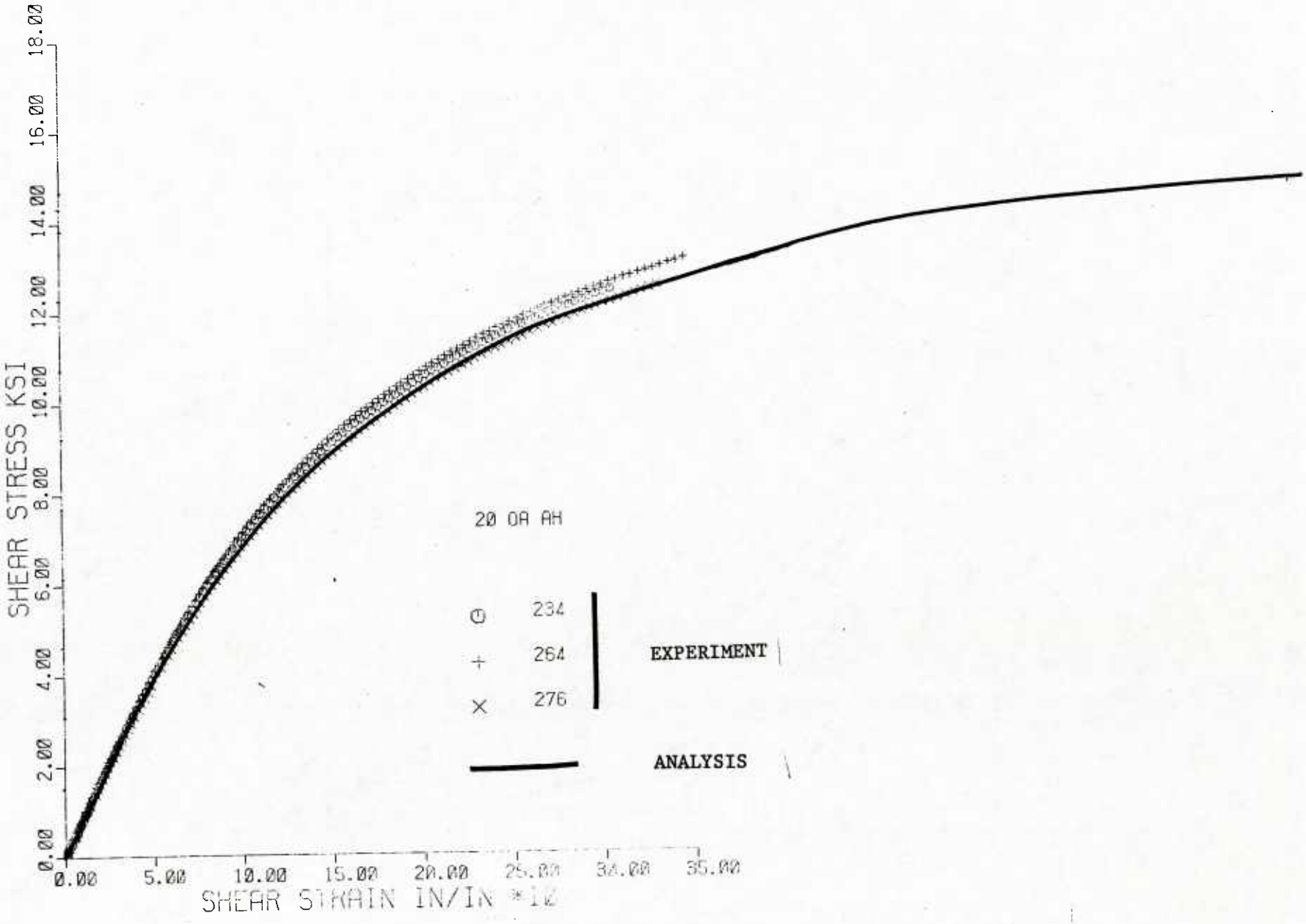

Figure 58. Shear Stress (τ_{12}) versus Shear Strain (γ_{12}) Curves for 20^{o} Off-axis Specimens with Square Tabs and Hinged Grips

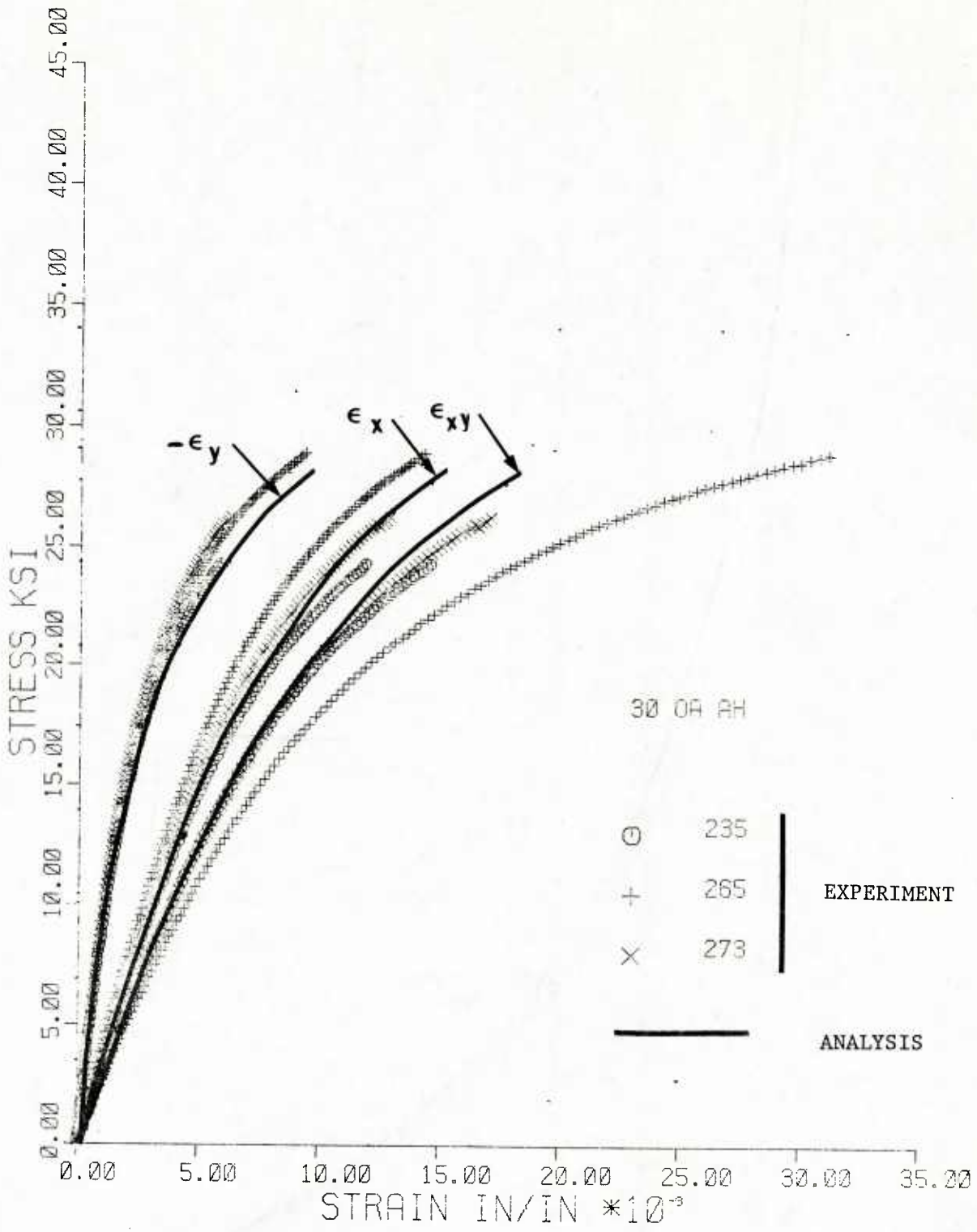

Figure 59. Axial Stress versus Axial, Transverse and Shear Strain Curves for 30^{o} Off-axis Specimens with Square Tabs and Hinged Grips

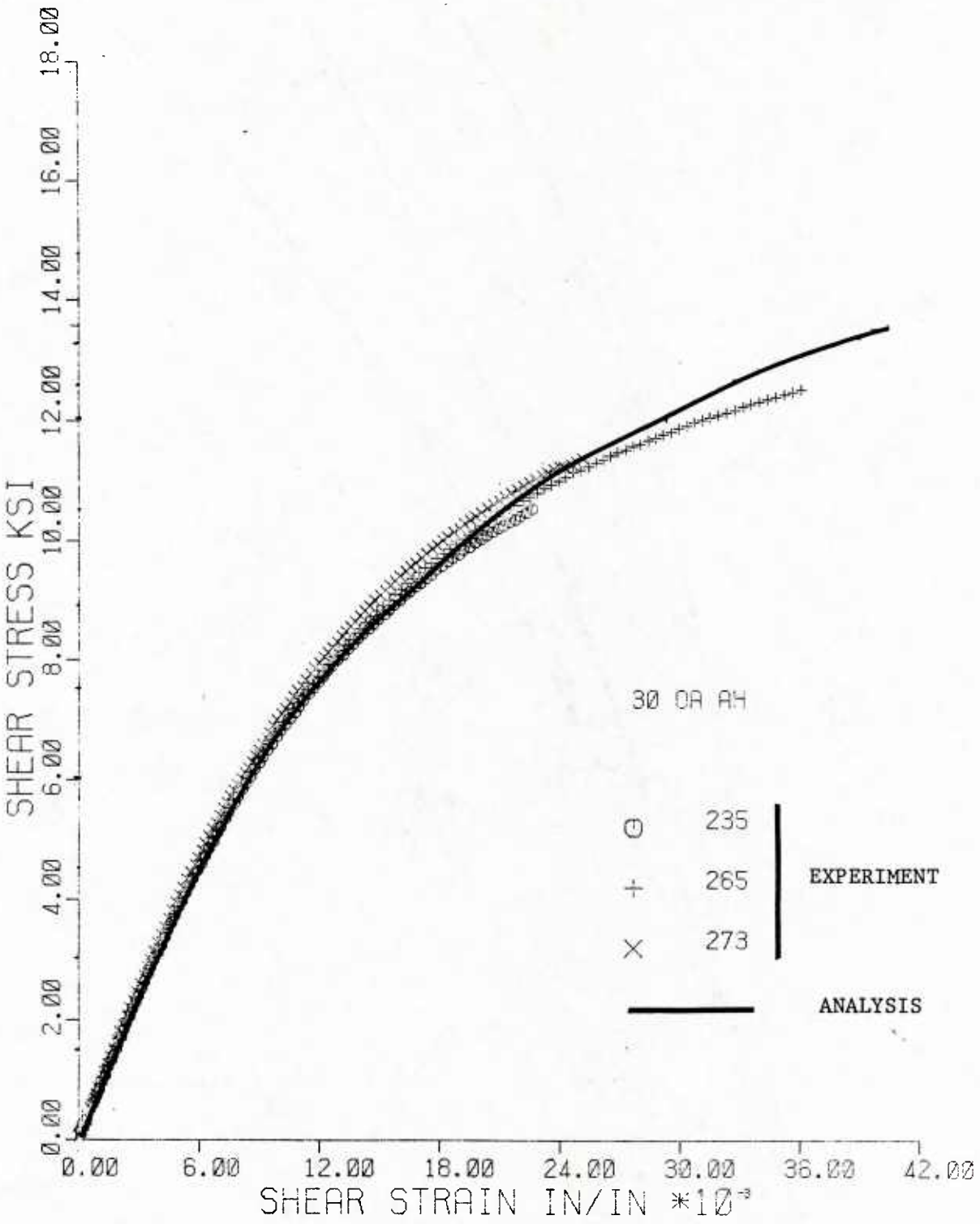

Figure 60. Shear Stress (τ_{12}) versus Shear Strain (γ_{12}) Curves for 30° Off-axis Specimens with Square Tabs and Hinged Grips

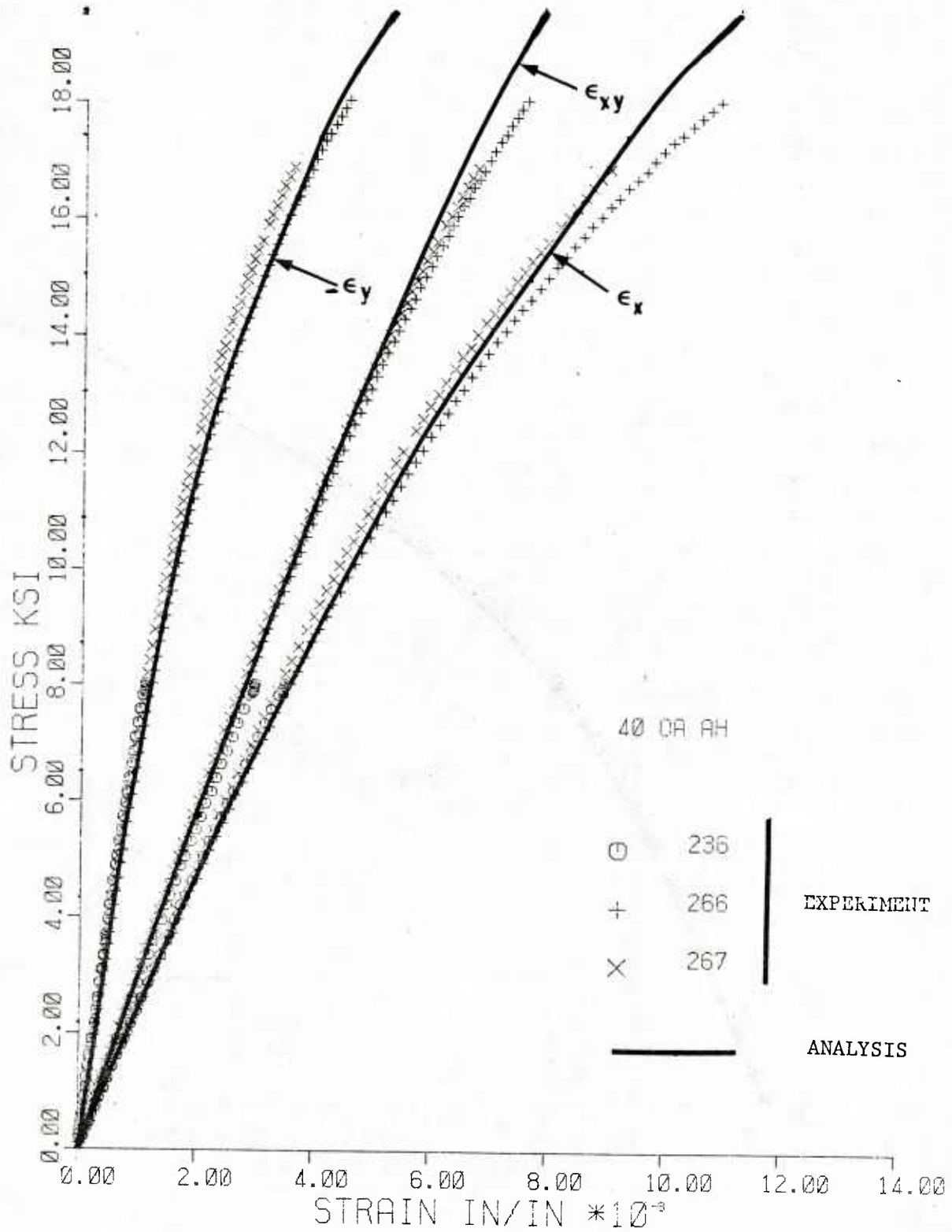

Figure 61. Axial Stress versus Axial, Transverse and Shear Strain Curves for 40^{o} Off-axis Specimens with Square Tabs and Hinged Grips

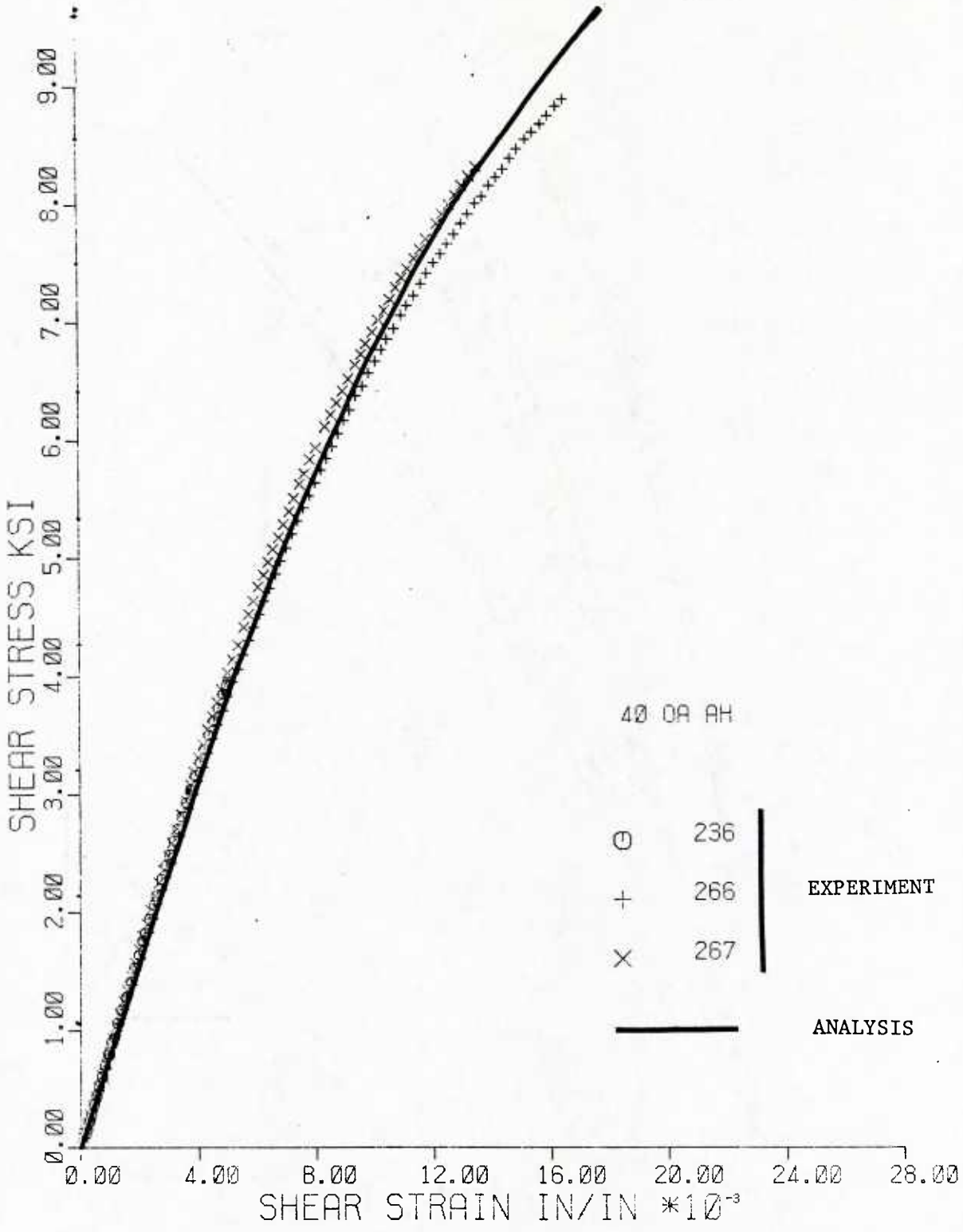

Figure 62. Shear Stress (τ_{12}) versus Shear Strain (γ_{12}) Curves for 40° Off-axis Specimens with Square Tabs and Hinged Grips

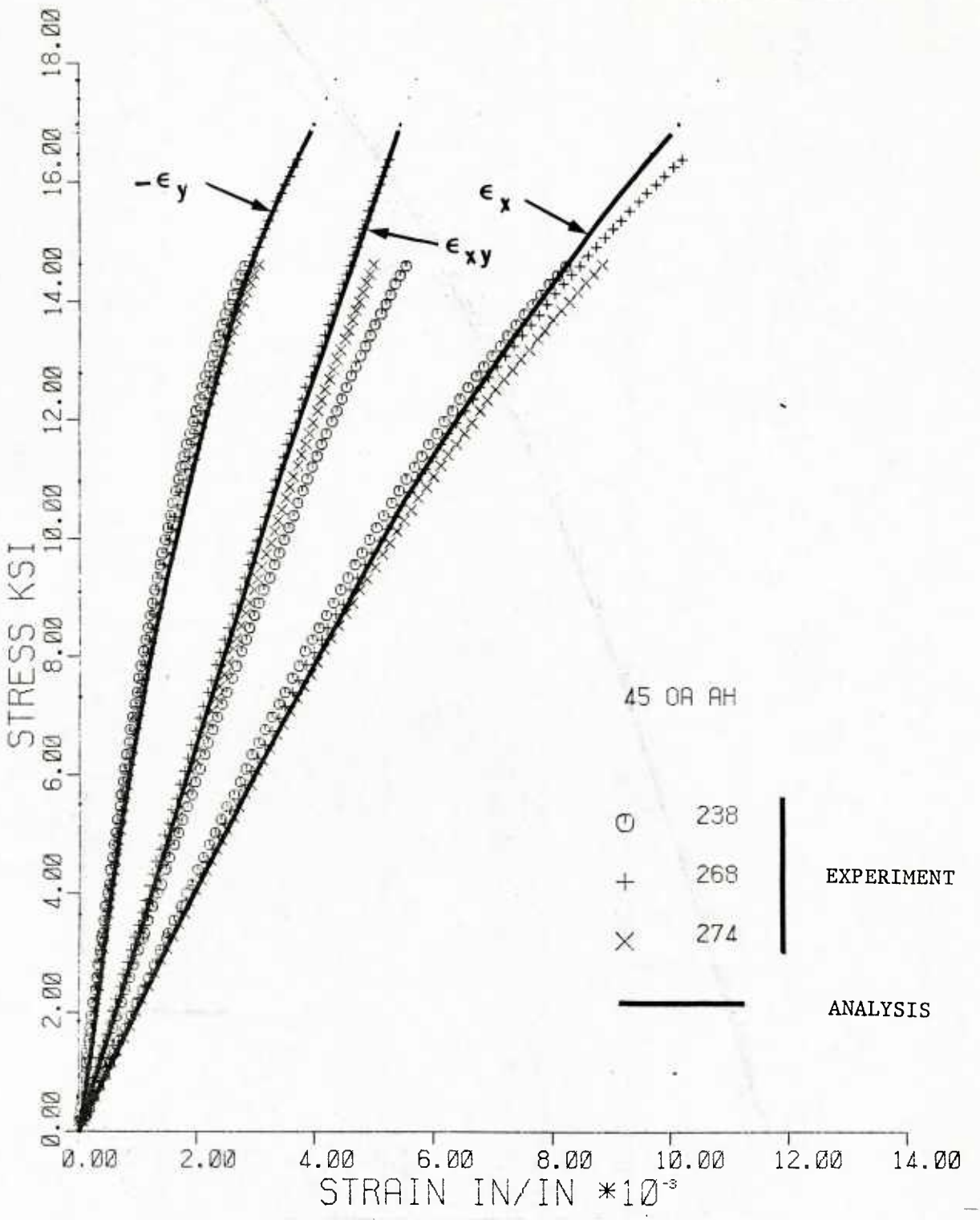

Figure 63. Axial Stress versus Axial, Transverse and Shear Strain Curves for 45^{o} Off-axis Specimens with Square Tabs and Hinged Grips

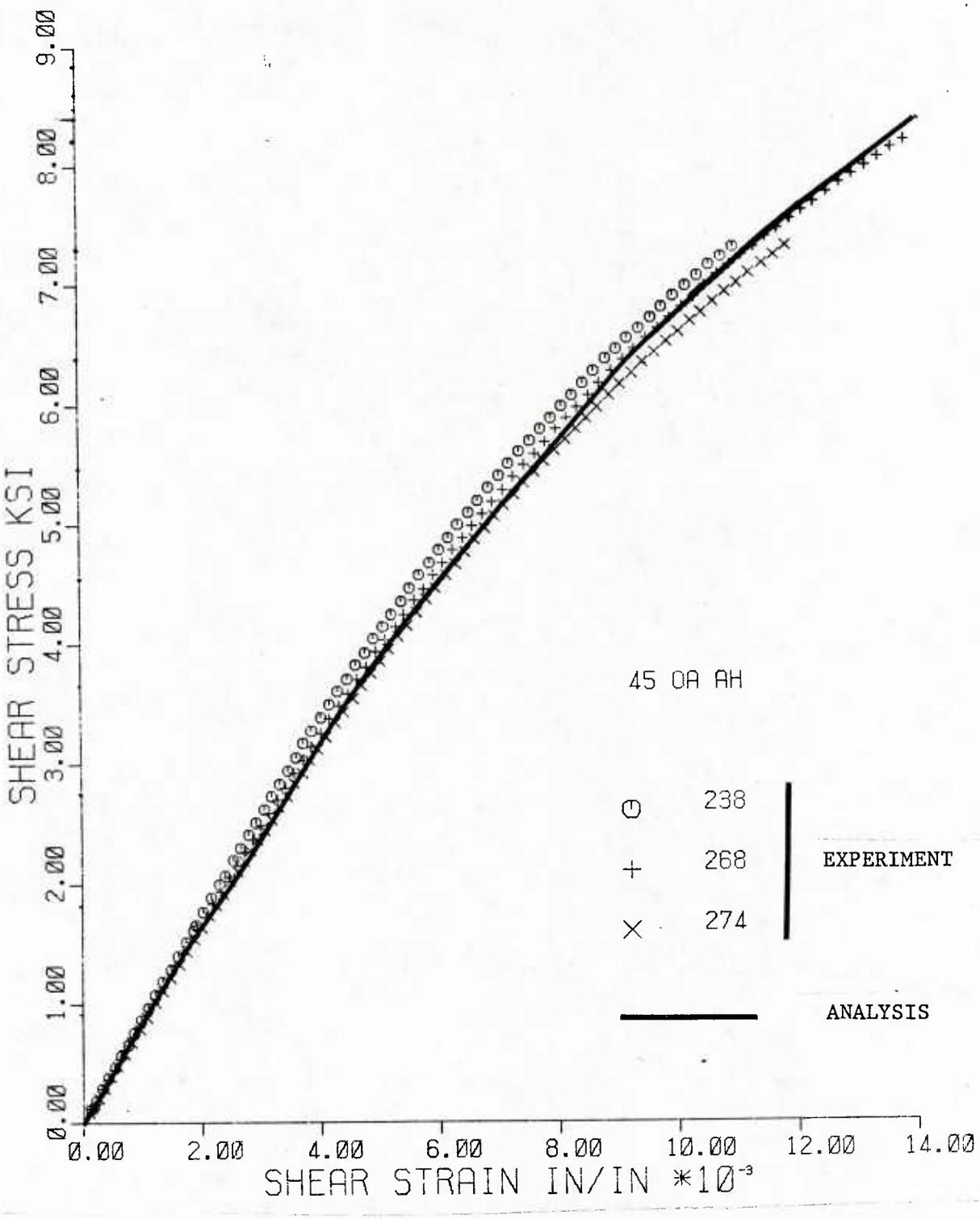

Figure 64. Shear Stress (τ_{12}) versus Shear Strain (γ_{12}) Curves for 45° Off-axis Specimens with Square Tabs and Hinged Grips

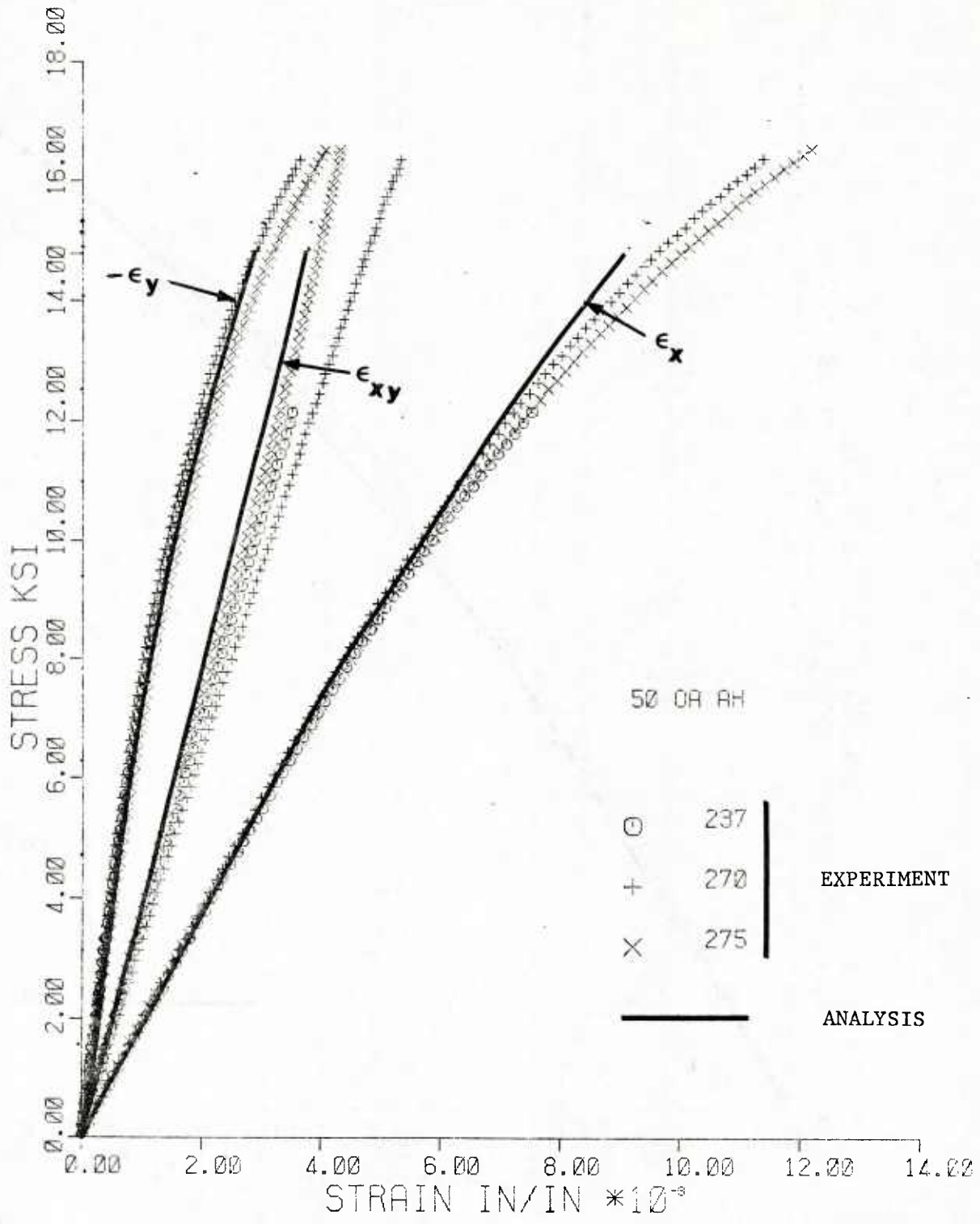

Figure 65. Axial Stress versus Axial, Transverse, and Shear Strain Curves for 50^{o} Off-axis Specimens with Square Tabs and Hinged Grips

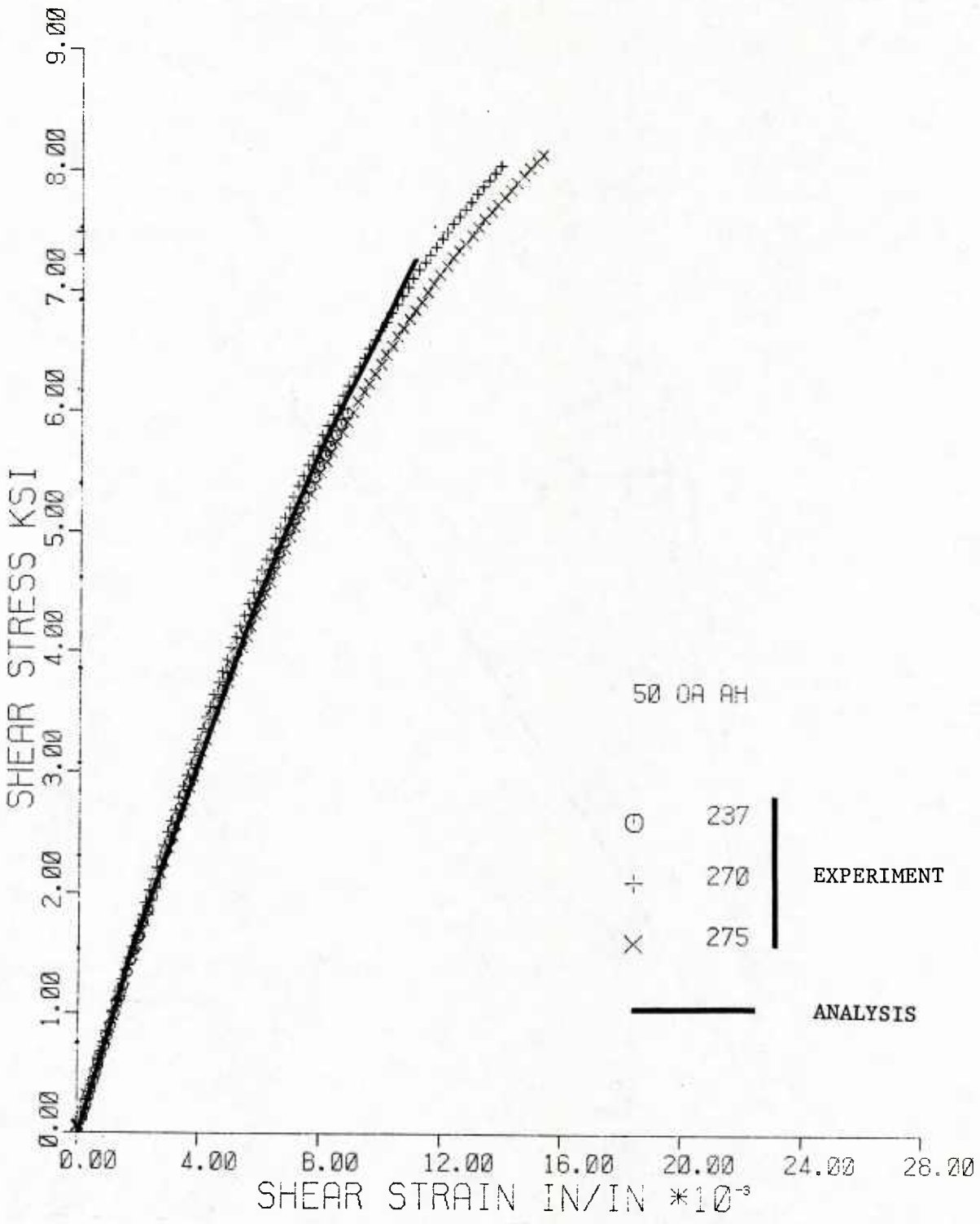

Figure 66. Shear Stress (τ_{12}) versus Shear Strain (γ_{12}) Curves for 50° Off-axis Specimens with Square Tabs and Hinged Grips

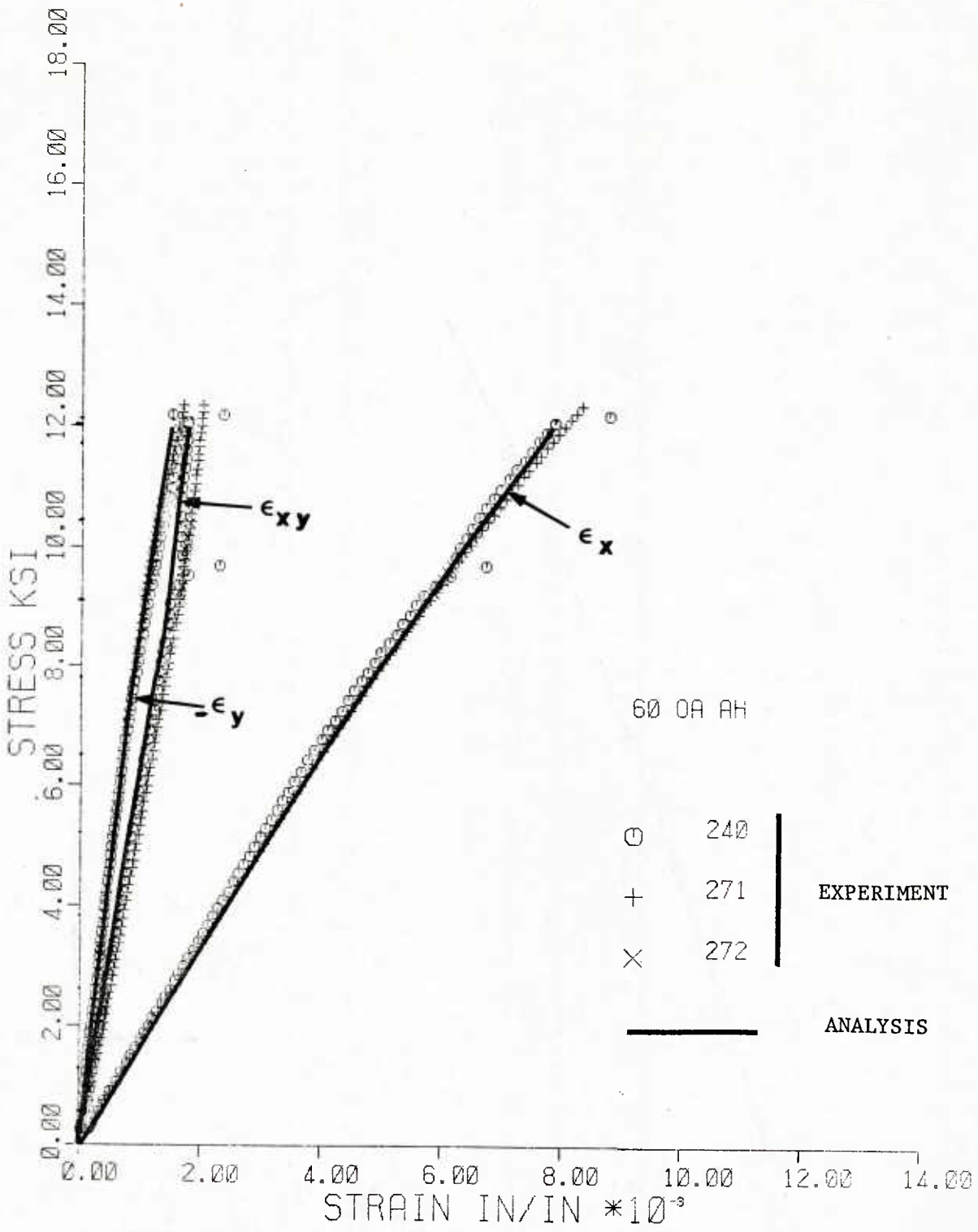

Figure 67. Axial Stress versus Axial, Transverse, and Shear Strain Curves for 60^{o} Off-axis Specimens with Square Tabs and Hindged Grips

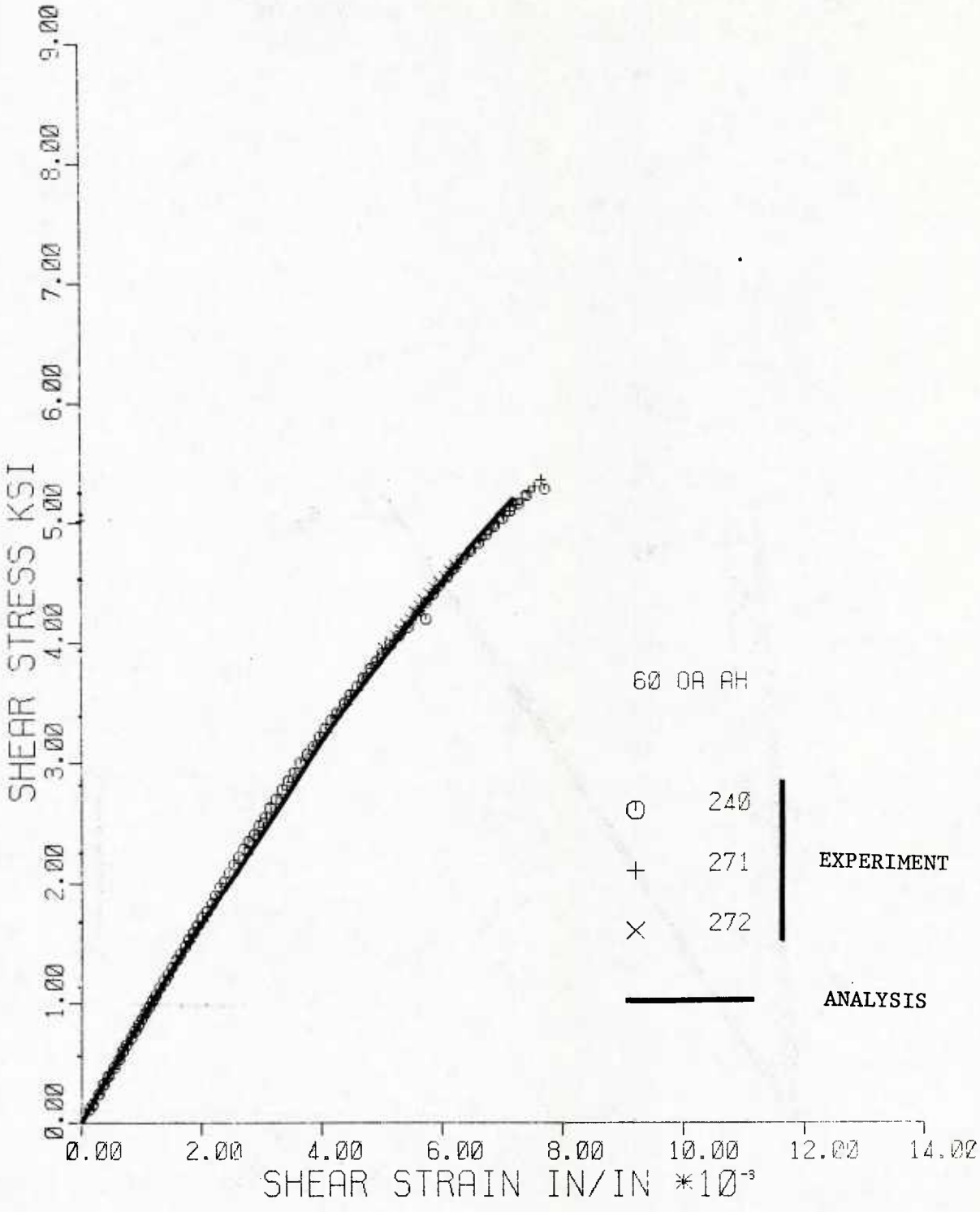

Figure 68. Shear Stress (τ_{12}) versus Shear Strain (γ_{12}) Curves for 60° Off-axis Specimens with Square Tabs and Hinged Grips

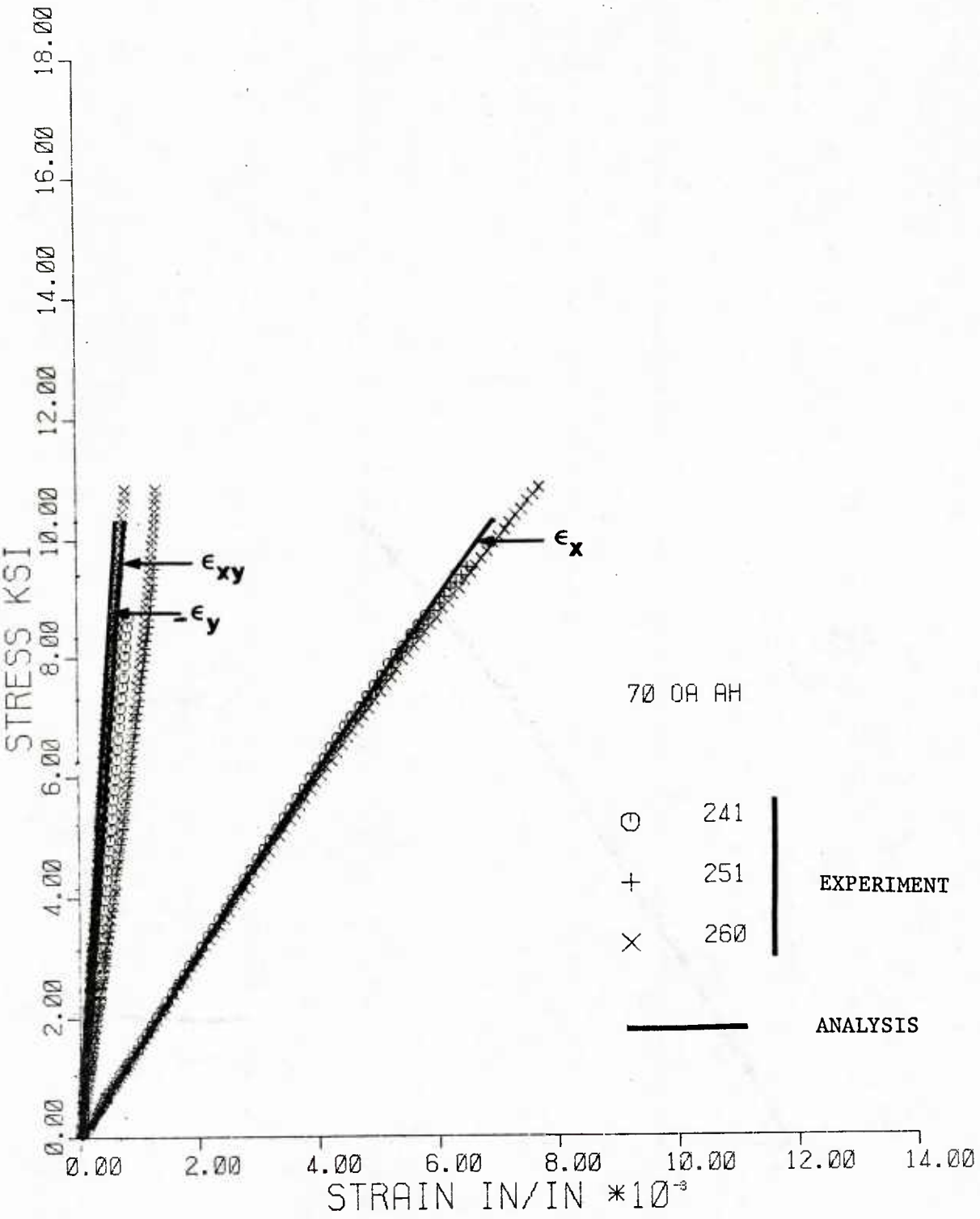

Figure 69. Axial Stress versus Axial, Transverse, and Shear Strain Curves for 70^{o} Off-axis Specimens with Square Tabs and Hinged Grips

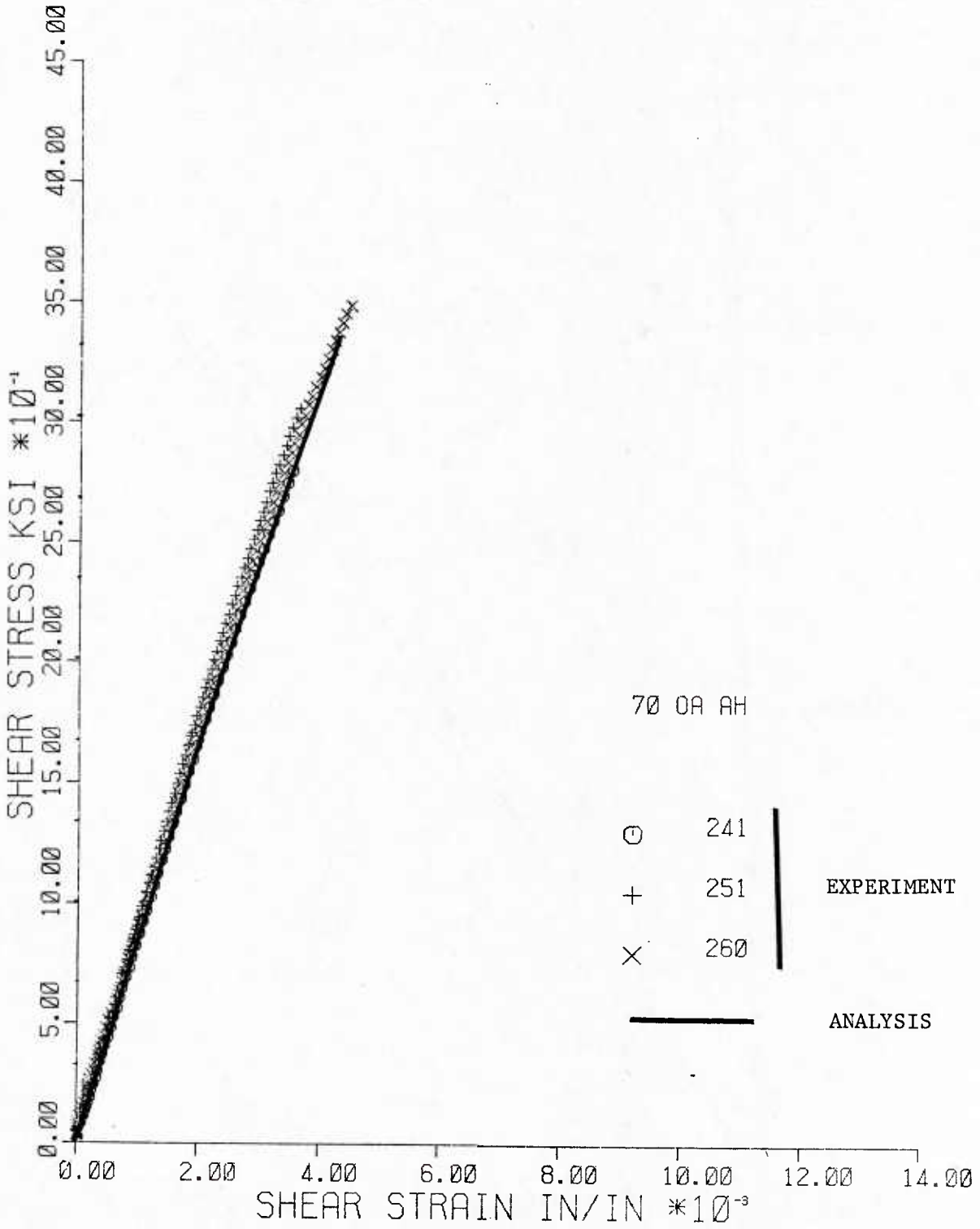

Figure 70. Shear Stress (τ_{12}) versus Shear Strain (γ_{12}) Curves for 70° Off-axis Specimens with Square Tabs and Hinged Grips

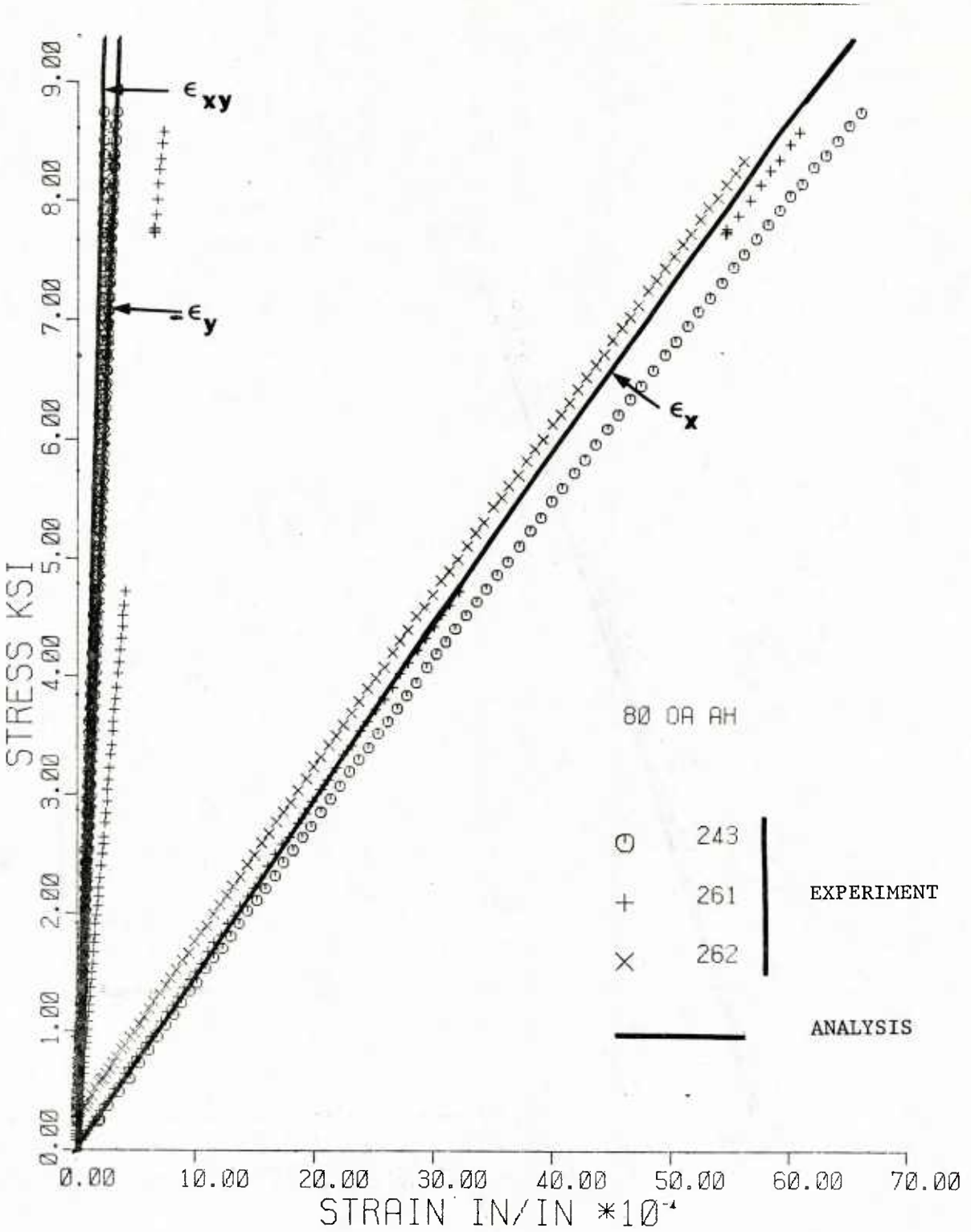

Figure 71. Axial Stress versus Axial, Transverse, and Shear Strain Curves for 80^{o} Off-axis Specimens with Square Tabs and Hinged Grips

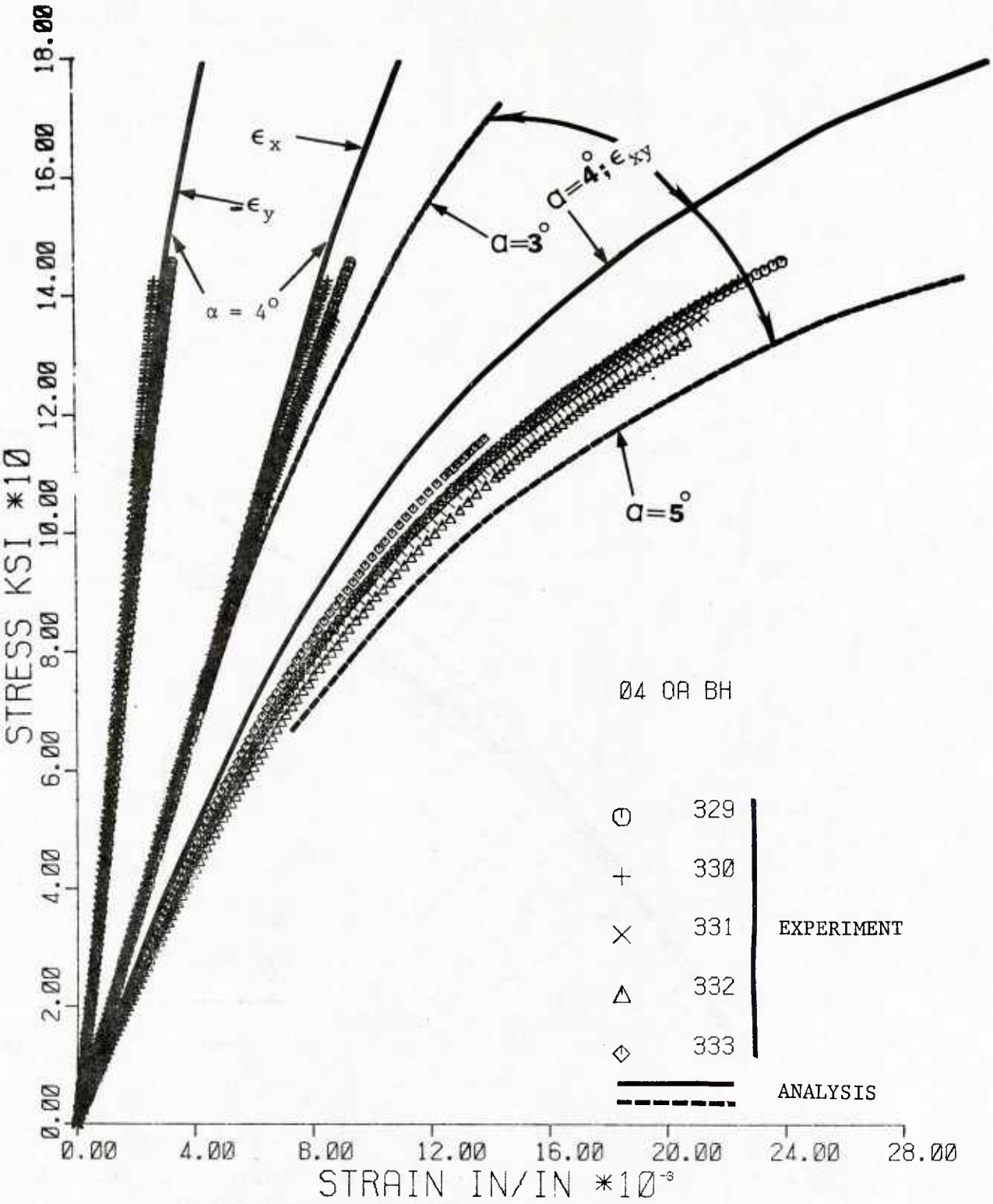

Figure 72. Axial Stress versus Axial Transverse, and Shear Strain Curves for 4° (nominal) Off-axis Specimens with Inclined Tabs and Hinged Grips

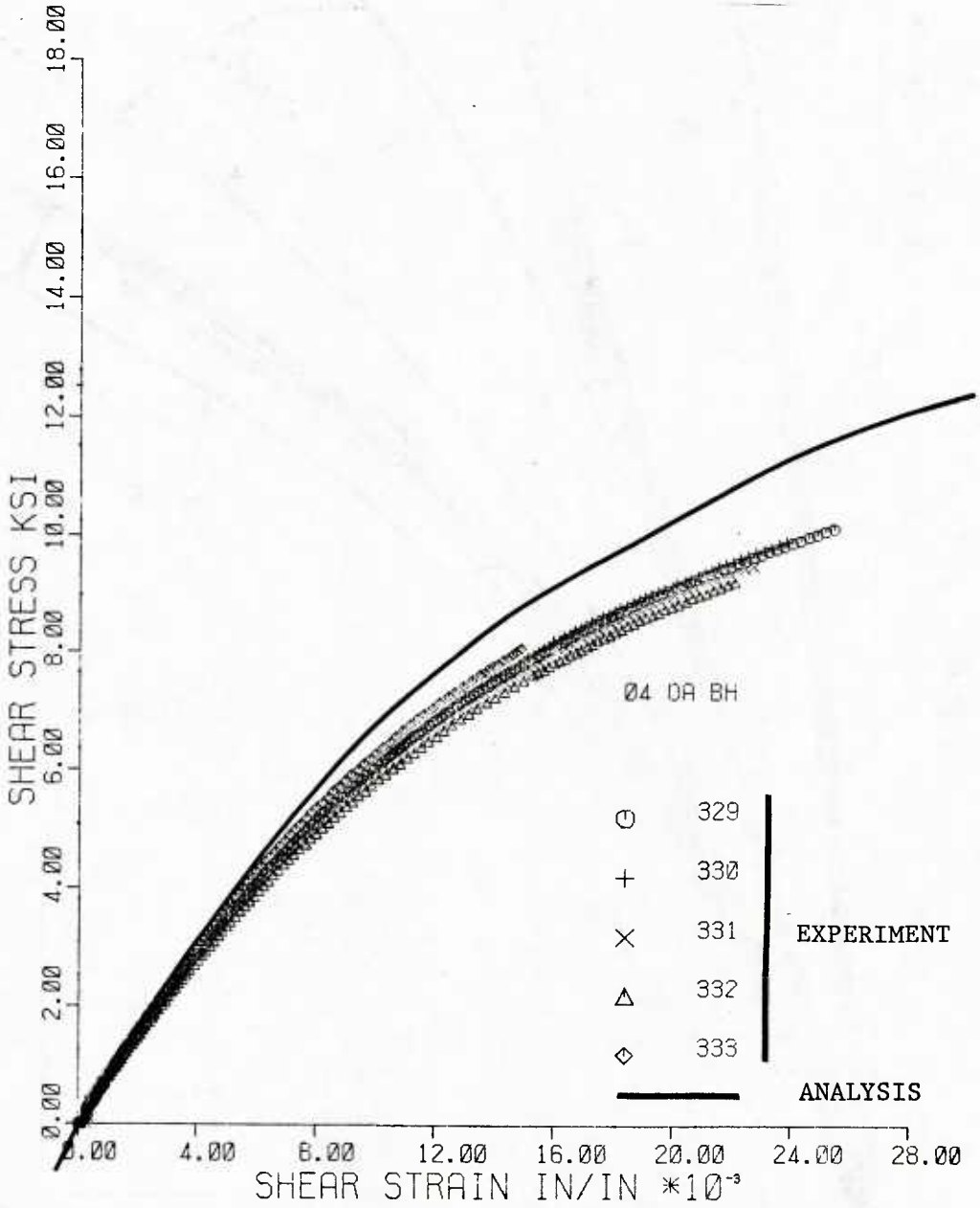

Figure 73. Shear Stress (τ_{12}) versus Shear Strain (γ_{12}) Curves for 4° Off-axis Specimens with Inclined Tabs and Hinged Grips

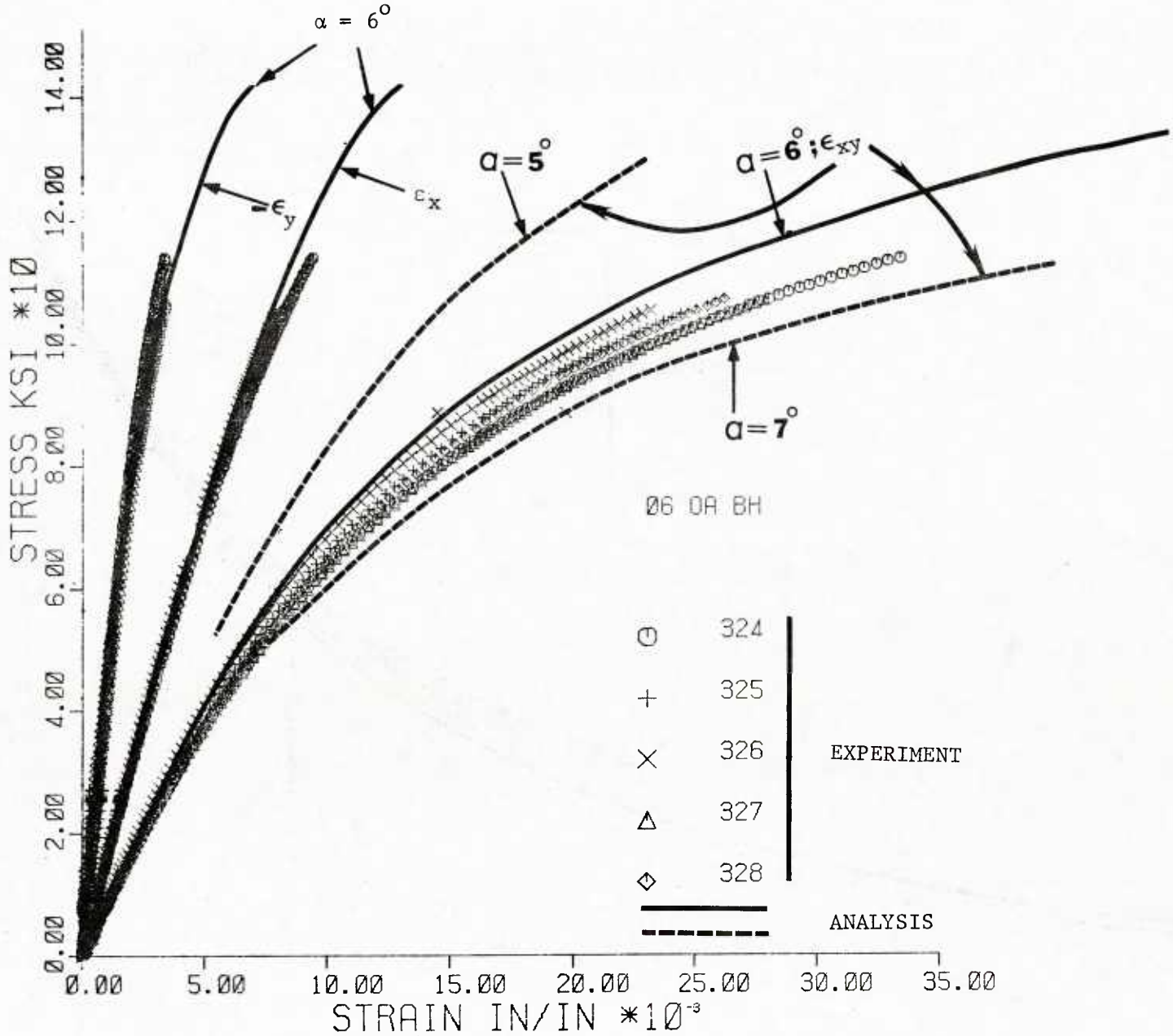

Figure 74. Axial Stress versus Axial, Tranverse, and Shear Strain Curves for 6° (nominal) Off-axis Specimens with Inclined Tabs and Hinged Grips

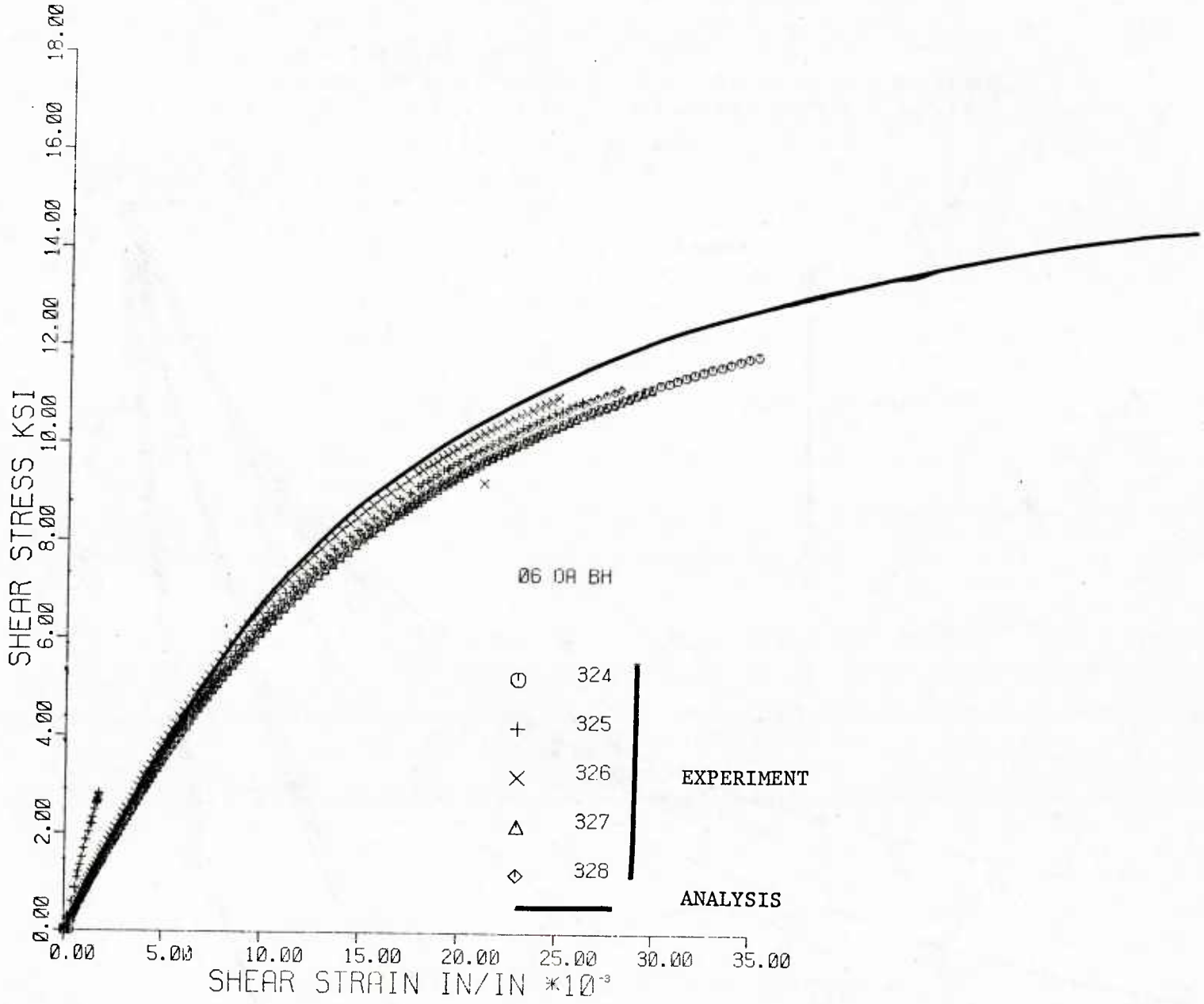

Figure 75. Shear Stress (τ_{12}) versus Shear Strain (γ_{12}) Curves for 6° Off-axis Specimens with Inclined Tabs and Hinged Grips

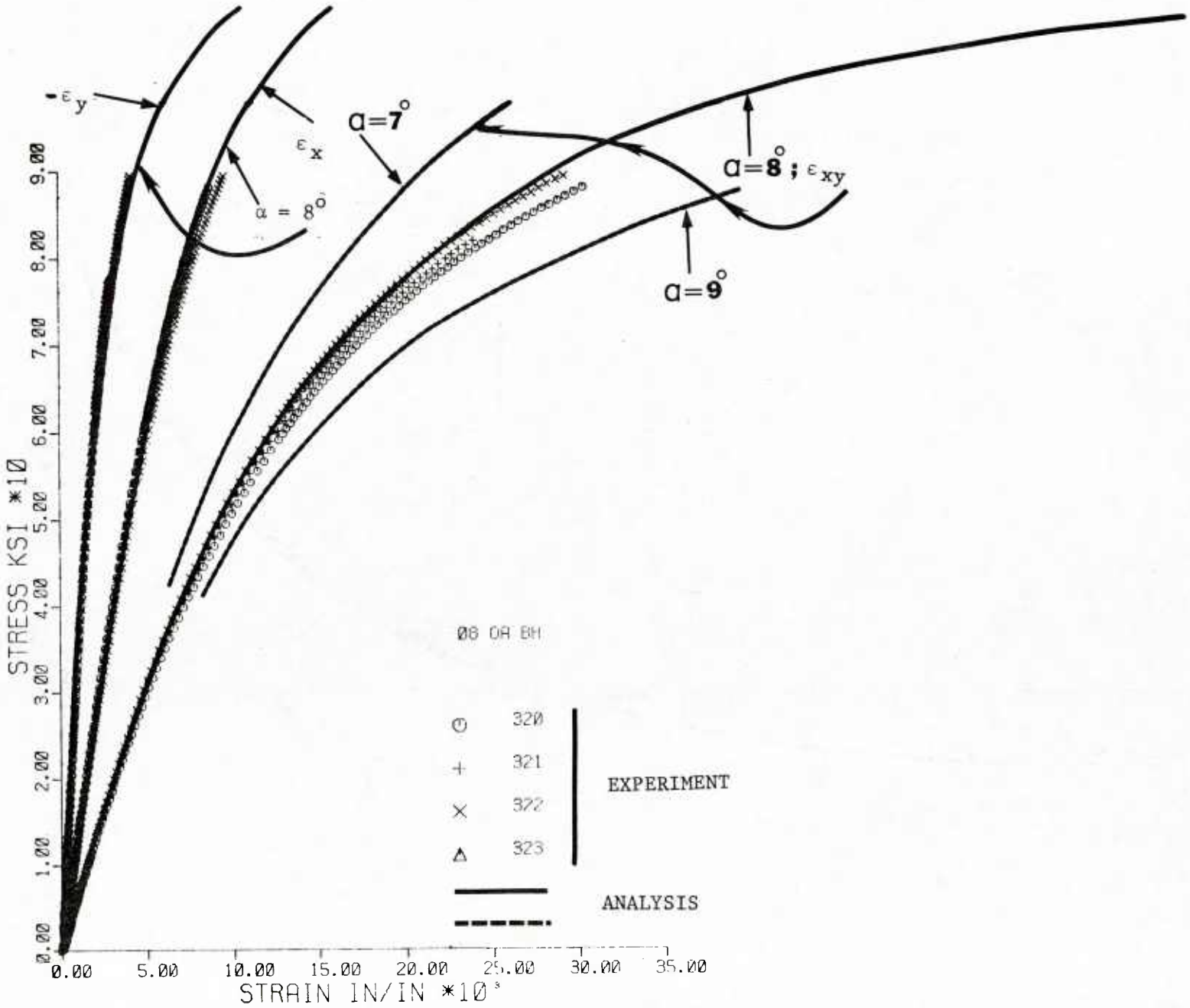

Figure 76. Axial Stress versus Axial, Transverse, and Shear Strain Curves for 8° (nominal) Off-axis Specimens with Inclined Tabs and Hinged Grips

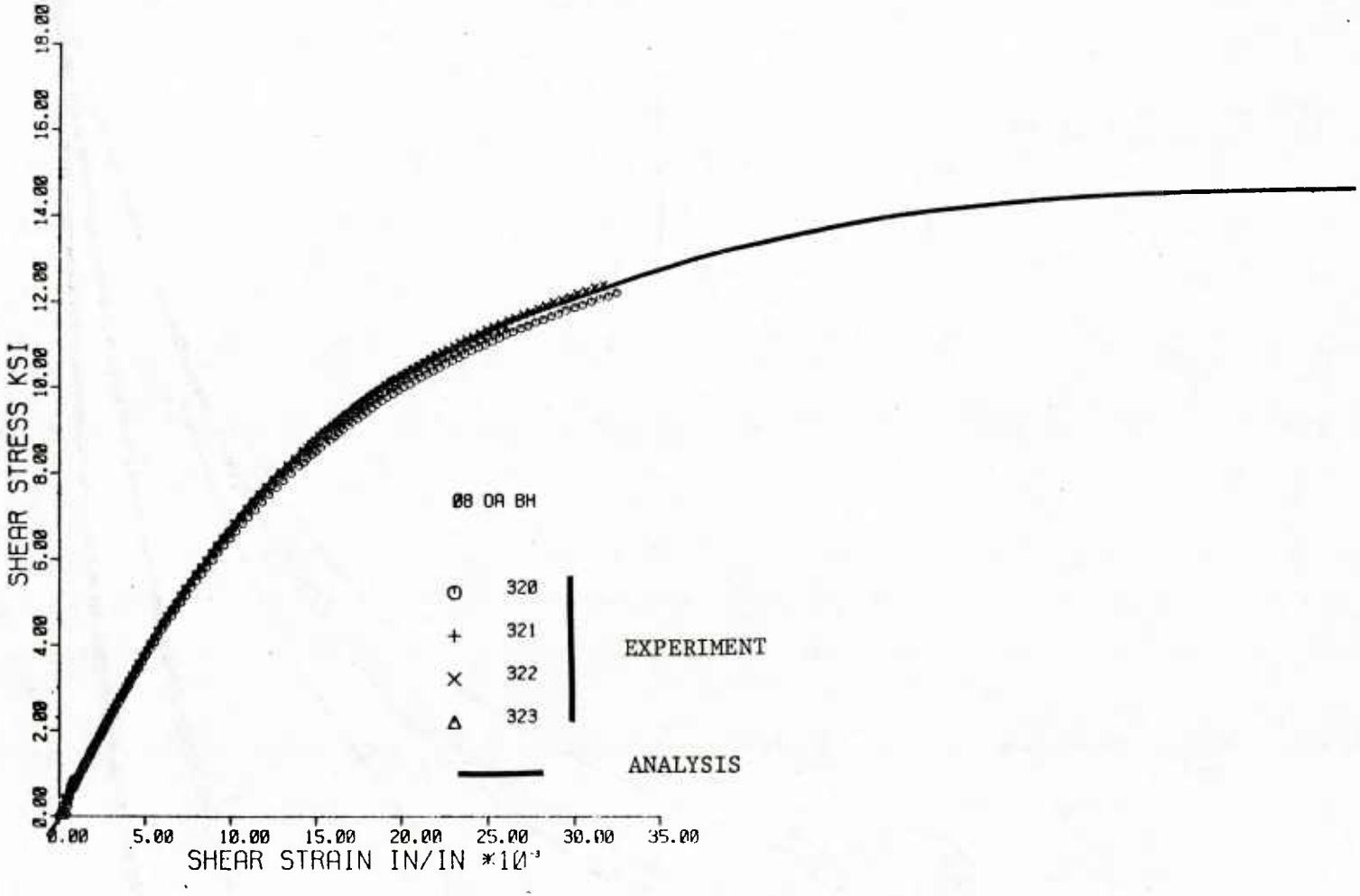

Figure 77. Shear Stress (τ_{12}) versus Shear Strain (γ_{12}) Curves for 8° Off-axis Specimens with Inclined Tabs and Hinged Grips

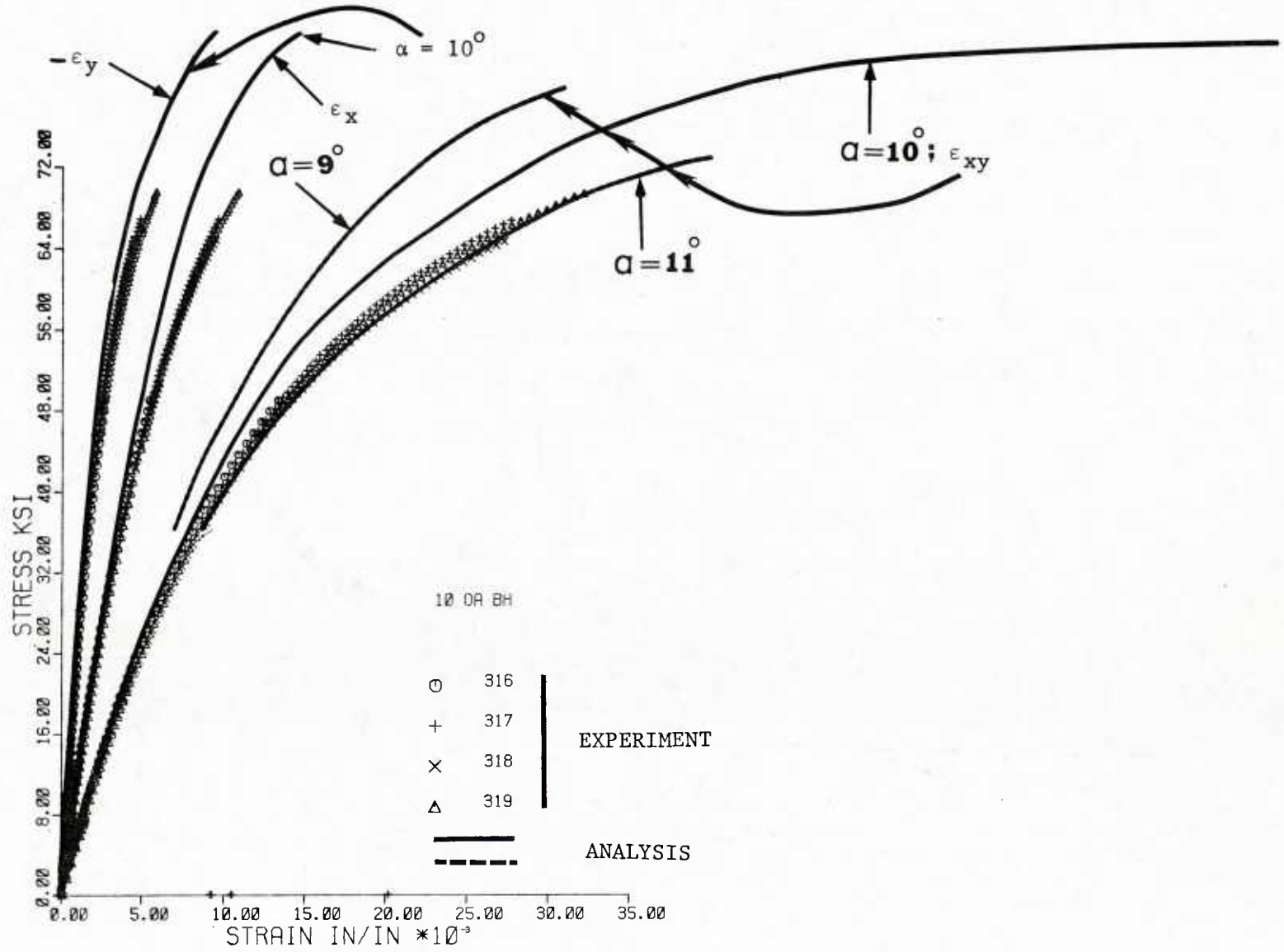

Figure 78. Axial Stress versus Axial, Transverse, and Shear Strain Curves for 10° (nominal) Off-axis Specimens with Inclined Tabs and Hinged Grips

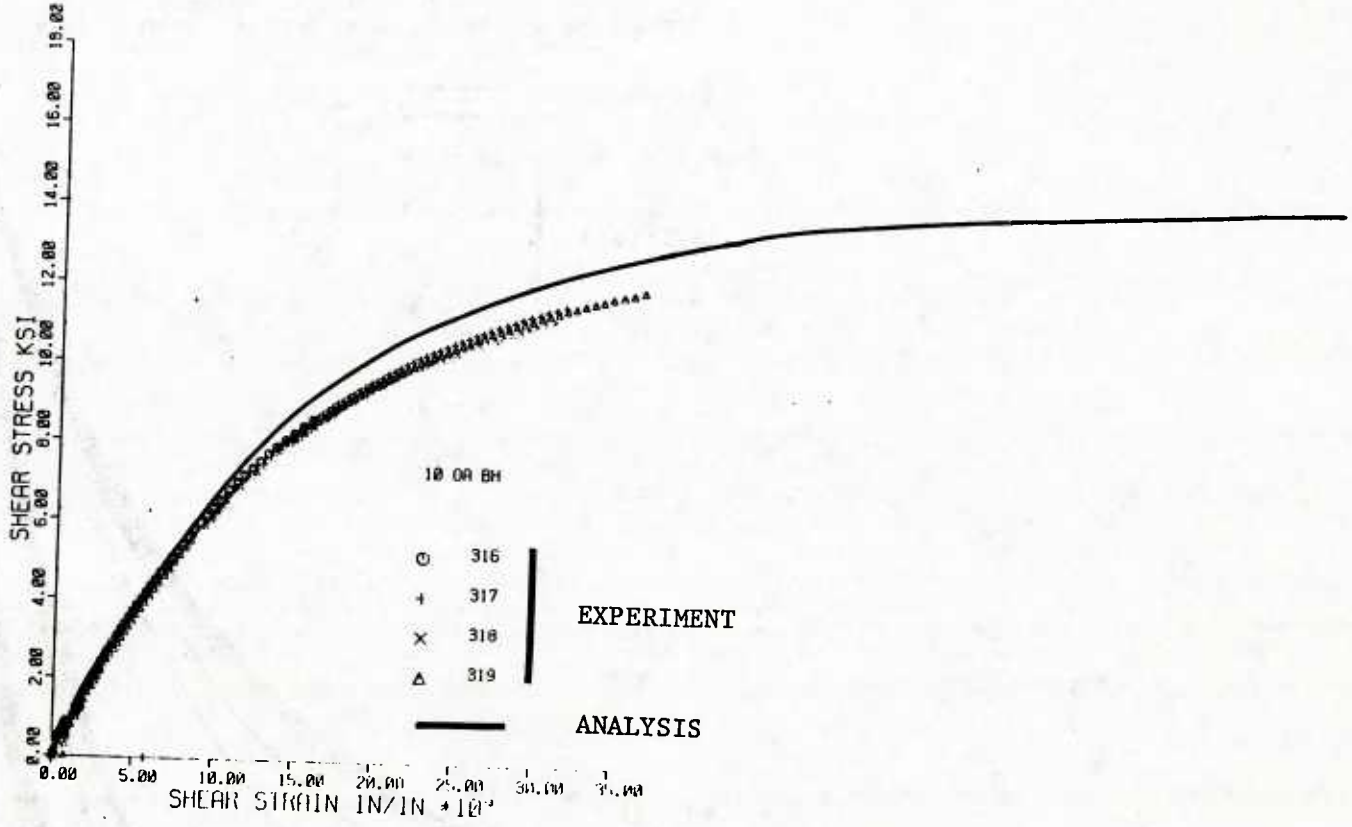

Figure 79. Shear Stress (τ_{12}) versus Shear Strain (γ_{12}) Curves for 10° Off-axis Specimens with Inclined Tabs and Hinged Grips

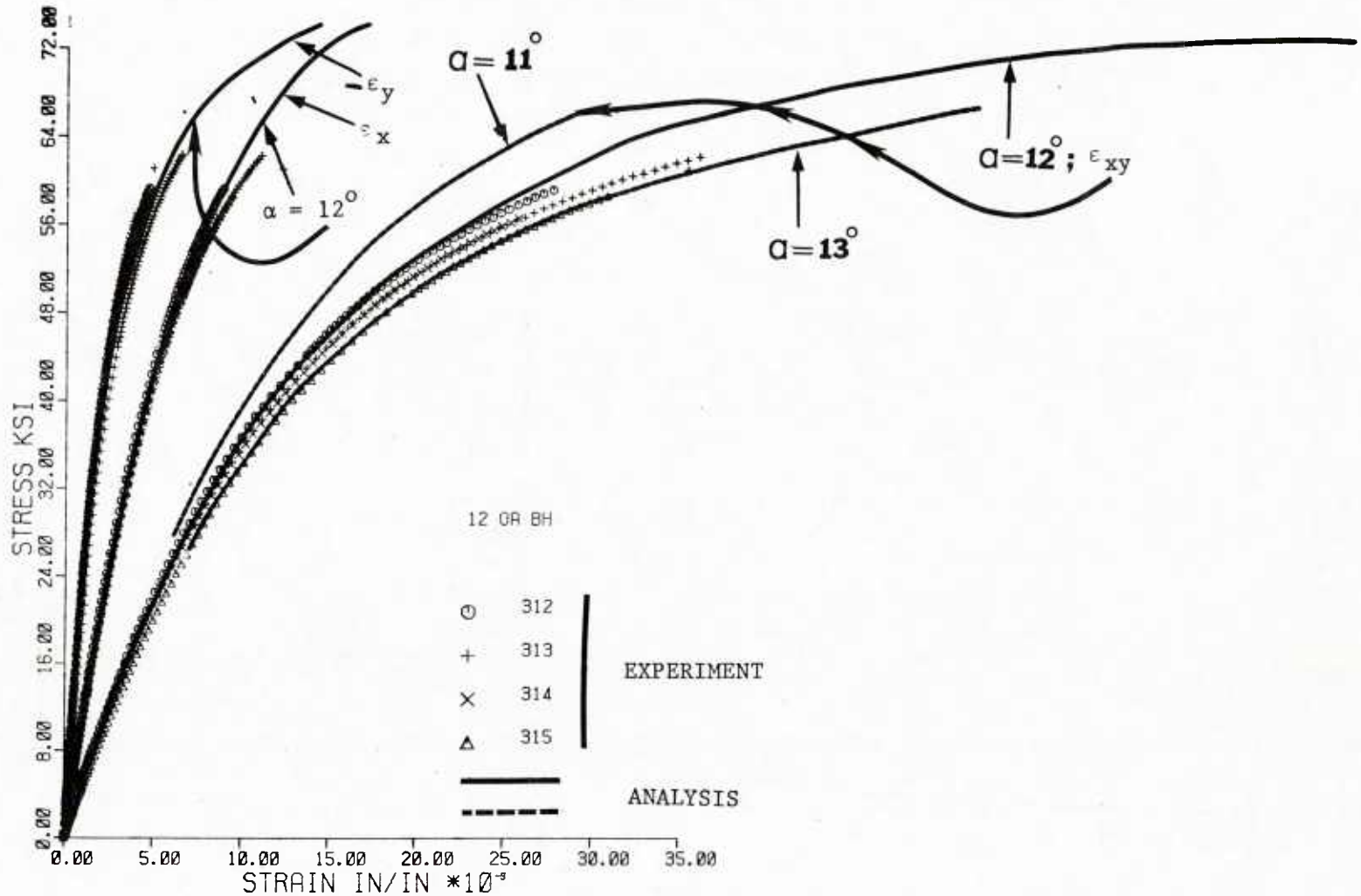

Figure 80. Axial Stress versus Axial, Transverse, and Shear Strain Curves for 12° (nominal) Off-axis Specimens with Inclined Tabs and Hinged Grips

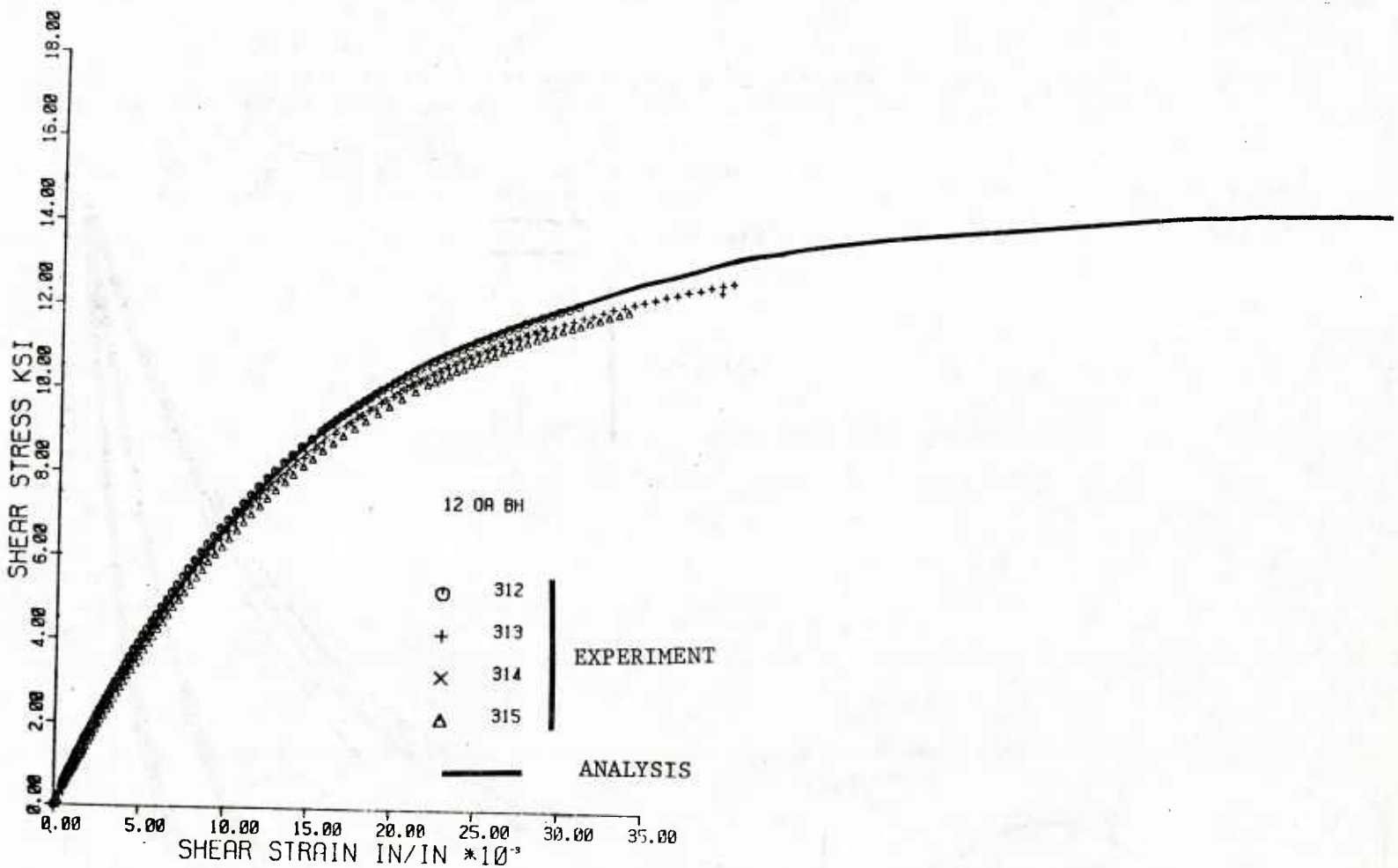

Figure 81. Shear Stress (τ_{12}) versus Shear Strain (γ_{12}) Curves for 12° Off-axis Specimens with Inclined Tabs and Hinged Grips

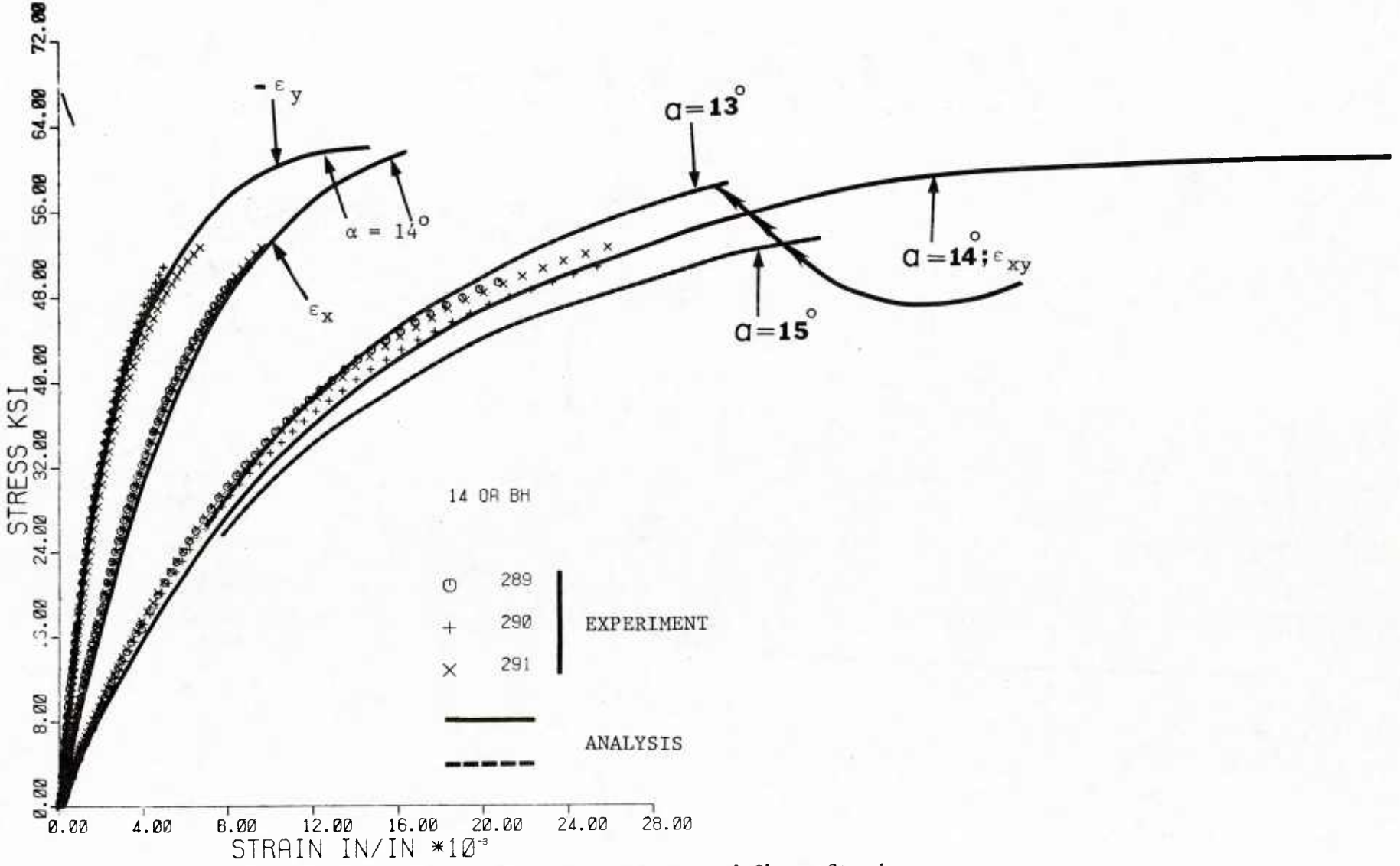

Figure 82. Axial Stress versus Axial, Transverse, and Shear Strain Curves for 14° (nominal) Off-axis Specimens with Inclined Tabs and Hinged Grips

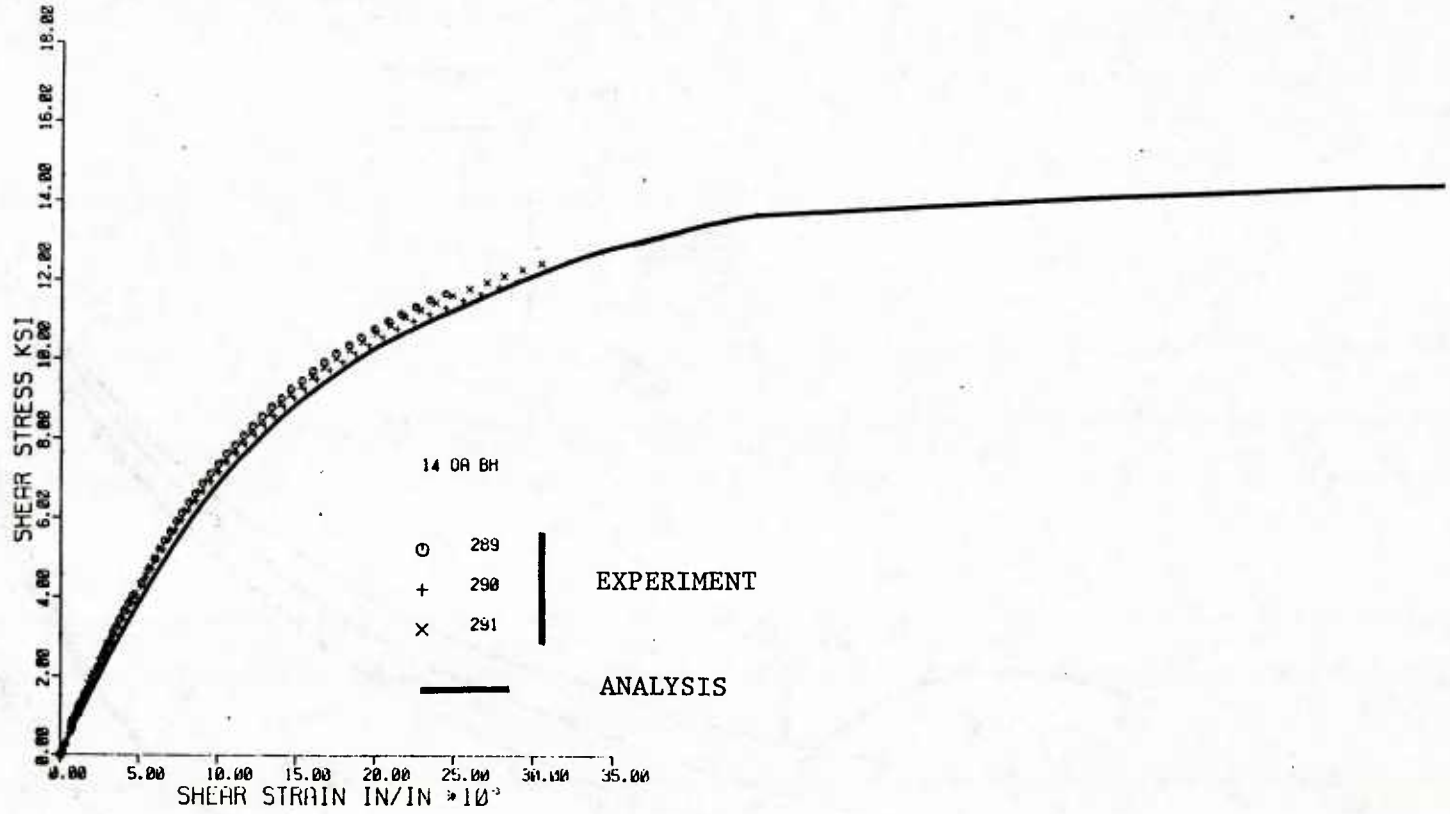

Figure 83. Shear Stress (τ_{12}) versus Shear Strain (γ_{12}) Curves for 14° Off-axis Specimens with Inclined Tabs and Hinged Grips

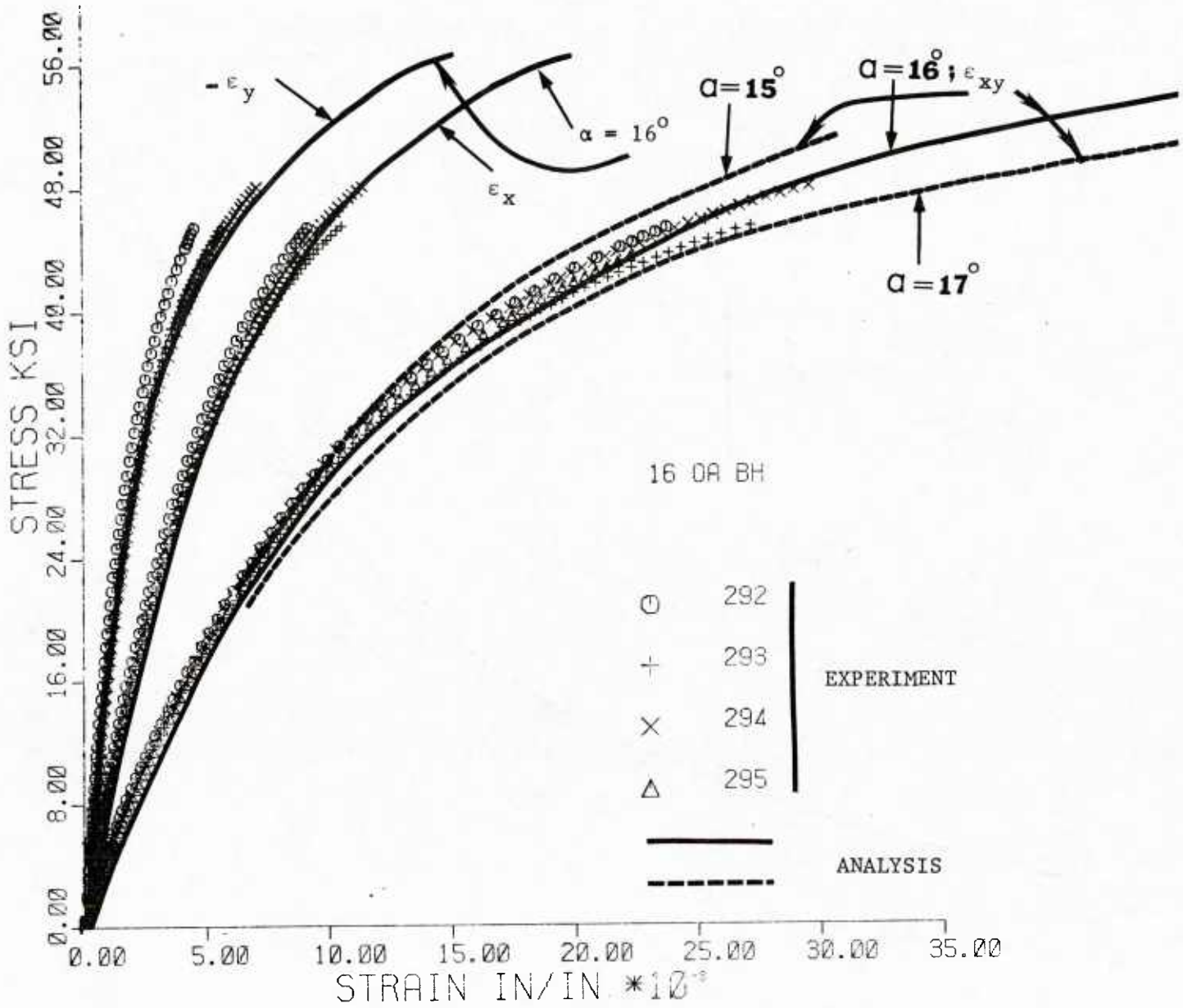

Figure 84. Axial Stress versus Axial, Transverse, and Shear Strain Curves for 16° (nominal) Off-axis Specimens with Inclined Tabs and Hinged Grips

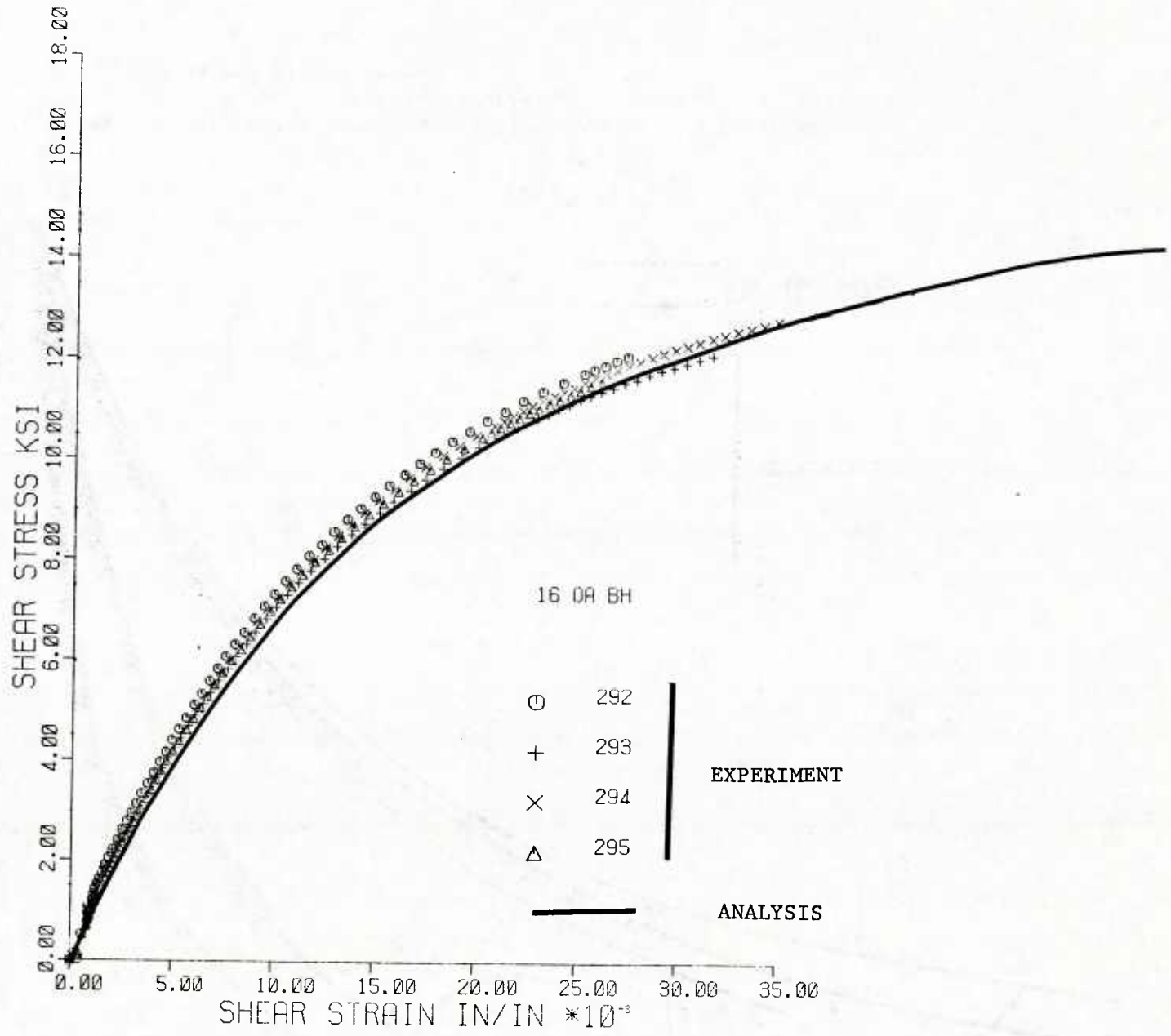

Figure 85. Shear Stress (τ_{12}) versus Shear Strain (γ_{12}) Curves for 16° Off-axis Specimens with Inclined Tabs and Hinged Grips

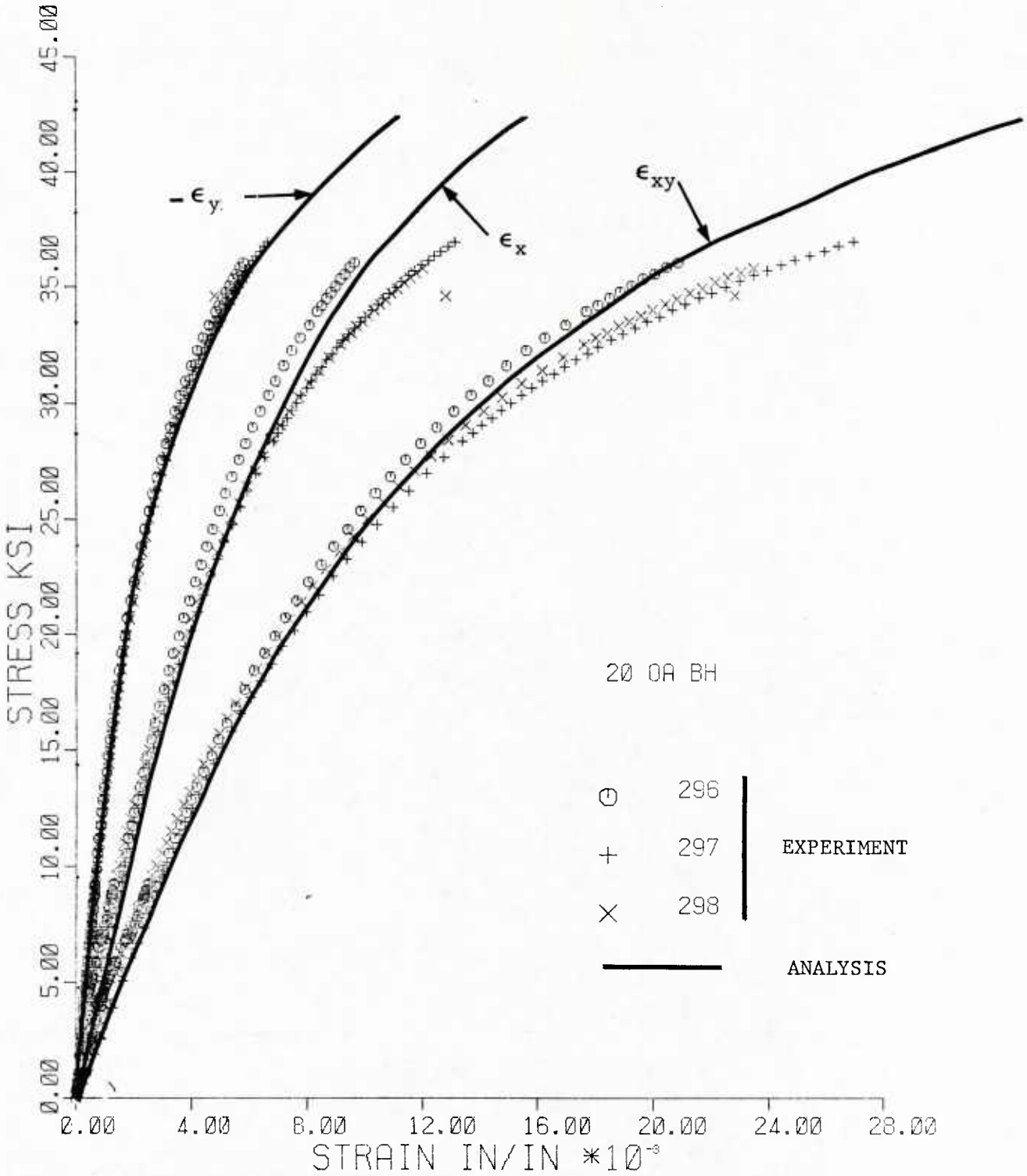

Figure 86. Axial Stress versus Axial, Transverse, and Shear Strain Curves for 20^{o} Off-axis Specimens with Inclined Tabs and Hinged Grips

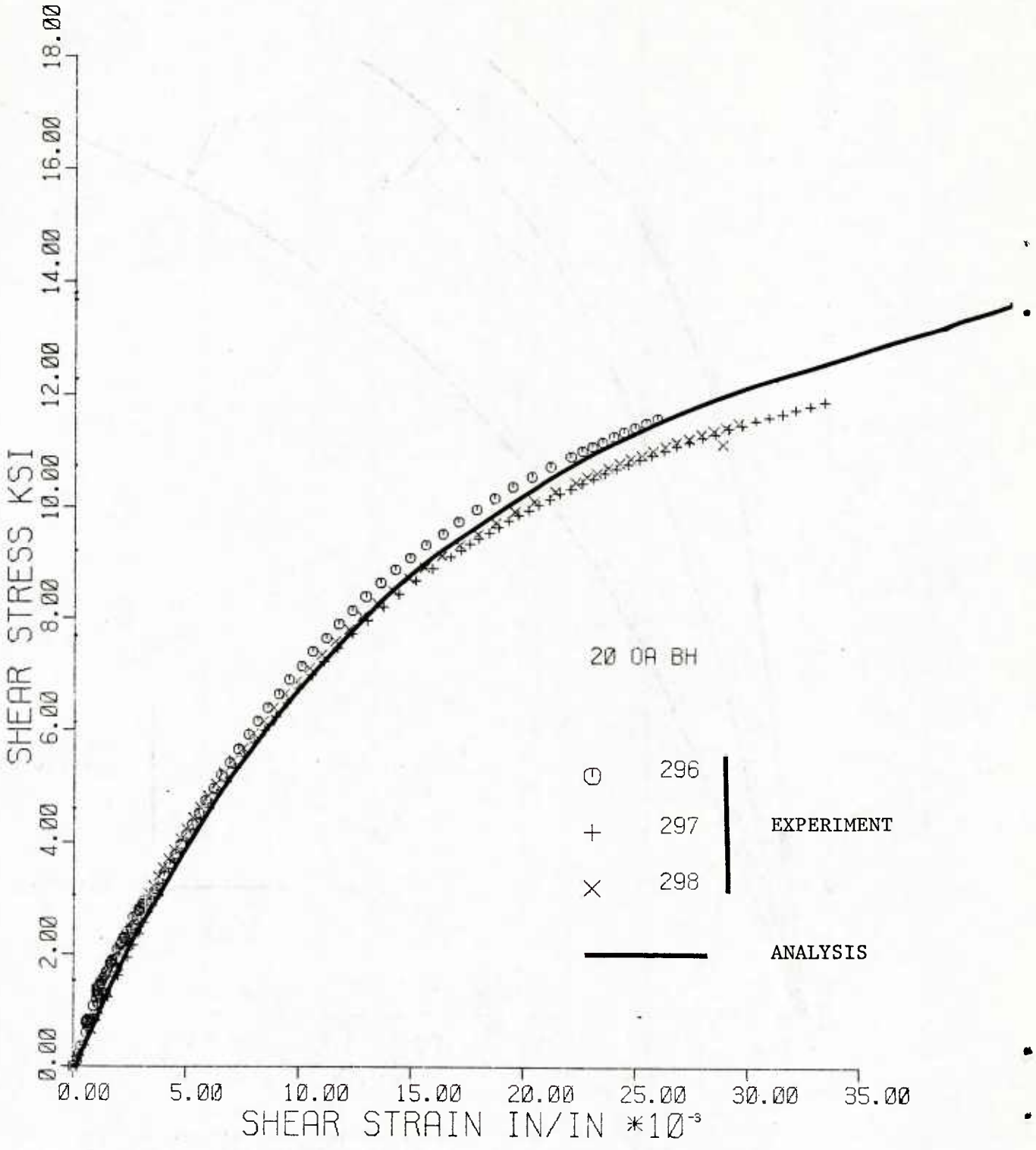

Figure 87. Shear Stress (τ_{12}) versus Shear Strain (γ_{12}) Curves for 20° Off-axis Specimens with Inclined Tabs and Hinged Grips

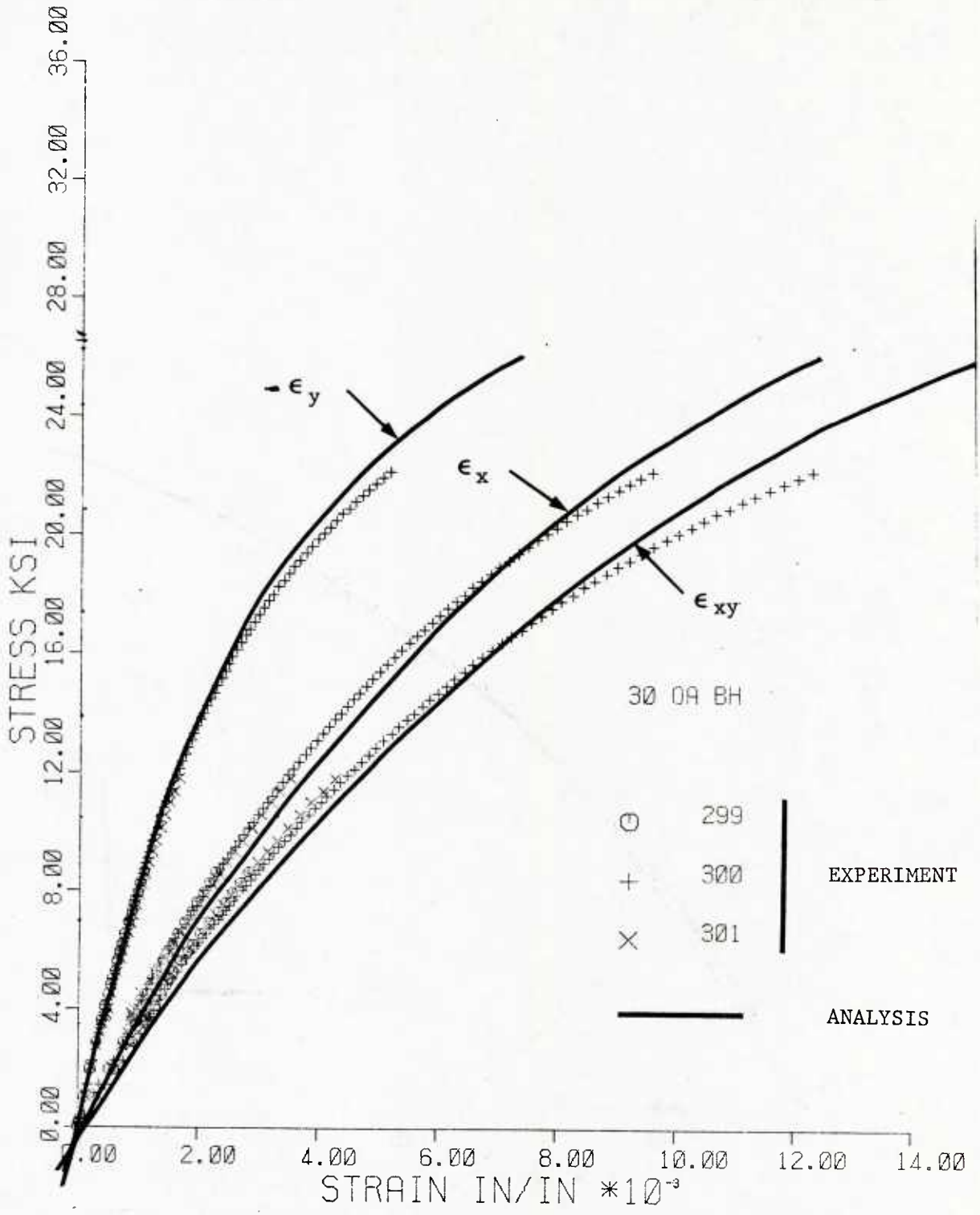

Figure 88. Axial Stress versus Axial, Transverse, and Shear Strain Curves for 30° Off-axis Specimens with Inclined Tabs and Hinged Grips

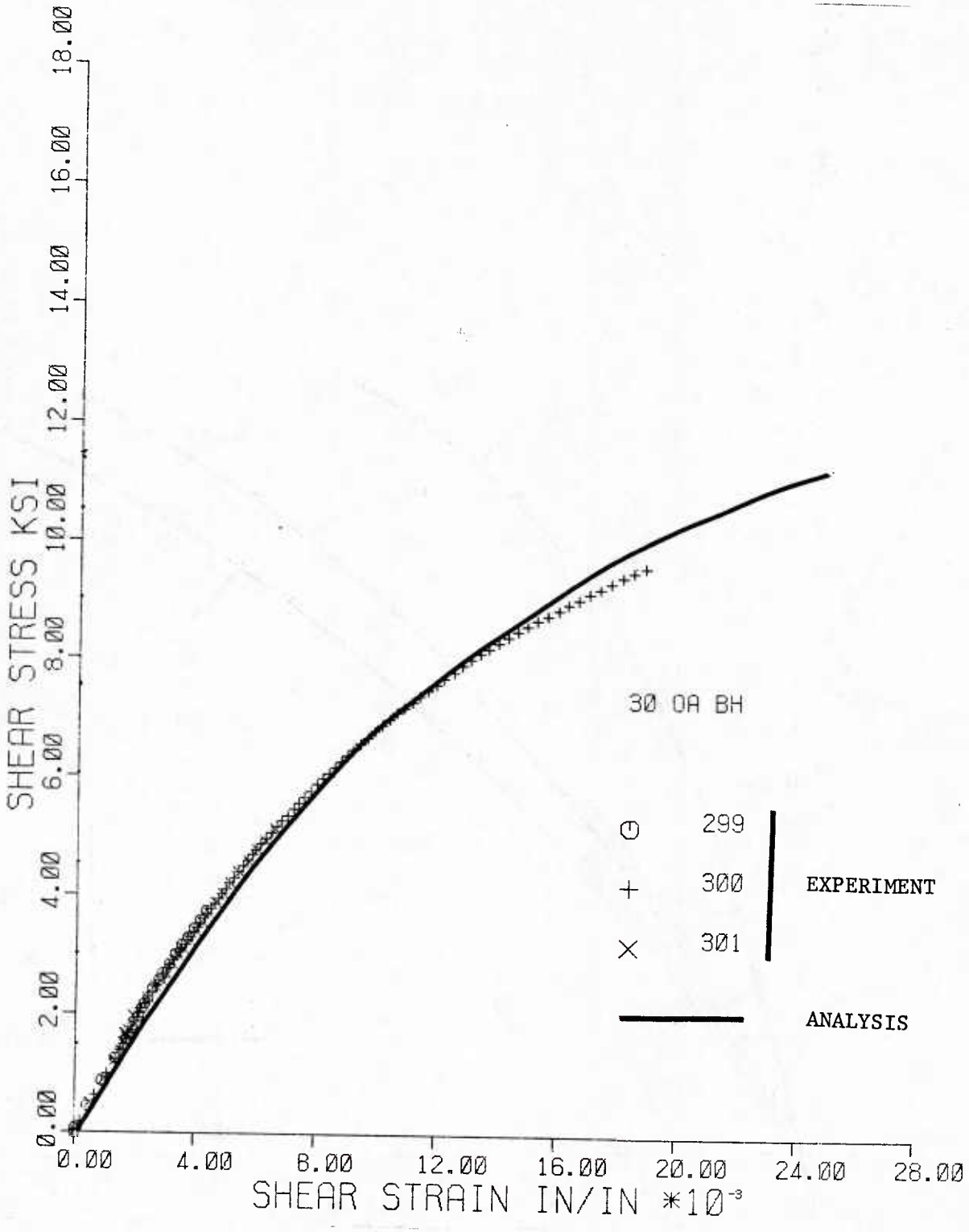

Figure 89. Shear Stress (τ_{12}) versus Shear Strain (γ_{12}) Curves for 30° Off-axis Specimens with Inclined Tabs and Hinged Grips

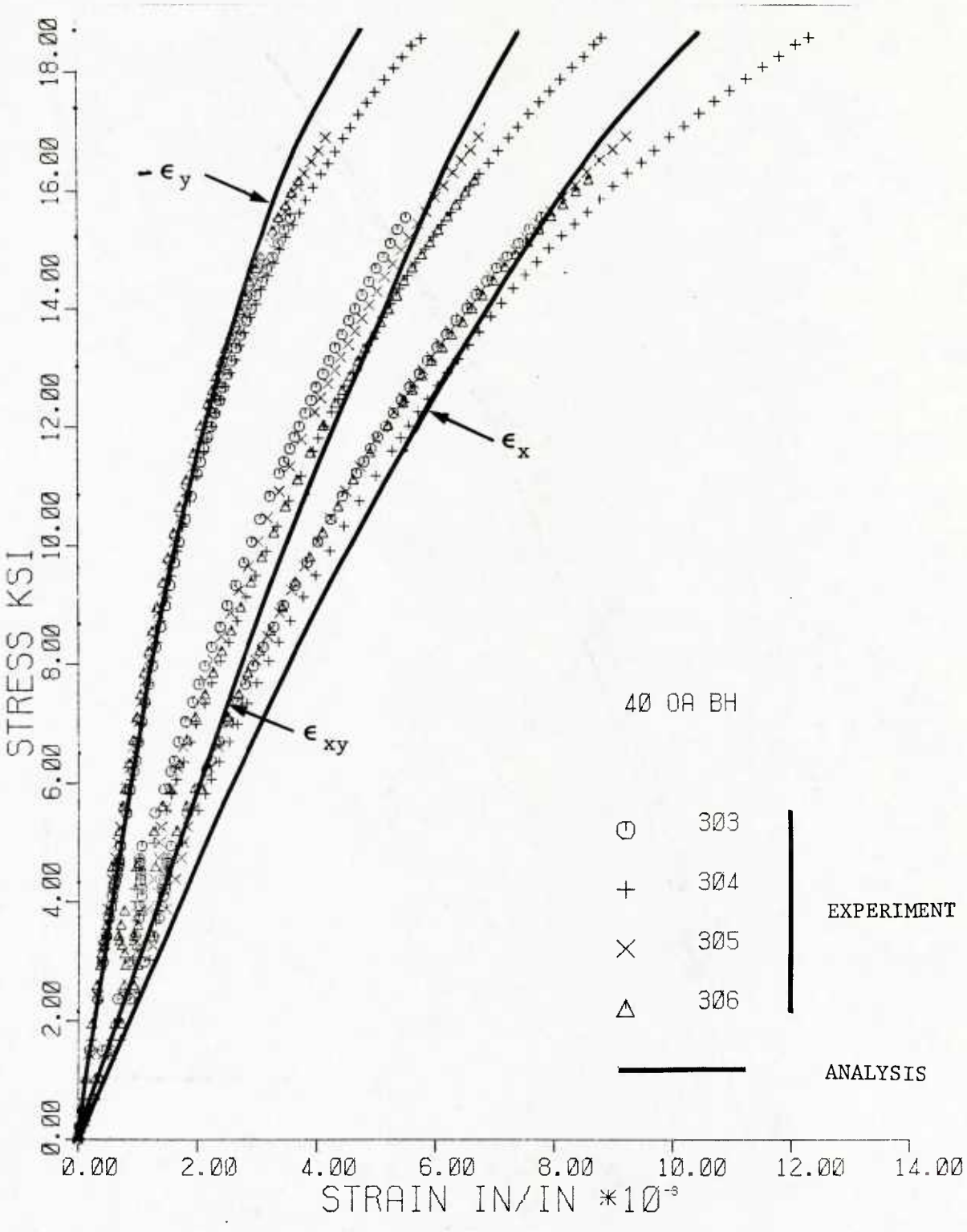

Figure 90. Axial Stress versus Axial, Transverse, and Shear Strain Curves for 40° Off-axis Specimens with Inclined Tabs and Hinged Grips

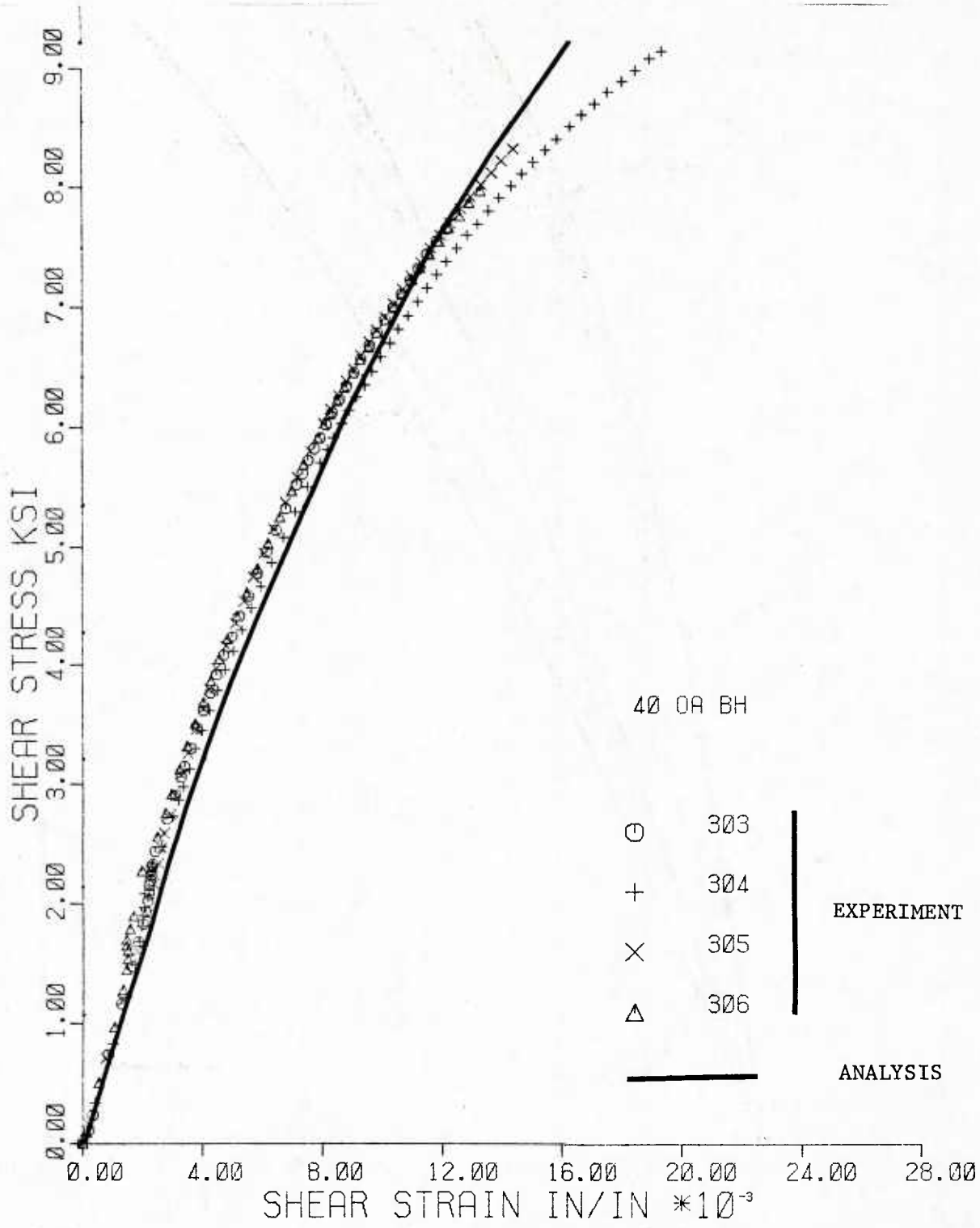

Figure 91. Shear Stress (τ_{12}) versus Shear Strain (γ_{12}) Curves for 40^{o} Off-axis Specimens with Inclined Tabs and Hinged Grips

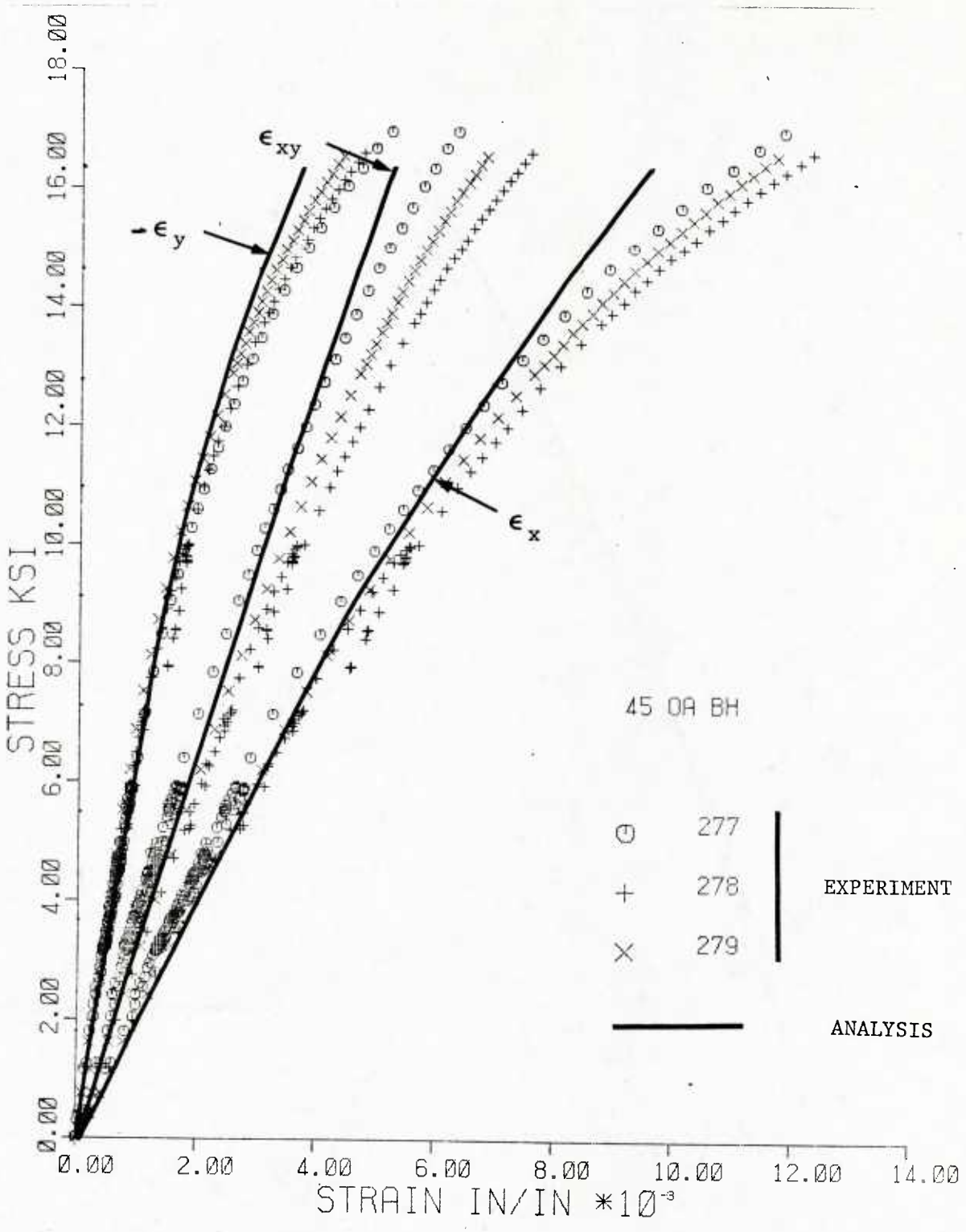

Figure 92. Axial Stress versus Axial, Transverse, and Shear Strain Curves for 45^{o} Off-axis Specimens with Inclined Tabs and Hinged Grips

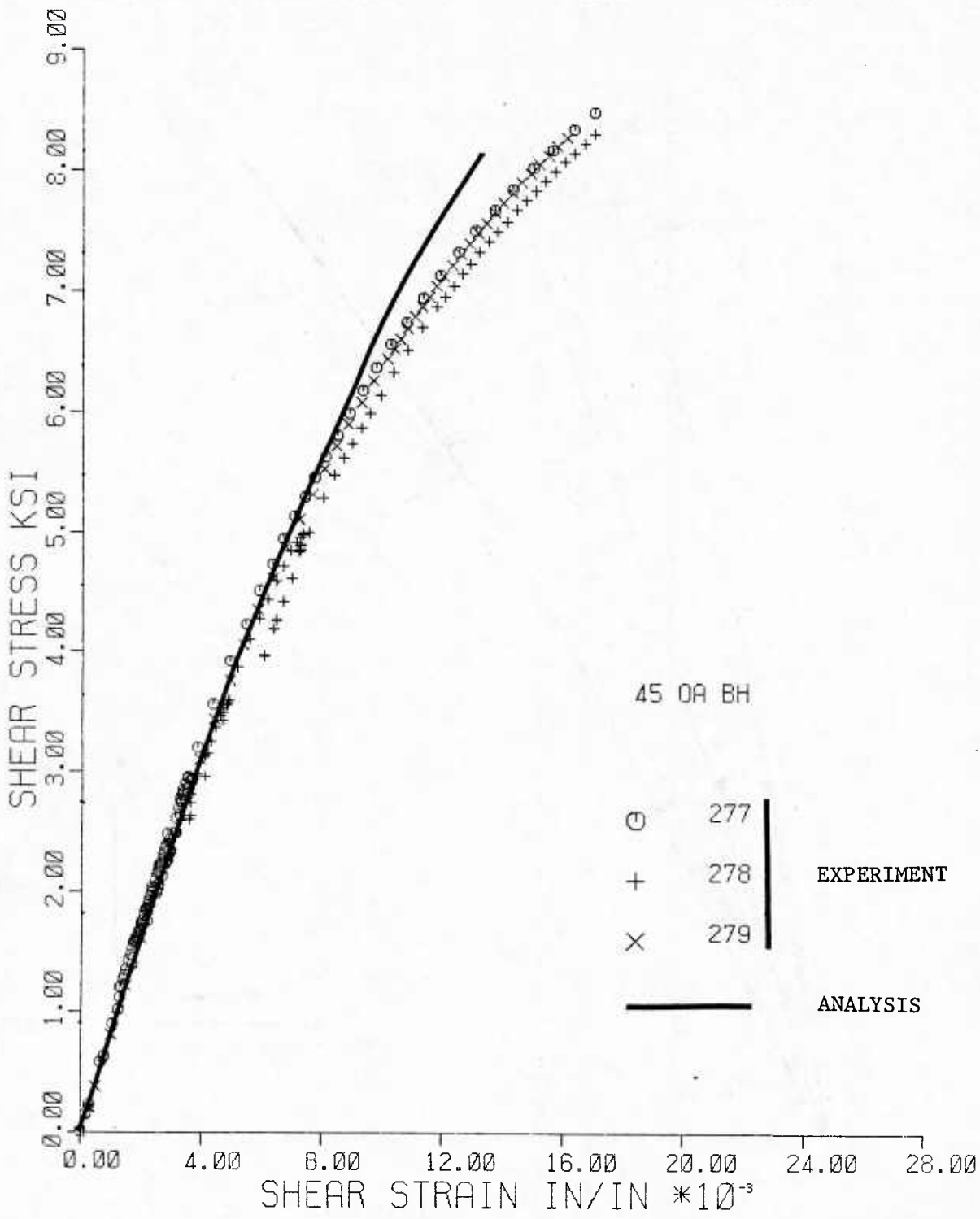

Figure 93. Shear Stress (τ_{12}) versus Shear Strain (γ_{12}) Curves for 45° Off-axis Specimens with Inclined Tabs and Hinged Grips

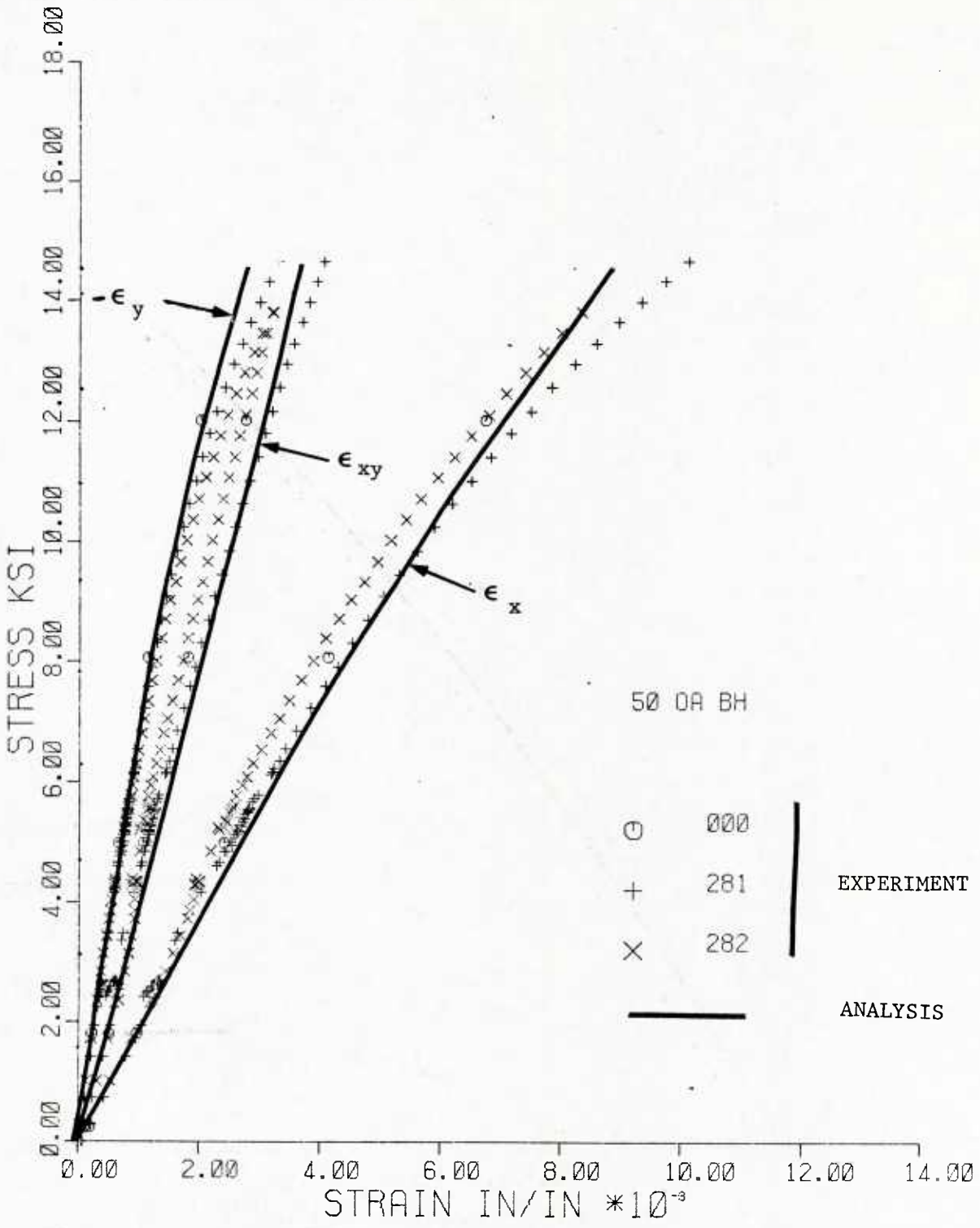

Figure 94. Axial Stress versus Axial, Transverse, and Shear Strain Curves for 50° Off-axis Specimens with Inclined Tabs and Hinged Grips

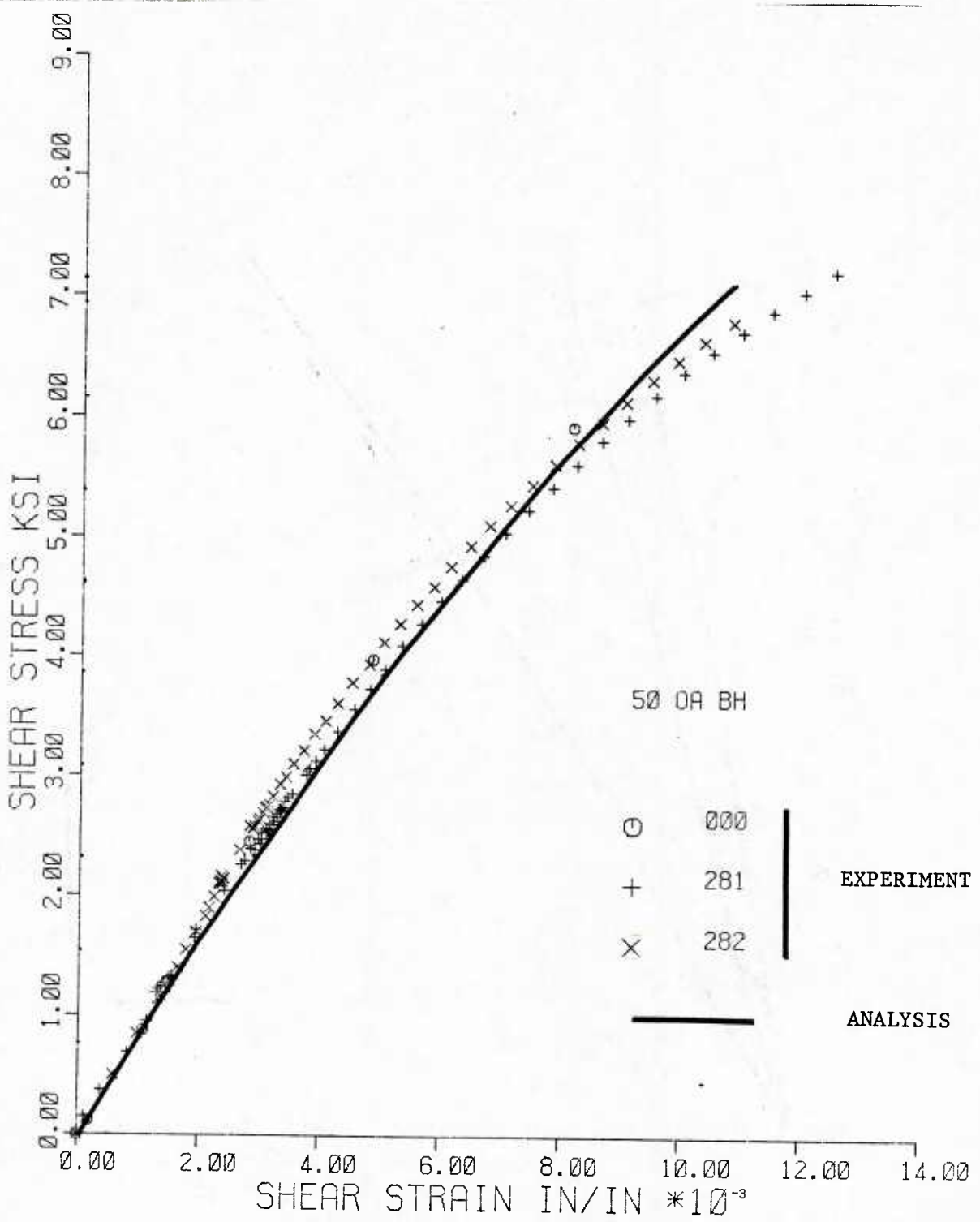

Figure 95. Shear Stress (τ_{12}) versus Shear Strain (γ_{12}) Curves for 50° Off-axis Specimens with Inclined Tabs and Hinged Grips

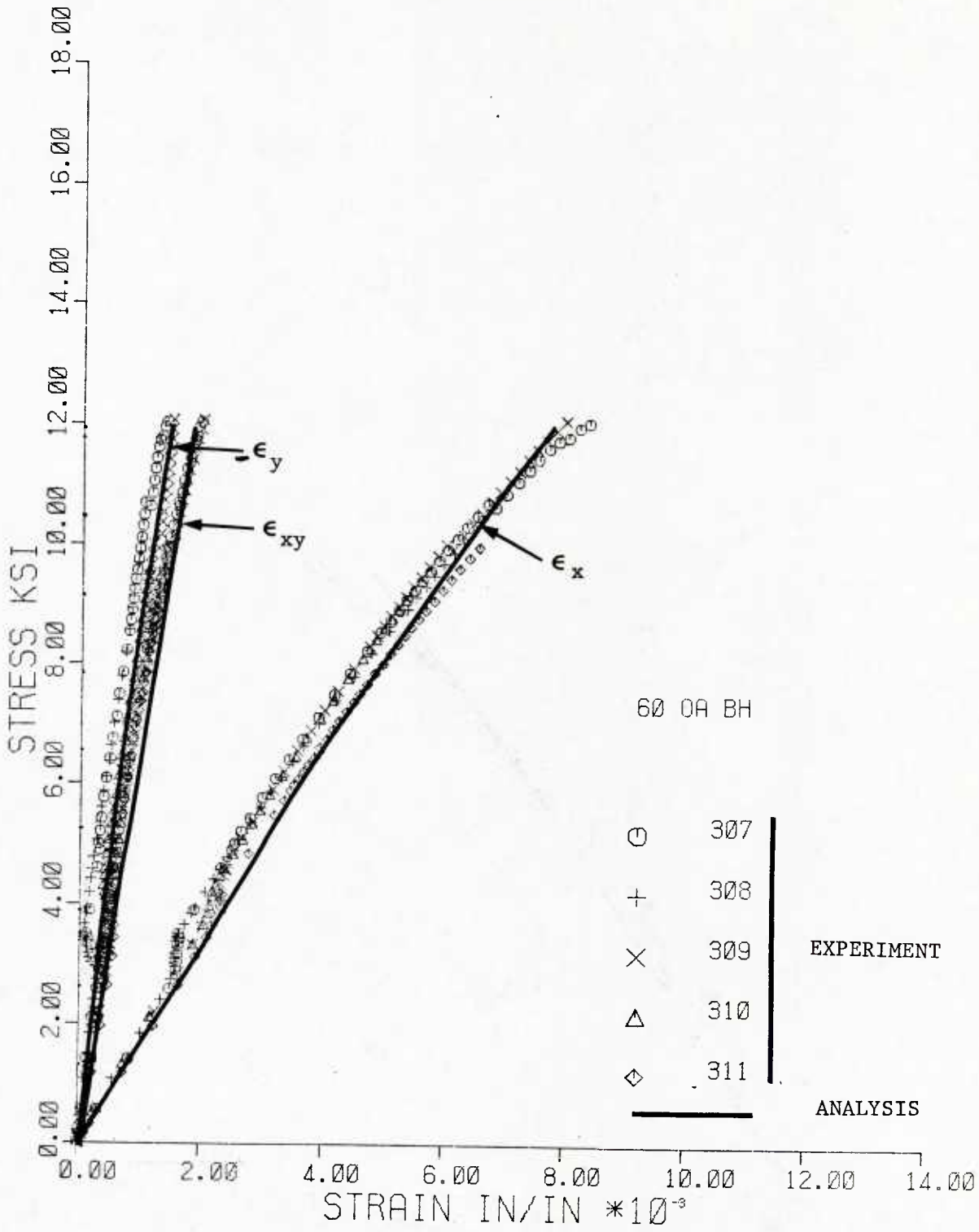

Figure 96. Axial Stress versus Axial, Transverse, and Shear Strain Curves for 60° Off-axis Specimens with Inclined Tabs and Hinged Grips

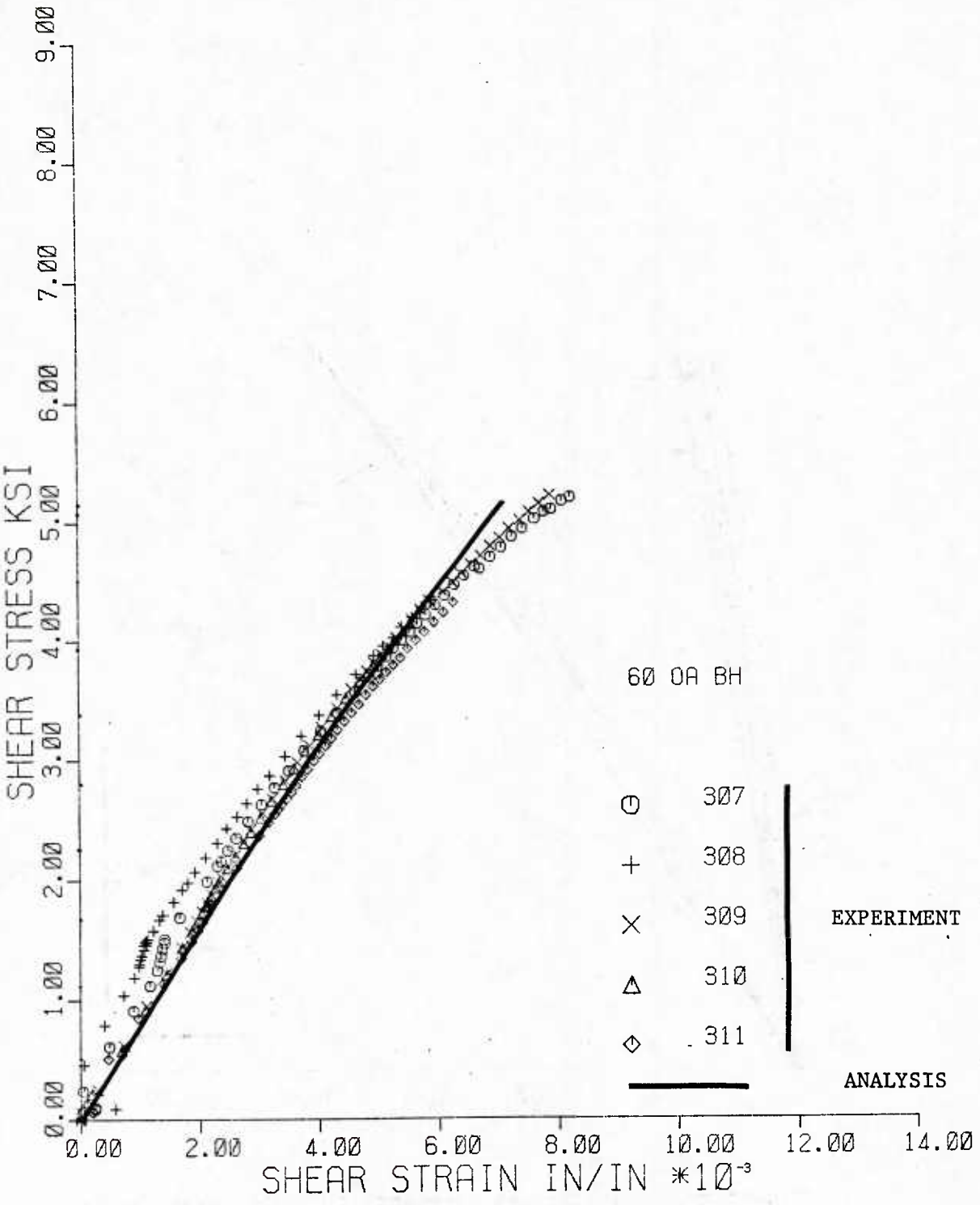

Figure 97. Shear Stress (τ_{12}) versus Shear Strain (γ_{12}) Curves for 60° Off-axis Specimens with Inclined Tabs and Hinged Grips

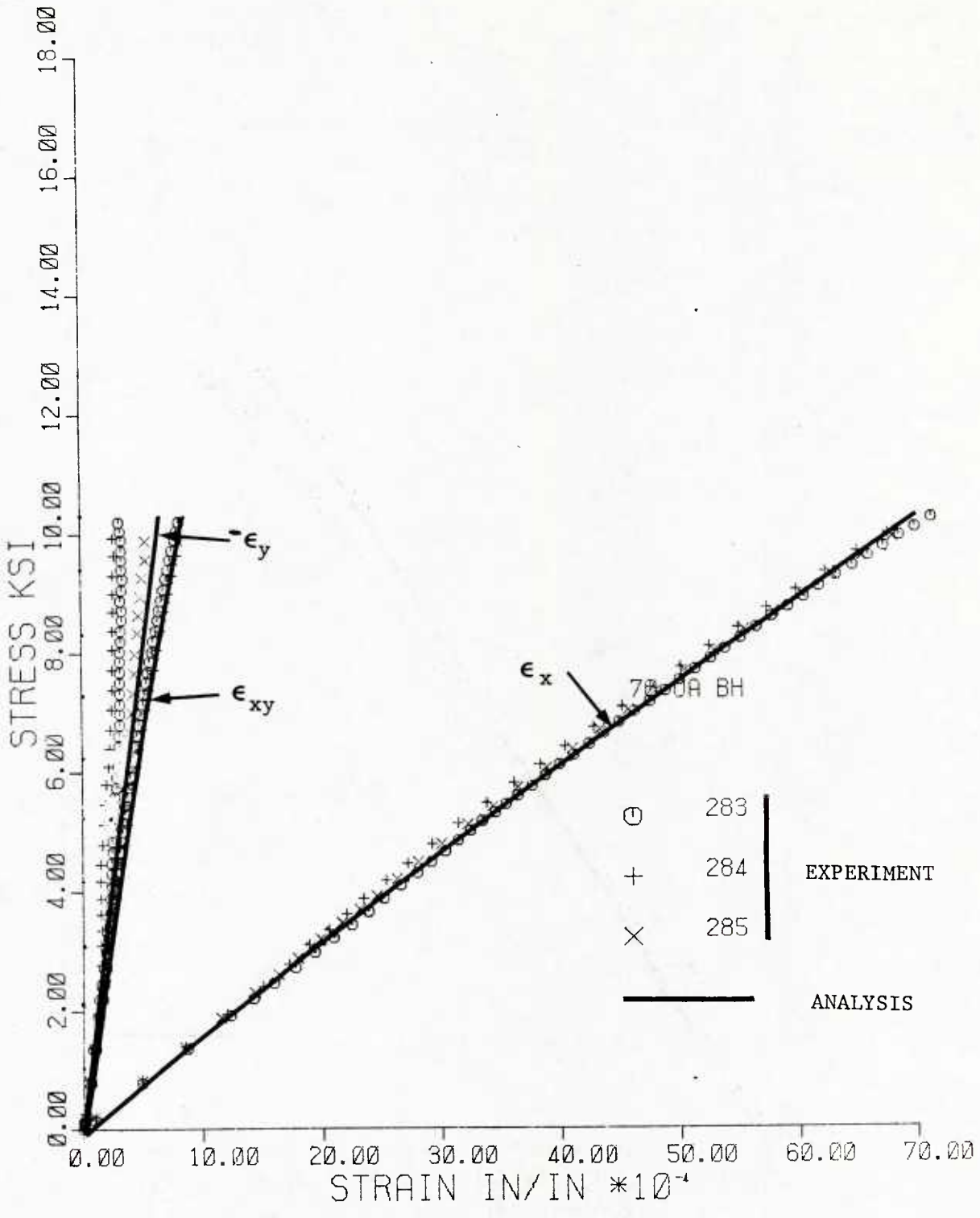

Figure 98. Axial Stress versus Axial, Transverse, and Shear Strain Curves for 70° Off-axis Specimens with Inclined Tabs and Hinged Grips

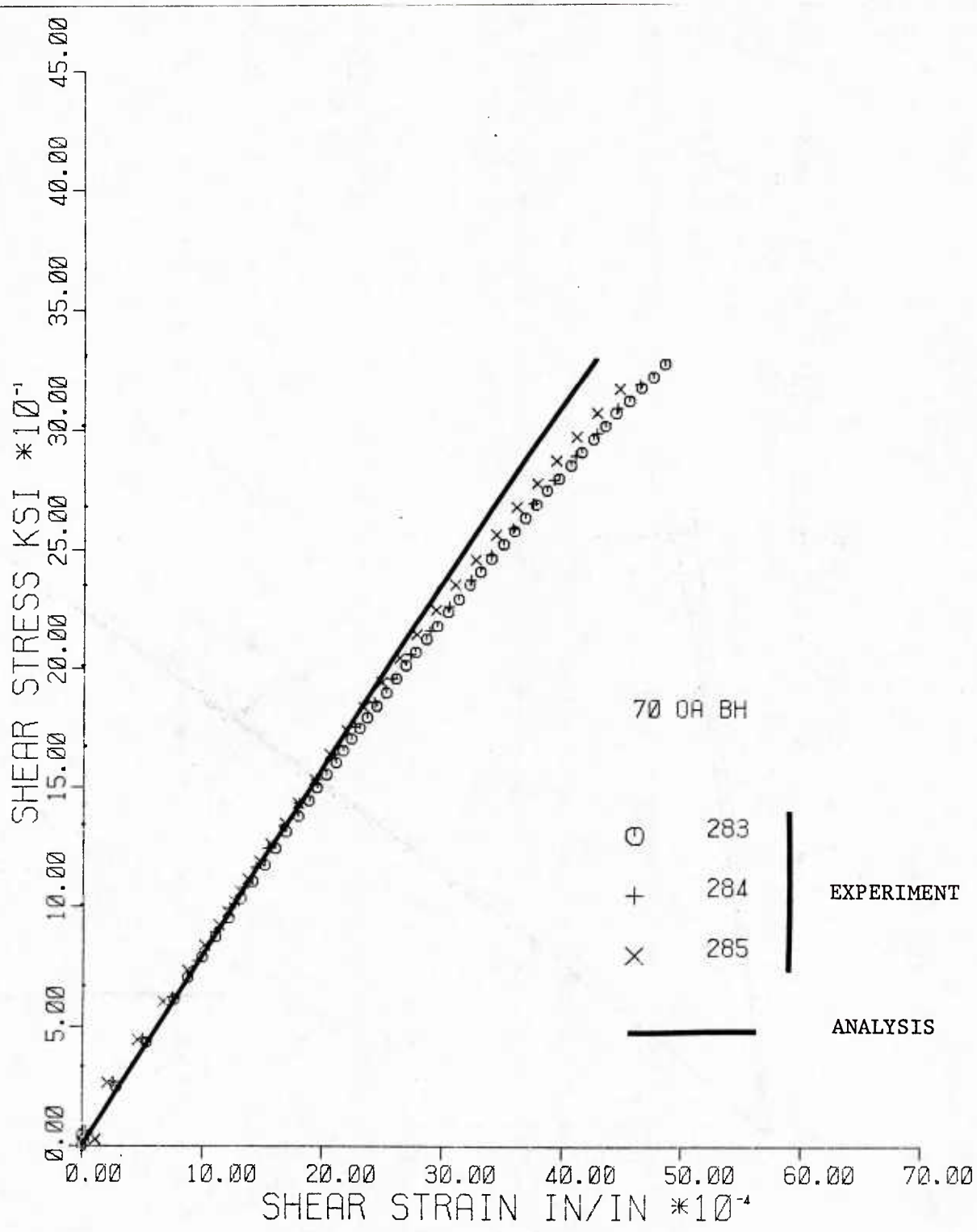

Figure 99. Shear Stress (τ_{12}) versus Shear Strain (γ_{12}) Curves for 70° Off-axis Specimens with Inclined Tabs and Hinged Grips

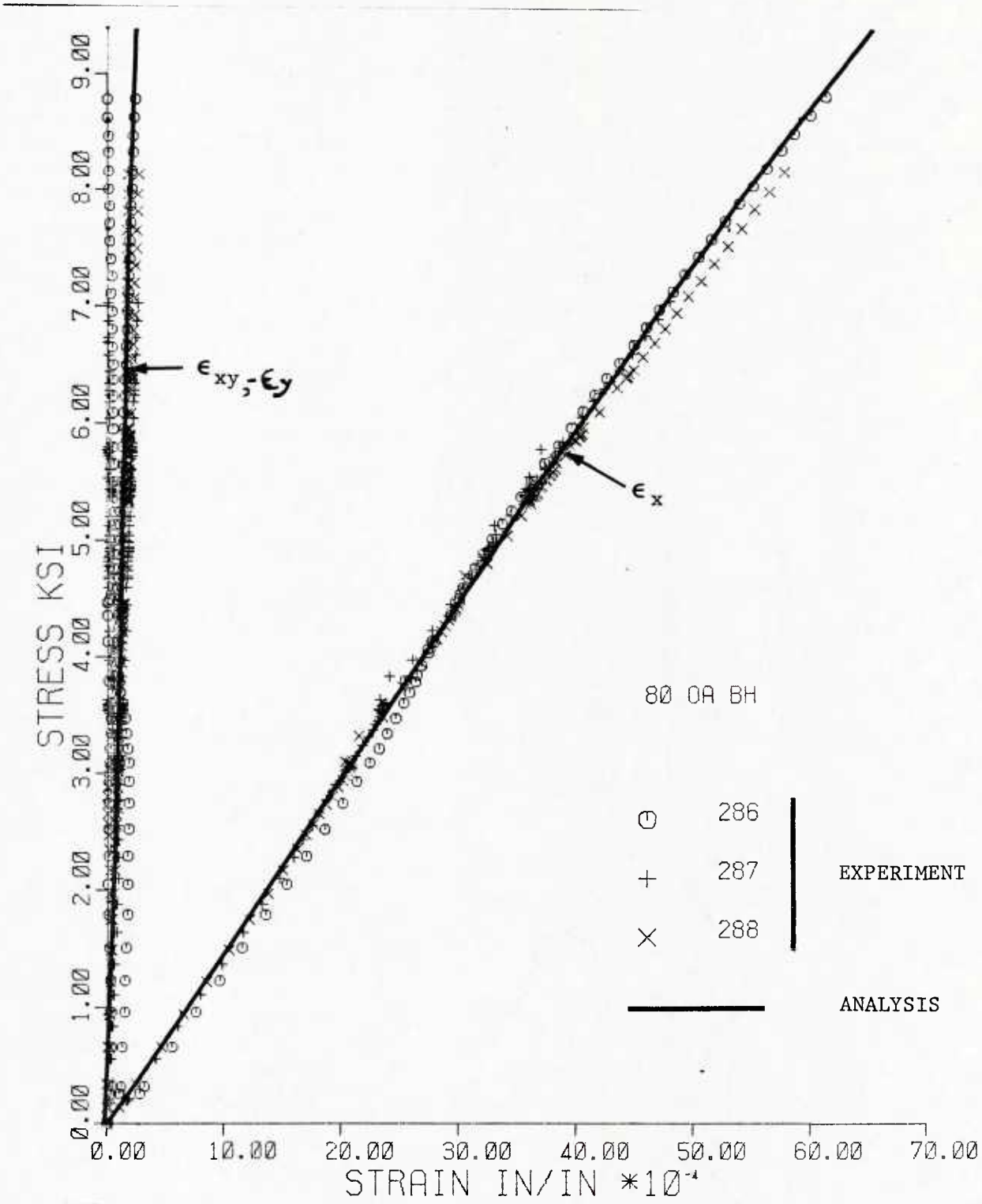

Figure 100. Axial Stress versus Axial, Transverse, and Shear Strain Curves for 80° Off-axis Specimens with Inclined Tabs and Hinged Grips

*U.S.Government Printing Office: 1985 — 559-065/20757